

BULLETIN 17

## **Regional bedrock geology for Coal River map area (NTS 95D), southeast Yukon**

by

Lee C. Pigage, Charles F. Roots and J. Grant Abbott

with contributions from Jim Crowley, Sandy McCracken, Godfrey Nowlan, Mike Orchard  
and Leanne Pyle

2015





2009 field crew at Grizzly Creek Lodge, upper Toobally Lake - (*back row, left to right*) Lee Pigage, Mike Dorsey and Grant Abbott; (*middle row, left to right*) Kristen Kennedy, Beth Hunt and Charlie Roots; (*front row, left to right*) Gavin Clarkson, Martina Bezzola and Casey Cardinal.

BULLETIN 17

## **Regional bedrock geology for Coal River map area (NTS 95D), southeast Yukon**

by  
Lee C. Pigage<sup>1</sup>, Charles F. Roots<sup>2</sup> and J. Grant Abbott<sup>1</sup>

with contributions from Jim Crowley, Sandy McCracken, Godfrey Nowlan, Mike Orchard and Leanne Pyle

---

1 retired geologist, Yukon Geological Survey  
2 Geological Survey of Canada

Published under the authority of the Minister of Energy, Mines and Resources, Government of Yukon  
<http://www.emr.gov.yk.ca>

© Minister of Energy, Mines and Resources, Government of Yukon

This, and other Yukon Geological Survey publications, may be obtained from:

Yukon Geological Survey  
102-300 Main Street  
Box 2703 (K-102)  
Whitehorse, Yukon, Canada Y1A 2C6  
phone (867) 667-3201  
fax (867) 667-3198  
email [geology@gov.yk.ca](mailto:geology@gov.yk.ca)

Visit the Yukon Geological Survey website at <http://www.geology.gov.yk.ca>

In referring to this publication, please use the following citation:

Pigage, L.C., Roots, C.F. and Abbott, J.G., 2015. Regional bedrock geology for Coal River map area (NTS 95D), southeast Yukon. Yukon Geological Survey, Bulletin 17, 155 p.

This bulletin is available in colour on the Yukon Geological Survey website.

**Cover photo:** Waterfall in upper part of Beaver River (NTS 95D/10), immediately upstream from field station 09TOA146 (636 644 E, 6 719 278 N). Cliffs consist of thick-bedded Sunblood Formation.

## FOREWORD

Recent collaborative geological mapping by Yukon Geological Survey (YGS) and Geological Survey of Canada (GSC) through the Central Foreland NATMAP project (fieldwork 2000-2002) provided a new and enhanced stratigraphic and structural framework for bedrock and surficial geology in southeast Yukon. Subsequent detailed geological mapping sponsored by YGS (fieldwork 2003-2007) further elaborated on an improved understanding of the bedrock geology for reassessing its mineral and hydrocarbon potential.

This report documents the revised bedrock geology of the Coal River map area (NTS 95D) in southeast Yukon, expanding upon the earlier studies. It results from a helicopter-supported 2009 collaborative mapping project between YGS and GSC which was funded through the Geoscience for Energy and Minerals (GEM) program of Natural Resources Canada. Isotopic dating and paleontology were organized by GSC; geochemical analysis of the igneous rocks was funded by YGS. In 2010, YGS sponsored one week of fieldwork as a follow-up to stratigraphic and structural questions from the 2009 project.

The current publication provides a contemporary bedrock geology framework of the Coal River map area which straddles the southern margin of Selwyn basin and occurs at the southeast end of the 'Tintina gold belt'. Both mineral domains constitute significant mineral resource provinces of Yukon. Bedrock geology consists of Neoproterozoic to Eocene stratigraphic units comprising 6 depositional successions and is described in a lithologic and paleogeographic context. Numerous small Cretaceous granitoid bodies have been identified in the northern half of the map area.

Mineral occurrences include Irish-type and Mississippi Valley-type Zn-Pb replacements in carbonate rock, massive sulfide mantos, tungsten and base metal skarns, and scattered intrusion-related precious-metal veins and replacements. For much of the area, carbonaceous sedimentary rocks appear to be over-mature as hydrocarbon source rocks although potential may exist for unconventional tight-shale gas; a coal resource has been identified locally.



Maurice Colpron

Senior Project Geologist  
Yukon Geological Survey  
Energy Mines and Resources  
Government of Yukon

## ABSTRACT

Coal River map area (NTS 95D) encompasses the southern extent of the early Paleozoic Selwyn basin, with Macdonald platform to the south. Neoproterozoic to Triassic strata constitute miogeoclinal sedimentary rocks deposited on the passive margin of Laurentia. Cambrian-Ordovician strata define an east-west facies change from silty limestone in the west to impure quartzose sandstone in the east. Alkali basalt occurs in multiple stratigraphic horizons within Cambro-Ordovician strata. Silurian-middle Devonian strata record a facies change from platform carbonate rocks in the south to deep marine carbonaceous shale in the north. Middle Devonian to Triassic shale and sandstone sequences record three transgressive/regressive cycles. Eocene strata consist of post-orogenic fluvial mudstone, siltstone and sandstone with interbedded coal seams preserved in an extensional half-graben.

Most of the small Cretaceous granitic stocks are highly magnetic and coincide with positive aeromagnetic anomalies. Other aeromagnetic anomalies may correspond to buried or unmapped intrusions.

The Coal River map area is characterized by steeply dipping, northwest to northeast-trending faults and folds. Contractional deformation structures and axial planar fabrics decrease in intensity from west to east. Late extensional deformation is manifested by normal faults. The largest of these structures is the Rock River fault which forms the western margin of the upper Eocene Rock River basin half-graben. Metamorphic mineral assemblages in the pelites regionally range from muscovite-chlorite zone in lower greenschist facies to biotite-garnet-staurolite-chloritoid zone in lower amphibolite facies. Higher grade rocks occur in a northeast-trending belt from the west-central to north-central part of the map area. Deformation and metamorphism are part of the Cordilleran orogeny, a manifestation of the amalgamation of Laurentia with allochthonous terranes.

Southeast Yukon is under-explored although it is geographically situated at the south margin of Selwyn basin and the southeast tail of the Tintina gold belt. Sediment-hosted mineralization may include sedimentary exhalative Zn-Pb±Ba deposits in black shale (SEDEX) and Irish-type or MVT Zn-Pb replacement deposits in carbonate rocks. Intrusion-related mineralization may include massive sulphide mantos, tungsten and base metal skarns, precious metal veins, sheeted veins and replacement deposits.

Carbonaceous sedimentary successions are overmature for source hydrocarbon potential. Conventional oil or gas reservoirs are probably not present. Potential does exist for unconventional tight shale gas resource. Coal resources have been identified in the late Eocene Rock River basin sediments.

# TABLE OF CONTENTS

<b>FOREWORD</b> .....	v
<b>ABSTRACT</b> .....	vi
<b>INTRODUCTION</b> .....	1
<b>LOCATION, PHYSIOGRAPHY AND ACCESS</b> .....	1
<b>GLACIAL HISTORY</b> .....	3
<b>PREVIOUS WORK</b> .....	3
<b>REGIONAL GEOLOGIC SETTING</b> .....	3
<b>STRATIGRAPHY OF COAL RIVER MAP AREA</b> .....	5
<b>SUCCESSION 1 - NEOPROTEROZOIC TO LOWER CAMBRIAN</b> .....	8
<i>Toobally Formation (PT)</i> .....	8
Introduction.....	8
Composition.....	9
Age, Correlation and Depositional Setting.....	9
<i>Hyland Group</i> .....	9
<i>Yusezyu Formation (Hyland Group) (PY)</i> .....	10
Introduction.....	10
Composition.....	10
Age, Correlation and Depositional Setting.....	11
<i>Vampire-Narchilla unit (Hyland Group) (PCVN, PCVN-m, PCVN-l, PCVN-v)</i> .....	12
Introduction.....	12
Composition.....	12
Age, Correlation and Depositional Setting.....	14
<i>Unit Cs (Sekwi-correlative unit)</i> .....	16
Introduction.....	16
Composition.....	16
Age, Correlation and Depositional Setting.....	17
<b>SUCCESSION 2 – UPPER CAMBRIAN TO LOWER ORDOVICIAN</b> .....	18
<i>Otter Creek Formation (COOC) [new]</i> .....	19
Introduction.....	19
Composition.....	19
Age, Correlation and Depositional Setting.....	20
<i>Rabbitkettle Formation (COR-n, COR-lp, COR-v)</i> .....	20
Introduction.....	20
Composition.....	21
Age, Correlation and Depositional Setting.....	22
<i>Crow Formation (EOC, EOC-v)</i> .....	23
Introduction.....	23
Composition.....	23
Age, Correlation and Depositional Setting.....	25
<b>SUCCESSION 3 – LOWER TO MIDDLE ORDOVICIAN</b> .....	25
<i>Sunblood Formation (OSu, OSu-v)</i> .....	25
Introduction.....	25
Composition.....	26
Age, Correlation and Depositional Setting.....	27

<b>SUCCESSION 4 – ORDOVICIAN(?) TO MIDDLE DEVONIAN</b> .....	28
<i>Sandstone of Ordovician and/or Silurian age (OSs)</i> .....	29
Introduction .....	29
Composition .....	29
Age, Correlation and Depositional Setting .....	30
<i>Silurian-Devonian massive carbonate (SDc)</i> .....	31
Introduction .....	31
Composition .....	31
Age, Correlation and Depositional Setting .....	32
<i>Road River Group (SDRR, SMRB)</i> .....	32
Introduction .....	32
Composition .....	33
Age, Correlation and Depositional Setting .....	33
<b>SUCCESSION 5 – MIDDLE DEVONIAN TO TRIASSIC</b> .....	34
<i>Besa River Formation (DMBR, SMRB)</i> .....	34
Introduction .....	34
Composition .....	35
Age, Correlation and Depositional Setting .....	36
<i>Mattson Formation (MM)</i> .....	36
Introduction .....	36
Composition .....	37
Age, Correlation and Depositional Setting .....	37
<i>Fantasque Formation (PF)</i> .....	38
Introduction .....	38
Composition .....	38
Age, Correlation and Depositional Setting .....	39
<i>Undivided Grayling and Toad formations (TGT)</i> .....	39
Introduction .....	39
Composition .....	40
Age, Correlation, and Depositional Setting .....	40
<b>SUCCESSION 6 – PALEOCENE TO LATE EOCENE</b> .....	40
<i>Paleocene unconsolidated sediments (Pssc)</i> .....	41
Introduction .....	41
Composition .....	41
Age, Correlation and Depositional Setting .....	41
<i>Eocene Rock River basin, coal-bearing sediments (ERR)</i> .....	41
Introduction .....	41
Composition .....	41
Age, Correlation and Depositional Setting .....	41
<b>IGNEOUS ROCKS</b> .....	42
<i>Introduction</i> .....	42
<i>Cambrian-Ordovician Alkali Basalt (PCVN-v, EOC-v, COR-v, and OSu-v)</i> .....	42
Introduction .....	42
Undivided Vampire-Narchilla unit volcanic rocks (PCVN-v) .....	42
Crow Formation volcanic rocks (EOC-v).....	45
Rabbitkettle Formation volcanic rocks (COR-v).....	45
Sunblood Formation volcanic rocks (OSu-v) .....	48
Discussion .....	48
<i>Cretaceous Intrusions (mKg)</i> .....	50

<b>STRUCTURE</b> .....	52
<i>Introduction</i> .....	52
<i>Domain A</i> .....	52
<i>Domain B</i> .....	54
<i>Domain C</i> .....	54
<i>Domain D</i> .....	55
<i>Late Extensional Deformation</i> .....	56
<i>Discussion</i> .....	56
<b>METAMORPHISM</b> .....	57
<b>MINERAL OCCURRENCES AND METALLOGENY</b> .....	58
<i>Sedimentary exhalative (SEDEX) mineralization</i> .....	58
<i>Carbonate replacement (MVT, Irish type) mineralization</i> .....	60
<i>Volcanic-related mineralization</i> .....	60
<i>Intrusion-related mineralization</i> .....	60
<i>New exploration targets</i> .....	62
<b>HYDROCARBON POTENTIAL</b> .....	62
<i>Oil and Gas potential</i> .....	62
<i>Coal potential</i> .....	63
<b>SUMMARY</b> .....	63
<b>ACKNOWLEDGEMENTS</b> .....	65
<b>REFERENCES</b> .....	67
<b>APPENDIX A - PALEONTOLOGY</b> .....	81
<b>APPENDIX B - DETRITAL ZIRCON ANALYSES</b> .....	87
<i>Sample 09LP014-1 (PY)</i> .....	90
<i>Sample 09TOA098 (PCVN)</i> .....	99
<i>Sample 09TOA094 (PCVN)</i> .....	108
<i>Sample 09TOA095 (Cs)</i> .....	111
<i>Sample 09TOA096 (Cs)</i> .....	120
<i>Sample 09LP093-1 (OSs)</i> .....	123
<i>Sample 09LP090-2 (MM)</i> .....	132
<b>APPENDIX C - WHOLE ROCK GEOCHEMISTRY</b> .....	141
<i>Vampire-Narchilla unit: volcanic rocks</i> .....	141
<i>Toobally and Crow formations: dikes and volcanic rocks</i> .....	143
<i>Crow Formation: dikes and volcanic rocks</i> .....	145
<i>Crow Formation: volcanic rocks</i> .....	149
<i>Rabbitkettle Formation: volcanic rocks</i> .....	151
<i>Sunblood Formation: volcanic rocks</i> .....	154
<b>APPENDIX D - ROCK-EVAL ANALYSIS</b> .....	155

# PLATES

**Plate 1.** Bedrock geology of Coal River map area (NTS 95D), Yukon (1:250 000 scale). Yukon Geological Survey, Open File 2011-1

## LIST OF FIGURES

<b>Figure 1.</b> Location of Coal River map area in Yukon.....	2
<b>Figure 2.</b> Lower Paleozoic paleogeographic elements of Coal River map area.....	4
<b>Figure 3.</b> Distribution of stratigraphic successions in Coal River map area.....	6
<b>Figure 4.</b> Schematic N-S and E-W correlation charts for stratigraphic successions in Coal River map area.....	7
<b>Figure 5.</b> Pebbly mudstone of the Toobally Fm.....	8
<b>Figure 6.</b> Yusezyu Fm sandstone.....	10
<b>Figure 7.</b> Concordia and relative probability diagrams for geochronology of detrital zircons from Yusezyu Fm.....	11
<b>Figure 8.</b> Olive green, silty phyllite of the undivided Vampire-Narchilla unit.....	13
<b>Figure 9.</b> Banded maroon and green phyllite of the undivided Vampire-Narchilla unit.....	13
<b>Figure 10.</b> Siltstone interbedded with light brown quartz sandstone in the undivided Vampire-Narchilla unit.....	13
<b>Figure 11.</b> Staurolite-garnet-biotite schist of the undivided Vampire-Narchilla unit.....	13
<b>Figure 12.</b> Regional correlation of stratigraphic units in Selwyn basin.....	14
<b>Figure 13.</b> Concordia and relative probability diagrams for geochronology of detrital zircons from undivided Vampire-Narchilla unit (sample 09TOA098).....	15
<b>Figure 14.</b> Concordia and relative probability diagrams for geochronology of detrital zircons from undivided Vampire-Narchilla unit (sample 09TOA094).....	15
<b>Figure 15.</b> Grey, calcareous phyllite at the base of the Sekwi-correlative unit.....	17
<b>Figure 16.</b> Limestone with archeocyathids from middle section of Sekwi-correlative unit.....	17
<b>Figure 17.</b> Concordia and relative probability diagrams for geochronology of detrital zircons from Sekwi correlative unit (sample 09TOA095).....	18
<b>Figure 18.</b> Concordia and relative probability diagrams for geochronology of detrital zircons from Sekwi correlative unit (sample 09TOA096).....	18
<b>Figure 19.</b> Massive limestone of Otter Creek Fm.....	19
<b>Figure 20.</b> Massive limestone with irregular carbonate veinlets, Otter Creek Fm.....	20
<b>Figure 21.</b> Shale in Otter Creek Fm.....	20
<b>Figure 22.</b> Nodular limestone with silt interbeds, Rabbitkettle Fm (east nodular facies).....	21
<b>Figure 23.</b> Massive limestone beds within nodular limestone, Rabbitkettle Fm (east nodular facies).....	21
<b>Figure 24.</b> Thin bedded, phyllitic limestone, Rabbitkettle Fm (west facies).....	22
<b>Figure 25.</b> Silty limestone, Rabbitkettle Fm (west facies).....	22
<b>Figure 26.</b> Autobrecciated volcanoclastic basalt in Rabbitkettle Fm.....	22
<b>Figure 27.</b> Pink, thick-bedded sandstone of the Crow Fm.....	24
<b>Figure 28.</b> Maroon, argillaceous siltstone in Crow Fm.....	24
<b>Figure 29.</b> Quartz pebble clasts within sandstone of the Crow Fm.....	24
<b>Figure 30.</b> Planar-bedded tuff in the Crow Fm.....	25
<b>Figure 31.</b> Well-bedded limestone of the Sunblood Fm.....	26
<b>Figure 32.</b> Pink and tan burrowing texture on bedding plane of Sunblood Fm.....	26
<b>Figure 33.</b> Thick-bedded dolostone of Sunblood Fm.....	27

<b>Figure 34.</b> Altered basalt breccia within the Sunblood Fm.....	27
<b>Figure 35.</b> Dolomitic sandstone interbedded with silty shale, unit OSS. ....	29
<b>Figure 36.</b> Aerial view of sandstone in unit OSS. ....	29
<b>Figure 37.</b> Concordia and relative probability diagrams for geochronology of detrital zircons from unit OSS (station 09LP093).....	30
<b>Figure 38.</b> Thick-bedded limestone of unit SDC.....	31
<b>Figure 39.</b> Brecciated limestone of unit SDC.....	31
<b>Figure 40.</b> Graptolitic, silty shale of the Road River Group.....	33
<b>Figure 41.</b> Dark grey, silty limestone of the Road River Group.....	33
<b>Figure 42.</b> Grey dolostone with discontinuous black chert lenses, Road River Group.....	33
<b>Figure 43.</b> Limestone with 2-hole crinoids indicative of middle Devonian in Road River Group.....	34
<b>Figure 44.</b> Noncalcareous, brown-weathering, silty shale of Besa River Fm.....	35
<b>Figure 45.</b> Black, silty shale of the undivided Road River-Besa River map unit.....	35
<b>Figure 46.</b> Limestone nodules in silty shale of the undivided Road River-Besa River map unit. ....	35
<b>Figure 47.</b> Sandstone interbedded with recessive shale of the Mattson Fm.....	37
<b>Figure 48.</b> Thick-bedded sandstone of Mattson Fm.....	37
<b>Figure 49.</b> Concordia and relative probability diagrams for geochronology of detrital zircons from Mattson Fm (station 09LP090).....	38
<b>Figure 50.</b> Siliceous shale of the Fantasque Fm.....	39
<b>Figure 51.</b> Limestone nodule in siliceous shale of Fantasque Fm.....	39
<b>Figure 52.</b> Dark grey, recessive shale of the undivided Grayling-Toad fm.....	40
<b>Figure 53.</b> Sample location map of volcanic rock samples with whole rock geochemistry.....	43
<b>Figure 54.</b> Geochemical and tectonic discriminant diagrams for volcanic rocks of undivided Vampire-Narchilla unit.....	44
<b>Figure 55.</b> Geochemical and tectonic discriminant diagrams for volcanic rocks and intrusions of Crow Fm.....	46
<b>Figure 56.</b> Geochemical and tectonic discriminant diagrams for volcanic rocks of Rabbitkettle Fm.....	47
<b>Figure 57.</b> Geochemical and tectonic discriminant diagrams for volcanic rocks of Sunblood Fm.....	49
<b>Figure 58.</b> First vertical derivative of regional aeromagnetic survey with granitic intrusions indicated.....	51
<b>Figure 59.</b> Structural domains in Coal River map area.....	53
<b>Figure 60.</b> Stereonet of structural elements in domain A, Coal River map area.....	53
<b>Figure 61.</b> Stereonet of structural elements in domain B, Coal River map area.....	54
<b>Figure 62.</b> Stereonet of structural elements in domain C, Coal River map area.....	55
<b>Figure 63.</b> Stereonet of structural elements in domain D, Coal River map area.....	56
<b>Figure 64.</b> Mineral occurrences in Coal River map area.....	59
<b>Figure 65.</b> Summary of stratigraphic history and tectonic evolution in Coal River map area.....	64

## LIST OF TABLES

<b>Table 1.</b> Table of formations and successions.....	7
<b>Table 2.</b> List of plutons and isotopic ages.....	51
<b>Table 3.</b> Metamorphic mineral assemblages, undivided Vampire-Narchilla unit.....	57

## LIST OF TABLES - APPENDICES

<b>Table A1.</b> Fossil collections, arranged by formation.....	81
<b>Table B1.</b> Detrital zircon sample locations.....	87
<b>Table B2a.</b> Geochronological data for detrital zircon grains for sample 09LP014 (PY) .....	90
<b>Table B2b.</b> Trace element data for detrital zircon grains for sample 09LP014 (PY) .....	93
<b>Table B2c.</b> Calculated ratios and values for detrital zircon grains for sample 09LP014 (PY) .....	96
<b>Table B3a.</b> Geochronological data for detrital zircon grains for sample 09TOA098 (PCVN) .....	99
<b>Table B3b.</b> Trace element data for detrital zircon grains for sample 09TOA098 (PCVN).....	102
<b>Table B3c.</b> Calculated ratios and values for detrital zircon grains for sample 09TOA098 (PCVN) .....	105
<b>Table B4.</b> Geochronological data for detrital zircon grains for sample 09TOA094 (PCVN) .....	108
<b>Table B5a.</b> Geochronological data for detrital zircon grains for sample 09TOA095 (CS).....	111
<b>Table B5b.</b> Trace element data for detrital zircon grains for sample 09TOA095 (CS) .....	114
<b>Table B5c.</b> Calculated ratios and values for detrital zircon grains for sample 09TOA095 (CS).....	117
<b>Table B6.</b> Geochronological data for detrital zircon grains for sample 09TOA096 (CS).....	120
<b>Table B7a.</b> Geochronological data for detrital zircon grains for sample 09LP093 (OSs) .....	123
<b>Table B7b.</b> Trace element data for detrital zircon grains for sample 09LP093 (OSs).....	126
<b>Table B7c.</b> Calculated ratios and values for detrital zircon grains for sample 09LP093 (OSs) .....	129
<b>Table B8a.</b> Geochronological data for detrital zircon grains for sample 09LP090 (MM).....	132
<b>Table B8b.</b> Trace element data for detrital zircon grains for sample 09LP090 (MM).....	135
<b>Table B8c.</b> Calculated ratios and values for detrital zircon grains for sample 09LP090 (MM).....	138
<b>Table C1.</b> Lithogeochemistry for volcanic rocks in undivided Vampire-Narchilla unit .....	141
<b>Table C2a.</b> Lithogeochemistry for dikes and volcanic rocks in Toobally and Crow fms (2003) .....	143
<b>Table C2b.</b> Lithogeochemistry for dikes and volcanic rocks in Crow Fm (2004-2005).....	145
<b>Table C2c.</b> Lithogeochemistry for volcanic rocks in Crow Fm (2009-2010).....	149
<b>Table C3.</b> Lithogeochemistry for volcanic rocks in Rabbitkettle Fm.....	151
<b>Table C4.</b> Lithogeochemistry for volcanic rocks in Sunblood Fm .....	154
<b>Table D1.</b> Rock-Eval-6 analyses for samples (2009-2010).....	155

## INTRODUCTION

Recent fieldwork by the Yukon Geological Survey and the Geological Survey of Canada (Pigage, 2006; Pigage and MacNaughton, 2004; Pigage, 2009) in southeast Yukon resulted in major revisions to the previously reported stratigraphy and igneous history. Southeast Yukon includes rocks which regionally host SEDEX, MVT/Irish-type and intrusion-related mineralization. The mineral potential of southeast Yukon is under-evaluated both scientifically and economically relative to the central part of the territory; additional discoveries are possible with an updated geological information base.

To this end the Yukon Geological Survey and Geological Survey of Canada completed a helicopter-assisted bedrock mapping program in the Coal River (NTS 95D<sup>1</sup>) map area between late June and early August 2009 using federal funds provided by the 'Geo-Mapping for Energy and Minerals' program administered by Natural Resources Canada. A Bell206B helicopter provided daily set-outs of traverse pairs and enabled spot-checking of isolated rock exposures. An inflatable boat with jet outboard motor provided access to outcrops along the Coal River. The 10-person crew was based for 2 weeks at a mineral exploration camp on the south shore of Quartz (Hulse) Lake, and then at a private facility on the east side of the northernmost (upper) of the Toobally Lakes.

In 2010 the Yukon Geological Survey funded five days of helicopter-assisted field checks to resolve geological inconsistencies arising from the 2009 fieldwork. The 2009-2010 project produced a preliminary bedrock map (Plate 1) and surficial geology report (Kennedy, 2010) as well as a regional aeromagnetic map of the Yukon portion of the adjacent map area immediately to the north (Flat River, NTS 95E; Kiss, 2010a,b,c,d).

This report complements the 1:250 000-scale bedrock geological map (Plate 1) for the Coal River map area by providing descriptions of the rock units, structures, mineral occurrences and discussion of their geologic context; it should be read in conjunction with the bedrock geological map, Yukon Geological Survey Open File 2011-1 (included as Plate 1).

## LOCATION, PHYSIOGRAPHY AND ACCESS

The area of study is approximately 100 km east of Watson Lake, Yukon with bounding geographic coordinates of 60° and 61°N latitude and 126° and 128°W longitude (Fig. 1). It occurs largely within southeast Yukon with the northeast corner being in the Northwest Territories. Most of the map area is within the Hyland Highland physiographic region with the northwest corner being within the Logan Mountains (Mathews, 1986). Most of the 12 100 km<sup>2</sup> area consists of rounded, forest-covered hills with incised stream drainages. The map area is characterized by three broad, north-trending valleys extending the entire length of the area. The Coal (west valley) and Rock (central valley) rivers flow south into the Liard River. The east valley contains the Smith River (south flowing), Beaver River (southeast flowing) and Caribou River (northeast flowing). All rivers ultimately flow into the Mackenzie River and Arctic Ocean. Elevations range from 550 m (1800 ft) to 1980 m (6500 ft). Bedrock exposures constitute about 3% of the area and are restricted largely to ridge tops above timberline, rivers and glacial meltwater channels.

The Alaska Highway traverses the southwest corner of Coal River map area. Abandoned logging roads locally radiate northward from the highway. A few unpaved tracks and winter haulage trails (referred to as the Sulpetro and Smith River trails) cross the southern and central parts of the map area. Extensive forest cover limits places where helicopters can land. The upper Coal, West Coal and Rock rivers are

---

1 National Topographic System: <https://www.nrcan.gc.ca/earth-sciences/geography/topographic-information/maps/9763>

amenable to shallow-draft boats, as is the stream connecting the Toobally Lakes. The Smith River is boulder-strewn and rapid-filled, and class 3 and 4 rapids in downstream canyons on the Coal River prevent boat access from the Alaska Highway. A 500 m long gravel airstrip located near the head of Otter Creek was utilized for mineral exploration (Mel, Jeri, Jeri North, Joni). Float-equipped planes have used Hulse (Quartz), Roy, Gusty and the Toobally lakes to supply camps.

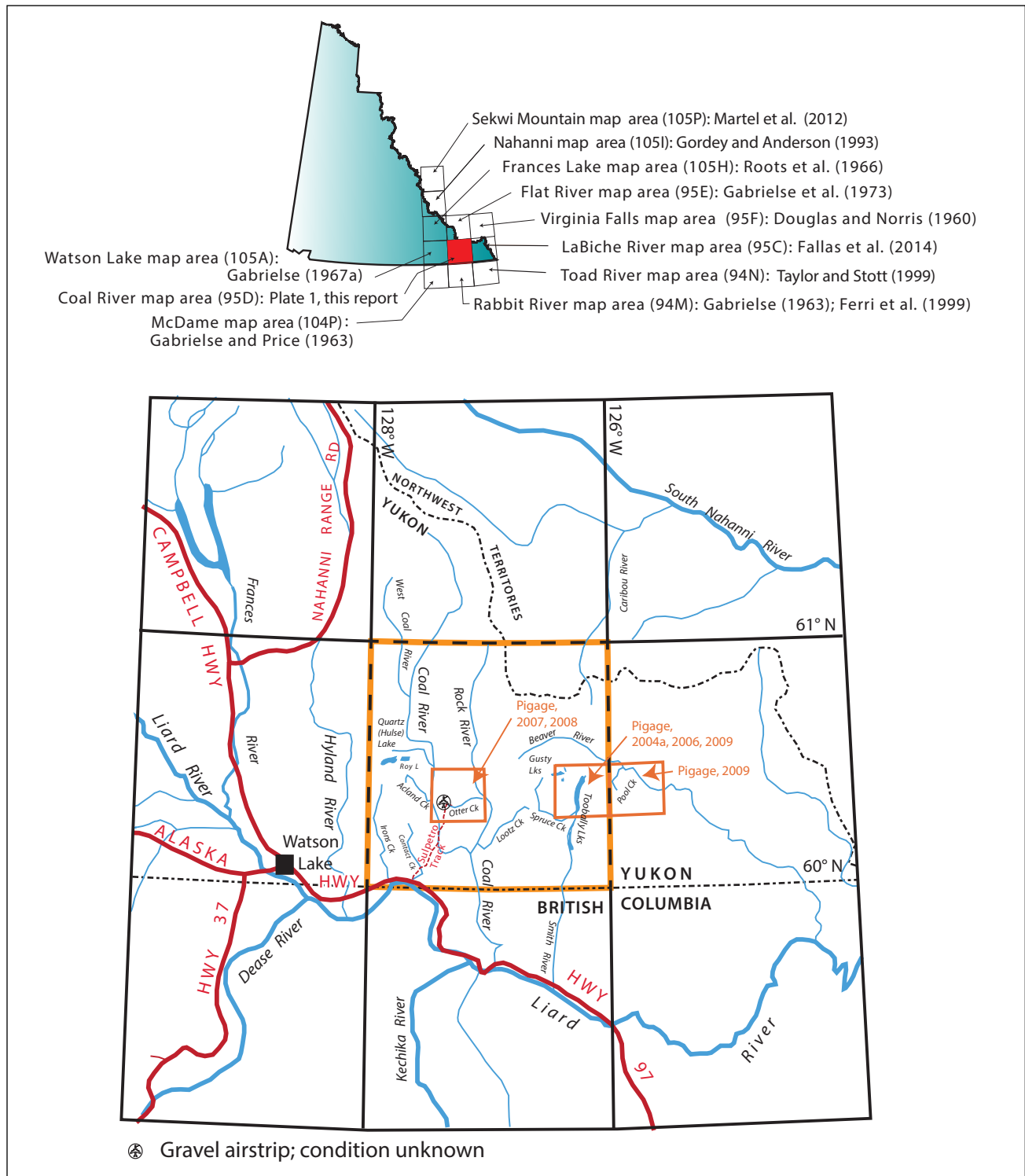


**Figure 1.** Map areas (with reference to geological reports), roads and water courses surrounding Coal River map area.

## GLACIAL HISTORY

Central and southern Yukon has a complex Pleistocene glacial history. Bostock (1966) and Duk-Rodkin *et al.* (2004) documented multiple advances of the Cordilleran ice sheet. Immediately to the west (in the Watson Lake area) Klassen (1987) described a lengthy glacial history with four till units interbedded with four non-glacial units. The uppermost till unit records late Wisconsinan glacial ice that flowed northeastward from the Cordilleran Ice Sheet. He also completed a surficial geology reconnaissance of the west half of the Coal River map area, documenting extensive glaciofluvial and glaciolacustrine sediments (Klassen, 1983). Surficial mapping, to the east of the Coal River project area, by Smith (2000) demonstrated that the continental Laurentide Ice Sheet advanced west and coalesced with the Cordilleran Ice Sheet just east of the Coal River map area along the western margin of the LaBiche River map area during the Wisconsinan glacial maximum. Coalescence resulted in thickening of the ice sheets that likely covered all but the highest peaks in the region (Kennedy, 2010).

Kennedy (2010) indicated that most of the glacial geomorphic features in the Coal River map area are probably related to the most recent Wisconsinan McConnell advance of the Cordilleran Ice Sheet. McConnell Glaciation attained its maximum extent around 23 000 <sup>14</sup>C years BP (Duk-Rodkin *et al.*, 1996) with much of it disappearing by approximately 13 000 <sup>14</sup>C years BP (Jackson *et al.*, 1991). Deglaciation in the Coal River area resulted in the deposition of extensive glaciolacustrine and glaciofluvial deposits associated with glacial lakes formed by the Cordilleran and Laurentide ice masses blocking south and east-flowing drainages. Deep, east-trending meltwater channels became incised and resulted in the formation of large deltas as the meltwater channels debouched into the major south-trending drainages and glacial lakes. The northwest and north-central parts of the map area possibly remained unglaciated during the Cordilleran glacial advances (Klassen, 1987; Kennedy, 2010).

## PREVIOUS WORK

Reconnaissance geological mapping by the Geological Survey of Canada (GSC), mostly during 1967, resulted in an outcrop style geology map at 1:253,440 scale and an accompanying report (Gabrielse and Blusson, 1968, 1969). Abbott (1981) conducted a regional mapping program in 1978-1979 which was largely north of the Coal River area, overlapping into the northwestern part of NTS 95D. Subsequent government-sponsored research was limited to visits to mineral exploration camps, until two regional total-field aeromagnetic surveys using a line spacing of 800 m (Natural Resources Canada, 2009) were completed in 1995 and 1996. Yukon Geological Survey conducted detailed (1:50 000 scale) bedrock geology mapping near Toobally Lakes (NTS 95D/8) and surrounding the Mel Pb-Zn occurrence (NTS 95D/6) between 2003 and 2008 (Pigage, 2004a, 2006, 2007, 2008; Pigage and MacNaughton, 2004), culminating in a final report (Pigage, 2009).

Mineral exploration occurred intermittently from the 1960s into the 2000s, but the poor exposure, difficult access and moderately promising results discouraged more extensive activity. As a result regional exploration has been limited, and detailed exploration has focused on the few known targets, namely the McMillan Pb-Zn-Ag replacement deposit (Yukon MINFILE 095D006), the Hyland Gold intrusion-related Au replacement deposit (Yukon MINFILE 095D011) and the Mel Pb-Zn-Ba MVT/Irish-type replacement deposit (Yukon MINFILE 095D005 and associated occurrences - Yukon MINFILE 095D027, 032, 035). Grassroots regional exploration targets include tungsten skarn, intrusion-related gold, and sediment-hosted zinc, lead and barite.

## REGIONAL GEOLOGIC SETTING

The Coal River map area is located along the northwest (present orientation) passive continental margin of Laurentia which formed after the breakup of the Proterozoic supercontinent Rodinia (Colpron *et al.*, 2002). An aggregate total of >14 000 m of miogeoclinal sedimentary and minor volcanic rocks

of Neoproterozoic through Triassic age are present in various parts of the map area. Most of the formations or their time-equivalent correlatives extend along the ancient margin, from east-central Alaska along the Mackenzie and Rocky mountains through the United States into Mexico. They were uplifted and exposed as a result of eastward contraction during the Cordilleran orogeny (Middle Jurassic to Paleocene fold-and-thrust belt; e.g., Gabrielse *et al.*, 1991).

The main Neoproterozoic to Middle Devonian geographic elements (Fig. 2) are shallow water carbonate and clastic strata transitioning westerly to southwesterly to deeper water strata, constituting Selwyn basin (Gabrielse, 1967b; re-defined by Cecile, 1982, and Gordey and Anderson, 1993). Selwyn basin is a 900 km long, up to 350 km wide, northwest-trending area of the central and eastern Yukon underlain by Late Proterozoic to Middle Devonian dark clastic strata. It is flanked to the north and east by the time-equivalent, carbonate-dominant Mackenzie platform (Lenz, 1972; *a.k.a.*, Blackwater platform of Cecile *et al.*, 1997; Mackenzie-Peel shelf of Morrow, 1999). A southern extension of relatively deep-water strata about 50 km wide continues 600 km farther south and is known as Kechika trough (Douglas *et al.*, 1970); it is flanked to the east by Macdonald platform. The southwest margin of both Selwyn basin and Kechika trough is the Tintina fault, and the fault-offset equivalent strata are present in central Alaska (McGrath quadrangle). Coal River is located at the northern margin of Macdonald platform and the southern edge of Selwyn basin.

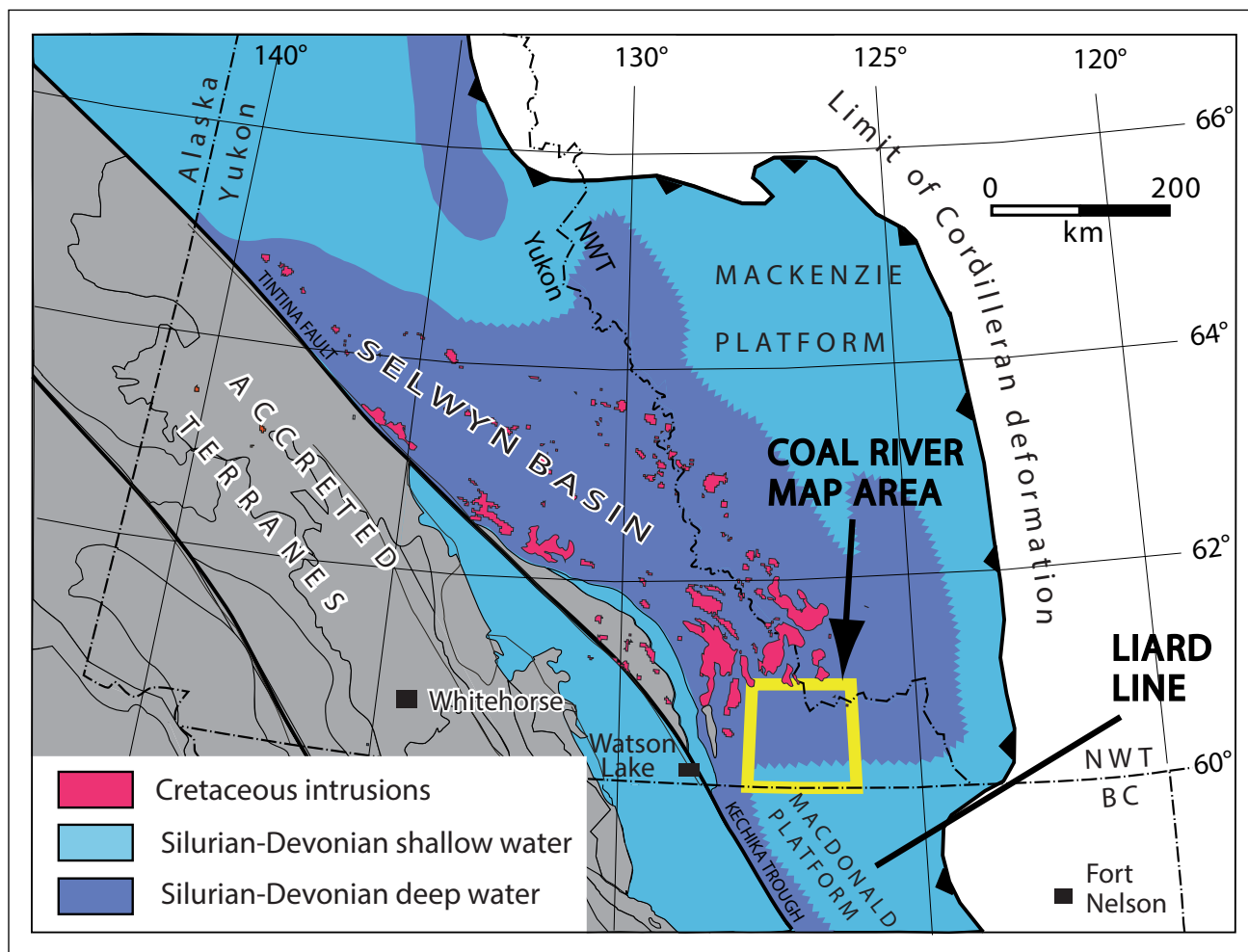


**Figure 2.** Paleozoic (Silurian-Devonian) tectonic elements of eastern Yukon and northern BC. Accreted terranes are undifferentiated (grey) and movement of Tintina fault is not restored. Terranes adapted from Wheeler and McFeely (1991). Cretaceous intrusions from Gordey and Makepeace (2003).

Middle Devonian to Mississippian transgressive, carbonaceous shale and chert overlying the Mackenzie and Macdonald platform shelf carbonate rocks denote a major change in depositional environment and tectonics (Abbott *et al.*, 1986) and represent the cessation of the Selwyn basin-Mackenzie and Macdonald platform paleogeography. Extensional rifting during this time is indicated by locally sourced conglomerate and the presence of depositional growth faults within the former Selwyn basin (Abbott *et al.*, 1986; Gordey *et al.*, 1982). Late Mississippian deposition in the Coal River area is dominated by silts and sands of a large, prograding marine and fluvial delta complex.

Deposition in Pennsylvanian through Triassic time delineates multiple transgressive-regressive cycles of fine-grained clastic rocks and chert of relatively shallow water, marine origin separated by unconformities (Abbott *et al.*, 1986).

Jurassic-Paleocene deformation is manifested primarily by widely spaced, high-angle reverse faults and asymmetric folds. Intensity of deformation and depth of burial exposed at surface increase from east to west, with penetrative fabrics being well developed only in the west. Metamorphism associated with deformation ranges from lowermost greenschist facies (muscovite-chlorite zone) in the east to upper greenschist facies (biotite-garnet zone) and locally lower amphibolite facies (staurolite zone) in the west.

Numerous small, undeformed, approximately circular Cretaceous intrusions are scattered across the northern half of the map area (Plate 1). These intrusions represent the southeast extent of the Tay River plutonic suite (Mortensen *et al.*, 2000; Plate 1; Fig. 2). Post-orogenic (Upper Eocene) fine-grained, fluvial and lacustrine, coal-bearing deposits occupy a north-trending half graben in the centre of the map area (Rock River basin; Long and Sweet, 1994).

The Coal River map area lies north of the Liard Line (Fig. 2), a northeast-trending zone defined primarily by the absence of Ordovician to Lower Devonian strata southward (Cecile *et al.*, 1997). The Liard Line is interpreted as an ancestral transfer fault zone across which there is an interpreted reversal in the asymmetry direction of the original rift zone along the western edge of Laurentia (Cecile *et al.*, 1997). North of the Liard Line, Selwyn basin exposures are interpreted as being in the footwall of the continental marginal rift, and the Macdonald platform exposures to the south are thought to be in the hanging wall of the continental marginal rift. There is no surface expression of the Liard Line, and its location is poorly constrained.

## **STRATIGRAPHY OF COAL RIVER MAP AREA**

This report divides the miogeoclinal strata into six formation-delineated 'successions' of strata ranging in age from Neoproterozoic through late Eocene (Fig. 3). Each succession consists of one or more formations with related lithologic facies and depositional environments (Table 1). Tectono-stratigraphic relationships markedly differ between successions (*cf.*, Morrow and Geldsetzer, 1991). Internally the successions may locally contain unconformities. North and east-striking schematic correlation charts (Fig. 4) illustrate the regional distribution and stratigraphic relationships of the formations and sedimentary successions.

Succession 1 consists of Neoproterozoic-lower Cambrian siliciclastic sedimentary rocks (Yusezyu, Narchilla and Vampire formations, and an interval of silty phyllite and limestone interbeds considered equivalent to the Sekwi Formation) that are exposed throughout the western half of the map area. Mafic volcanic rocks occur locally near the top of this succession. A small isolated occurrence of Neoproterozoic(?) conglomerate (Toobally Formation) occurs in the immediate hanging wall of the Toobally fault in the east-central part of the map area.

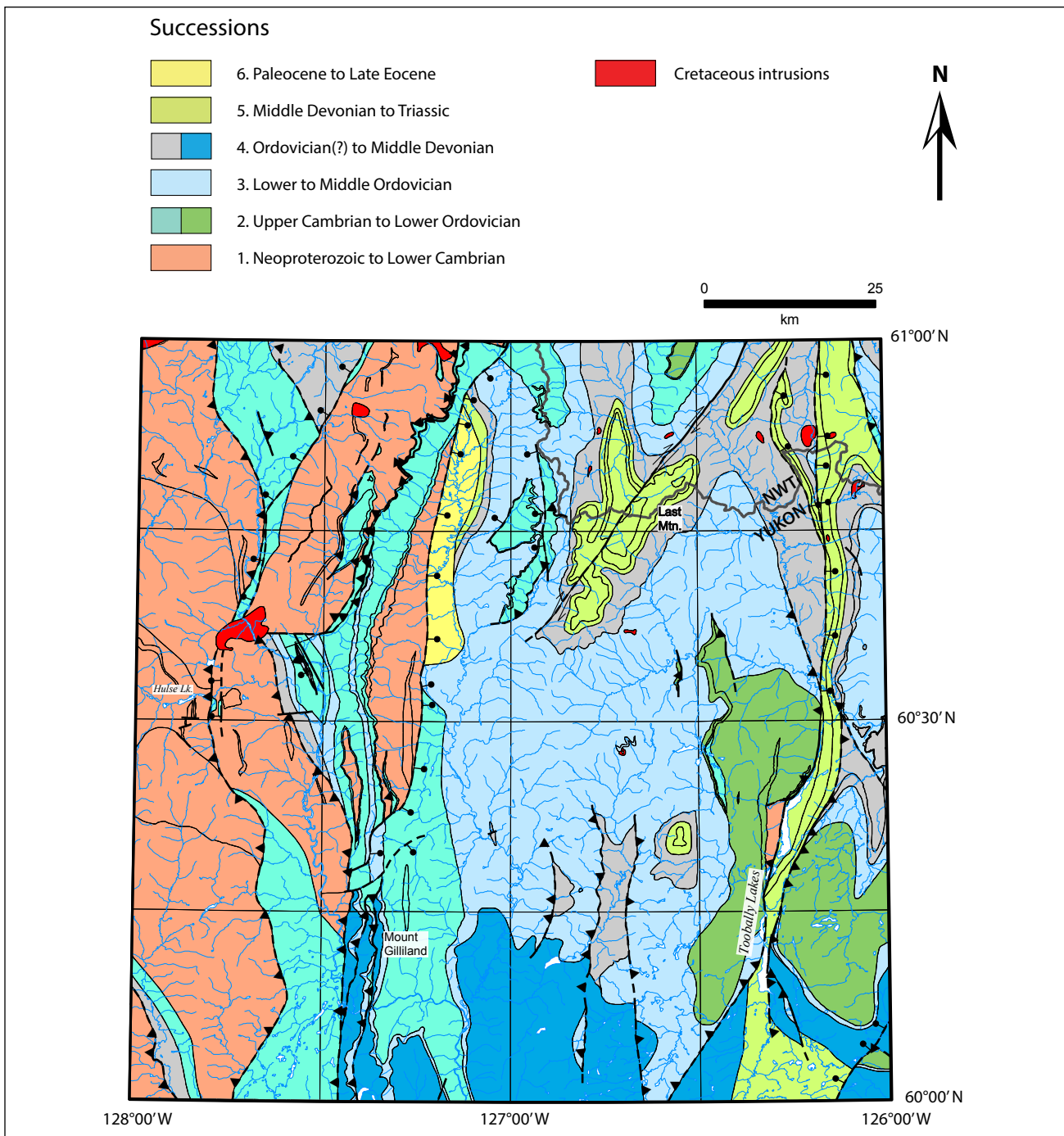


**Figure 3.** Coal River map area, showing the six stratigraphic successions and Cretaceous intrusions, based upon 2009-2010 fieldwork and previous mapping by Gabrielse and Blusson (1969). The map area at 1:250 000 scale is shown in Plate 1.

Succession 2 is upper Cambrian through Lower Ordovician in age; it exhibits a dramatic facies change from limestone and silty limestone in the west (Otter Creek and Rabbitkettle formations) to shallow water and subaerial strata dominated by subarkosic sandstone and maroon siltstone in the east (Crow Formation). Both facies contain intervals of mafic volcanic rocks.

Succession 3 is presently exposed throughout the eastern two-thirds of the map area and consists of Lower to Middle Ordovician shallow, platformal carbonate (Sunblood Formation). This succession is absent in the southwest and northwest corners of the Coal River map area.

**Table 1.** Formations in Coal River map area.

Succession	Map Unit	Main Lithology	Thickness (m)
6	Rock River (ERRs)	mudstone	>445 - 1100 ?
6	Paleocene clastic (Pssc)	siltstone, sandstone and conglomerate	160
5	Toad and Grayling (TGT)	shale	>240
5	Fantasque (PF)	shale	1000 - 1700
5	Mattson (MM)	sandstone	500 - 1450
5	Besa River (DMBR)	shale	300
4	Siluro-Devonian carbonate (SDc)	dolostone	100 - 1000
4	Road River (SDRR, SMRR)	shale, siltstone	2000
4	Ordovician-Silurian sandstone (OSs)	sandstone to pebbly sandstone	220
3	Sunblood (OSu)	dolostone or limestone	0 - 2700
2	Rabbitkettle (COR-n, COR-lp, COR-v)	limestone, calc-phyllite	300 - 1500
2	Otter Creek (COOC)	limestone	65 - 500
2	Crow (COC, COC-v)	sandstone	? - >5000
1	Sekwi-correlative (CS)	phyllite to siltstone, sandstone	400
1	Vampire and Narchilla (PCVN, PCVN-m, PCVN-l, PCVN-v)	phyllite to pelite	0 - 2500
1	Yusezyu (PY)	sandstone, pebbly sandstone	3500 ?
1	Toobally (PT)	pebbly mudstone	>1800

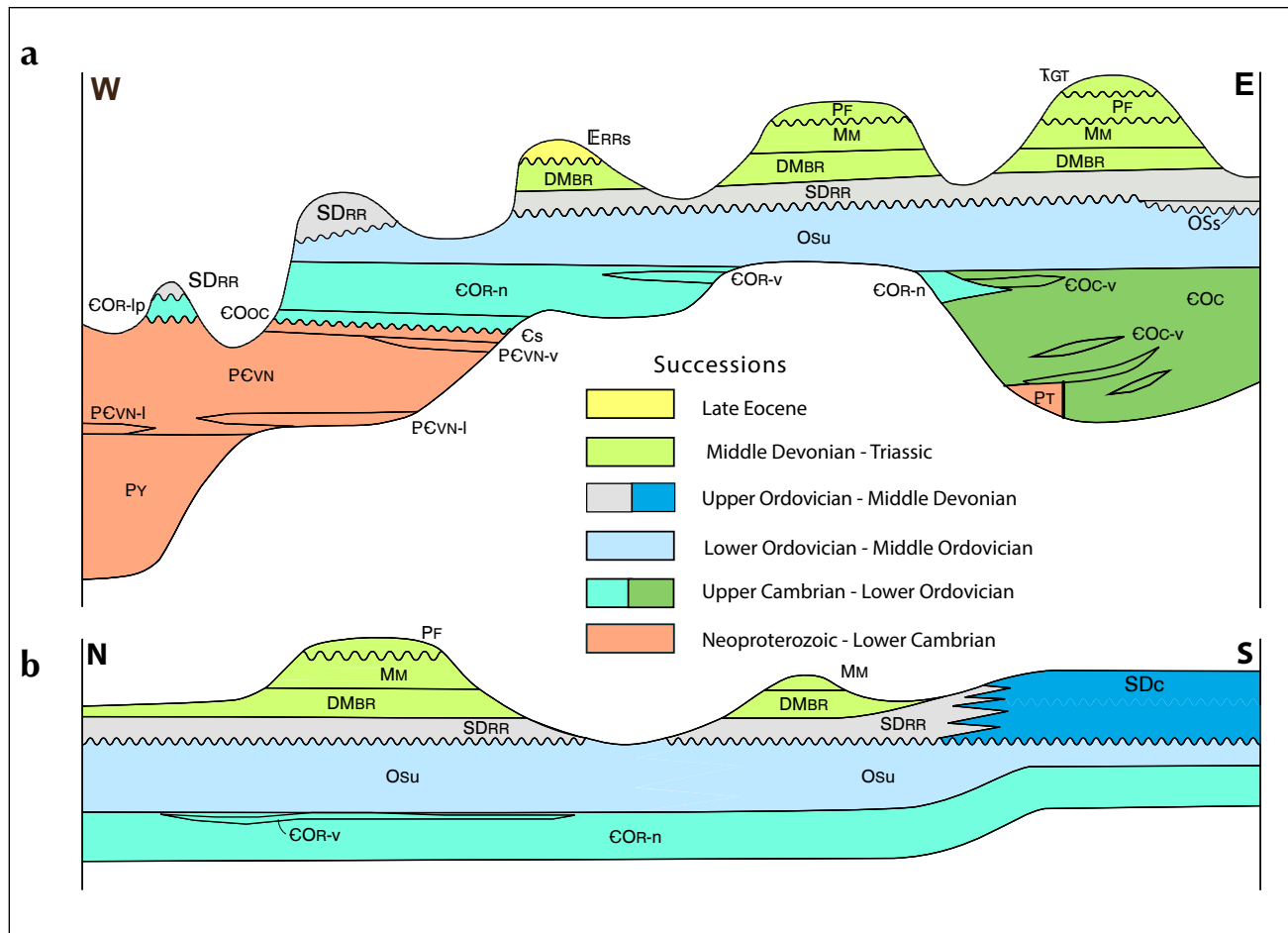


**Figure 4.** Schematic correlation diagrams of stratigraphic successions, from (a) west to east and (b) north to south across the Coal River map area.

Succession 4 includes the lateral transition from lower Silurian to Middle Devonian carbonate platformal sedimentary rocks of Macdonald platform (single map unit combining the Nonda, Muncho-McConnell, Stone and Dunedin formations) in the southern third of the map area, to fine clastic, basinal sedimentary rocks of Selwyn basin (Road River Group, undivided) northward. A basal coarse-grained, siliciclastic unit (Oss) occurs only in the eastern part of the map area.

Succession 5 comprises Middle Devonian through Triassic shallow marine shale, siltstone and sandstone (Besa River, Mattson, Fantasque and undivided Grayling-Toad formations) that represent multiple regional transgressive-regressive cycles separated by unconformities.

Succession 6 consists of the late Eocene fluvial strata and coal in the intermontane Rock River basin occurring in the north-central part of the map area and a single occurrence of Paleocene basalt and fluvial sediments on the far eastern edge of the map area.

The descriptions of these lithologic units augment those previously published for southeast Yukon (Pigage, 2006, 2009). Regional correlations include more recent information from adjacent regions (specifically northeastern British Columbia). Geographic place names used in the following descriptions are indicated on Plate 1 and Figure 1.

## **SUCCESSION 1 - NEOPROTEROZOIC TO LOWER CAMBRIAN**

Predominantly siliciclastic sediments and minor carbonate and volcanic rocks are exposed extensively in the western third of the Coal River map area. A smaller exposure lies west of the upper Toobally Lake in the east-central part of the area. The western region includes Yusezyu and Narchilla formations of the Hyland Group, Vampire Formation, and silty phyllite, sandstone, and limestone considered equivalent to Sekwi Formation. The areally limited exposures in the east comprise the Toobally Formation. Proterozoic sandstone (unit **Ps** of Pigage, 2009) and argillite (unit **Pa** of Pigage, 2009) are exposed immediately east of Coal River map area, and possibly underlie the Toobally Lakes region.

### ***Toobally Formation* (PT)**

#### **Introduction**

The Toobally Formation (Pigage and MacNaughton, 2004) occurs in scattered exposures immediately west of upper Toobally Lake. It consists of a monotonous succession of orange-weathering, polymictic, matrix-supported conglomerate to pebbly mudstone (Fig. 5) with a minimum thickness of 1800 m (assuming a regional 45° dip). The lower contact is structural as the unit occurs in the immediate hanging wall of the east-verging Toobally reverse fault. The upper contact with the overlying Crow Formation is unconformable.



**Figure 5.** *Pebbly mudstone of the Toobally Formation, with slaty cleavage, dipping to the left (west). Hammer handle is 33 cm long. West of upper Toobally Lake, station 03LP006.*

## Composition

Bedding generally cannot be seen at outcrop scale. In rare cases, normally graded to indistinctly gradational beds can be recognized within the unit. It contains a moderately developed, pervasive slaty cleavage which gradually becomes more intense toward the Toobally fault to the east.

The matrix for the conglomerate to mudstone consists of dark brown to dark grey, brown, buff, or orange-weathering silty shale to siltstone and accounts for 50 to 80% of the total rock volume. Clasts are most commonly within the granule to pebble size range; cobbles are rarely present. They are angular to subrounded, without preferred orientation. Numerous clast compositions were observed, including quartzitic meta-sandstone, calcareous sandstone, lithic sandstone, mudstone, massive lime mudstone and dolo-mudstone, laminated lime mudstone, massive grainstone and rare fragments of vesicular to amygdaloidal basalt. At one locality the formation contains a large olistolith of orange-weathering, unfossiliferous, microcrystalline to very finely crystalline, thinly bedded dolostone at least 20 m thick. The upper contact of the dolostone has not been observed; the lower contact is sharp and stained red (see Pigage, 2009, p. 22, for more description).

The Toobally Formation is cut by dark green, orange-weathering, fine-grained, diabase to gabbro dikes and sills from less than 10 cm to greater than 10 m thick (too small to show on the map). In many outcrops the dikes and sills are extensively altered to a pale grey, orange-weathering, pyritic carbonate-sericite assemblage. The geochemistry of the dikes and sills is similar to that for the Crow Formation volcanic rocks, and they are considered to be feeders for the overlying Crow Formation volcanic rocks (Pigage, 2009); the analyses are listed in Appendix C but are not included in the discriminant diagrams.

## Age, Correlation and Depositional Setting

Fieldwork in 2003 (Pigage and MacNaughton, 2004) found no definitive evidence for glacial deposition (*i.e.*, dropstone and lonestone in associated sediment, till pellets, striated clasts). This polymictic lithotype can be deposited under glacial or non-glacial conditions (Eyles, 1990). Pigage and MacNaughton (2004) interpreted the Toobally Formation as being deposited from relatively viscous, sediment-gravity flows in a marine slope to toe-of-slope setting.

Pigage (2009) discussed possible depositional ages for this stratigraphic unit. One detrital zircon sample contained a youngest detrital zircon age of about 650 Ma (2 grains; see Pigage, 2009). The preferred depositional age is late Neoproterozoic (post-650 Ma). Rare basaltic clasts indicate an earlier period of volcanism in the paleo-drainage (Pigage, 2009).

In spite of the lack of direct evidence for the Toobally Formation being a glacial deposit, Pigage and MacNaughton (2004) noted that the unit resembles Neoproterozoic Sturtian and Marinoan glacial diamictites previously documented in northwestern Canada: the Shezal Formation (Eisbacher, 1978, 1981) and the Ice Brook Formation (Aitken, 1991). A recent U-Pb single grain dating (CA-ID-TIMS) on a volcanic tuff within the Sayeuni Formation stratified diamictites resulted in a date of  $716.5 \pm 0.2$  Ma for the earlier Sturtian glaciation (Macdonald *et al.*, 2010). A Re-Os date of  $662.4 \pm 3.9$  Ma for the Twitya Formation (Rooney *et al.*, 2014) places a maximum age constraint on the Ice Brook Formation (Marinoan glaciation). Detrital zircon results for the Toobally Formation (see above) are consistent with correlation of the Toobally Formation with the Ice Brook Formation of the Windermere Supergroup.

## Hyland Group

The Hyland Group (Gordey and Anderson, 1993) is the oldest widely exposed unit of Selwyn basin. It outcrops nearly continuously from the Alaska-Yukon border north of the Yukon River, southeast to

the Northwest Territories-Yukon border, and extends 130 km into northern British Columbia and the headwaters of the Tuchodi River (59°N; Wheeler and McFeely, 1991). Where defined in the southern Little Nahanni River map area (140 km northwest along structural grain from the northwest corner of Coal River map area; Fig. 1) it consists of pebbly sandstone with interbedded shale of the Yusezyu Formation, overlain by greyish green and maroon shale of the Narchilla Formation. The uppermost part of the Yusezyu Formation contains numerous discontinuous orange-weathering, dark, shaly to silty limestone lenses that Gordey and Anderson (1993) informally called the limestone member. This middle carbonate is increasingly prominent northward, and Cecile (2000) formally established the Algae Formation in Nidderly Lake map area (400 km north of Coal River). Regionally the Yusezyu Formation is Neoproterozoic (Ediacaran), and the Narchilla Formation is Neoproterozoic (Ediacaran) to possibly lower Cambrian (Fortunian; uppermost stage 2?).

The Hyland Group strata are the oldest strata in the western third of the Coal River map area. Only the Narchilla and Yusezyu formations are recognized; a mappable Algae Formation is not present and mappable calcareous strata occur entirely within the Narchilla Formation.

### ***Yusezyu Formation (Hyland Group) (PY)***

#### **Introduction**

The Yusezyu Formation (Gordey and Anderson, 1993) is exposed in two northwest-trending belts in the westernmost Acland thrust fault panel of the Coal River map area (Plate 1). The base of the formation was not observed; the upper contact with the overlying Narchilla Formation is gradational, although locally faulted (Plate 1). The contact with the overlying Narchilla Formation was placed at the gradational transition demarcated by an up-section decrease in the amount of pebbly sandstone and quartz sandstone and a corresponding increase in green and/or maroon, noncalcareous, silty phyllite; this transition occurs over an interval of tens of metres to hundreds of metres.

At the type section (in the Little Nahanni River map area), the Yusezyu Formation is at least 3000 m thick (Gordey and Anderson, 1993). In the Coal River map area only the upper part of the formation is exposed, and a lack of marker horizons make structural repetition difficult to recognize. An inferred thickness of approximately 3500 m is used in the cross section interpretation (Plate 1).

#### **Composition**

In Coal River the Yusezyu Formation consists predominantly of noncalcareous, grey to cream sandstone to pebbly sandstone (Fig. 6) interbedded with brown-weathering, non-calcareous, medium to pale green phyllite and rare fine-grained, grey limestone. In the pebbly sandstones the predominant coarse clasts are clear to bluish quartz with lesser subangular, white feldspar. Bedding is on a scale of centimetres to metres; exposures typically have gentle dips. In contrast to the type area of the Yusezyu Formation (Gordey and Anderson, 1993) no limestone is present at the top of the Yusezyu Formation in the Coal River map area.



**Figure 6.** Yusezyu Formation sandstone, showing the bedding contact between coarse and fine-grained beds. White granules are quartz in a noncalcareous, coarse-sand matrix. Black bars on scale at right are in cm. From 20 km north of Hulse (Quartz) Lake, station 09RAS058.

## Age, Correlation and Depositional Setting

In the Coal River map area the Yusezyu Formation is unfossiliferous. Regionally the upper part of the formation is of latest Precambrian age (Ediacaran) based on primitive trace fossils reported by Fritz *et al.* (1983).

The pebbly sandstone of the Yusezyu Formation is correlated by Fritz *et al.* (1983) with the lower member of the Backbone Ranges Formation (*cf.* MacNaughton *et al.*, 2008) on the basis of trace fossils in overlying strata and stratigraphic position. Moynihan (2014) correlated the Yusezyu Formation with an uppermost member of the Blueflower Formation in the northernmost Selwyn basin area. These two correlations are compatible only if the entire Backbone Ranges Formation indicated by Moynihan corresponds to only the upper member of the Backbone Ranges Formation.

The Yusezyu Formation is a thick succession of coarse-grained turbidite flows that reflect rapid erosion of a sedimentary source terrane of unknown extent and location (Gordey and Anderson, 1993). Scarce paleocurrent indicators suggest that the source area is located to the northwest. The suggested depositional environment is a series of upper or mid-fan submarine channels in shallow to moderate water depth (Gordey and Anderson, 1993).

One sample of Yusezyu Formation (09LP014) from the west side of the Coal River map area was submitted for detrital zircon study. The table of analyses from this sample is contained in Appendix B (Tables B2a,b,c). Figure 7 illustrates the Concordia diagram and the probability distribution plot for the sample. The sample contains two Neoproterozoic to Mesoproterozoic ages,  $631 \pm 29$  Ma and  $1115 \pm 109$  Ma. All other dates are Paleoproterozoic and Archean. The probability distribution plot has a dominant peak centred on 1859 Ma and a lesser peak at 2719 Ma. Scattered peaks range between 1937 Ma and 2606 Ma. The oldest dated grain has an Archean age of  $2745 \pm 51$  Ma. The dominant age distribution of detrital zircons corresponds to the Laurentia Type I signature identified by Hadlari *et al.* (2012); the zircons could be derived from the Wopmay orogen and the Archean Slave province east and northeast (current orientation) of the Coal River map area.

This interpretation contrasts with a northwestern source indicated by the limited paleocurrent data of Gordey and Anderson (1993). The western extent of the Yusezyu Formation is unknown because it is truncated by the Tintina fault. As a result the provenance of Yusezyu Formation remains unresolved.

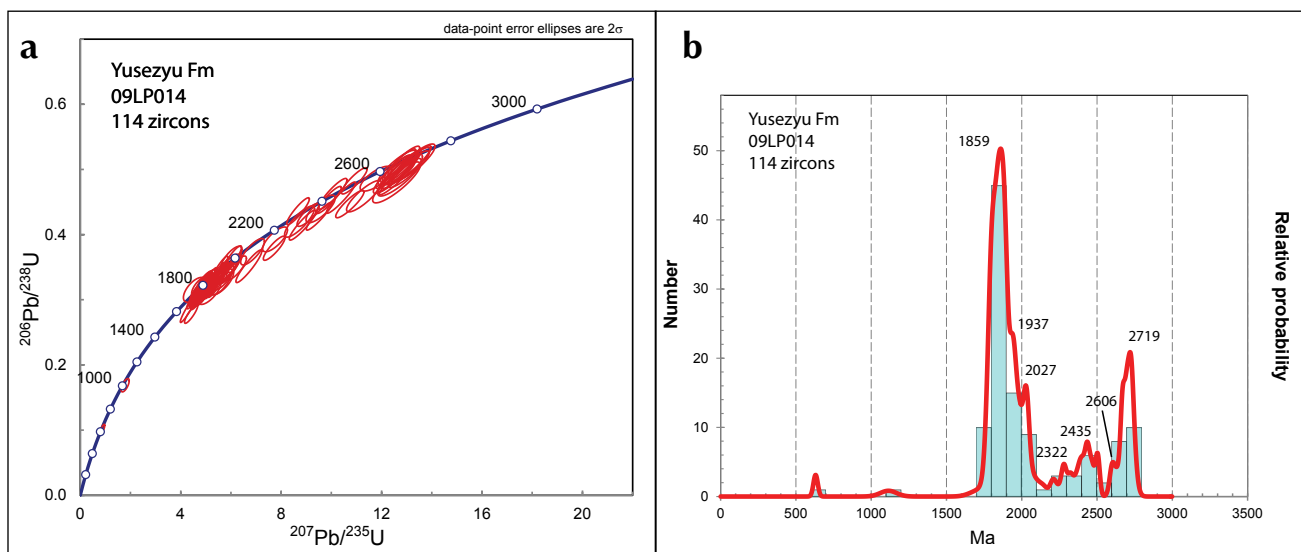


**Figure 7.** Results of geochronological analysis of 114 detrital zircon grains from sample 09LP014 of Yusezyu Formation sandstone: (a) concordia diagram; (b) probability distribution diagram. Data and methods are shown in Appendix B (Table B2).

## ***Vampire-Narchilla unit (Hyland Group)* (PЄVN, PЄVN-m, PЄVN-l, PЄVN-v)**

### **Introduction**

Shaly strata lithologically similar to both the Narchilla Formation (Gordey and Anderson, 1993) and Vampire Formation (Fritz, 1982) are exposed in the western third of the map area. Observations of previous workers in the northern part of the Coal River map area (Abbott, 1981) and in areas farther north (Fritz, 1982; Gordey and Anderson, 1993) indicate a west-to-east transition from Narchilla Formation (dominantly slate to phyllite) through Vampire Formation (dark weathering siltstone interbedded with quartzose sandstone) to the upper member of the Backbone Ranges Formation (sandstone; MacNaughton *et al.*, 2008). In 2009 we were unable to consistently differentiate the Vampire and Narchilla formations. Consequently we chose to map these units as an undivided Vampire-Narchilla unit.

The lower contact with the Yusezyu Formation is poorly exposed but appears to be a gradational decrease up-section in the amount of subarkosic pebbly sandstone and a corresponding increase in shale and siltstone. In the central part of the map area immediately west of the Rock River, the unit is conformably overlain by siltstone, sandstone and carbonate rocks of unit **Єs**, the lower Cambrian Sekwi-correlative unit. The undivided Vampire-Narchilla unit is unconformably overlain by the late Cambrian to Early Ordovician Rabbitkettle or Otter Creek formations in the western part of the map area.

The thickness of the Narchilla Formation at the type section is 828 m (Gordey and Anderson, 1993). The type section of the Vampire Formation is 930 m thick (Fritz, 1982). In the Coal River area the thickness of the Vampire-Narchilla unit is interpreted to be significantly greater, based upon the geometric requirements of a structurally plausible cross section; the thickness of this unit could be as much as 2500 m.

### **Composition**

The predominant lithology (Fig. 8) is a pale olive green, rusty brown-weathering, noncalcareous, laminated, silty phyllite (**PЄVN**). Bedding within the phyllite is denoted by colour variations and is on the scale of centimetres to metres. Locally the pale green phyllite contains interbeds of reddish maroon to dark maroon phyllite (**PЄVN-m**; Fig. 9); this maroon phyllite is regionally characteristic of the Narchilla Formation. West of the West Coal River, maroon interbeds are common within the green silty phyllites. In contrast maroon interbeds are rare in the southwestern quadrant of the map area. No maroon intervals were observed in the silty phyllite immediately west of the Rock River.

The phyllite contains interbeds of medium to dark grey, cream-weathering siltstone, cream-weathering, quartzose sandstone (Fig. 10), cream-weathering, pebbly quartzose sandstone and pale to medium grey, thick-bedded to massive limestone (**PЄVN-l**). The sandstone, pebbly sandstone and limestone intervals locally reach thicknesses of 100 m or more without apparent structural repetition. Only the interbedded limestone units have been differentiated as separate lithologies in the legend.

The Vampire-Narchilla unit consistently displays a pervasive slaty cleavage (Figs. 8, 9, 10). Locally it also contains a later, spaced crenulation cleavage. Throughout most of the area the phyllite contains sericite and chlorite, placing it in the lower greenschist facies of metamorphism. In a north to northeast-trending linear zone extending from south of Roy Lake northeastward to Mt. Skonseng, the phyllite contains ubiquitous biotite with local garnet and staurolite (Fig. 11). The areal extent of the biotite-bearing phyllite was not well defined by the few traverses completed in 2009.



**Figure 8.** Olive green, silty phyllite of the undivided Vampire-Narchilla map unit. Slaty cleavage (steeply dipping north-northeast) offsets the horizontal bedding, which is marked by a thin, recessive siltstone layer. From 20 km northwest of the eastward bend of the Coal River, station 09LP028. Hammer handle is 33 cm long.



**Figure 9.** Banded maroon and green phyllite of the undivided Vampire-Narchilla map unit. The colour change represents oxidation-reduction fronts during diagenesis of the muddy sediment and typically follows layering. From east of Coal River and west of the headwaters of Otter Creek, station 07LP003.



**Figure 10.** Phyllitic siltstone interbedded with light brown quartz sandstone in the undivided Vampire-Narchilla map unit. Note the centimetre-scale cross-beds (mostly dipping to the left in the photograph) in the sandstone beds and slaty cleavage in the phyllitic siltstone beds (dipping to the right). Outcrop 20 km north of Alaska Highway, station 09LP022.

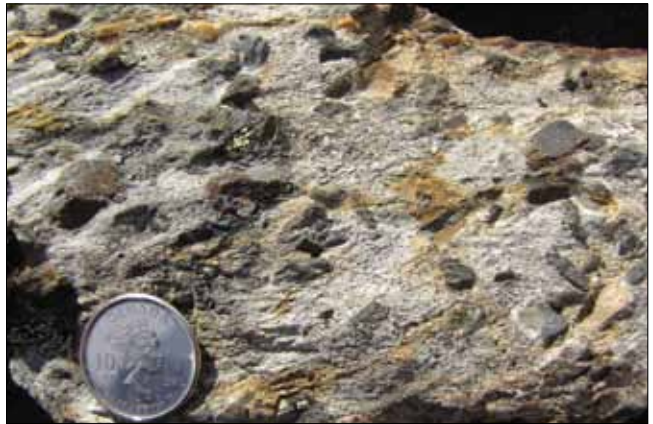


**Figure 11.** Staurolite-garnet-biotite schist of the undivided Vampire-Narchilla map unit. From 30 km northeast of Roy Lake, station 09TOA076. The coin is 2.5 cm in diameter.

In the central Coal River map area, immediately west of the Rock River, the upper part of the Vampire-Narchilla unit contains extensive greyish-green to green, fine-grained, locally amygdaloidal to vesicular basalt which we have differentiated as a separate unit (PCVN-v). Lower and upper contacts are not exposed; these could be flows or sills. Locally the basalt is intruded by fine to medium-grained, equigranular, chloritized hornblende diabase that likely represents feeders. The basalt and diabase form a mappable unit up to 1300 m thick. Their geochemistry is discussed in the section on Cambro-Ordovician alkali basalt (see p. 42).

## Age, Correlation and Depositional Setting

We did not recognize any fossils in the Vampire-Narchilla unit in the Coal River map area. Regionally the Vampire Formation contains ichnofossils from biozones *Rusophycus avalonensis* and *Cruziana tenella* (Fritz *et al.*, 1983; MacNaughton and Narbonne, 1999). The first appearance (datum) of trilobites and archeocyathids occurs within the very uppermost Vampire Formation and the overlying Sekwi Formation (Handfield, 1968). The age of the Vampire-Narchilla unit is therefore early Cambrian (Terreneuvian: Stages Fortunian and 2). Occurrences of the ichnofossil *Oldhamia radiata* in the upper part of the unit in Nidderly Lake map area (Hofmann and Cecile, 1981) are consistent with the upper portion of the unit being within Cambrian Stage 2 (Herbosch and Verniers, 2011).

Time-correlative formations north of the Coal River map area display a complex succession of interlayered coarse and fine siliciclastic formations (Fig. 12) deposited in Selwyn basin.

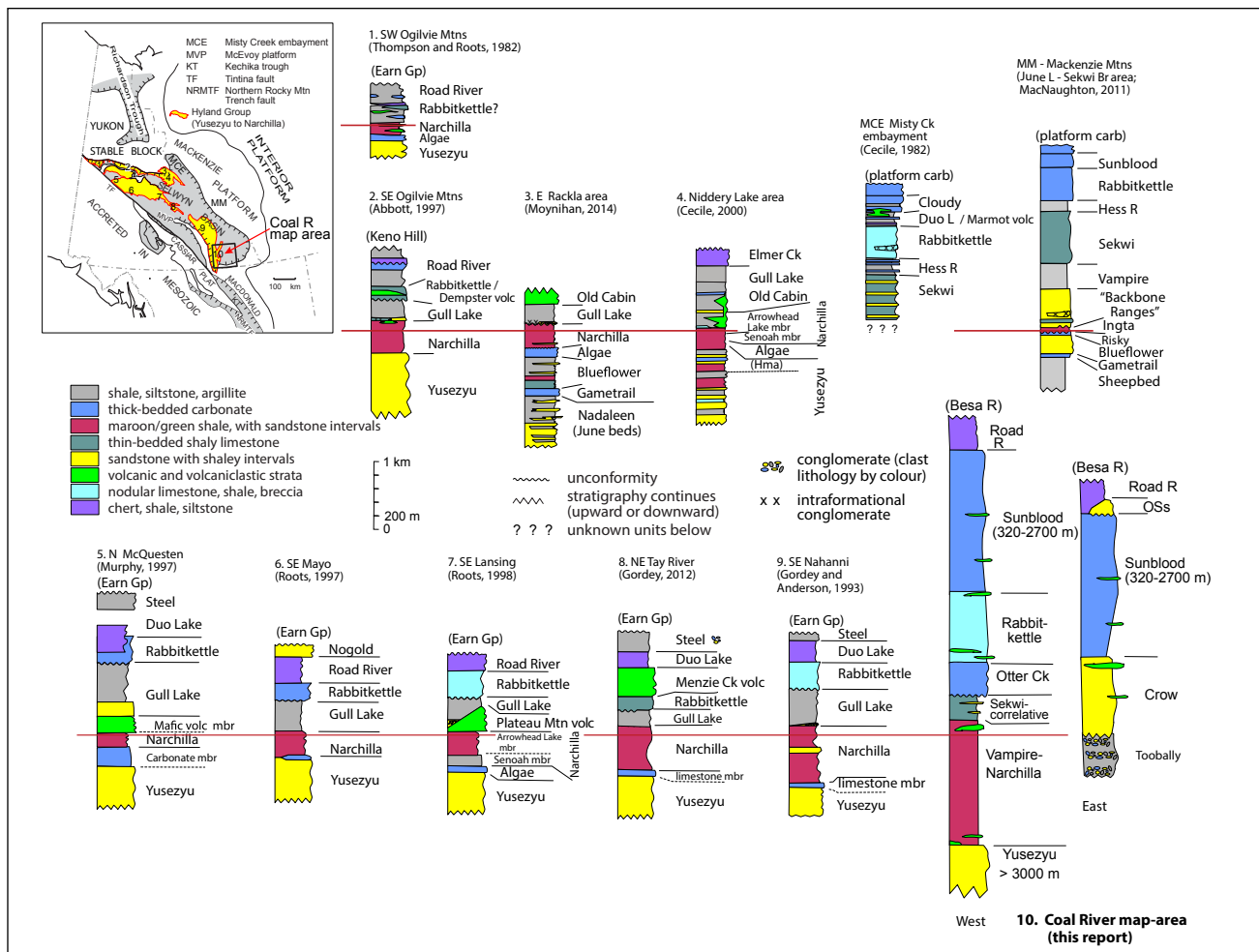


**Figure 12.** Regional correlation of stratigraphic units that compose Selwyn basin (and Mackenzie Mountains [MM] for comparison). Representative columns were selected from the numbered areas and depict thicknesses as given in the citations; the datum is approximately the Cambrian-Precambrian boundary. Overlying units are labeled in parentheses. This figure is modified from Figure 36 in Gordey and Anderson (1993) and Figure 5 in Cecile (2000).

Two sandstone samples from the undivided Vampire-Narchilla unit were examined for detrital zircon geochronology (09TOA098 and 09TOA094). Results are tabulated in Appendix B (Tables B3 and B4) and illustrated in Figures 13 and 14. Four zircon grains from sample 09TOA098 indicate a maximum

age of 644 Ma, and one grain from sample 09TOA094 indicates a maximum age of 560 Ma for the unit.

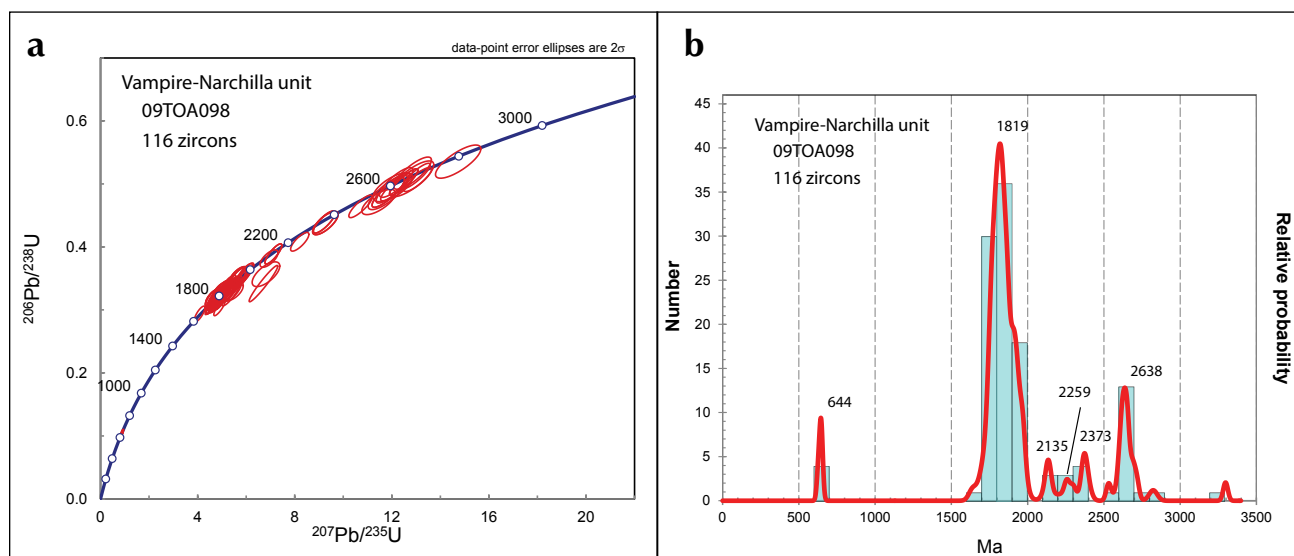


**Figure 13.** Results of geochronological analysis of 116 detrital zircon grains from sample 09TOA098 of undivided Vampire-Narchilla map unit sandstone: (a) Concordia diagram; (b) probability distribution diagram. Data and methods are shown in Appendix B (Table B3).

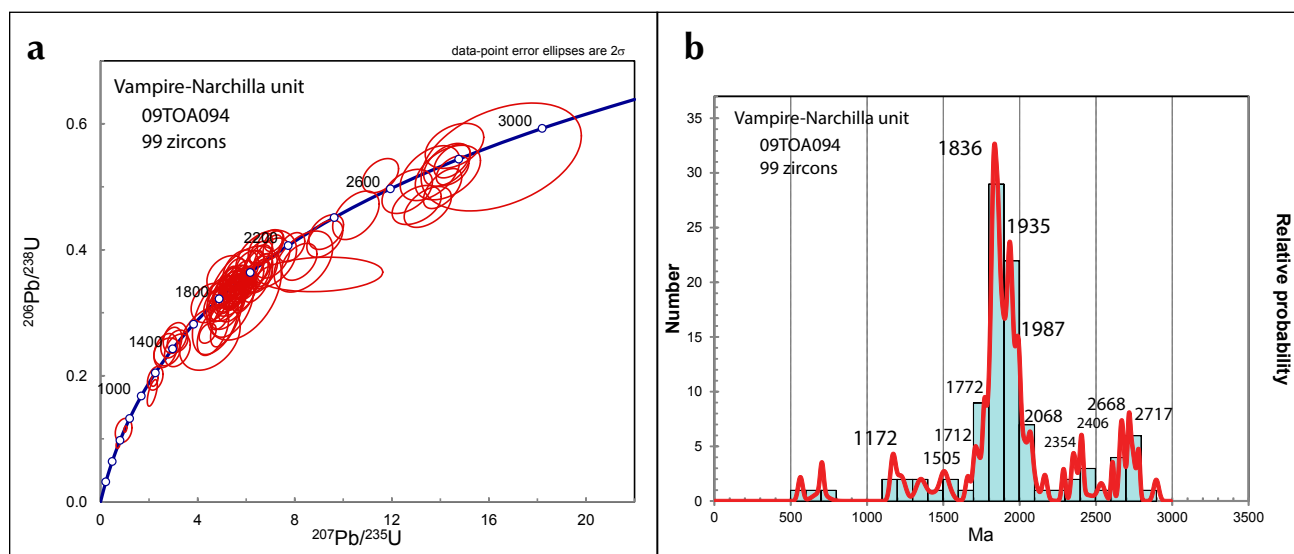


**Figure 14.** Results of geochronological analysis of 99 detrital zircon grains from sample 09TOA094 of undivided Vampire-Narchilla map unit sandstone: (a) Concordia diagram; (b) probability distribution diagram. Data and methods are shown in Appendix B (Table B4).

Sample 09TOA098 has a similar probability plot to that of the Yusezyu Formation with a major peak at 1819 Ma and lesser peaks at 2373 Ma and 2638 Ma. In contrast, sample 09TOA094 contains a different zircon age distribution. About 15% of the analyzed grains are within the interval from 1000-1550 Ma. More than 30% of the grains are between 1700 and 1800 Ma.

Hadlari *et al.* (2012) identified two major detrital zircon signatures for Cambrian strata in the Northwest Territories. These signatures closely match those identified above for samples 09TOA094 and 09TOA098. The Laurentia type I signature (sample 09TOA098) is dominated by Paleoproterozoic and Archean detrital zircon ages with potential sources including the Great Bear magmatic zone, Fort

Simpson terrane, Hottah terrane, Coronation margin and Slave craton. The Laurentia type II signature (sample 09TOA094) contains abundant Mesoproterozoic ages. The source area is dominated by Grenville-aged detrital zircons; proximate sources are most likely Proterozoic strata of the Mackenzie Mountains and Shaler supergroups. The fewer grains of Paleoproterozoic and Archean age could have the same source area as the Laurentia type I signature. Both of these source areas are east to northeast of the Coal River map area.

In summary, detrital zircon ages from the two samples are consistent with erosion of Paleoproterozoic and Archean bedrock in northern Alberta and Northwest Territories. A small number of zircon grains are most likely recycled from exposed Mackenzie Mountains Supergroup strata at the time of deposition of this Vampire-Narchilla unit. An easterly source was also determined for the Backbone Ranges Formation (Leslie, 2009).

Although we chose to assign these lithologies to a combined Vampire-Narchilla map unit, in a broader context the Narchilla and Vampire formations are differentiated regionally (Abbott, 1981; Fritz, 1982). For consistency with the regional treatment of this stratigraphic interval we assign our combined map unit to different formations in the Yukon-wide geology compilation according to the structural panel in which it appears. The western-most domain A structural panel is considered to be the Narchilla Formation, and exposures in the two more easterly structural panels have been assigned to the Vampire Formation.

### ***Unit Cs (Sekwi-correlative unit)***

#### **Introduction**

Ridges west of the Rock River in the north-central map area contain exposures of silty phyllite, silty, archeocyathid-bearing limestone, arkosic sandstone and quartzose sandstone. We have informally called this unit the 'Sekwi-correlative' unit because it is correlative in time with the Sekwi Formation. We are not calling it the Sekwi Formation because lithologies in the Coal River area differ from the predominant carbonate rocks described for the Sekwi Formation at the type section (Handfield, 1968) located 300 km to the north.

Unit **Cs** conformably overlies the Vampire-Narchilla unit and is unconformably overlain by carbonate rocks of the upper Cambrian-lower Ordovician Otter Creek Formation. The overall thickness of unit **Cs** is approximately 400 m where it is most completely exposed. The unit could not be traced beyond a strike length of 22 km; this is a minimum extent because we were unable to recognize it with our limited traverses. Alternatively it may have been removed by the unconformity beneath the overlying Otter Creek Formation.

#### **Composition**

Unit **Cs** consists predominantly of pale green to tan, brown-weathering, laminated, locally calcareous, silty phyllite (Fig. 15). Interbedded with the silty phyllite are rusty brown-weathering, thin bedded arkosic sandstone, cream-weathering, fine-grained quartzose sandstone and laminated, silty limestone. The lower contact with the Vampire-Narchilla unit is denoted by the first appearance of recessive-weathering limestone nodules in the siltstone (Fig. 15), the occurrence of trilobites, and the presence of green, argillaceous siltstone. A silty limestone bed occurs at this basal contact. Arkosic sandstone intervals up to 10 m thick occur throughout the lower part of the unit. A cream-weathering, noncalcareous, quartzose sandstone forms a distinctive thick-bedded unit 70 m thick at the top of the unit. Medium to dark grey and orange-weathering limestone near the middle of the unit contains archeocyathids (Fig. 16) and occurs locally as bioherms or bioclastic sediments (Handfield, 1971). Trilobites were found in the silty phyllite stratigraphically below and above the archeocyathid-bearing limestone (Handfield, 1971).



**Figure 15.** Light brown-weathering, grey, calcareous phyllite at the base of the Sekwi-correlative unit. Dark hollows up to 3 cm long are recessive-weathering carbonate nodules. From 17 km northeast of the confluence of Quartz Creek with Coal River, station 09TOA15. Scale card at top edge of photo is in cm.



**Figure 16.** Thick limestone near the middle of the Sekwi-correlative unit (Cs) containing archeocyathids. Outcrop is 3 km northeast of the confluence of Quartz Creek with Coal River, station 09TOA017.

### Age, Correlation and Depositional Setting

The trilobite and archeocyathid fossils (see Appendix A) indicate the formation is lower Cambrian, contemporaneous with the Sekwi Formation. Although differing in detail, the trilobite identifications by Handfield (1971) and L. Bohach (pers. comm. 2009) indicate the age of unit Cs is lower Cambrian Series 2 (Stage 3 or Stage 4). Fritz (1972) delineated three trilobite zones within the type Sekwi Formation (Fallotaspis, Nevadella and Bonnia-Olenellus zones); these correspond to Stages 3 and 4 in Series 2 of lower Cambrian (Peng *et al.*, 2012).

Unit Cs is a deeper water facies-equivalent of the Sekwi Formation. In the Selwyn basin area, the lower Cambrian shale facies is known as Gull Lake Formation (Fig. 12; Gordey and Anderson, 1993), but the strata in Coal River map area is more calcareous and siltier than Gull Lake Formation. The unit is envisaged to have been deposited on a westward deepening, homoclinal ramp, similar to that described in Sekwi Mountain map area 100 km to the north (Fischer and Pope, 2012).

The northern part of the Kechika trough southwest of the Coal River map area, contains a facies change from interbedded early Cambrian siliciclastic rocks and carbonate rocks eastward to deeper water siliciclastic rocks, possibly indicative of the western edge of Kechika trough (Ferri *et al.*, 1999). Archeocyathids in the carbonate intervals indicate the package is correlative with the Sekwi Formation (and with Unit Cs in the Coal River map area).

Two samples (09TOA095 and 09TOA096) from this unit were analyzed for detrital zircon geochronology. Analytical results are illustrated in figures 17 and 18; analytical tables are listed in Appendix B (Tables B5 and B6). The zircons of both samples can be grouped into three clusters: those consistent with Mesoproterozoic Grenville age (1.0-1.5 Ga); those of Paleoproterozoic age possibly derived from the Hottah terrane and Great Bear Magmatic zone (1.8-2.1 Ga); and those of Archean Slave craton (>2.5 Ga) age. The detrital zircons indicate a mix of the Laurentia type I and type II signatures as identified by Hadlari *et al.* (2012). All three clusters can be attributed to basement and Mackenzie Mountain Supergroup sources that are exposed to the east in Alberta and Northwest Territories.

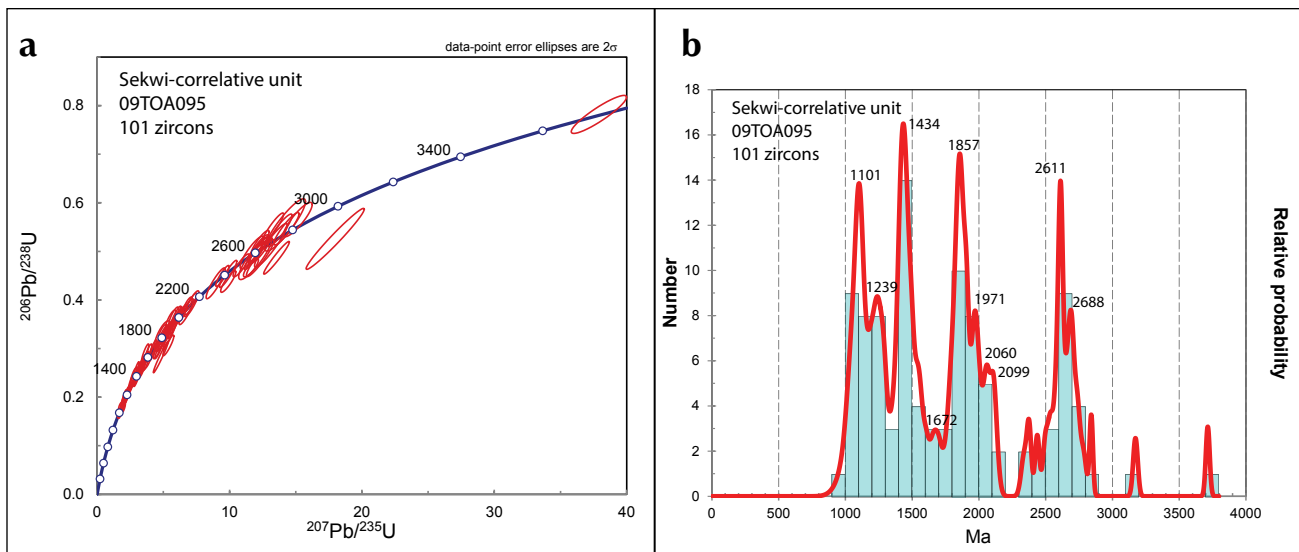


**Figure 17.** Results of geochronological analyses of 101 detrital zircon grains from sandstone in Sekwi-correlative unit: **(a)** Concordia diagram; **(b)** probability distribution diagram. Data and methods are shown in Appendix B (Table B5), station 09TOA095.

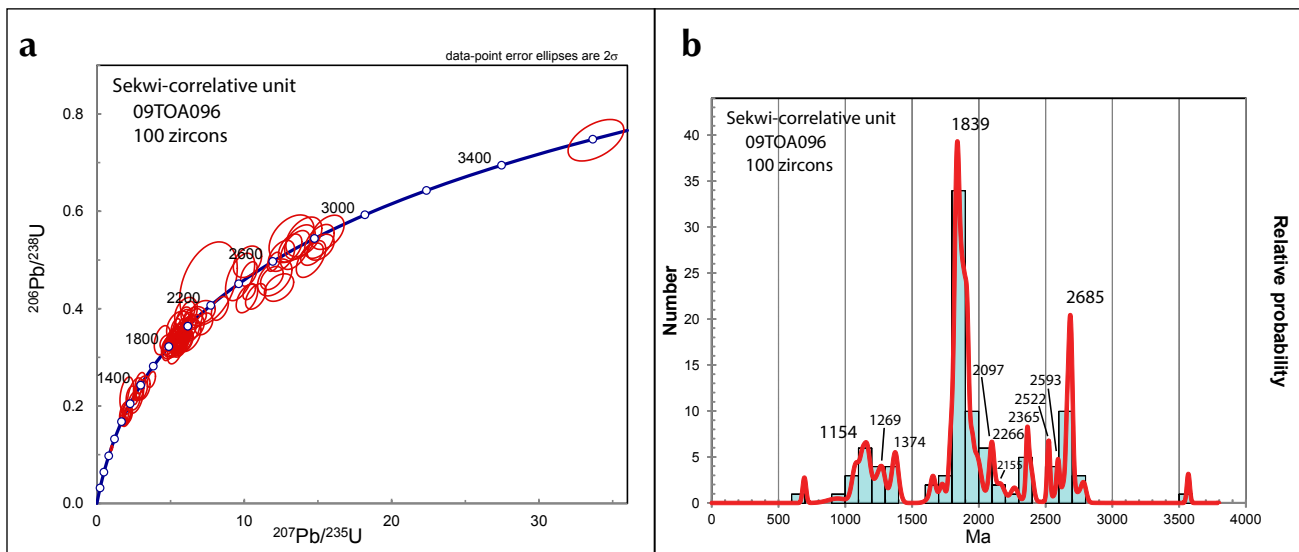


**Figure 18.** Results of geochronological analysis of 100 detrital zircon grains from uppermost sandstone of Sekwi-correlative unit: **(a)** Concordia diagram; **(b)** probability distribution diagram. Data and methods are shown in Appendix B (Table B6), sample 09TOA096.

## SUCCESSION 2 – UPPER CAMBRIAN TO LOWER ORDOVICIAN

Succession 2 consists of three stratigraphic units having a composite age range of late Cambrian through Early Ordovician and a combined thickness of approximately 5000 m. The lowermost unit in the succession is a thick-bedded to massive limestone and dolostone, outcropping largely in the central part of the map area; this unit is defined in this report as the Otter Creek Formation. Silty to phyllitic limestone of the Rabbitkettle Formation conformably overlies the Otter Creek Formation. The western half of the Coal River map area contains two facies of the Rabbitkettle Formation. In the eastern half of the map area quartzose sandstone of the Crow Formation appears to interdigitate with the time-equivalent Rabbitkettle Formation. The lower contact of this entire succession is unconformable, and the upper contact is conformable.

## ***Otter Creek Formation (EOOC) [new]***

### **Introduction**

This unit comprises massive limestone and lesser dolostone (mapped by Gabrielse and Blusson (1969) as unit 5, presumed lower Cambrian), here defined as the Otter Creek Formation. Several narrow belts of exposure lie between the Rock and Coal rivers (Plate 1). The type area for the formation is in NTS 95D/06 at the Mel property (UTM NAD83 587 950 E/6 692 150 N) where a complete section of this formation is exposed (Fig. 19) in the overturned steep limb of an east-verging, asymmetric anticline-syncline fold couplet. The type area is located near the headwaters of Otter Creek, after which the formation is named.



**Figure 19.** Massive limestone of Otter Creek Formation in the overturned steep limb of an asymmetric syncline. View northward at the head of Otter Creek, near the MEL occurrence, from station 06LP008. This is the proposed type location for the Otter Creek Formation.

Both upper and lower contacts are recessive and not observed at surface in the dense vegetation cover. The contacts were recognized in diamond drill holes on the Mel property. The lower contact is sharp and interpreted as a major unconformity above the lower Cambrian Vampire-Narchilla unit. The conformable upper contact with the calcareous shale and silty limestone of the Rabbitkettle Formation is sharp.

On the Mel property, the Otter Creek Formation is approximately 160 m thick. Thickness estimates in the Coal River map area range from 65 m on the Jeri North property (Yukon MINFILE 095D035) to 500 m in outcrops west of the Rock River in the northern part of the Coal River map area.

### **Composition**

The Otter Creek Formation weathers light grey to off-white, and consists of finely crystalline, indistinctly bedded to massive, resistant limestone (Fig. 20) with lesser interbeds of buff to tan-weathering dolostone. The limestone typically contains ghosted white calcite and tan siderite veinlets. In at least one location the limestone has ghost textures reminiscent of burrow mottling. In the type area the limestone contains small, irregular lenses of pale green to cream, noncalcareous phyllite to mudstone (Fig. 21).

Dolostone lenses have a massive, sucrosic texture. Miller (1977) described three stratiform, discontinuous dolostone intervals up to 30 m thick and ranging from 60 to 500 m in length. One dolostone occurrence, up to 30 m thick, occurs adjacent to a late steep fault and clearly crosscuts primary bedding.

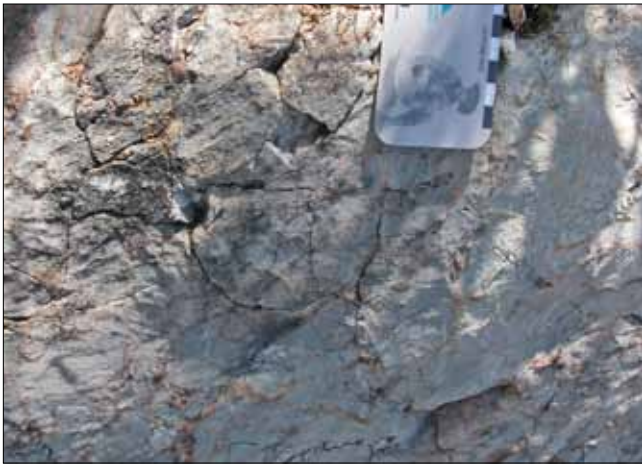


**Figure 20.** Light coloured, massive, fine-grained limestone with irregular network of buff to tan-weathering dolostone veinlets, Otter Creek Formation. From the headwaters of Otter Creek near the MEL occurrence, station 06LP008.



**Figure 21.** Olive-green mudstone with limestone (light grey), Otter Creek Formation. Drill core from 254 ft depth in Hole 74-6 (Bostock core collection) at the MEL mineral occurrence. Scale bar is in cm.

### Age, Correlation and Depositional Setting

Identified brachiopods and trilobite fragments (Norford, 1984; Miller and Wright, 1986) from the limestone are late Cambrian to Early Ordovician; on this basis Pigage (2008) describes the limestone as a basal member of the Rabbitkettle Formation. Additional occurrences recognized during regional mapping in 2009 prompts its reinterpretation as a distinct carbonate unit underlying silty limestone of the Rabbitkettle Formation.

Gordey and Anderson (1993) describe a Cambrian-Ordovician to Silurian dolostone, the Haywire Formation, partially underlying Rabbitkettle Formation in the Little Nahanni River map area. Otter Creek Formation is considered correlative with the lowermost part of the Haywire Formation. It represents the western margin of the shallow carbonate platform during late Cambrian to Early Ordovician.

### **Rabbitkettle Formation** (€OR-n, €OR-lp, €OR-v)

#### Introduction

Rabbitkettle Formation, as defined by Gabrielse *et al.* (1973) in southwestern Mackenzie Mountains, is a silty limestone widely recognized in Selwyn basin. It occurs in north-trending belts in the western and central Coal River map area, in the core of the Caribou anticline, and in one exposure near the Gusty Lakes. Fissile carbonate outcrops in the northeast corner of the map area were visually identified from the helicopter as Rabbitkettle.

In the western part of the map area, the Rabbitkettle Formation unconformably overlies the undivided Vampire-Narchilla unit and is in turn unconformably overlain by carbonaceous strata of the Road River Group. In the central part of the map area the lower contact with the Otter Creek Formation and the upper contact with the Sunblood Formation are both conformable.

A well-exposed section of the Rabbitkettle Formation, between the Coal and Rock rivers in the north-central part of the map area, is estimated to be 1500 m thick. Its thickness in the Mel property area ranges from 300 to 1050 m.

## Composition

The predominant unit of the eastern facies (**COR-n**) consists of a light grey to brownish grey-weathering, silty to argillaceous, nodular limestone (Fig. 22). Nodules are typically up to 10 cm long and 5 cm thick and consist of pale grey, recessive-weathering, fine-grained limestone which is locally parallel laminated. The limestone contains a well-developed, but discontinuous, slaty cleavage which anastomoses around the nodules; because of this texture the formation has previously been informally termed the 'wavy-banded limestone'. The nodular limestone commonly contains lesser interbeds of pale grey, fine-grained, massive limestone up to 2 m thick which constitute 50% or less of any outcrop (Fig. 23). Locally the nodular limestone contains intervals of grey-weathering, interbedded argillaceous limestone and laminated limestone up to tens of metres thick. Alternation of these two limestone types in an outcrop is on a scale of 5-30 cm.



**Figure 22.** A characteristic texture of Rabbitkettle Formation; eastern facies is nodular limestone with mud-silt interbeds up to 2 cm thick. Near the MEL occurrence at the headwaters of Otter Creek (station 06LP021).

West of the Coal River, the Rabbitkettle Formation has a distinctive shaly facies (**COR-lp**) which consists of a light to medium grey, silvery-weathering, thin-bedded, phyllitic limestone (Fig. 24). This western facies contains a well-developed, pervasive slaty cleavage; primary bedding is only commonly observed in small intervals within the slaty cleavage. Yellow-weathering, silty, laminated limestone exposed along the Coal River near the Sulpetro Road (NTS 95D/03) has been included within the Rabbitkettle Formation shaly facies. In the northwestern Coal River map area, outcrops of typical Rabbitkettle phyllitic limestone are overlain by a dark grey, orange-weathering, pin-striped, silty limestone (Fig. 25); this unit is also included within the western shaly facies of the Rabbitkettle Formation.

Siltstone and silty limestone near the top of the Crow Formation are more than 700 m thick in a stream flowing east to upper Toobally Lake. These strata are considered a tongue of Rabbitkettle Formation within pinkish sandstone of the upper Crow Formation near its western extent (Pigage, 2009). In the Caribou anticline a similar thickness of Rabbitkettle Formation overlies a thin sandstone unit reinterpreted as Crow Formation (see next section).



**Figure 23.** Two massive limestone interbeds within recessive weathering, nodular limestone of the Rabbitkettle Formation. Outcrop at headwaters of Otter Creek near the MEL occurrence (station 07LP010).

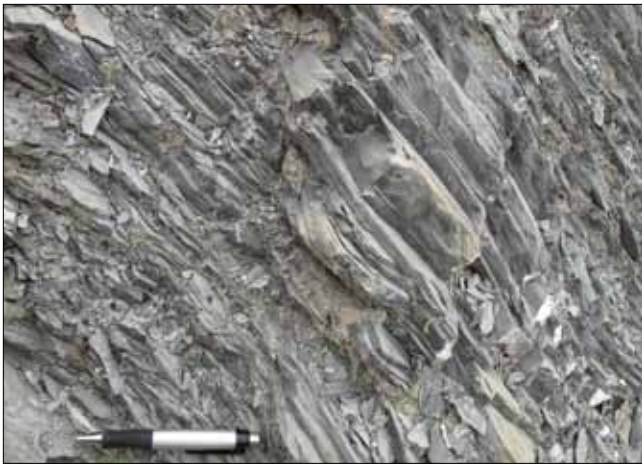


**Figure 24.** Grey, phyllitic limestone of the west facies of the Rabbitkettle Formation, showing slaty cleavage. View northward at roadcut on the Alaska Hwy at Contact Creek, south edge of the map area (station 09RAS150).

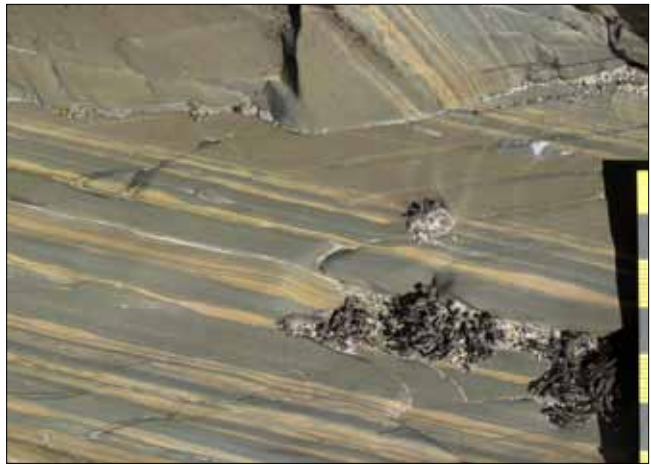


**Figure 25.** Calcareous, grey mudstone with yellow-weathering silt laminae, assigned to the Rabbitkettle Formation (west facies). Spaced slaty cleavage dips gently to the left in the photograph. Outcrop beside rapids on the Coal River, 15 km north of its confluence with the West Coal River (station 09RAS050). Scale bar (right side) in cm.

A horizon of medium green, silvery green-weathering, alkali basalt, breccia and lithic tuff (€OR-v) occurs near the base of the Rabbitkettle Formation on the Jeri North property (Pigage, 2007; this volcanic horizon is too small to show on the map at 1:250 000 scale). East of the Rock River in the northern Coal River map area, an extensive volcanic horizon is discontinuously exposed for 30 km near the upper contact of the Rabbitkettle Formation; this occurrence is the informal ‘Coal River volcanics’ of Goodfellow *et al.* (1995). It locally contains pillowed basalt flows. Breccia textures with angular basalt clasts in a chloritic fine-grained matrix are common (Fig. 26). Tuffs are interlayered with the flows and coarse breccias. The geochemistry of the basalt is discussed in the section on Cambro-Ordovician alkali basalt.

**Figure 26 (right).** Angular basalt blocks in a chloritic fine-grained matrix in the volcanic horizon at the top of Rabbitkettle Formation. View northward, on the Yukon-Northwest Territories border, east of the Rock River (station 09TOA164).



### Age, Correlation and Depositional Setting

The Rabbitkettle Formation is sparsely fossiliferous. Regionally the brachiopod and conodont collections range from late Cambrian through late Middle Ordovician (Gabrielse *et al.*, 1973; Tipnis *et al.*, 1978; Cecile, 1982; Gordey and Anderson, 1993). Conodont collections in 2007 and 2009 from the Coal River map area are all Early Ordovician, ranging from early Tremadocian to late Floian (Plate 1; Appendix A in this report).

Regionally Rabbitkettle Formation extends across the Selwyn basin during late Cambrian-Early Ordovician time (see Fig. 12). South of the Nahanni River (150 km northwest of Coal River map area) nodular, silty limestone changes southwestward to evenly laminated, argillaceous limestone (Gordey and Anderson, 1993). Shallow shelf (Mackenzie platform) correlatives of Rabbitkettle Formation are

the Broken Skull and Franklin Mountain formations (Gabrielse *et al.*, 1973; Gordey and Anderson, 1993; Martel *et al.*, 2012). South of the Coal River map area and along structural grain, Rabbitkettle correlates with the early Ordovician Kechika Formation. This grey, phyllitic, calcareous shale and thin-bedded, argillaceous limestone and grainstone (Pyle and Barnes, 2000) thickens from 200 to 1400 m in a westerly direction.

Fossil collections (Appendix A in this report) indicate that Rabbitkettle Formation in the northern Coal River map area is laterally correlative with Sunblood Formation in the east-central Coal River map area.

Fine lamination and the dark colour of the carbonate indicate that Rabbitkettle deposition was in a quiet water, sub-wave base, off-shelf setting. Analogous to the Kechika trough located to the south, it accumulated on a broad, gentle ramp, transitioning from shallow to deeper water facies (Cecile and Norford, 1979). These upper Cambrian to Ordovician basinal strata reflect post-rift passive margin thermal subsidence following Neoproterozoic to middle Cambrian extension (Pyle and Barnes, 2000).

## **Crow Formation (€OC, €OC-v)**

### **Introduction**

The Crow Formation (Pigage, 2009) forms two large exposures flanking the Toobally Lakes in the eastern Coal River map area. There it consists of a thick sequence of bedded sandstone with interbeds of amygdaloidal alkali basalt, and maroon, silty argillite.

A third occurrence, in the core of the Caribou anticline, is a 30 m-thick interval of sandy dolostone beneath the Rabbitkettle Formation and above a volcanic and volcanoclastic unit. Gabrielse and Blusson (1969) assigned this latter exposure to the Sekwi Formation. The underlying volcanic rocks are chemically similar to the Rabbitkettle and Crow volcanic rocks, but distinct from the volcanic rocks within the Vampire-Narchilla unit (see section on Cambro-Ordovician alkali basalt). On the strength of general stratigraphic position and the correlation of the underlying volcanic strata, we here reassigned the sandy dolostone and the volcanic strata to the upper Crow Formation.

In a limited area immediately west of the upper Toobally Lake, the Crow Formation unconformably overlies the Toobally Formation. Elsewhere in the map area the lower contact of the Crow Formation is not observed; it is truncated by the Toobally fault (western exposure) or a parallel reverse fault east of the Toobally fault (eastern exposure). To the east, the Crow Formation unconformably overlies Proterozoic strata and intrusive rocks (Pigage, 2009). It is conformably overlain by the Sunblood Formation. A minimum thickness of 5000 m is inferred from the extensive outcrops of Crow Formation on the west side of upper Toobally Lakes (Pigage 2009) if the outcrops are considered to be a monoclinical succession dipping westward at 45°; the succession may have been thickened by unmapped thrust fault repetition.

### **Composition**

Pinkish, indistinctly bedded, quartzose to subarkosic sandstone is the predominant lithology (Fig. 27) with interbeds of maroon, noncalcareous, argillaceous siltstone (Fig. 28) up to several tens of metres thick occurring throughout. Bedding thickness of the sandstone typically ranges from 20 to 70 cm. Locally the sandstone contains scattered argillite and quartz pebble clasts (Fig. 29). In several locations the sandstone has well-developed crossbeds; other areas exhibit mudcracks.

West of the upper Toobally Lake, we have interpreted a thick limestone and dolostone interval as being within the upper part of the formation. Alternatively this carbonate horizon may be basal Sunblood Formation structurally overlain by Crow Formation (see Pigage *et al.*, 2012 for discussion). A tongue of

nodular limestone of the Rabbitkettle Formation, within the upper part of the Crow Formation, is also documented in the same general area (Pigage, 2009).



**Figure 27.** Pink, thick-bedded, quartzose to subarkosic sandstone of the Crow Formation. View looking west, 11 km west-northwest of upper Toobally Lake (station 05LP075).



**Figure 28.** Maroon, non-calcareous, argillaceous siltstone constitutes up to several metre-thick interbeds within Crow Formation sandstone. From ridge approximately 8 km west of north end of upper Toobally Lake (station 04LP053).

**Figure 29 (right).** Argillite and quartz pebble clasts within sandstone of the Crow Formation. From ridge approximately 8 km west of north end of upper Toobally Lake (station 05LP057).



Pigage (2009) mapped four alkali basalt horizons (COC-v) within the Crow Formation. Massive to pillowed, amygdaloidal flows and lapilli tuffs are the predominant lithologies. These horizons have previously been informally termed the Gusty Lakes and Toobally volcanics (Gabrielse and Blusson, 1969; Goodfellow *et al.*, 1995). The geochemistry of the basalt was presented in Pigage (2009) and is further described in the subsequent section on Cambro-Ordovician alkali basalt.

A 2 m-thick interval of medium green, fine-grained, porphyritic, rhyolitic tuff occurs along the Beaver River within sandstone of the Crow Formation (see Appendix C, Table C2c, sample 10TOA024), slightly below the uppermost alkali basalt horizon. It contains approximately 15% K-feldspar phenocrysts and 15% subhedral quartz phenocrysts, both 1-3 mm in diameter. About 25% of the tuff consists of brown, fine-grained volcanic lithic fragments containing feldspar microlites and small broken quartz microphenocrysts. The matrix consists of a fine-grained mixture of chlorite and sericite with small broken phenocrysts of K-feldspar and quartz. Flow banding and spheroidal textures are apparent in hand sample and thin section.

A basalt occurrence at this stratigraphic level in the core of the Caribou anticline in the northeast corner of the Coal River map area (McDougall, 1976; Stammers, 1983) is included in unit COC-v. Both amygdaloidal flows and several lithic tuff horizons (Fig. 30) are present. The lower contact of the basalt is not exposed, and its thickness is undetermined.



**Figure 30.** Planar cross-bedded tuff in the core of Caribou anticline, assigned to Crow Formation because it underlies a thin sandstone unit. The subangular to subrounded basalt clasts are enclosed in a fine-grained, chlorite-rich matrix. Outcrop is 2 km northwest of the main fork in the upper Caribou River (station 09LP083). Scale card is 9 cm wide.

### Age, Correlation and Depositional Setting

Conodont collections from the Crow Formation in the Coal River area are Early to Middle Ordovician (Pigage, 2009; Plate 1; Appendix A). Zircon grains from the rhyolite tuff (sample 10TOA024), interpreted as primary volcanic crystals, give a weighted mean  $^{206}\text{Pb}/^{238}\text{U}$  age of  $491.04 \pm 0.13$  Ma (Early Ordovician or late Cambrian; Pigage *et al.*, 2012). The Crow Formation is time correlative with the Rabbitkettle Formation (see Fig. 12) and the two are interpreted to be interdigitated in the subsurface of the eastern Coal River map area.

Mud cracks and ripple marks in the Crow Formation indicate deposition in a shallow water to subaerial environment (Pigage, 2009). The limited lateral extent and unusual thickness of the Crow Formation suggest deposition in a river delta complex with sediments derived from a granitic and quartz-rich source. Detrital zircon studies from the Crow Formation (Pigage, 2009) indicate that the zircon provenance could be the Archean Slave province and the adjacent Wopmay orogen. A small number of zircon grains from one Crow Formation sample (05LP034) are ~1000-1350 Ma, similar in age to those found in the Mackenzie Mountains Supergroup, possibly representing erosion of these strata (Hadlari *et al.*, 2012; Rainbird *et al.*, 1992, 1997).

### SUCCESSION 3 – LOWER TO MIDDLE ORDOVICIAN

Succession 3 consists solely of the Sunblood Formation which records shallow water carbonate deposition in a shelf environment. The carbonate unit is exposed in the central and eastern part of the Coal River map area; in the western third it is not present, and carbonaceous shale of the Road River Group occurs in the same stratigraphic position.

#### ***Sunblood Formation*** (OSu, OSu-v)

##### **Introduction**

The Sunblood Formation (Kingston, 1951; the updated reference section by Gabrielse *et al.*, 1973 is 110 km north of the Coal River map area) outcrops extensively along the Rock River and several smaller streams and meltwater channels in the central and eastern parts of the map area. In the west-central part of the map area it is preserved in north-trending synclinal fold keels. Gabrielse and Blusson (1969) concluded that the Sunblood Formation was presumably removed by erosion beneath unit SDC in the southern quarter of the Coal River map area. Mapping in 2009, however, confirmed that the unit is thin but present beneath unit SDC, and probably extends farther south into British Columbia. Sunblood Formation is not present in the southwestern corner of the map area (Irons Creek drainage) and the northwest corner of the map area (Coal River and West Coal River drainage). In both areas black shale

of the Road River Group overlies the Rabbitkettle Formation and is likely a facies equivalent of the Sunblood Formation.

The Sunblood Formation conformably overlies the Rabbitkettle Formation in the west and the Crow Formation in the east within the map area. It is unconformably overlain by a dolomitic sandstone unit (OSS) in the east, while in the southern part of the area it is unconformably overlain by massive carbonate (SDc). Elsewhere it is unconformably overlain by shales of the Road River Group. The Sunblood Formation ranges from 2700 m thick in the Caribou anticline northeast part of map area to 320 m thick near Mount Gilliland in the southwest part of the map area. It attains its greatest thickness in the central part of the map area. Immediately to the east in NTS 95C/5 it has a minimum thickness of 150 m (Pigage, 2006).

### Composition

In the northern part of the Coal River map area, the Sunblood Formation consists of medium grey, thick-bedded, finely crystalline limestone (Fig. 31). The limestone is typically tan to pink, flaggy or platy, with silty intervals and chert nodules locally. Bedding ranges from 2 to 60 cm in thickness. Bedding planes have a mottled appearance indicating extensive bioturbation (Fig. 32a,b). Macrofossils, including brachiopods, bryozoans, trilobites, ostracods, cephalopods, and gastropods (especially *Maclurites* sp.) are common (Gabrielse and Blusson, 1969). Recent karst solution cavities are conspicuous on limestone-topped ridges north of the Beaver River.



**Figure 31.** Well-bedded limestone of the Sunblood Formation. Bedding planes are mottled grey and tan from bioturbation. This unit locally develops modern, karst sinkholes. From ridge 5 km north of upper Beaver River (station 09LP075). Hammer for scale.

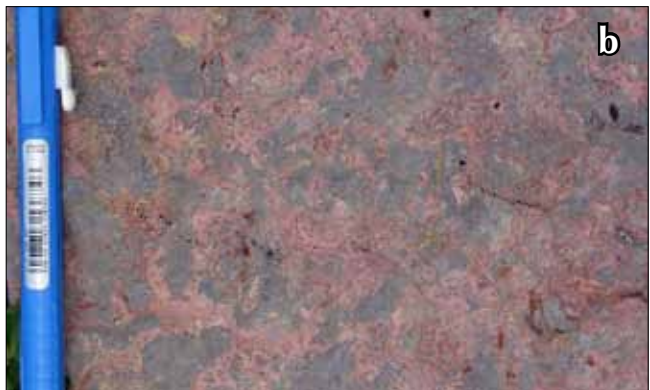


**Figure 32.** Bioturbation on bedding plane of Sunblood Formation limestone; (a) tan-weathering; (b) pink weathering; a defining characteristic of this formation farther north (Gabrielse et al., 1973). From ridge 5 km north of upper Beaver River (station 09LP075). Eraser for scale is 1 cm wide.

In the southern part of the Coal River map area, the Sunblood Formation consists largely of thick-bedded, pale grey, laminated to bioturbated dolostone interbedded with thick-bedded, dark grey, bioturbated dolostone (Fig. 33). Bedding ranges from 10 cm to 2 m in thickness. These rocks are

typically tan to buff-weathering, although locally they weather to a brownish-orange (the distinctive colour of the Sunblood Formation where it was named in the Nahanni River region). Bedding planes have a mottled appearance due to bioturbation (similar to the limestone). This southward transition from limestone to dolostone is attributed to secondary dolomitization of the primary limestone.

The Sunblood Formation contains green, brown-weathering, alkali basalt breccia and flows (OSu-v) in two localities, one near the headwaters of Spruce Creek and the other northeast of Lootz Lake. Flows are commonly pillowed. Breccia consists of angular clasts in a dark green, fine-grained, chloritic matrix (Fig. 34). The volcanic rocks in the headwaters of Spruce Creek occur at the top of the unit. North of Lootz Lake the volcanic rocks occur at a lower stratigraphic level within the Sunblood Formation. The chemistry of the basalt occurrences is described further in the Cambro-Ordovician alkali basalt section.



**Figure 33.** Pale grey, tan-weathering, laminated dolostone interbedded with dark grey, orange-grey-weathering, bioturbated dolostone, Sunblood Formation. Cliff is approximately 70 m high. From Rock River 3 km north of the mouth of Otter Creek (station 06LP043).



**Figure 34.** Altered basalt breccia within the Sunblood Formation. Looking north at outcrop (2 m high), 12 km northeast of Lootz Lake (station 08RAS304).

### Age, Correlation and Depositional Setting

In the type area the Sunblood Formation is of Middle Ordovician age (Gabrielse *et al.*, 1973; Ludvigsen, 1975). Age dating of conodonts collected more recently from the Coal River (NTS 95D) and LaBiche River (NTS 95C) map areas document an age range from Early Ordovician (Tremadocian) to Late Ordovician (Sandbian) (Pigage, 2009; Plate 1; Appendix A). The range in fossil ages for the Sunblood and Rabbitkettle formations indicates that the basal Sunblood contact is diachronous, varying in age from Tremadocian to Floian. The older Tremadocian ages occur in the east-central part of the area (NTS 95D/8 and 10); the younger Floian ages are represented farther north (NTS 95D/10 and 15) and south (NTS 95D/02 and 03). The diachroneity means that lower Sunblood Formation overlying the Crow Formation in the east-central part of the map area undergoes a lateral facies transition to Rabbitkettle Formation in the northeast part of the map area. Pohler and Orchard (1990) described a similar lateral transition between Haywire Formation and Rabbitkettle Formation north of Coal River map area. An analogous diachronous age variation of the lower contact of the Sunblood Formation was noted in Pigage (2009), varying easterly from Tremadocian to Floian.

Conodont collections from near the top of the formation suggest an Upper Ordovician (Sandbian to Katian) age for the upper contact in the eastern part of the map area. This younger age is also recorded in some of the fossil samples in the Pool Creek map area immediately to the east (Pigage, 2009). The

youngest ages for the upper contact appear to be restricted to the same general area as the older ages for the lower contact. The variation in age range for the upper contact can be interpreted to indicate that the Sunblood carbonate platform was restricted to a small geographic area in Upper Ordovician time, or that subsequent erosion has removed younger Sunblood strata in most areas except for the eastern Coal River and western LaBiche River map areas.

The Sunblood Formation is absent in the southwestern and northwestern parts of the map area. Although the contact is not exposed, carbonaceous, siliciclastic sediments of the Road River Group appear to directly overlie Rabbitkettle calcareous phyllite in these areas. An early Ordovician age for Road River Group strata north of Coal River (Abbott, 1981) indicates that the absence of Sunblood Formation in northwest Coal River results from a lateral facies change from Sunblood carbonate rocks to Road River Group clastic strata on the western margin of the Ordovician Sunblood carbonate platform.

The Sunblood Formation was deposited in a widespread sub-tidal, carbonate platform environment up to 100 km wide (Ludvigsen, 1975). It records a transgressive high-stand tract which terminated with a period of erosion in latest Ordovician-Early Silurian time.

It is widely distributed in the southeast Yukon and southwest Northwest Territories. Its western limit lies in the Coal River map area where Road River Group shale occurs in the same stratigraphic position (overlying Rabbitkettle Formation). In the Little Nahanni River map area (150 km northwest) it is in part correlative with the Cambro-Ordovician to Silurian Haywire Formation (Gordey and Anderson, 1993) that is an outer-shelf equivalent of the Rabbitkettle, Broken Skull, Sunblood, and possibly Whittaker formations (Gabrielse *et al.*, 1973). The schematic relations of these units are shown in Figure 17 of Gordey and Anderson (1993) where the Sunblood conformably overlies Broken Skull Formation and is unconformably overlain by Whittaker Formation. All three are relatively thick shelf carbonate units.

On the Macdonald platform in northeastern British Columbia, thick-bedded dolostone of the Middle Ordovician Skoki Formation is equivalent to the Sunblood Formation (Cecile and Norford, 1979; Pyle and Barnes, 2000).

The Sunblood Formation, in the Coal River map area, represents a westward extension of the Mackenzie platform during early and middle Ordovician, including overlap of the Crow Formation. It may also represent a northward extension of the Macdonald platform during the same time interval. Conodont fauna from near its base document its local transgression (expansion) away from the east-central part of the Coal River map area during the early Ordovician to middle Ordovician.

#### **SUCCESSION 4 – ORDOVICIAN(?) TO MIDDLE DEVONIAN**

Succession 4 indicates a south to north facies transition, from thick-bedded carbonate of the Macdonald platform in the south to siliciclastic, marine shale, laminated to thin-bedded limestone, and sandstone of Selwyn basin in the north. In the Coal River map area, carbonate rocks are represented by the undivided Nonda, Muncho-McConnell, Stone and Dunedin formations (collectively map unit **SDc**) which comprise Macdonald platform. The carbonaceous shale and limestone belong to the Road River Group (map units **SDRR** and part of **SMRB**) which represent the southeastern extent of the classic Selwyn basin (see below). In the east-central part of the map area, the Road River Group is underlain by a thin succession of quartzose sandstone to pebbly sandstone (unit **OSS**) of uncertain age.

## Sandstone of Ordovician and/or Silurian age (OSs)

### Introduction

Creamy white, tan to pale grey-weathering, fine-grained, dolomitic sandstone (Unit OSs; Fig. 35) is discontinuously exposed near the eastern edge of the Coal River map area and extends farther east into the adjacent map area. In contrast to Pigage (2009), this unit is assigned to Succession 4 because it is interpreted to represent easterly derived clastic sedimentation in concert with the eastward transgressive extension of Selwyn basin. Known as Meilleur River embayment (Basset and Stout, 1966), this eastward expansion began north of the Coal River map area in the Middle Ordovician and extended more than 200 km into the southwestern Northwest Territories during the Silurian (Cecile and Norford, 1993).

**Figure 35 (right).** Pale grey and light brown-weathering, dolomitic sandstone of Ordovician and/or Silurian age (map unit OSs). From the north bank of a west-flowing stream, 30 km east of Last Mountain and 5 km west of east edge of map area (station 09LP096).

The base of unit OSs is an abrupt change from thick-bedded dolostone of the Sunblood Formation to sandstone, and is probably unconformable (see Fig. 12). At the top, the unit is overlain by the Road River Group. A maximum thickness of 220 m has been estimated from mapping along the Beaver River (Fig. 36, below; NTS 95D/09).



**Figure 36 (left).** Dark-weathering sandstone of unit OSs is estimated to be 220 m thick in this exposure just north of the Beaver River, 1 km northeast of upper Toobally Lake.

### Composition

Quartz-rich, non-calcareous to slightly calcareous, quartzose to arkosic sandstone forms beds from 10 cm to 2 m thick. The sandstone weathers with a tan to orange-brown surface coating. Fine to medium, subround to round, sand clasts are predominantly monocrystalline quartz. Other clasts, in minor amounts, include black shale, quartz sandstone, K-feldspar, plagioclase, volcanic rock and chert.

Interbedded with the sandstone are lesser amounts of recessive-weathering, bioturbated, dolomitic siltstone and minor pebbly sandstone to conglomerate. The dolomitic siltstone is light grey and weathers tan. It contains minor, discontinuous, dark grey, shaly partings. Pebbles in the pebbly sandstone to conglomerate consist predominantly of white, blue and lesser pale green quartz pebbles in a quartz sand matrix. Typically they are matrix-supported, although locally they are extensive enough to be clast-supported.

### Age, Correlation and Depositional Setting

Diagnostic fossils constraining the depositional age have not been found. The unit is broadly constrained by the known ages of the underlying Sunblood Formation (Middle Ordovician) and overlying Road River Group (early Silurian). Its age range is probably much less as the lower contact is an unconformity.

In northeastern British Columbia, a 180 m-thick interval of interbedded shale and quartzite with minor dolostone occurs in the Road River Group (unit ORD of Cecile and Norford, 1979; Ware member of the Ospika Formation of Pyle and Barnes, 2000); it is of upper Middle Ordovician to Upper Ordovician age and may be a correlative unit. Sandstone is also present on the Macdonald platform within lower Silurian strata in places where the Nonda Formation rests directly on Precambrian basement rocks (Cecile and Norford, 1993).

Unit OSs coarse sandstone and conglomerate are proximal clastic facies, representing a transitional depositional environment from platform carbonate sedimentation to euxinic, basinal siliciclastic sedimentation. Abundant bioturbation in shaly intervals (Pigage, 2009) indicate a below-wave base environment. The unit is missing to the west in the central Coal River map area, and the source provenance is considered to be to the north or east. Primary sedimentary features indicating source direction were not observed.

Detrital zircon geochronology on one sample from unit OSS (09LP093) is shown on a probability density plot and concordia diagram (Fig. 37; analyses in Appendix B). This age distribution corresponds to the Laurentia type I signature of Hadlari *et al.* (2012), consistent with a Canadian Shield provenance.

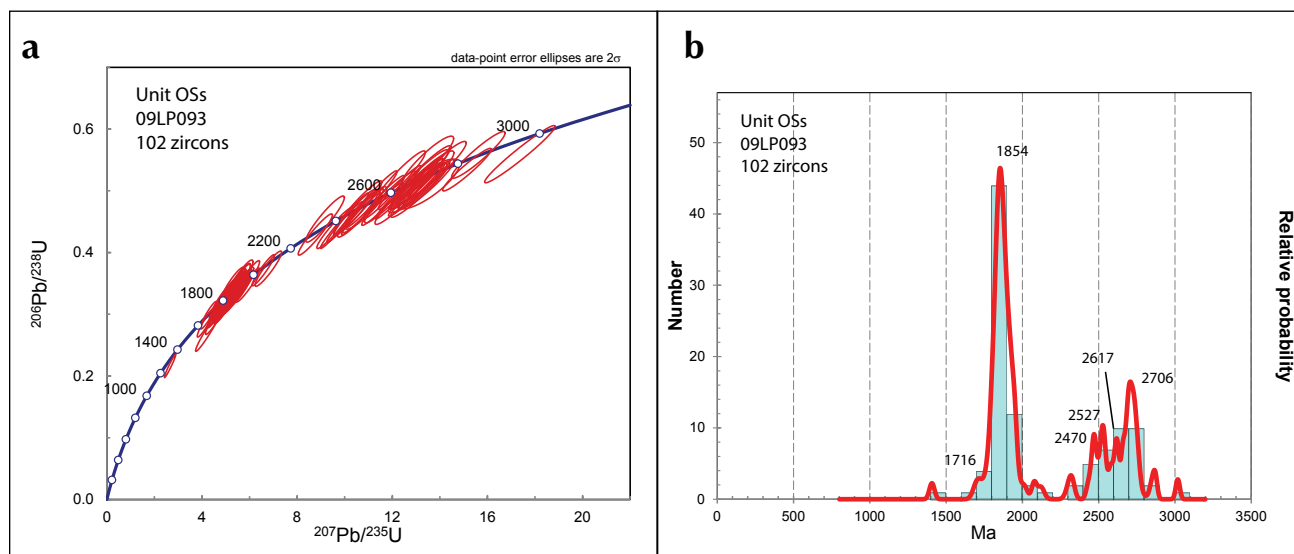


**Figure 37.** Results of geochronological analysis of 102 detrital zircon grains from OSs unit sandstone (sample 09LP093): (a) Concordia diagram; (b) probability distribution diagram. Data and methods are shown in Appendix B (Table B7).

## ***Silurian-Devonian massive carbonate (SDc)***

### **Introduction**

The southern part of the Coal River area contains cliff-forming exposures of thick-bedded, pale grey to cream-weathering dolostone and limestone (Fig. 38), representing the northern extent of the Macdonald platform. They form resistant ridges which exhibit modern karst features. The medium to coarsely crystalline secondary dolostone alteration obliterates distinction of the Nonda, Muncho-McConnell, Stone and Dunedin formations described for the Macdonald platform to the south (Thompson, 1989; Cecile and Norford, 1991, 1993; Taylor and MacKenzie, 1970).

**Figure 38 (right).** *Thick-bedded, pale grey to cream-weathering limestone of unit SDc forms the high-standing hills that constitute the northern extent of the Macdonald platform along the south edge of the map area. Looking northeast near Barney Lake (station 09TOA120).*

The lower contact with the underlying Sunblood Formation is sharp. The upper contact is eroded from much of the southern half of the Coal River map area. The thickness of the remaining strata is approximately 1000 m near Mount Gilliland, immediately east of the Coal River fault. In the southeast, near Smith River, the carbonate succession is many tens to hundreds of metres thick; the upper contact with the overlying Besa River Formation is abrupt.

### **Composition**

Bedding in the carbonate rocks is locally visible and generally ranges from 1-10 m in thickness. Metre-scale, convex-upward domes in the beds likely represent algal mounds, while darker bands commonly contain lighter-coloured macrofossils, including pelecypods, brachiopods, corals and crinoid hash. Areas of white to grey dolostone are totally recrystallized and sucrosic in places, reflecting diagenetic alteration. Post-depositional brecciation (Fig. 39) is extensive, with development of vugs up to 2 cm across. Vugs and clasts commonly are enclosed by cream hydrothermal dolomite.

Internal stratigraphic divisions within the carbonate could not be readily distinguished in the Coal River area. Strata comprising this unit can be separated into multiple formations to the east (e.g., Pigage, 2009) and to the south on the Macdonald platform (e.g., Taylor and MacKenzie, 1970; Morrow, 1978; Ferri *et al.*, 1999).



**Figure 39.** *Limestone of the undifferentiated SDc unit that has been brecciated with abundant secondary calcite (white). Hilltop 1 km northwest of Mount Gilliland (station 09TOA178). Hammer handle is 45 cm long.*

## Age, Correlation and Depositional Setting

Two fossil collections in the lower part of the unit northwest of Mount Gilliland are of Silurian age (Appendix A); Road River shale and limestone in the same stratigraphic position contain Silurian graptolites. A collection near the top of Mount Gilliland is Early Devonian. Near Tropical Creek, in the southeast, the carbonate locally contains recognizable crinoid columns with twin axial canals (2-hole crinoids), indicating their Early to Middle Devonian age. Contiguous carbonate in the Rabbit River map area to the south are of Early and Middle Devonian age (Gabrielse, 1963).

Unit **SDC** constitutes the northern edge of the Macdonald platform, which in British Columbia ranges in age from Ordovician through Middle Devonian. It includes the Nonda, Muncho-McConnell, Stone and Dunedin formations as a dominantly carbonate tract extending 500 km south-southeast from the Coal River map area. Regionally the Macdonald platform strata unconformably overlie Cambrian and older units (e.g., McMechan *et al.*, 2012), implying preceding uplift and erosion. The northward transition to Road River Group shale appears to be abrupt with the shale facies being present near Lootz Lake. Time-equivalent rocks of the Mackenzie platform (nearest point is 260 km north of unit **SDC**) include the Camsell, Sombre, Arnica, Grizzly Bear, Funeral, Delorme, Whittaker, Tsetso, Mount Kindle, Franklin Mountain, Nahanni, Headless, Bear Rock, Hume and Natla formations (Gabrielse *et al.*, 1973; Gordey and Anderson, 1993; Cecile and Norford, 1993; Morrow and Geldsetzer, 1991).

## Road River Group (SDRR, SMRB)

### Introduction

Jackson and Lenz (1962) defined the Road River Formation as Lower Cambrian to Lower Devonian strata in northern Yukon (Richardson trough) with a type section where the base was faulted. Gabrielse *et al.* (1973) extended the unit into the Selwyn basin and later into the Northern Rocky Mountains. Fritz (1985) and Gordey and Anderson (1993) elevated the Road River Formation to formal group status, although some regional publications (e.g., Cecile, 2000) avoid the term in favour of more precise formation nomenclature. In this report the breadth of Road River Group is appropriate because internal stratigraphic boundaries and defining paleontologic control are lacking.

Recessive weathering, carbonaceous, silty shale, limestone, dolostone, siltstone, and chert of the Road River Group are exposed along rivers, streams and glacial meltwater channels in the Coal River map area. The base is abrupt and marked by the first appearance of a carbonaceous, locally graptolitic unit. In most areas it unconformably overlies the Sunblood Formation. In areas where Unit **OSs** is present, carbonaceous strata abruptly overlie this sandstone unit. In the westernmost part of the map area it abruptly overlies the Rabbitkettle Formation. In much of the northern Coal River area carbonaceous shale of the Road River Group is conformably overlain by carbonaceous shale of the Besa River Formation.

In northern British Columbia the Kwadacha Formation (Pyle and Barnes, 2000) consists of tan-weathering, dolomitic, bioturbated siltstone forming the uppermost unit in the Road River Group. The Steel Formation (Gordey and Anderson, 1993) in the Little Nahanni map area (NTS 1051) is a similar unit that occurs in the same stratigraphic position. This distinctive lithology is a useful marker horizon for delineating the top of the Road River Group and the base of the overlying shale (like the Besa River Formation). Tan-weathering siltstone outcrops that resemble the Steel Formation were observed along the Coal River in the northwest corner of the map area. We were not able to identify this siltstone unit along Spruce Creek and in the northern part of the map area, resulting in the use of a combined map unit (**SMRB**) encompassing Road River and Besa River strata.

Near Spruce Creek the estimated thickness of the Road River Group is approximately 200 m and the estimated thickness of the Besa River Formation in the same general area is approximately 300 m. The combined unit has a similar thickness in the Last Mountain area. In the northeastern quadrant of the map area its broad extent and deep exposure in the Caribou River canyon suggests structural thickening by internal reverse faults and folds.

### Composition

The dominant lithology of the Road River Group in Coal River map area is a dark grey to black, noncalcareous to calcareous, locally graptolitic, silty shale (Fig. 40). Another major lithology is a dark grey, thin-bedded, silty limestone or dolostone (Fig. 41), locally containing thin black, discontinuous chert lenses or beds (Fig. 42). Intervals of dark grey to black, bedded chert also occur locally. The common distinctive characteristics of the Road River Group are the dark grey to black colour related to high organic material and the local occurrence of graptolites, especially near the base of the unit.



**Figure 40.** Dark grey, locally graptolitic, silty shale of the Road River Group. From glacial meltwater channel about 9 km north of Lootz Lake (station 09LP074).



**Figure 41.** Dark grey, silty, parallel-laminated limestone of Road River Formation. From 7.5 km north of Lootz Lake (station 09LP062).

### Age, Correlation and Depositional Setting

Fossil collections from previous work in the Coal River and LaBiche River map areas indicate an age range of lower Silurian to Lower Devonian for the Road River Group (Gabrielse and Blusson, 1969; Pigage, 2009). Fossil collections from the 2009 fieldwork are consistent with that age assignment (Appendix A). Lenses of limestone containing two-hole crinoids (Fig. 43) were observed in outcrops on the Coal River in the northwest part of the Coal River map area, indicating an Early to early Middle Devonian (Emsian to Eifelian) age. Abbott (1981) reported a Lower Ordovician conodont sample collected from the Road River Group from NTS 95E (north of the Coal River area), indicating that in the northwestern part of the Coal River map area



**Figure 42.** Grey dolostone with discontinuous black chert layers, Road River Group. On Spruce Creek (station 09LP091). Scale divisions are in cm.

the lower Road River Group probably includes Ordovician carbonaceous strata. Northwestward across Selwyn basin Road River Group is widespread, in some areas divided into Duo Lake or Elmer Creek formations, overlain by Steel Formation (see Fig. 12).



**Figure 43.** Limestone containing two hole crinoids indicative of Early to Middle Devonian age, undivided Road River-Besa River map unit. Outcrop on the Coal River 4 km west of Mt. Skonseng (station 10TOA005). Canadian coin is 2.5 cm in diameter.

The Macdonald platform units – Skoki, Nonda, Muncho-McConnell, Wokkash, Stone and Dunedin formations (Morrow and Geldsetzer, 1991) are time-correlative with Road River Group. On the Mackenzie platform, Camsell, Sombre, Arnica, Grizzly Bear, Bear Rock, Funeral and Natla formations (Morrow and Geldsetzer, 1991) are time-correlative with Road River Group.

Road River Group abruptly overlies sandstone and carbonate, attesting to a rapid change to a deeper water depositional environment. The dark, thin-bedded shale reflects reduced conditions, although the presence of deep-water limestone indicates deposition above the carbonate compensation depth. Chert deposition suggests that the basin was relatively starved of clastic input.

## SUCCESSION 5 – MIDDLE DEVONIAN TO TRIASSIC

The single depositional entity Selwyn basin was destroyed by uplift (locally block faulting) in Middle Devonian time (Gordey and Anderson, 1993). Subsequent Middle Devonian through Triassic strata are preserved in the eastern half of the Coal River map area as three sequences separated by regional unconformities. They record alternating regional transgressions and regressions in a broad, shallow marine depositional environment. Map units are the Middle Devonian to Lower Mississippian Besa River Formation (DMBR, SMRB), the Mississippian Mattson Formation (MM), the Permian Fantasque Formation (PF) and the Triassic undivided Grayling and Toad formations (TGT).

### ***Besa River Formation*** (DMBR, SMRB)

#### **Introduction**

Recessive, dark grey to black, pale grey-weathering, noncalcareous, silty shale with lesser interbeds of tan-weathering sandstone and limestone (Fig. 44) outcrop extensively along streams and rivers in the southeast part of the map area, constituting the Besa River Formation (Kidd, 1963). In the southeast Coal River map area, the lower contact with the underlying SDC unit of the Macdonald carbonate platform is sharp. In the northern Coal River map area, the similar units of the Besa River Formation and the underlying Road River Group mean that the lower contact of the Besa River Formation is not accurately located, and the nature of the contact is unknown. Exposures of dark silty shale lacking stratigraphic context could not be attributed with certainty to either Road River Group or Besa River Formation and thus were mapped as a combined unit (SMRB). The upper contact with the overlying

Mattson Formation is gradational over tens of metres; the contact is placed at the first major bed of indurated, grey, quartzose sandstone.

The type section, about 200 km southeast of Coal River map area, is 672 m thick (Kidd, 1963). Besa River Formation thins northwestward (Bamber *et al.*, 1968) and a thickness of greater than 300 m is estimated from exposures in the Spruce Creek area. Greater thicknesses in the northern part of the map area most likely result from structural thickening.



**Figure 44.** Outcrop exposure of the Besa River Formation, consisting of brown and grey-weathering, noncalcareous, silty shale with interbeds of tan-weathering sandstone and limestone. Looking northward at cliffs above Spruce Creek, 14 km west of Toobally Lakes (station 09TOA131).

### Composition

The predominant lithology consists of dark grey to black, thin-bedded, noncalcareous, silty shale that locally is pale grey or rusty brown-weathering (Fig. 45). Bedding is typically on a scale of 1-5 cm. Some intervals are siliceous enough to be considered porcellanites. The silty shale commonly contains limestone nodules up to 2 m in diameter (Fig. 46). Interbeds of dark grey limestone up to 10 m thick occur locally.



**Figure 45.** Rusty brown to dark grey-weathering exposure of black, silty shale of the undivided Road River-Besa River map unit. Outcrop is 3 m high. Exposure on the Beaver River 2 km north of upper Toobally Lake (station 09LP077).



**Figure 46.** Limestone nodules or concretions in silty shale of the undivided Road River-Besa River map unit in the headwaters of the Coal River (southern Flat River map area; station 10TOA006). Hammer handle is 45 cm long.

## Age, Correlation and Depositional Setting

Two conodont samples collected immediately east of Coal River map area are Devonian to Mississippian (Table IV-10 in Pigage, 2009). Both upper and lower contacts are diachronous with the age range decreasing in an eastward direction (Bamber and Mamet, 1978; Richards, 1989); the maximum age range is from Middle Devonian (Giventionian) to Middle Mississippian (Viséan). Bamber and Mamet (1978) described the westward shaleout of Dunedin Formation carbonate rocks to Besa River Formation in northeastern British Columbia.

In southeast Yukon and southwest Northwest Territories Besa River Formation is laterally equivalent to the carbonate rocks of the Pekisko, Prophet and Flett formations and the clastic sediments of the Yohin, Clausen and Golata formations (Richards, 1989). In northeastern British Columbia, Besa River Formation is correlative with carbonate rocks of the Upper Keg River, Slave Point, Kakiska, Trout River, Tetcho, Kotcho, Banff, Pekisko, Shunda and Debolt formations and with shales of the Horn River, Muskwa, Fort Simpson, Exshaw and Golata formations (Ferri *et al.*, 2011). In Selwyn basin and Kechika trough, Besa River Formation is laterally equivalent to the Earn Group (Gordey, 1991; Ferri *et al.*, 2011).

The western margin of Laurentia was inundated by dark clastic sediments between Middle Devonian and Middle Mississippian time; this diachronous transgression eastward extended well into the North American interior. The dark clastic sediments overlie early Paleozoic platform and basin depositional elements.

Three Devonian-Mississippian clastic assemblages were deposited in Yukon: the Earn assemblage, the Imperial assemblage and the Besa River assemblage (Gordey, 1991). In northern Yukon the Imperial assemblage shale, siltstone and sandstone delineate the westward and southwestward influx of coarse foreland clastic sediments from the Ellesmerian orogeny (Pugh, 1983; Norris, 1985). Northwest and southwest of the Coal River map area the Earn assemblage consists of black shale and siltstone interbedded with sandstone and chert pebble conglomerate; the clasts were derived from eroded Selwyn basin units and deposited in submarine channels and fans (Gordey *et al.*, 1982; Gordey and Anderson, 1993; Gordey, 2013). Extension and local contraction in the outer parts of Selwyn basin and Kechika trough (Abbott *et al.*, 1986; Gordey *et al.*, 1982) during rifting or transtensional extension can account for the northwest to west provenance of Earn Group sediments. In contrast the Besa River Formation occurs immediately northwest (outboard) of barrier reefs (Ferri *et al.*, 2011) with extensive back-reef evaporates and sediments to the southeast. Richards (1989) considered the fine-grained, clastic sediments of the Besa River Formation to be derived from a north to northeast source.

## **Mattson Formation (MM)**

### **Introduction**

Pale grey and rusty-brown-weathering sandstone interbedded with shale is exposed in the Caribou syncline and comprises a strip trending north from Toobally Lakes. These are the westernmost outliers of the Mattson Formation (Patton, 1958) that is widely exposed in southeast Yukon and eastward to the Liard River in the Franklin Mountains. Reddish orange transported gossans are common where streams incise this unit.

The lower contact is conformable, placed at the base of the first major sandstone bed (Fig. 47) above Besa River shale. Shale-rich strata of the middle Permian Fantasque Formation unconformably overlie the Mattson Formation. Near Last Mountain the Mattson Formation is estimated to be 500 m thick. At the type locality, 31 km west of Nahanni Butte, it is 1138 m thick (Patton, 1958), and the greatest known thickness, 1410 m (Richards, 1989), is 60 km east of the Coal River map area near the Yukon-NWT border.

## Composition

Grey, thick-bedded, fine-grained, quartz sandstone (Fig. 48) is the predominant lithology. Bedding is rarely observed and few other primary sedimentary features are visible in the sandstone. The sandstone contains minor interbeds of dark grey to black, noncalcareous shale. In the northeastern part of the map area, the middle of the formation consists of thick, noncalcareous, black shale with quartzose sandstone above and below it. The Last Mountain barite occurrence is at, or near, the base of the Mattson Formation.



**Figure 47.** Grey and brown-weathering sandstone interbedded with recessive shale of the Mattson Formation. Looking northward at Last Mountain, northeast Coal River map area.



**Figure 48.** Thick-bedded, quartz sandstone of Mattson Formation. From ridgetop 5 km north of Spruce Creek (station 09LP090).

## Age, Correlation and Depositional Setting

Fossils were not found in the Mattson Formation in the Coal River map area. East of the map area conodonts from the carbonate-bearing upper part of the formation are Viséan to Serpukhovian (Table IV-4 in Pigage, 2009), similar to those from thicker intervals farther east, indicating a Middle to Late Mississippian age (Richards *et al.*, 1993).

The Mattson Formation correlates with the Stoddart Group (Rutgers, 1958; Bamber and Mamet, 1978) in northeastern British Columbia. Time-equivalent and lithologically identical units to the north and northwest are the Heritage Trail Formation of the Tischu Group (Cecile, 2000; Martel *et al.*, 2012) on the Northwest Territories-Yukon border, and the Keno Hill quartzite, north of Dawson City, Yukon (Tempelman-Kluit, 1970; Gordey and Anderson, 1993).

Regionally the Mattson Formation constitutes a large, south to southwest-prograding delta complex with interbedded eolian sand, coal, fluvial deposits, channel-fill deposits, submarine channels, and delta shoreline deposits (Richards *et al.*, 1993). The scarcity of heavy minerals and non-quartz clasts in the sandstone suggests the grains are multicyclic, representing more than one weathering cycle. Paleocurrents and spatial relationships between delta plain and marine lithofacies indicate a northern provenance (Richards, 1989; Fallas, *et al.*, 2002).

Detrital zircon geochronology was completed on one sandstone sample (09LP090) from the Mattson Formation. Analytical results are listed in Appendix B; the probability distribution and Concordia plots are shown in Figure 49. The youngest zircons form a peak at 432 Ma. The distribution of zircon grain ages, from Mesoproterozoic to Archean, is consistent with the Laurentia type II signature of Hadlari

et al. (2012); the detrital zircon grains are likely recycled from erosion of Paleozoic and Proterozoic strata. Lemieux et al. (2011), Beranek, et al. (2010) and Leslie (2009) noted that early Paleozoic to Neoproterozoic detrital zircon ages first appear in Cordilleran strata in Late Devonian to Mississippian time with the influx of clastic sediments from a northern exotic source region contributing detrital zircons. Suggested exotic source regions include Baltica, Siberia, or the east Greenland Caledonides (Lemieux et al., 2011; Beranek et al., 2010).

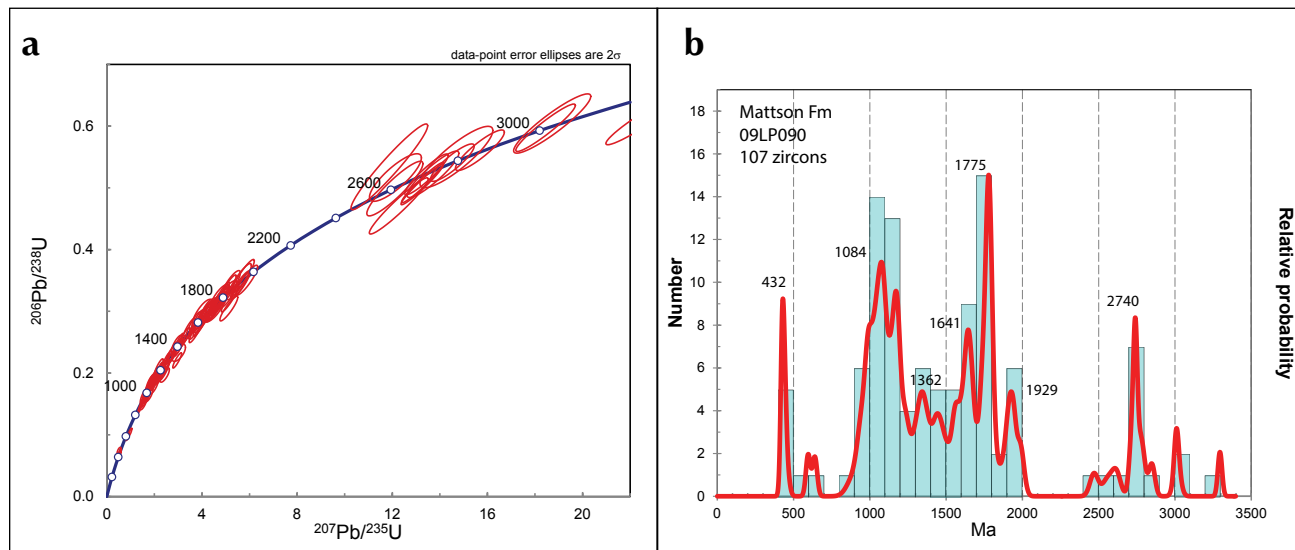


**Figure 49.** Results of geochronological analysis of 107 detrital zircon grains from Mattson Formation sandstone (sample 09LP090): (a) Concordia diagram; (b) probability distribution diagram. Data and methods are shown in Appendix B (Table B8).

## Fantasque Formation (PF)

### Introduction

Rusty brown-weathering, dark grey, siliceous shale in the eastern part of the Coal River map area is assigned to the Permian Fantasque Formation (Harker, 1961). It unconformably overlies the Mattson Formation and is in turn unconformably overlain by the Triassic Grayling-Toad unit. Its thickness ranges from 1000 m (northeast Coal River map area) to 1700 m (upper Toobally Lake area). At its type section (about 100 km east of Toobally Lakes) however, its thickness is 180 m. It is therefore possible that in the Coal River map area it is tectonically thickened or may include some of the underlying Tika unit (K. Fallas, pers. comm., 2014).

### Composition

The formation consists predominantly of rusty brown-weathering, dark grey, siliceous shale (Fig. 50). The shale is internally bedded on a scale of 5 to 20 cm. Beds with abundant limestone nodules are scattered through the shale succession (Figs. 50 and 51). In the upper Toobally Lakes area the formation contains a thin-bedded, dark grey limestone interval estimated to be 800 m thick (Pigage 2009); poor outcrop precludes determining where this carbonate interval occurs within the formation. This limestone was not encountered elsewhere in the Coal River map area.



**Figure 50.** Rusty brown-weathering, dark grey, siliceous shale of the Fantasque Formation. Bedding dips steeply to the right in the photograph; slaty cleavage dips moderately to the left. Limestone nodules visible locally. From the core of the Skinboat syncline, in northeastern Coal River area (station 09TOA203).



**Figure 51.** Large limestone nodule in siliceous shale of Fantasque Formation. From 700 m east of upper Toobally Lake (station 04LP013). Hammer head is 20 cm long.

### Age, Correlation and Depositional Setting

A conodont sample from the east side of upper Toobally Lake was broadly Permian; another three were of indeterminate age (Table IV-12 in Pigage, 2009). Regionally the Fantasque Formation is upper Artinskian through Wordian (early Permian through middle Permian) (Bamber *et al.*, 1968; Henderson *et al.*, 1993). Sponge spicules are the diagnostic fauna for this unit although an elasmobranch fish impression was found near the base of the formation (Harker, 1961).

The Fantasque Formation is a thin but laterally persistent unit from Pine Pass throughout northeastern British Columbia and extends to the southern Mackenzie Mountains. Regionally the shale is typically interbedded with chert, and siltstone interbeds contain lag deposits of phosphate, chert pebbles, and chert nodules. It reflects a slope to basinal environment.

Correlative strata in the Rocky Mountains to the southeast include the Ranger Canyon and Mowitch formations of the Ishbel Group (Henderson *et al.*, 1993). In central Yukon correlative strata include the Mount Christie Formation, defined in Little Nahanni River map area (100 km north of the Coal River), consisting of buff to orange weathering shale, siliceous shale, chert, and minor sandstone of Early Permian age (Gordey and Anderson, 1993). In the southern Ogilvie Mountains correlative units are a mid-Permian limestone, the Takhandit Formation, and overlying green and red slate with minor chert (Green, 1972). The Fantasque Formation was deposited in a shallow water marine environment, below wave base.

### **Undivided Grayling and Toad formations (TGT)**

#### **Introduction**

A single locality of Triassic strata in the Coal River map area occurs on the northwest side of upper Toobally Lake in the immediate footwall of the Toobally reverse fault. Outcrops of Triassic strata are sparse in southeast Yukon and previously mapped as undivided Grayling and Toad formations (Kindle, 1944; Fallas and Lane, 2001). It lies unconformably on the Fantasque Formation (Permian), and is unconformably overlain by Cretaceous strata to the east. In its type area, Grayling Formation (Lower

Triassic) is 305 m thick, conformably overlain by up to 730 m of Toad Formation (Middle Triassic) (Kindle, 1944).

### Composition

The exposure consists of dark grey, soft, recessive shale (Fig. 52) and lesser interbedded thin, tan-weathering sandstone. Mica is locally visible on the slaty cleavage surfaces of the shale. Thin interbeds of greenish grey, very fine grained sandstone reveal small load clasts, possible gutter casts and poorly preserved horizontal burrows. Both the shale and sandstone are locally concretionary (Pigage, 2009).



**Figure 52.** Dark grey, soft, recessive shale interbedded with thin, tan-weathering sandstone comprise the undivided Grayling-Toad unit. In the immediate footwall of the Toobally fault on the west side of upper Toobally Lake (station 03LP008).

### Age, Correlation, and Depositional Setting

Pollen samples for this unit in the Coal River area were identified as Lower Triassic with abundant Middle and Upper Devonian reworked spores (Pigage, 2009).

The unit is unlikely to be present elsewhere in the eastern Coal River map area, but is extensive (although poorly exposed) to the east and southeast. Correlation in the subsurface to the southeast includes the gas-bearing Montney and Doig formations (Gibson, 1993; Dixon, 2009). Northwest of the Coal River map area, the Jones Lake Formation, of late Middle to Late Triassic (Ladinian to Norian) age, is a correlative siltstone, sandstone and shale unit about 750 m thick (Gordey and Anderson, 1993).

Five facies associations are recognized in detailed sections measured to the east in NTS 95C/1 and NTS 95C/2 (MacNaughton, 2002). These facies associations are interpreted to represent depositional environments on a wave-dominated shelf, ranging from relatively distal, sand-poor settings below storm wave base to high-energy, proximal sand-rich, mid to upper shoreface settings. Sandstone from the Jones Lake Formation yielded Mississippian detrital zircons, a likely indication that Yukon-Tanana terrane elements were contributing to the shallow marine shelf sediments (Beranek *et al.*, 2010).

### SUCCESSION 6 – PALEOCENE TO LATE EOCENE

Two widely separated exposures constitute this succession. The western tip of an east-trending ridge projects into the Coal River map area at 60°28'N. In the north-central part of the map area, the Rock River valley contains exposures of poorly consolidated sediments over a 50 by 4 km area.

## ***Paleocene unconsolidated sediments* (PSSC)**

### **Introduction**

A greater than 160 m-thick succession of flat-lying, siltstone, sandstone and conglomerate unconformably overlies folded Road River Group strata. The upper extent of the unit is eroded.

### **Composition**

This outcrop extends eastward into the Pool Creek map area (NTS 95C/5), where its greater exposure permitted more thorough observation of bedding and lithologic variation (Pigage, 2009). There it consists predominantly of poorly consolidated pebbly sandstone with thinner interbeds of clay siltstone to mudstone and highly variable 'red beds'. Siltstone intervals are discontinuous across the section, occurring as thin lenses up to 20 m long. The uppermost sedimentary unit is a coarse, clast-supported conglomerate up to 21 m thick. The dominant clast component in the conglomerate is grey quartzite. The succession is capped by remnants of a Paleocene trachytic, locally columnar-jointed, olivine alkali basalt flow up to 20 m thick.

### **Age, Correlation and Depositional Setting**

A whole rock sample of the basalt flow was dated at  $56.7 \pm 0.7$  Ma using  $^{39}\text{Ar}/^{40}\text{Ar}$  methods (Pigage, 2009), providing a minimum late Paleocene age for the sediments.

The strata indicate a subaerial, fluvial depositional environment. Imbrication and bar forms indicate an east to southeast paleoflow direction (Pigage, 2009).

## ***Eocene Rock River basin, coal-bearing sediments* (ERR)**

### **Introduction**

Eocene strata are poorly exposed along the banks of the Rock River, and in diamond drill core from coal exploration in the Rock River valley in 1986 and 2006. Drill holes penetrated Cenozoic sediments to a depth of 445 m (Aurora Geosciences Ltd., personal communication 2014). Gravity surveys on east-west lines were used to calculate an 1100 m thickness for the poorly consolidated sediments overlying lower Paleozoic sedimentary rocks in the northern part of the basin (Wright and Miller, 1986). The lower contact is unconformable, and there are no overlying units recognized.

### **Composition**

The succession is dominated by drab, dark to light grey, poorly consolidated mudstone with thin sandstone beds and thick lenses of coal (Long and Sweet, 1994; Wright and Miller, 1986). The coal horizon in the single outcrop exposure is over 5 m thick; in two drill holes, coal seams up to 4.7 m thick amounted to about 50% of the core (Wright and Miller, 1986). Bedding in the single outcrop of Tertiary strata dips about  $15^\circ$  westward.

### **Age, Correlation and Depositional Setting**

Cenozoic strata encountered in the drill holes have a late Eocene age based on palynology (Long and Sweet, 1994). They were deposited in floodplains or wetlands associated with a stable single or multiple-channel fluvial system (Long and Sweet, 1994).

In early Cenozoic time several intermontane depositional basins or half-grabens developed along active extensional faults in eastern Yukon and adjacent Northwest Territories (320 km north-northwest; see Martel *et al.*, 2012). The west side of the poorly consolidated sediments in the north-central part of the Coal River map area is a postulated normal fault; the eastern limit is eroded. We interpret these to be remnants of a depositional basin whose strike length is approximately 50 km (based upon its gravity expression; Wright and Miller, 1986), and maximum width is 4 km.

## **IGNEOUS ROCKS**

### ***Introduction***

Coal River map area contains several volcanic rock horizons within Proterozoic through Late Ordovician strata. The exposures range from approximately 50 m to about 1300 m thick, consisting of multiple flow units, breccia and tuff. Similar textural characteristics and geochemistry warrant their treatment together in this section.

Fifteen plutons are currently known in the northern half of the Coal River map area. Most are small and poorly exposed, underlying heavily forested areas. Age dating and chemical analysis indicate that most of the plutons have a similar chemistry, with crystallization ages between 97 Ma and 100 Ma (Pigage *et al.*, 2014).

### ***Cambrian-Ordovician Alkali Basalt (PЄVN-v, ЄOC-v, ЄOR-v, and OSu-v)***

#### **Introduction**

Lenticular belts of volcanic rock are present within the undivided Vampire-Narchilla unit, Crow Formation, Rabbitkettle Formation, and Sunblood Formation. Based upon the ages of the sedimentary units that overlie and underlie them they range from early Cambrian to Late Ordovician, thus representing a protracted interval of intermittent volcanism. Texturally the flows include massive, pillowed, and autobrecciated variants; these intercalations have been described previously with their respective stratigraphic units. Their volumetric abundance is minor and few dikes were noted outside of the immediate area of the volcanic rocks. It is surmised that these occurrences are remnants from many isolated extrusions, rather than a few eruptions of widespread extent.

The geochemical character of the different volcanic units is presented in this section. Whole rock and trace element analyses were completed on samples from the different volcanic units (Fig. 53); the analyses are presented in Appendix C. Samples were selected to avoid amygdules, veins, or alteration in fractures. All volcanic exposures contain secondary minerals, likely resulting from seawater alteration and burial and subsequent metamorphism. Volcanic rocks in the map area have been metamorphosed to at least lower greenschist facies based upon ubiquitous chlorite. Typical alteration includes modification of the alkali content, increase in carbonate and water (volatiles) and oxidation of the iron content (e.g., Rollinson, 1993). The moderate to large loss-on-ignition (LOI) contents in these samples attest to mobilization of some major and trace elements. Immobile elements during alteration and metamorphism have been utilized to minimize the effects of alteration and metamorphism and eliminate errors of classification (Pearce and Cann, 1973; Wood, 1980; Jenner, 1996).

#### **Undivided Vampire-Narchilla unit volcanic rocks (PЄVN-v)**

Two diabase dike samples and two samples from a flow within the Vampire-Narchilla unit differ in subtle ways from the other Paleozoic igneous rocks. They were selected from outcrops in a 17 km long, 1300 m wide area of this unit west of the Rock River fault (Plate 1). Based upon these samples, the total-iron to magnesium ratio is ~4; Cr and Ni content are below 20 ppm; and Nb is low (80-115 ppm).

TiO<sub>2</sub> is low (2.06-2.8%) and Zr ranges from 24 to 401 ppm (the latter may reflect the presence of a zircon crystal in the sample). These rocks contain high Ba (826-1095 ppm), and the Na<sub>2</sub>O to K<sub>2</sub>O ratio is 1.5-2. On the Zr/Ti vs Nb/Y composition plot (Pearce, 1996) these few samples occupy the alkali basalt field (Fig. 54a); trace element values normalized to primitive mantle broadly have an ocean island basalt (OIB) signature; the samples show significant depletions in Zr, Hf and Ti (Fig. 54b). The low vanadium content of all samples places them well away from the volcanic arc trend (Fig. 54c; Shervais, 1982).

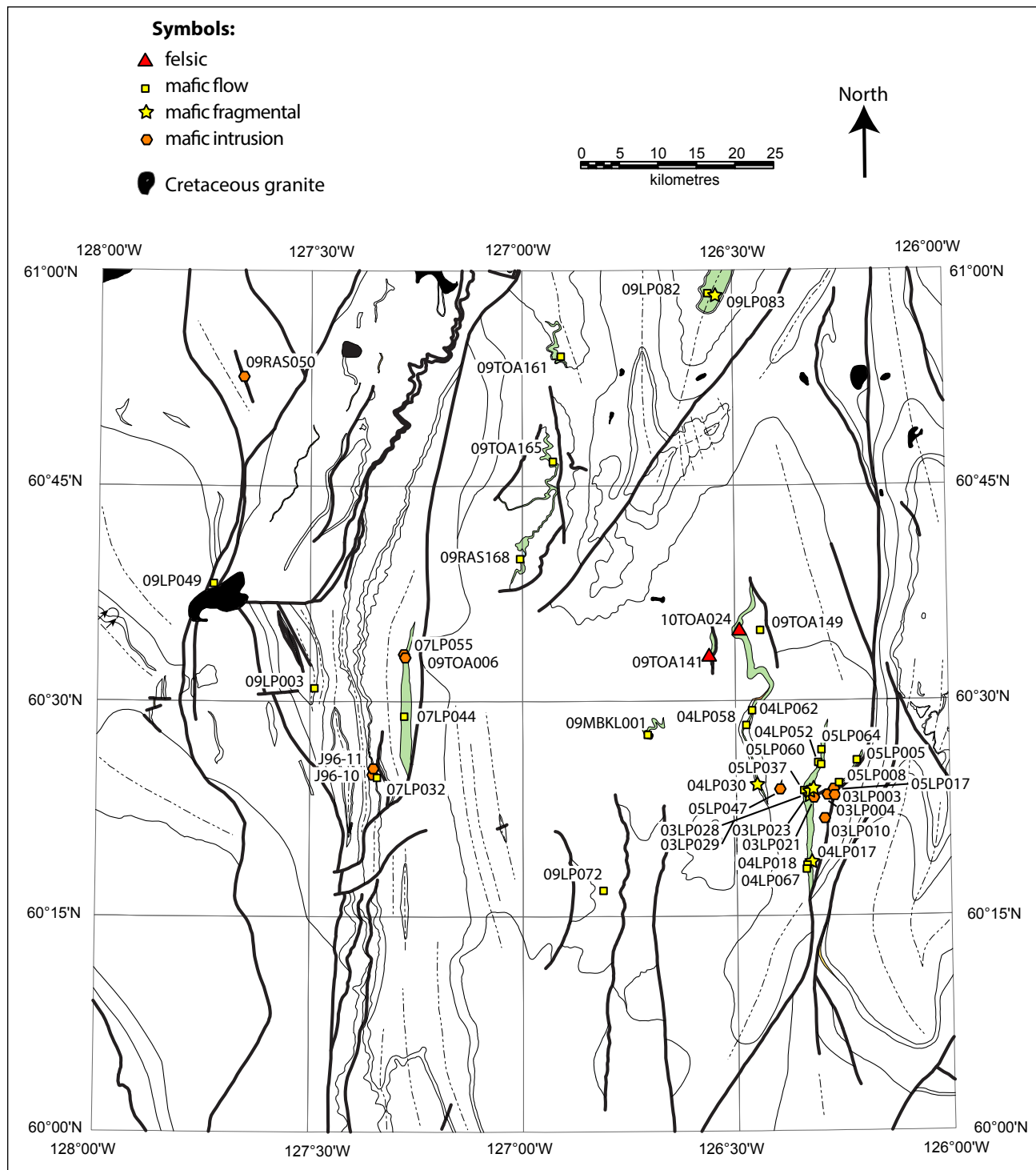


**Figure 53.** Distribution of volcanic rocks intercalated within four formations of the Coal River map area. Numbers indicate sample locations for geochemistry (Appendix C, Tables C1-C4).

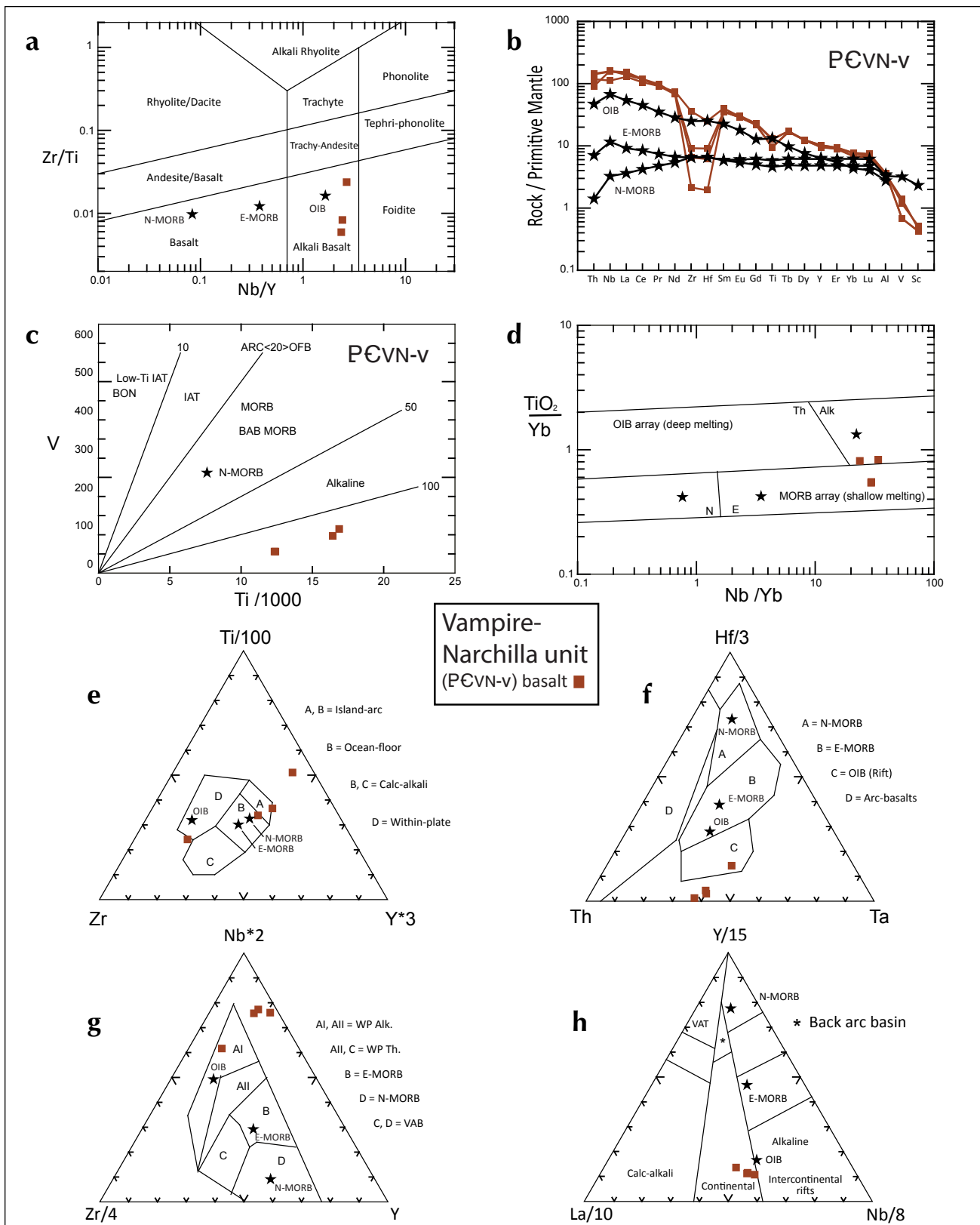


**Figure 54.** Geochemical and tectonic discriminant diagrams for volcanic rocks of the undivided Vampire Narchilla unit: (a) Zr/TiO<sub>2</sub>-Nb/Y diagram of Winchester and Floyd (1977), as modified by Pearce (1996); (b) primitive mantle-normalized, multi-element diagram; (c) Ti/V diagram of Shervais (1982); (d) TiO<sub>2</sub>/Yb-Nb/Y diagram of Pearce (2008); (e) Zr-Ti-Y diagram of Pearce and Cann (1973) for tholeiitic basalt; (f) Th-Hf-Ta diagram of Wood (1980); (g) Zr-Nb-Y diagram of Meschede (1986); and (h) La-Y-Nb diagram of Cabanis and Lecolle (1989) for basalt.

In general these rocks are poorly discriminated on ternary diagrams (Fig. 54e-h). They straddle multiple fields on the ternary Ti-Zr-Y plot designed for tholeiitic basalt (Fig. 54e; Pearce and Cann, 1973), and are so low in Hf and Zr that most plot outside the established fields on the other diagrams (Fig. 54f,g).

The alkali basalt designation is confirmed by Figure 54a,c,d. Figure 54b and d suggest an enriched mantle source with minimal to no crustal contamination; limited crustal contamination of the magma suggests rapid extrusion from the mantle source area.

### **Crow Formation volcanic rocks (€OC-v)**

Volcanic rocks form narrow belts of exposure within the Crow Formation west of upper Toobally Lake and in the core of the Caribou anticline (Plate 1). The previous study of Pigage (2009) is augmented by additional analyses here. Analyses on eight samples returned a loss-on-ignition (LOI) greater than 10% [flows: 05LP008, 04LP018-1, 05LP060; altered dikes/sills: 03LP003, 03LP010, 03LP017; altered breccia: 03LP023, 04LP017]. The high volatile content likely reflects metamorphism and alteration. These samples also have anomalous CaO (indicative of secondary carbonate); they were not included in the diagrams. Two samples (09TOA141 and 10TOA024) have SiO<sub>2</sub> compositions indicative of andesite to rhyolite; these samples are included in the Appendix C tables but are also excluded from the discriminant and composition diagrams that are appropriate for basaltic rocks.

The total iron to magnesium ratio ranges from 1.5-4, with variable Cr (below 20 to 528 ppm), Ni (69-198 ppm) and uniform Nb (23-48 ppm). TiO<sub>2</sub> is low (1.4-3.3%) as is Zr (87-413 ppm), and P<sub>2</sub>O<sub>5</sub> content is low to moderate (0.18-1.12%). K<sub>2</sub>O is equal to or greater than Na<sub>2</sub>O in half the samples; Ba is either low (<50 ppm) or relatively high (300-946 ppm). From the composition and discriminant plots these rocks are clearly alkaline basalt (Fig. 55a,b,c) in the 'within plate' and OIB fields (Fig. 55e,f,g) with a few samples near the boundary between continental and intercontinental rifts (Fig. 55h). Trace-element and rare earth element (REE) patterns normalized to primitive mantle range between OIB and enriched mid-ocean ridge basalt (E-MORB).

The tectonic discriminant diagrams indicate deep melting of enriched mantle with minimal contamination from crust during ascent (Pearce, 2008; and others listed in the caption for Fig. 54).

### **Rabbitkettle Formation volcanic rocks (€OR-v)**

Five flows, one sill and two undefined samples (from drill core at Jeri-North prospect) represent the igneous component of the Rabbitkettle Formation. Volatile contents range from 3% to 8%; silica contents are typical of basalt. The total iron to magnesium ratio approaches 2, and all have low Nb (10-57 ppm), Cr (40-470 ppm, by ICP-MS) and Ni (below 20 to 240 ppm). TiO<sub>2</sub> ranges from 0.67 to 3.2%, and Zr from 131-272 ppm. The rocks are sodic (Na<sub>2</sub>O: K<sub>2</sub>O is 3-10), and some contain appreciable Ba (up to 1591 ppm).

On the Zr/Ti vs Nb/Y composition diagram the Rabbitkettle volcanic samples are andesitic basalt to alkali basalt (Fig. 56a), the samples plot in both the alkaline, OIB and MORB fields (Fig. 56c,d). On ternary discriminant diagrams, the samples occupy the 'within plate' and OIB fields (Fig. 56e,f,g), although the high La in the samples pulls them into the calc alkaline field (Fig. 56h). The composition normalized to primitive mantle indicates depletions in Nb and Ti for some of the samples (Fig. 56b), suggesting slight crustal contamination for the basalt; this indication of crustal contamination is also suggested by several of the samples plotting above the MORB array in Figure 56d. A continental, within-plate, extensional environment with slight crustal contamination of an enriched mantle source is suggested.

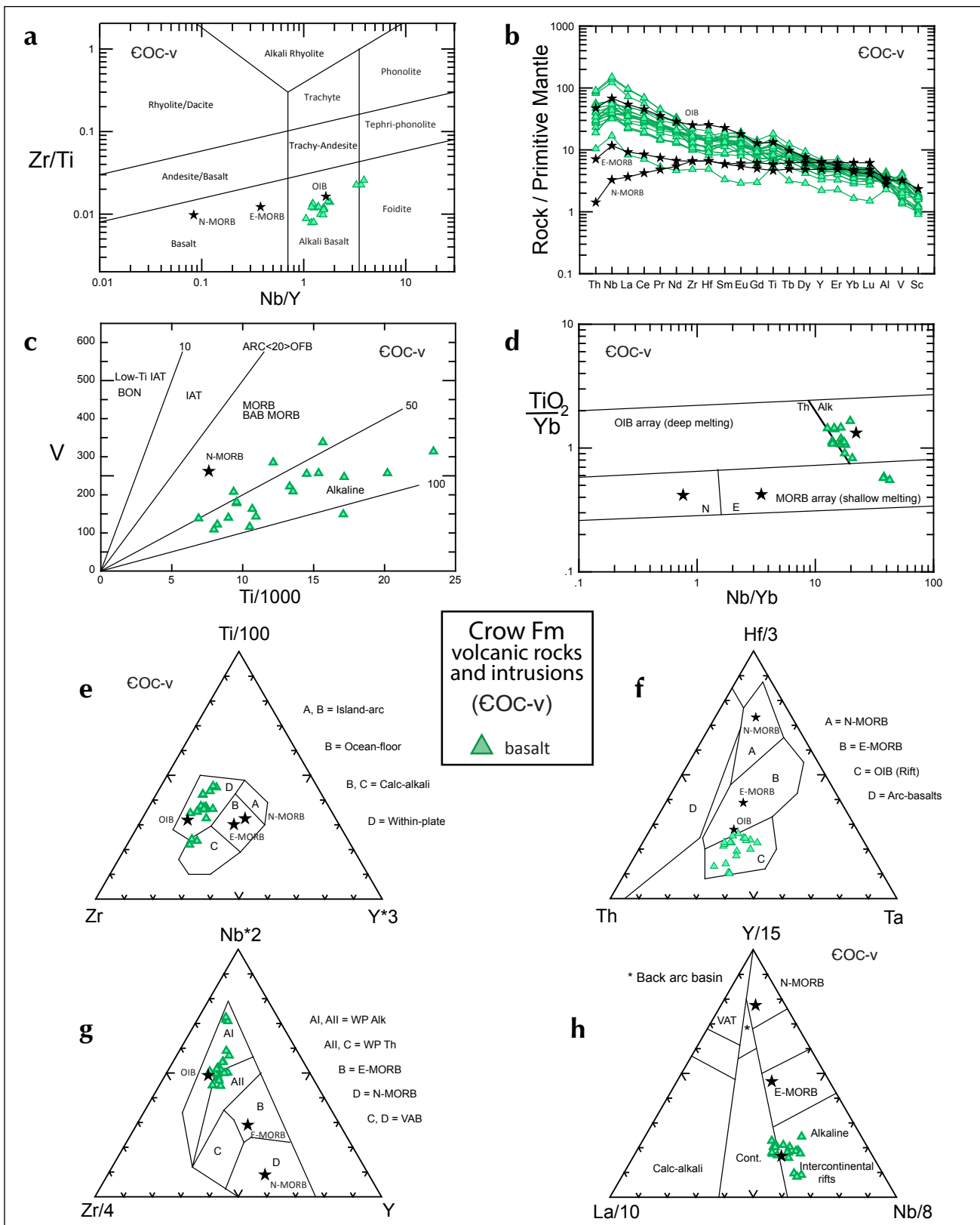


**Figure 55.** Geochemical and tectonic discriminant diagrams for volcanic rocks and intrusions of the Crow Formation: **(a)** Zr/TiO<sub>2</sub>-Nb/Y diagram of Winchester and Floyd (1977), as modified by Pearce (1996); **(b)** primitive mantle-normalized, multi-element diagram; **(c)** Ti/V diagram of Shervais (1982); **(d)** TiO<sub>2</sub>/Yb-Nb/Y diagram of Pearce (2008); **(e)** Zr-Ti-Y diagram of Pearce and Cann (1973) for tholeiitic basalt; **(f)** Th-Hf-Ta diagram of Wood (1980); **(g)** Zr-Nb-Y diagram of Meschede (1986); and **(h)** La-Y-Nb diagram of Cabanis and Lecolle (1989) for basalt.

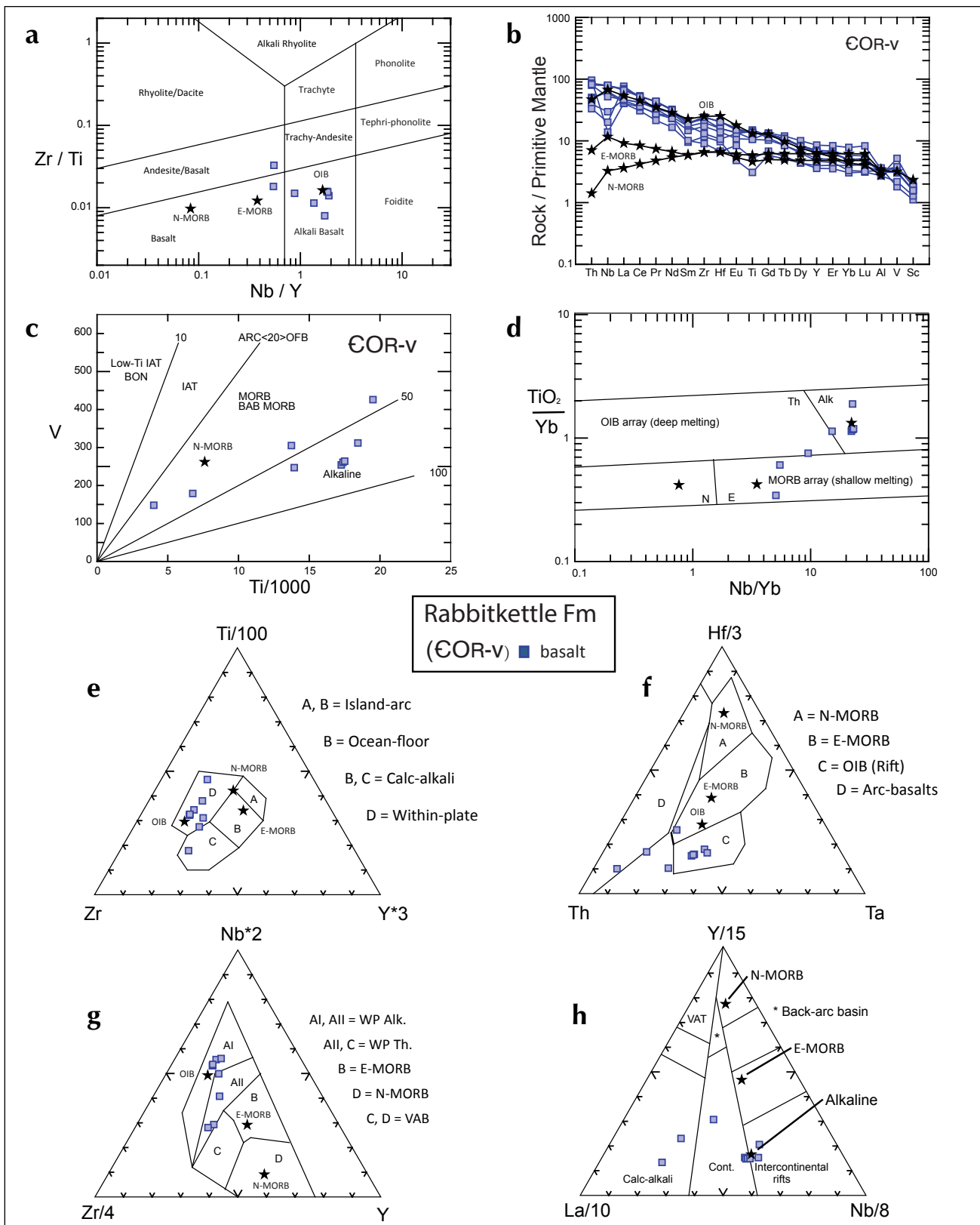


**Figure 56.** Geochemical and tectonic discriminant diagrams for volcanic rocks of the Rabbitkettle Formation: (a) Zr/TiO<sub>2</sub>-Nb/Y diagram of Winchester and Floyd (1977), as modified by Pearce (1996); (b) primitive mantle-normalized, multi-element diagram; (c) Ti/V diagram of Shervais (1982); (d) TiO<sub>2</sub>/Yb-Nb/Y diagram of Pearce (2008); (e) Zr-Ti-Y diagram of Pearce and Cann (1973) for tholeiitic basalt; (f) Th-Hf-Ta diagram of Wood (1980); (g) Zr-Nb-Y diagram of Meschede (1986); and (h) La-Y-Nb diagram of Cabanis and Lecolle (1989) for basalt.

## Sunblood Formation volcanic rocks (OSu-v)

Two samples were selected from flows within the Sunblood Formation. The composition of one may be less reliable because its carbonate and hydrous mineral content amounted to 7.2% LOI. Both samples show roughly equal total iron to magnesium ratios, low Nb (~30 ppm), variable Cr (69-348 ppm) and Ni (40-160 ppm). One sample has high K<sub>2</sub>O (5.2%) but lower Ba (517 ppm, in contrast to 875 ppm in the other) suggestive of alteration, given its high volatile content. On the Zr/Ti vs Nb/Y composition diagram the samples plot within the alkali basalt field (Fig. 57a). Trace element patterns normalized to primitive mantle match that of OIB (Fig. 57b), and the samples plot neatly within the OIB and 'within-plate' fields on various discriminant diagrams (Fig. 57c-h), similar to those for the Crow and Rabbitkettle formations.

## Discussion

The volcanic rocks in the Coal River map area are part of a widespread assemblage of mafic volcanic rocks of similar ages and composition that are distributed throughout Selwyn basin and adjacent Mackenzie platform (Goodfellow *et al.*, 1995), as well as more sparsely along the eastern half of the southern Canadian Cordillera. The chemistry of the assemblage indicates an enriched mantle source, similar to OIB, but reflects intermittent extension within unstable, thinned continental crust of the outer continental margin.

Dominantly mafic, submarine volcanic rocks from lower Cambrian to Middle Devonian age form lenticular occurrences in east central Alaska, eastward and southeast to the Coal River map area (Goodfellow *et al.*, 1995). Significant exposures include the southern Ogilvie Mountains (Roots, 1988), the axis of the Misty Creek embayment (Marmot Formation; Cecile, 1982) and the Anvil Range north of Faro (Menzie Creek formation; Jennings and Jilson, 1986; Pigage, 2004b).

Locally quartz and feldspar-phyric flows and intrusions occur in the western Ogilvie mountains, near the Dempster Highway (Roots, 1988), near the Marg VMS deposit northeast of Mayo and in Crow and Rabbitkettle formations within the Coal River map area (this report). Their composition is rhyolite, with high K<sub>2</sub>O and Ba, although these elements may be secondarily enriched.

The mafic localities have similar depositional environment and tectonic settings. They dominantly form subaqueous, low magma volume volcanic edifices (individual occurrences estimated to contain <20 km<sup>2</sup>; greatest thicknesses are in Misty Creek embayment (500 m in Porter Puddle Complex; Goodfellow *et al.*, 1995) and at Fossil Creek (610 m; Wheeler *et al.*, 1986)). They overlie and are intercalated with clastic sediments of the upper Hyland Group (typically Narchilla formation), Rabbitkettle Formation and Road River Group (e.g., Hess River, Rabbitkettle, Elmer Creek/Duo Lake and Steel formations). Many occurrences are overlapped by limestone patch reefs, although the Sunblood Formation of southeast Yukon is one of only two regionally widespread platform carbonate units to contain volcanic horizons (the other is the Haywire Formation). Typically, flows low in the volcanic successions are pillowed, while some upper sections contain conglomerate and maroon breccia that indicate emergence (Roots, 1988; Goodfellow *et al.*, 1995). The preservation of subaerial facies between flow units and relatively deep water sediments indicates rapid subsidence of parts of the volcanic edifice.

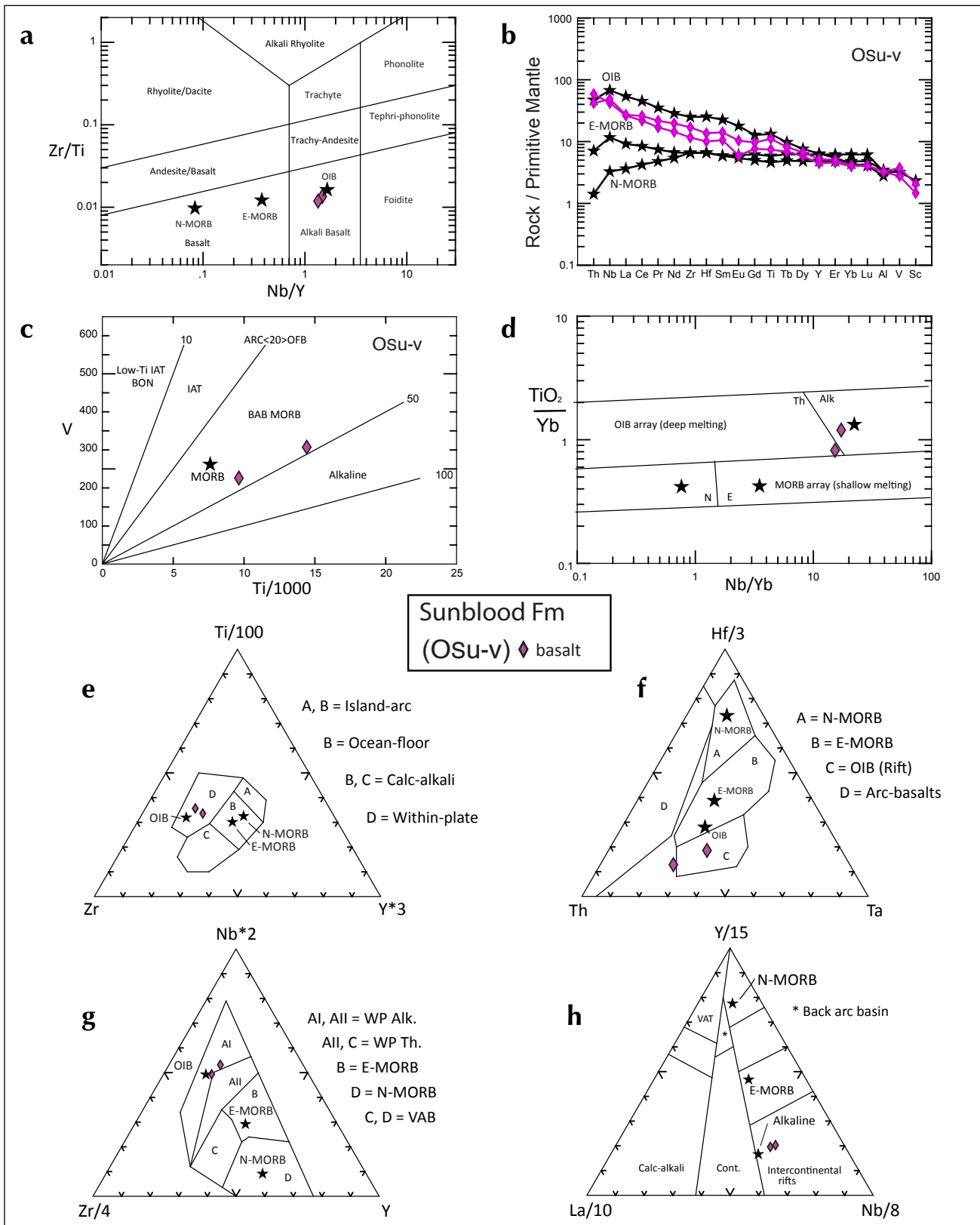


**Figure 57.** Geochemical and tectonic discriminant diagrams for volcanic rocks of the Sunblood Formation: **(a)** Zr/TiO<sub>2</sub>-Nb/Y diagram of Winchester and Floyd (1977), as modified by Pearce (1996); **(b)** primitive mantle-normalized, multi-element diagram; **(c)** Ti/V diagram of Shervais (1982); **(d)** TiO<sub>2</sub>/Yb-Nb/Y diagram of Pearce (2008); **(e)** Zr-Ti-Y diagram of Pearce and Cann (1973) for tholeiitic basalt; **(f)** Th-Hf-Ta diagram of Wood (1980); **(g)** Zr-Nb-Y diagram of Meschede (1986); and **(h)** La-Y-Nb diagram of Cabanis and Lecolle (1989) for basalt.

The discontinuous and interdigitating nature of the volcanic outcrops suggests that they issued from fissures; their primary geometry is masked by subsequent folding and faulting and poor exposure. The range in age suggests that Selwyn basin (*i.e.*, early Paleozoic continental margin) underwent episodic tensional stress that reactivated deep fractures in the continental margin. Their alkalic nature and within-plate chemistry are consistent with this extensional tectonic regime (Barberi *et al.*, 1982; Bailey, 1985). The volcanic magma was sourced from enriched mantle, and ascended with only minor crustal contamination. Slight differences in the chemistry of the Coal River volcanic rocks attest to heterogeneity in the source region, with no indication of progressive change over time.

### **Cretaceous Intrusions (mKg)**

Fifteen plutons (Table 2) are scattered across the northern half of the map area where they generally occupy low lying, heavily forested areas. Nine were either discovered during this program or were previously only recorded on industry maps. The intrusions are typically subcircular and range from 335 m to about 8380 m across. Aeromagnetic anomalies aided detection and mapping of the intrusions (Fig. 58).

Since the intrusive bodies are poorly exposed, their full size, contact relationships and metamorphic effects such as hornfelsing, skarn development and alteration remain unclear and poorly documented. The Kostiuk, Spork and Ivo-Salivo plutons consist of the southern portions of large plutons primarily located in adjacent Frances Lake (NTS 105H) and Flat River (NTS 95E) map areas.

The plutons of the Coal River map area consist predominantly of biotite  $\pm$  hornblende, metaluminous granodiorite to quartz monzodiorite. Textures range between porphyritic and equigranular. Porphyritic variants are typically crowded with plagioclase phenocrysts up to 5 mm across in a fine-grained, grey matrix; hornblende, biotite, and minor quartz also occur as phenocrysts. The Main pluton is the only body which contains primary muscovite. Many of the intrusions are incipiently to extensively altered, with chlorite replacing hornblende and biotite, and sericite dust occurring within feldspar.

Geochronology and geochemistry of the plutons are described in Pigage *et al.* (2014). All sampled intrusions (except for the Main pluton; see discussion below) belong to the Tay River suite as outlined by Rasmussen (2013; see also Heffernan, 2004; Hart *et al.*, 2004; Mortensen *et al.*, 2000). They are the southernmost exposures of the Tay River suite, a belt of contemporaneous and compositionally coherent intrusions extending 450 km northwest.

Crystallization ages for nine of the plutons were determined using CA-TIMS geochronology on single zircon grains. These ages are tightly clustered, ranging from  $97.70 \pm 0.03$  Ma to  $99.80 \pm 0.03$  Ma. Pigage *et al.* (2014) described their compositions, suggesting that the intrusions are partial melts from a reasonably homogenous, igneous, infracrustal source rock. They further suggested that partial melting was related to subduction with flattening of the subducting slab resulting in the Tay River plutonic suite being 400 km inboard of the postulated subduction trench.

The Gabe, Main and Spork plutons occur within the north to northeast-trending belt defined by a positive aeromagnetic anomaly (Fig. 58) and rocks of higher metamorphic grade. The aeromagnetic anomaly may be caused by the presence of metamorphic pyrrhotite or magnetite in the thermal aureole of a large intrusion, or a magnetic phase of a buried pluton.

**Table 2.** Intrusions in Coal River map area. Coordinates are UTM zone 9N, NAD83 datum.

Name	UTM East (m)	UTM North (m)	Age Ma $\pm$ 2 sigma*	Reference
Powers	658 872	6 743 596	98.2 $\pm$ 1.3	Rasmussen <i>et al.</i> , 2007
Jorgensen	645 250	6 751 550	98.35 $\pm$ 0.13	Pigage <i>et al.</i> , 2014
Last 1	621 360	6 751 642	-	
Last 2	620 192	6 745 800	98.52 $\pm$ 0.13	Pigage <i>et al.</i> , 2014
Gabe	570 761	6 722 414	97.83 $\pm$ 0.13	Pigage <i>et al.</i> , 2014
Kostiuk	555 895	6 762 820	99.39 $\pm$ 0.13	Pigage <i>et al.</i> , 2014
Oudder	625 672	6 723 074	97.70 $\pm$ 0.13	Pigage <i>et al.</i> , 2014
Lookout	655 673	6 752 196	98.20 $\pm$ 0.13	Pigage <i>et al.</i> , 2014
Spork	597 672	6 764 282	98.09 $\pm$ 0.13	Pigage <i>et al.</i> , 2014
Main	586 791	6 754 152	-	
Gusty	626 261	6 704 777	99.79 $\pm$ 0.13	Pigage <i>et al.</i> , 2014
Balsam	655 415	6 737 047	-	
Caribou	652 311	6 752 434	98.27 $\pm$ 0.13	Pigage <i>et al.</i> , 2014
Patterson	631 695	6 751 436	97.5 $\pm$ 0.5	Heffernan, 2004
Ivo-Salivo	606 595	6 764 260	-	

\* For a discussion of error, see Pigage *et al.* (2014).

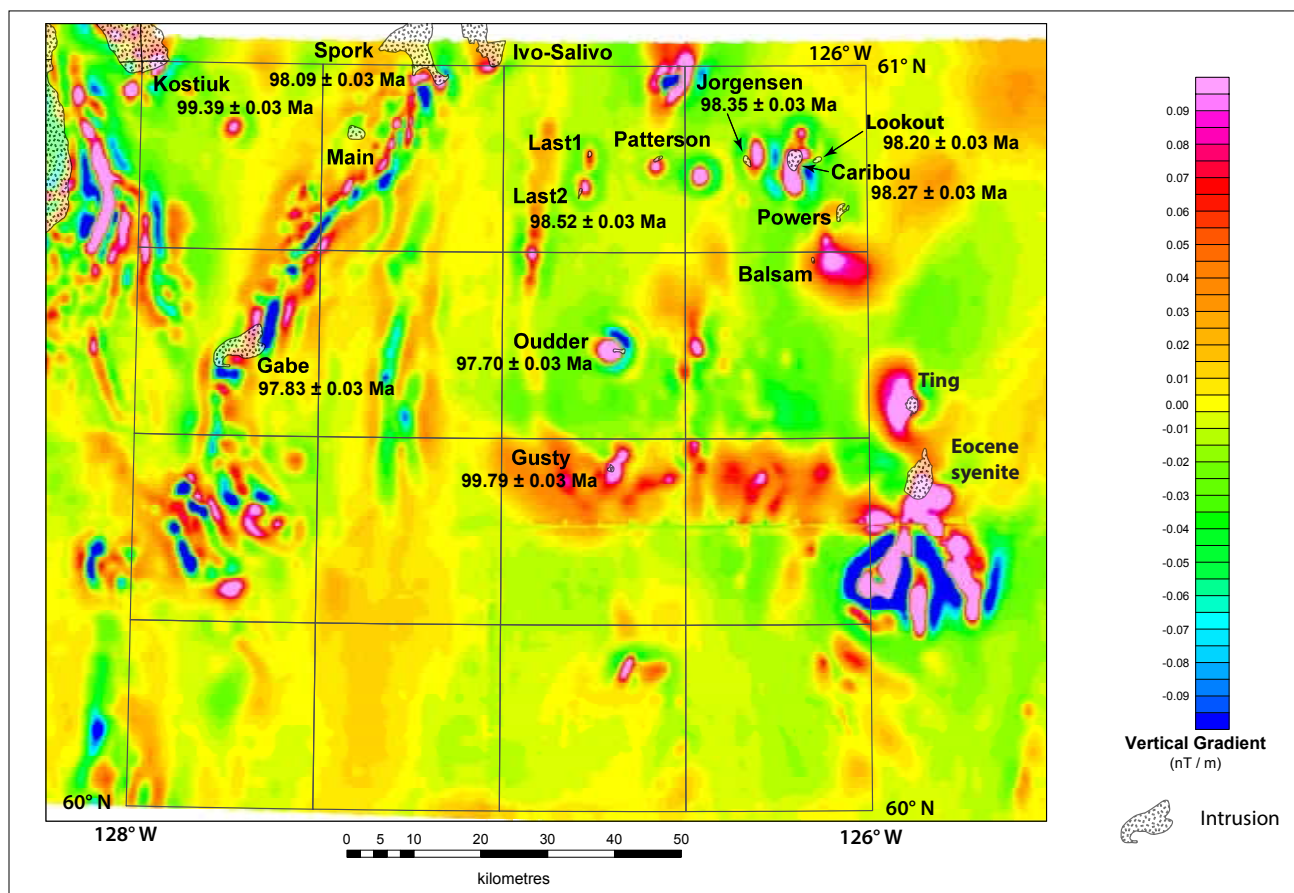


**Figure 58.** First vertical derivative of regional aeromagnetic survey with Cretaceous and Cenozoic granitic intrusions superimposed. Eocene syenite from Pigage (2009). Ting intrusions from Harrison (1982).

The sample from the Main pluton is a medium-grained, equigranular, foliated, medium grey, muscovite-tourmaline-garnet granite. The feldspar is exclusively plagioclase. Subhedral plagioclase and interstitial quartz constitute approximately 90% of the mode. Staining reveals very minor, fine-grained, interstitial K-feldspar. The chemistry is also significantly different from the other plutonic samples (Pigage *et al.*, 2014). The Main sample (sample10TOA019) yielded such poor quality zircon that isotopic dating was not attempted (Pigage *et al.*, 2014).

Another linear positive magnetic anomaly extends westerly from the eastern boundary of the map area to very near the Rock River (Fig. 58). It may also represent a series of buried plutons. The eastern end of this anomaly, in the Pool Creek map area (NTS 95C/5), contains exposures of a magnetite-bearing, Eocene biotite syenite (Pigage, 2009). Boulders of granite (Gusty pluton) were found over the most magnetic part of the anomaly. Elsewhere along this trend the surface exposures are siliciclastic and carbonate rocks with little to no magnetic expression.

## STRUCTURE

### *Introduction*

The Coal River map area is characterized by steeply dipping, northwest to northeast-trending faults and folds. It has been divided into four domains (domains A-D, Fig. 59), and structural measurements are plotted on equal area stereonet (Figs. 60-63). The domains, described here from west to east, reflect decreasing intensity of deformation and waning penetrative structural fabrics.

In domains A and B and the western part of domain C folds are associated with a penetrative axial planar slaty cleavage in argillaceous units. Second-phase refolding of earlier contractional structures by north-trending, open cross-folds (domains A, B and C) resulted in the local development of an axial planar crenulation cleavage in argillaceous units. A penetrative slaty cleavage fabric is not readily visible in domain D.

### *Domain A*

The westernmost structural domain A is bounded to the east by the interpreted east-verging Acland thrust fault. Stratigraphic units in the domain are the Yusezyu Formation, undivided Vampire-Narchilla unit, Rabbitkettle Formation, and Road River Group. The domain is characterized by northwest-trending, southwest-verging, asymmetric folds with an associated pervasive, axial planar, slaty cleavage. Poles to bedding form a broad girdle with a best-fit trend/plunge of 330/11 (Fig. 60a). The axial planar slaty cleavage is dominantly steep (Fig. 60b); lineations plunge both to the northwest and southeast with a mean trend/plunge of 328/11. Locally these early folds are refolded with the development of later, small, north-trending, east-verging, open folds with an associated axial planar crenulation cleavage.

Lack of stratigraphic markers in the Yusezyu Formation hinder recognition of structures larger than outcrop scale. Consistent bedding and structural orientations over fairly large areas hint at the existence of large-scale folds. Northwest-trending anticlines cored by Yusezyu Formation have been interpreted in domain A on the basis of these structural relations between bedding and the pervasive slaty cleavage.

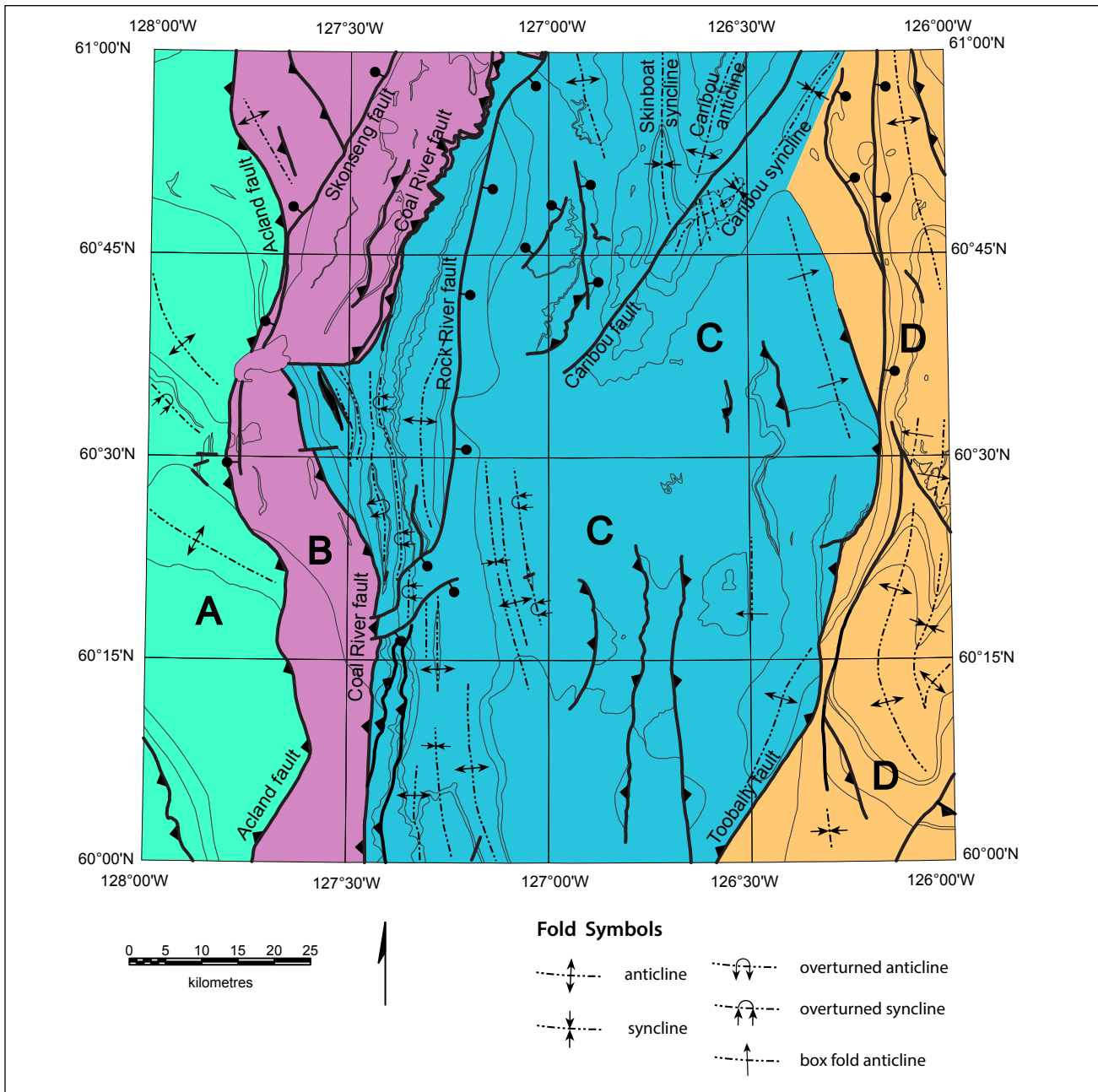


Figure 59. Structural domains in Coal River map area.

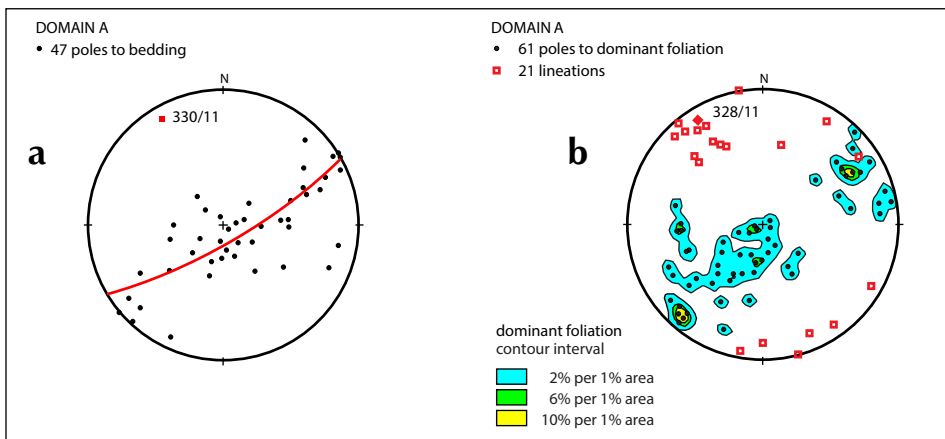


Figure 60. Structural domain A structural fabrics; (a) poles to bedding; (b) poles to dominant foliation, lineations associated with dominant foliation.

## Domain B

The next structural panel to the east is cored by the undivided Vampire-Narchilla unit and bounded to the east by the Coal River thrust fault array. Bedding and foliation measurements are dispersed (Fig. 61), but generally correspond with trends of the aeromagnetic anomalies. Documented early folding consists of north-trending, east-verging, large-scale, tight, asymmetric folds with steep to vertical limbs and gently west-dipping limbs (Fig. 61a); poles to bedding form a broad girdle with a best fit pole of 188/11. Rocks in these folds have an associated pervasive, axial planar, slaty cleavage dipping moderately to the west (Fig. 61b); associated lineations plunge gently to the north-northeast and south-southwest with an average trend/plunge of 196/14. Structural domain B also contains locally extensive development of later, small-scale, north-trending, east-verging folds with an associated axial planar crenulation cleavage which refolds the earlier folds (Fig. 61c); the crenulation cleavage dips gently to moderately to the west. Associated lineations plunge gently to the north-northeast and southwest.

The Skonseng fault in the northwest corner of the map area separates rocks containing muscovite-chlorite (west) from rocks containing biotite-staurolite-garnet (east). The change in metamorphic grade is abrupt and is interpreted as a post-peak metamorphism normal fault.

The Coal River fault array consists of two or more closely spaced east-verging reverse faults. Rock units between the faults in the northern part of the map area are strongly foliated, suggesting that the reverse faults developed in hinge zones of tight folds. The faults are locally well exposed towards their north end, and dip moderately west. Displacement is estimated to be 2000-3000 m.

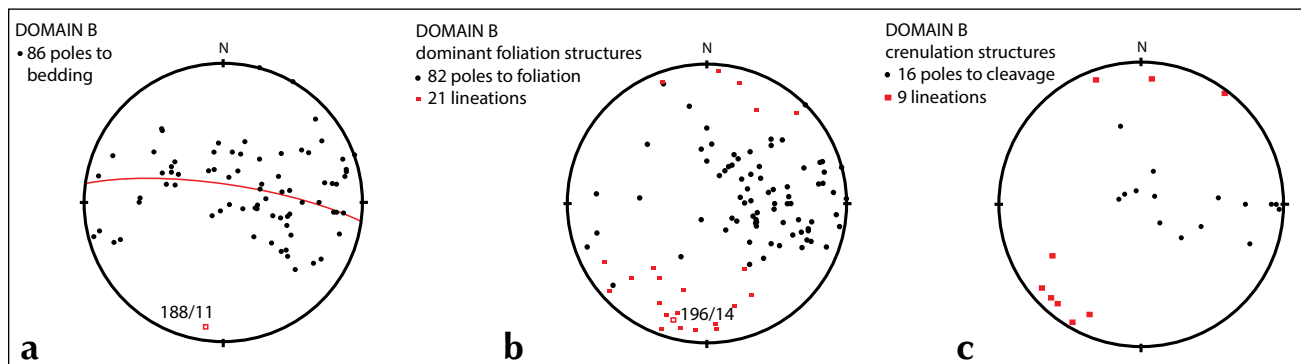


**Figure 61.** Structural domain B structural fabrics, (a) poles to bedding; (b) poles to dominant foliation, lineations associated with dominant foliation; (c) poles to crenulation cleavage, lineations associated with crenulation cleavage.

## Domain C

Domain C underlies the central part of the map area and is bounded by the Coal River reverse fault to the west and the Toobally reverse fault to the east. It is characterized by asymmetric to overturned, east-verging folds with associated pervasive, west-dipping, axial planar, slaty cleavage in the west-central part of the map area. These folds are particularly well developed in the immediate Otter Creek area (Mel mineral occurrence - Yukon MINFILE 95D 005). To the south, the folds decrease in intensity and become more open and symmetrical; to the north the folds are replaced by east-verging reverse faults separated by west-dipping sedimentary strata. To the east, folding becomes less intense and transitions to a generally west-dipping, homoclinal stratigraphic succession with locally developed, macro-scale, east-verging reverse faults and box-style folds. Some small-scale, west-verging reverse faults and/or normal extensional faults are also present; these structures generally trend northerly.

Poles to bedding indicate a predominant, moderate west dip (Fig. 62a). The pervasive axial planar cleavage dips steeply to the west (Fig. 62b); associated lineations plunge gently to north and south (Fig. 62b).

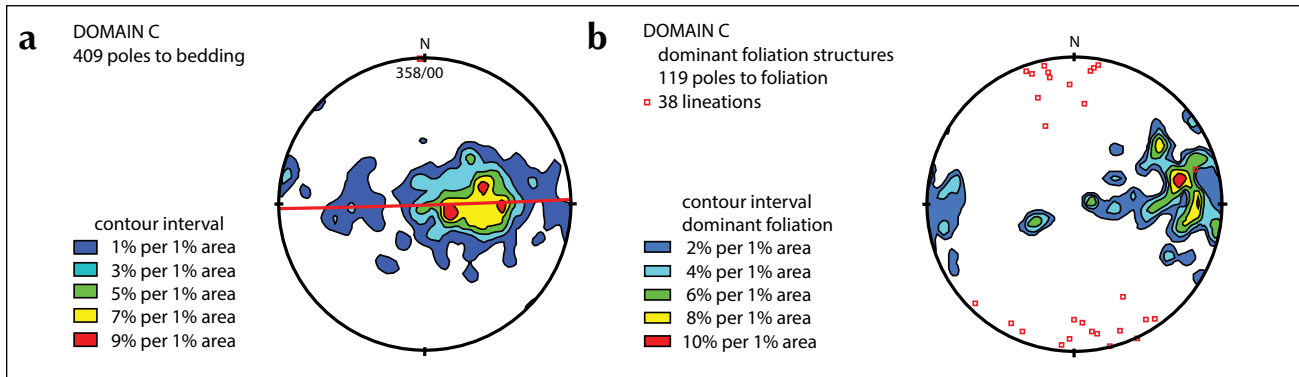


**Figure 62.** Structural domain C structural fabrics; (a) poles to bedding; (b) poles to dominant foliation, lineations associated with dominant foliation.

The northern part of domain C is dominated by the Caribou anticline (Gabrielse and Blusson, 1969) and its associated adjacent synclines. The Caribou anticline is a south-plunging, symmetrical structure. The herein named Skinboat syncline immediately west of the Caribou anticline is a tight, symmetrical, south-plunging syncline cored by the Permian Fantasque Formation.

In contrast, the Caribou syncline (Gabrielse and Blusson, 1969), located southeast of the Caribou anticline, is open and northeast-trending with very gently dipping limbs. The Caribou syncline is refolded by open, north-trending cross folds.

In the upper Toobally Lake area the east-verging Toobally fault (Gabrielse and Blusson, 1969) places the Proterozoic(?) Toobally Formation and the Cambrian-Ordovician Crow Formation in the hanging wall structurally on top of the undivided Triassic Grayling-Toad formations in the footwall. Structural displacement across this fault is difficult to determine because of differences in the thicknesses of the formations between structural panels C and D. Displacement across the Toobally fault decreases both to the north and south away from upper Toobally Lake.

The Rock River fault (Gabrielse and Blusson, 1969) forms the west margin of the Eocene Rock River basin sediments. Gabrielse and Blusson (1969) interpret it as an east-verging thrust fault. In contrast we propose that an east-dipping normal fault would permit deposition of Eocene sediments in a north-trending, extensional half-graben.

### **Domain D**

The easternmost domain D is bounded on the west by the Toobally fault in the south and central parts of the map area, and the Caribou syncline in the northern part of the map area. In the north it is dominated by a north-plunging anticline cored by Mattson Formation and Sunblood Formation in the centre. Immediately north of the Toobally-Crow fault it has a box-fold style with a wide flat hinge zone and straight, moderately dipping limbs. South of the Toobally-Crow fault a similar, doubly plunging anticline is cored by Crow Formation. Slaty cleavage is not generally developed in argillaceous units in this domain.

Poles to bedding outline a girdle with trend/plunge of 189/07 (Fig. 63). The predominant bedding dip is moderately to the west.

Domain D also contains several north-trending faults with small displacements. In the north, the faults have been interpreted as normal; one fault in the central area has been interpreted as a west-verging, small-scale, back-thrust.

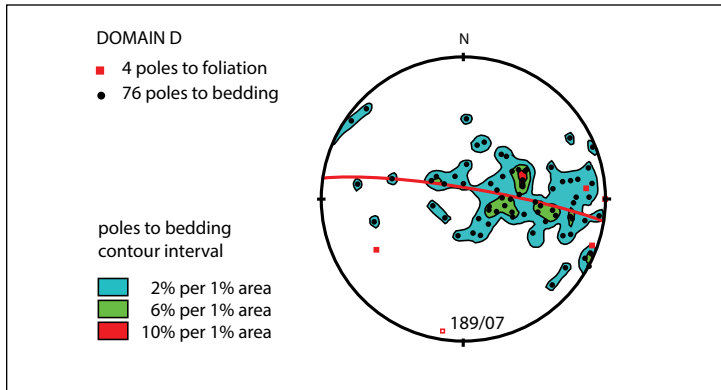


**Figure 63.** Structural domain C structural fabrics; poles to bedding, poles to dominant foliation.

### **Late Extensional Deformation**

Extensional deformation is manifested by normal faults documented in the Coal River area. These structures are late-stage because they displace and offset earlier contractional fold and fault structures. The largest of these extensional features is the Rock River fault which forms the western margin of the upper Eocene sedimentary rocks. Because the upper Eocene sedimentary rocks east of the Rock River fault dip gently west, movement on the fault is inferred to be syn-late Eocene with faulting being concurrent with deposition of the late Eocene Rock River basin strata. The Rock River fault juxtaposes undivided Vampire-Narchilla unit against Road River Group and Eocene strata. A minimum displacement across the fault is at least 450 m (the known thickness of Eocene strata); a possible thickness of 1100 m for the Eocene strata (Wright and Miller, 1986) suggests a significantly greater minimum displacement across the fault.

### **Discussion**

Fold structures and associated slaty cleavage in domain A trend northwest and are truncated by the north-trending Acland reverse fault, suggesting the contractional deformation associated with the folding in this domain predates the predominant north to northeast-trending folds occurring in the other domains. We infer that the locally developed, north-trending, east-verging minor folds and associated axial planar crenulation cleavage in domain A are correlated with the predominant fold and fault structures occurring in the other domains. The timing of the earlier deformation is poorly constrained to being post-lower Cambrian strata and pre-middle Cretaceous thrust faults.

The predominant contractional deformation (in domains B, C, D) at this structural level (now at surface) is constrained to post-Early Triassic time because Triassic and older argillaceous strata are folded and contain the pervasive slaty cleavage. It is further constrained to pre-middle Cretaceous time as the mid-Cretaceous plutons that crosscut fold and fault structures regionally are undeformed (Gordey and Anderson, 1993). Contractional structures are inferred to flatten into a shallow, west-dipping detachment located in pre-Hyland Group strata (cross section on Plate 1). Displacement at depth on this detachment may well have continued after emplacement of the Cretaceous intrusions.

Deformation in the Coal River area is considered to be part of the Cordilleran orogen (Gabrielse *et al.*, 1991; Nelson and Colpron, 2007; Nelson *et al.*, 2013), a manifestation of the amalgamation of Laurentia with allochthonous terranes.

The Rock River fault and associated half-graben occurred when east-directed compressional deformation ceased in Paleocene or Eocene, and dextral motion was initiated on the northwest-trending Tintina fault (Nelson *et al.*, 2013).

## METAMORPHISM

Metamorphic mineral assemblages in the pelitic rocks regionally range from muscovite-chlorite zone in lower greenschist facies to biotite-garnet-staurolite-chloritoid zone in lower amphibolite facies (Table 3). All mineral assemblages in the basaltic volcanic rocks contain epidote, calcite and chlorite. The biotite-garnet-staurolite grade rocks occur in a northeast-trending belt extending from near the Hyland Gold MINFILE occurrence (Roy Lake) to north of the Coal River map area. The aluminosilicate minerals (andalusite, kyanite, sillimanite) were not observed in the pelitic rocks.

The dominant foliation (S1) and the later crenulation cleavage (S2) are delineated by matrix muscovite, chlorite and biotite. The porphyroblastic minerals garnet, staurolite, biotite and chloritoid contain planar inclusion trails which pass into the external, dominant foliation; the S2 crenulation cleavage wraps around the porphyroblasts. These different textures indicate maximum metamorphic conditions occurred during, or after, the formation of the S1 foliation, and before the formation of the S2 cleavage.

**Table 3.** Metamorphic assemblages in Vampire-Narchilla unit, Coal River map area. Coordinates are UTM zone 9N, NAD83 datum.

Station	UTM East (m)	UTM North (m)	Mineral Assemblage
09LP001	570845	6706095	quartz-muscovite
09LP050	583278	6742306	quartz-muscovite-chlorite-biotite
09LP051	582745	6742319	quartz-muscovite-biotite
09LP055	580956	6743751	quartz-muscovite-biotite
09RAS048	591454	6758267	quartz-muscovite-biotite-garnet-staurolite
09RAS085	591270	6762014	quartz-muscovite-biotite
09RAS086	590101	6762277	quartz-muscovite-biotite-staurolite
09TOA009	595171	6714622	quartz-plagioclase-muscovite
09TOA084	577859	6738819	quartz-muscovite-chlorite-biotite-garnet-staurolite
09TOA090	580872	6738795	quartz-muscovite-chlorite-biotite
09TOA098	582139	6742420	quartz-feldspar-muscovite-biotite
09TOA109	577140	6733039	quartz-muscovite-biotite-garnet-staurolite
09TOA110	576299	6733094	quartz-chlorite-biotite-garnet-chloritoid
09TOA111	576053	6733332	quartz-muscovite-chlorite-garnet-staurolite

## MINERAL OCCURRENCES AND METALLOGENY

The Coal River map area offers potential for sediment-hosted base metal and intrusion-related base and precious metal mineralization. Sediment-hosted mineralization may include both sedimentary exhalative Zn-Pb±Ba in black shale (SEDEX) and Irish-type or MVT Zn-Pb replacements in carbonate rock. Intrusion-related mineralization may include massive sulphide mantos, tungsten and base metal skarns, precious metal veins, sheeted veins, and replacement deposits.

The basinal facies within both Selwyn basin and Kechika trough are characterized by stratiform mineral deposits. In the latter, 200 km south of Coal River map area, stratiform barite-lead-zinc deposits are hosted in sub-basins along the platform margin within Middle Ordovician, Lower Silurian and Upper Devonian strata (MacIntyre, 1992), including the Cirque, Fluke, and Elf deposits in the Gataga district (MacIntyre, 1992). In the former, stratiform barite-lead-zinc and barite deposits are hosted within Cambrian, Silurian, Devonian, and Mississippian carbonaceous shale (Abbott *et al.*, 1986).

The lower Paleozoic platform-to-basin transition of the Macdonald platform also hosts Mississippi Valley type (MVT) deposits, the most important is at Robb Lake (Macqueen and Thompson, 1978; Paradis *et al.*, 1999).

The recognition of nine additional plutons in the Coal River map area results in more exploration target areas for intrusion-related, base and precious metal mineralization.

The following mineral occurrence descriptions are summarized from government-maintained databases (Yukon MINFILE and NWT NORMIN; Fig. 64) with interpretation and clarification in light of recent fieldwork. MINFILE occurrences with no apparent economic significance are excluded from the following discussion. The 2009 mapping refined the geological setting of some of these occurrences and identified four new potential exploration targets.

### ***Sedimentary exhalative (SEDEX) mineralization***

Although the Road River Group has previously been considered a favourable host for SEDEX mineralization in the Coal River map area, no SEDEX occurrences have yet been found. A few MINFILE occurrences record elevated zinc concentrations, but these are considered to be typical values for much of the Road River Group and not related to SEDEX mineralization. In the eastern part of the map area the black shale is limited in extent and overlies thick sequences of Rabbitkettle and Sunblood carbonate rocks. Possibly, the carbonate prevented the formation of SEDEX deposits by reacting with expelled basinal fluids to form replacement deposits such as the MEL before they could reach the surface. More favourable environments may exist farther west along the Coal River, where the Road River Group is more extensive than previously thought and older strata are primarily siliciclastic.

Black shale of the Besa River Formation, although equivalent to the well-mineralized Devonian-Mississippian Earn Group, contains no known sedimentary exhalative sulphide deposits. This may be for the same reasons cited above for the Road River Group. Alternatively it may be because of an apparent lack of syndepositional tectonism as indicated by the absence of Devonian-Mississippian coarse siliciclastic facies and volcanism in this area.

Bedded barite is known in one locality in the Northwest Territories at the Last Mountain (NORMIN 095DNE0003) occurrence. There, finely laminated, but thick-bedded to massive barite between 3 and 10 m thick occurs in a structurally complex zone on the eastern limb of the Skinboat syncline. It has not been traced along strike due to lack of outcrop. The barite occurs close to the contact with basal quartzite of the Mattson Formation but whether it lies above or below the quartzite could not be determined due to poor exposure and cryptic structures. The Mattson Formation is Middle and

Late Mississippian in age; therefore the barite is likely to be Mississippian as well. The Tea deposit near Macmillan Pass (Dawson and Orchard, 1982) is another barite deposit of roughly equivalent age.

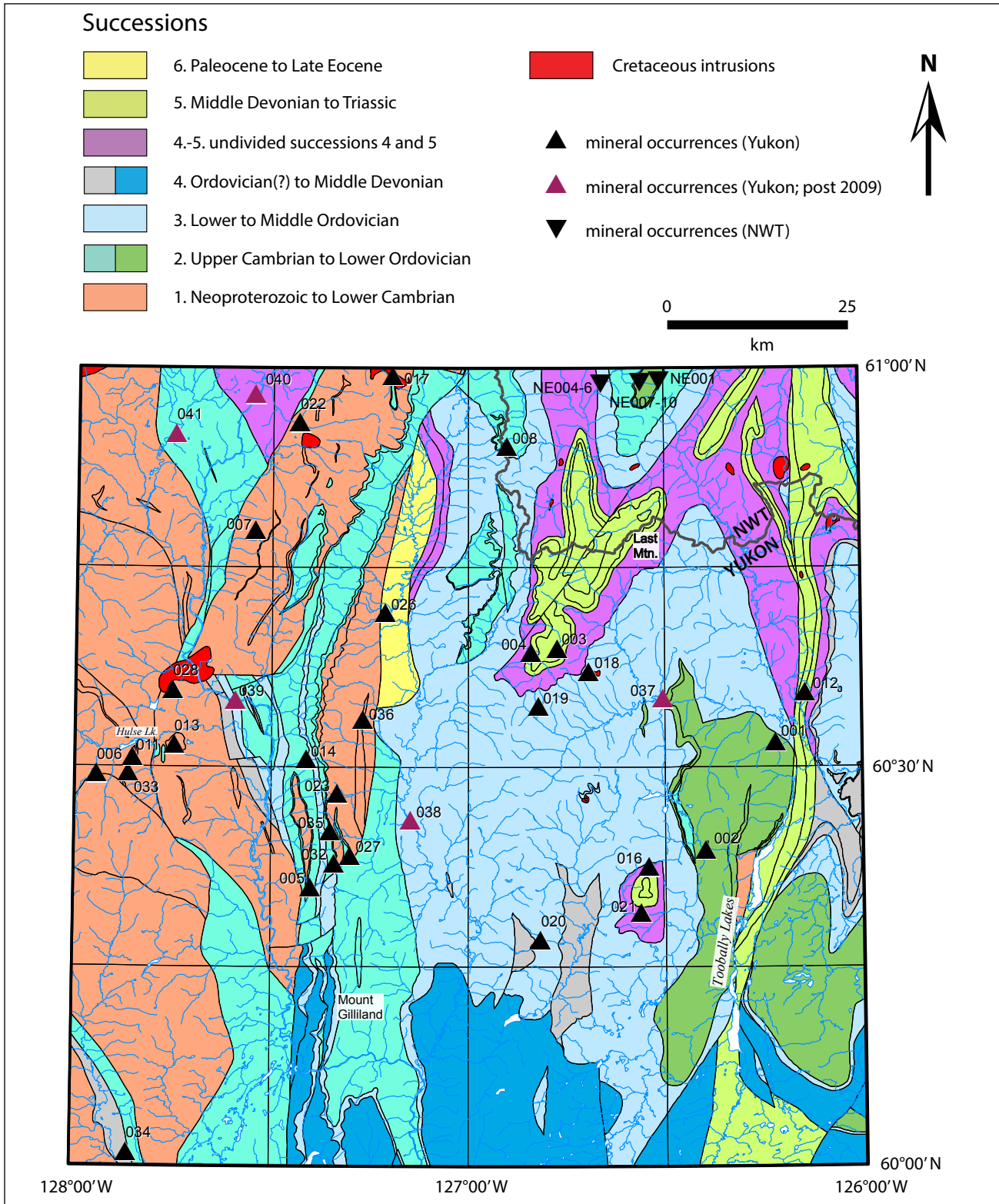


**Figure 64.** Mineral occurrences in Coal River map area. Numbers refer to Yukon MINFILE for 95D and NORMIN database (2010), and are referred to in the text.

### ***Carbonate replacement (MVT, Irish type) mineralization***

Four epigenetic, stratabound zinc±lead±barite deposits and showings (Yukon MINFILE 095D005, 095D027, 095D032 and 095D035) are located in NTS 95D/6. Each of these mineral occurrences is now considered to be hosted in massive, fine-grained limestone of the Otter Creek Formation at the contact with the overlying argillaceous limestone of the Rabbitkettle Formation. The following summary is condensed from a comprehensive description and discussion of the origin of these deposits by Pigage (2008).

The Mel (Yukon MINFILE 095D005) is the largest of these deposits with a published, pre-NI43-101, drill-indicated reserve of 6.78 MT (million tonnes) grading 54.69% barite, 7.10% Zn, and 2.03% Pb (King, 1995). It is a stratabound lens about 800 m long and up to 22 m thick near its centre, and it remains open at depth. It consists of very coarse grained, white barite and reddish-brown, coarse-grained sphalerite with late, interstitial galena occurring along fractures and as selvages.

The Mel-East showing (Yukon MINFILE 095D027) is poorly exposed for a strike length of 170 m. True width is unknown but may exceed 3 m. Mineralization consists of disseminated smithsonite blebs ranging from less than 1 mm to 20 mm in size that are associated with dolomitization and silicification of the massive limestone over a width of 10 m.

The Jeri occurrence (Yukon MINFILE 095D032), consists of smithsonite in silicified dolostone at three localities. The smithsonite forms veins and discontinuous masses up to 1 m thick with the total width of mineralization exceeding 11 m.

The Jeri North occurrence (Yukon MINFILE 095D035) is located north of the Jeri zone along strike. Mineralization consists of coarse brown sphalerite and quartz infilling fractures in strongly silicified limestone.

The Mel and nearby deposits are probably Devono-Mississippian in age on the basis of lead isotope data (Godwin and Sinclair, 1982; Godwin *et al.*, 1988), and best classified as epigenetic Irish-type replacement or MVT deposits (Pigage, 2008). Similar deposits may occur elsewhere in the Otter Creek Formation or other carbonate units. Limestone of unit SDc is commonly replaced by hydrothermal dolomite. Modern sinkholes and karst features demonstrate the susceptibility of unit SDc to dissolution and cavity formation, making it a possible candidate for MVT or Irish type mineralization. One possible target for Mel-type mineralization is the Watsit (Yukon MINFILE 095D014) occurrence, located on strike to the north of the Mel. There, a zinc soil geochemical anomaly up to 4500 ppm is located above limestone of the Rabbitkettle Formation near the contact with dolostone of the Sunblood Formation (Yukon MINFILE).

### ***Volcanic-related mineralization***

The Grant (Normin 095DNE0001), Chuck (Normin 095DNE0009), Gabe (Yukon MINFILE 095D008), and Gusty (Yukon MINFILE 095D002) copper occurrences are in Cambrian and Ordovician mafic volcanic rocks. All consist of scattered disseminations of chalcopyrite±bornite and malachite. None of these are known to have significant size or potential.

### ***Intrusion-related mineralization***

The McMillan massive sulphide replacement deposit (Yukon MINFILE 095D006) consists of two zones. The Main Zone contains pre-NI 43-101 reserves of 1.1 MT grading 8.3% Zn, 4.1%Pb, and 62g/t Ag, and the South Zone contains 0.4 MT grading 9.3%Pb, 1.7% Zn, and 214g/t Ag (Vaillancourt, 1983). The Main Zone forms a gently east dipping tabular body in quartzite and massive grey limestone.

Nearby maroon and green phyllite are associated with the quartzite and limestone, and the assemblage has herein been assigned to the Vampire-Narchilla unit. Textural relationships clearly show that mineralization is discordant to bedding. Lead isotopes (Godwin, *et al.*, 1988) indicate a Cretaceous age for mineralization.

The Hyland Gold mineralization (Yukon MINFILE 095D011) is a low-grade, oxidized, fault-controlled Au deposit. Quartzite, phyllite and limestone host rocks resemble the host rocks to the McMillan deposit 5 km to the west and are assigned to the Vampire-Narchilla unit. A NI43-101 inferred resource of 12.5 MT grading 0.9 g/t Au and 5.6 g/t Ag (using a 0.6 g/t Au equivalent cutoff; Armitage and Gray, 2012) has been identified in the Main Zone. Mineralization is controlled primarily by north-trending faults, but occurs in four settings: 1) breccia zones mainly in quartzite; 2) north-trending fault zones; 3) limestone replacement bodies up to 40 m thick containing pyrite, pyrrhotite, arsenopyrite and siderite; and 4) narrow quartz veins containing erratic pods of massive jamesonite.

The Cuz gold occurrence (Yukon MINFILE 095D033) is about 4 km south of the Hyland Gold deposit in a quartzite and granular sandstone-dominated assemblage that is herein assigned to the Yusezyu Formation of the Hyland Group. The mineralized zone is not well defined and consists primarily of float. Two types of mineralization have been recognized: 1) grey chalcedonic quartz veins containing fine-grained arsenopyrite in brecciated and altered host rock and 2) silicified and leached quartzite and conglomerate. Results from assays of specimens of Type 1 are as high as 9.0 g/t while Type 2 are as high as 3.7 g/t (Carne, 1996).

Six kilometres east of the Hyland Gold deposit, stratabound disseminations and veinlets of sphalerite replace coarse-grained marble and staurolite-chlorite schist in the Hulse (Yukon MINFILE 095D013) occurrence. Channel sampling results returned up to 0.85% Zn, 0.15% Pb and 2.7 g/t Ag over 0.9 to 5.5 m widths (Stockwell, 1975).

The McMillan, Hyland Gold, Cuz and Hulse occurrences represent different styles of epigenetic mineralization typically associated with granitic intrusions, suggesting that they are related to one or more intrusions occurring at depth. Alteration is widespread between the McMillan and Hyland deposits; high temperature metamorphism is only seen at the Hulse. There is no pronounced magnetic anomaly in the area; therefore the hypothetical pluton would have a low magnetic susceptibility, like the Gabe pluton located 10 km to the north-northeast. Alternatively, the Hyland and Cuz occurrences might be considered 'orogenic' and related to a large, deep-seated fault system (Hart and Lewis, 2006).

The Chuck (Normin Occurrences 095NE0007, 8 and 9) gold occurrence consists of east-trending quartz veins 4-10 cm wide in volcanic and carbonate rocks with low grades of gold and arsenic. Silt samples from a creek draining the area returned values greater than 500 ppb gold. Float in the creek included skarn fragments and subangular vein quartz up to 50 cm across which returned values up to 50 ppb Au and 212 ppb As (Vulimiri, 1986). A strong aeromagnetic anomaly coincides with the occurrence. The SITE 1,2,3 placer gold occurrence (Normin 095DNE0004, 5 and 6) is probably derived from it. The style of mineralization and association with a positive aeromagnetic anomaly suggests the Chuck occurrences are associated with a buried intrusion. Placer and lode gold occurrences are associated with the Macleod and Big Charlie plutons located 8 and 25 km respectively to the north (Rasmussen *et al.*, 2007).

The Herpes (Yukon MINFILE 095D022) and Oudder (Yukon MINFILE 095D018) exploration targets record anomalous values of scheelite in stream sediment and soil respectively near poorly exposed intrusions. No associated bedrock occurrences are known.

The Toobally (Yukon MINFILE 095D001) occurrence is a large alteration zone exposed along a north-trending creek. Sandstone of the Crow Formation is pervasively altered to white clay. A rusty, vertical,

east-trending limonite zone is located near the centre of the alteration zone. Early work reported anomalous lead values from the limonite. An assay from a sample of limonite taken in 2009 returned anomalous values for Pb (38 ppm), Zn (218 ppm), Ni (95 ppm), Co (90 ppm), Mn (>10000 ppm), Fe (33.2%) and As (185 ppm). An RGS sample and a silt sample taken in 1999 from the mouth of the creek contained no anomalous values, but they may not have been representative of the creek drainage because they were located well into the valley of the Beaver River. No aeromagnetic anomaly is associated with the alteration, but the most likely explanation for it is a buried intrusion.

### ***New exploration targets***

The localities described below arose from field work in 2007, 2009 and 2010.

#### **Gusty** occurrence (Yukon MINFILE 095D037)

An extensive alteration zone and colour anomaly in the Sunblood Formation is located in a small creek draining into the Beaver River. Dolostone is completely decalcified and disaggregated to sand. No anomalous values were obtained from geochemical analysis of the material or from a silt sample from the creek. The alteration zone coincides with a small aeromagnetic anomaly.

#### **Blood** occurrence (Yukon MINFILE 095D038)

Highly fractured dolostone of the Sunblood Formation exposed on the banks of the Rock River contains veins and replacement lenses of fine-grained nodular pyrite.

#### **Ferricrete** occurrence (Yukon MINFILE 095D039)

On the banks of the Coal River, ferricrete is draped over highly fractured dolostone of the Sunblood Formation along an inferred small fault zone.

#### **Argil** occurrence (Yukon MINFILE 095D040)

On the banks of the upper Coal River, a small outcrop of shattered cherty olive green argillite tentatively assigned to the Road River Group contains breccia zones cemented by fine-grained pyrite and manganese stained fractures. An assay of pyrite breccia returned anomalous values for Mo (8.57 ppm), Cu (110.6 ppm), Ni (198.4 ppm), Mn (>10000 ppm) and Fe (24.35%).

#### **Toe-in** occurrence (Yukon MINFILE 095D041)

A small outcrop on the banks of the West Coal River consists of fine grained, altered biotite granodiorite (Cretaceous?) intruding rusty-weathering pyritic, cherty hornfelsed sediment assigned to the Rabbitkettle Formation. Skarn and granodiorite coincide with a regional magnetic high.

## **HYDROCARBON POTENTIAL**

### ***Oil and Gas potential***

The Kotaneelee gas field in southeast Yukon is the only producing gas field in Yukon. Gas in the Kotaneelee field is located in stratigraphic traps related to karsting, diagenetic dolomitization and subsequent burial of Devonian carbonate rocks (Morrow *et al.*, 1990). Similar stratigraphy exists at

surface in the southern part of the Coal River map area. Carbonaceous shale and limestone in the Road River Group and Besa River Formation are possible hydrocarbon source rocks for conventional gas or oil reservoirs.

Carbonaceous silty shale and limestone from surface outcrops were collected and tested at the Geological Survey of Canada Organic Geochemistry Laboratory in Calgary for potential as hydrocarbon source rocks using Rock-Eval/TOC pyrolysis. The Rock-Eval 6 instrument provides information on type, maturity and quantity of organic matter present in the sample (Espitalié *et al.*, 1977). Appendix D presents results for the analyses; operating conditions during analysis are described in Pigage (2009).

All analyzed samples are from the Road River Group and/or Besa River Formation. Kirk Osadetz (GSC Calgary, personal communication 2009) kindly provided the following summary. Samples 09LP039, 09LP074, and 09LP062 have insufficient TOC to infer anything other than a lack of source rock potential. Samples 09CYA010, 09RAS106, 09LP093 and 09LP077 are overmature source rocks with S1 and S2 values below 0.2 mg/gm. The low S2 values mean the results may not be meaningful (Peters, 1986). Sample 09LP058 was flagged as being anomalous with an unusual low Tmax value. It was suggested that this sample was possibly contaminated by an organic fluid. Sample 10TOA035 is from the formation in the same general geographic area. Analytical results for 10TOA035 indicate an overmature source rock with low S1 and S2 values.

Organic-rich rocks in the Coal River map area have been subjected to temperatures which have essentially destroyed their capability of generating oil or gas locally. Any conventional hydrocarbon reservoir in the Coal River area would have to form through extensive lateral migration into the map area from a source area which has not been subjected to these higher temperatures. It is inferred that conventional reservoir potential in the map area is very limited.

Several of the samples analysed with rock-eval contain several percent total organic carbon. Although overmature, the samples could potentially have generated gas which could still be present if the formation was impermeable to gas migration. The possibility of a tight shale unconventional gas resource has not been tested in the Coal River area.

### ***Coal potential***

The Eocene Rock River basin in the north-central Coal River area contains a 5 m-thick outcrop of lignite coal along a tributary of the Rock River. Five diamond drill holes were completed in 1981 by Sulpetro Minerals Ltd. to test the regional extent of the coal seams (Wright and Miller, 1986). Significant near-surface coal was intersected in two of the holes. The coal ranges from lignite A to sub-bituminous C rank. Thermal content was reported as 6645 Btu/lb with 17.6% ash and 1.09% sulphur at equilibrium moisture of 26.3%. Maximum depth penetrated by drilling was 162 m. In contrast, the depth of Tertiary sediment based on gravity data was interpreted as being up to 1100 m (Wright and Miller, 1986), thus indicating the potential for coal seams at greater depth.

## **SUMMARY**

Bedrock geological mapping in 2009-2010 succeeded in redefining the understanding of the geologic history and mineral potential of southeastern Yukon. The area contains six successions of sedimentary rocks, ranging from Proterozoic to Eocene in age with a composite thickness exceeding 14 000 m. These strata record the evolution of the Laurentia passive continental margin, lateral facies changes associated with the development of Selwyn basin, and subsequent deformation and plutonism. Figure 65 schematically portrays the stratigraphic history, igneous history, tectonic evolution and setting of mineral occurrences in the region.

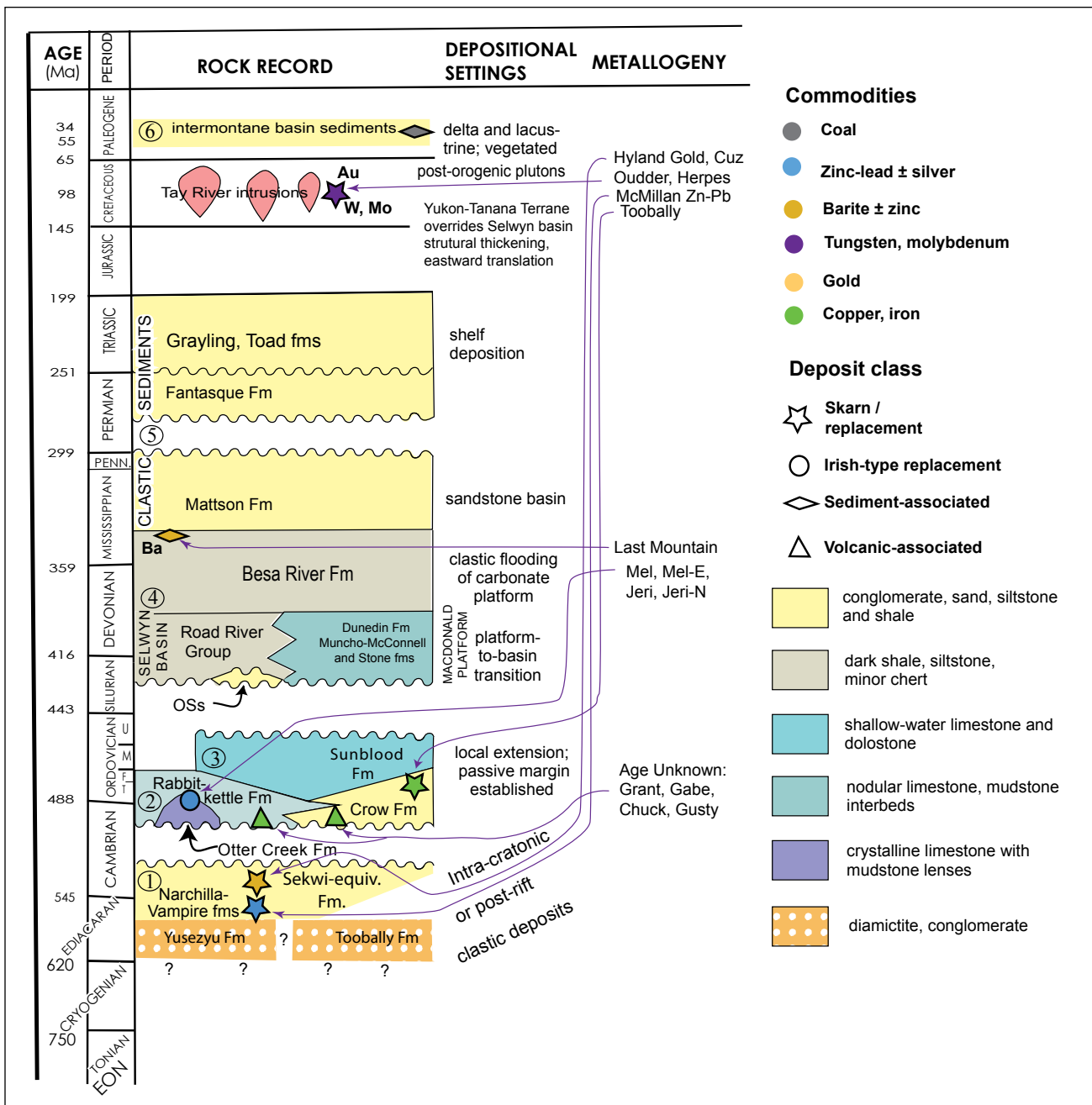


**Figure 65.** Summary of stratigraphic history and tectonic evolution in Coal River map area, and the geological relationship to mineral occurrences.

The earliest exposed deposition consists of Neoproterozoic to early Cambrian, dominantly siliciclastic sedimentary units documenting the initiation of rifting of Rodinia to form the western passive continental margin of Laurentia.

Deposition in late Cambrian to Middle Ordovician chronicles the initiation of an extensive continental carbonate platform along the western margin of Laurentia. The Sunblood Formation first developed near upper Toobally Lake in earliest Ordovician time and expanded laterally. Rabbitkettle Formation, coeval with both Crow and lower Sunblood formations, represents the gentle ramp-slope deposition of carbonate debris away from the Sunblood carbonate platform. The thick but aerially restricted siliciclastic Crow Formation defines a delta complex fed by a large river draining the east and northeast.

The Silurian through Middle Devonian carbonate platform lacks a ramp facies; it is an abrupt northward change to carbonaceous, fine-grained sediment of the locally anoxic deeper water of Selwyn basin. In Middle Devonian through Mississippian time the platform was flooded and deposition of carbonaceous sediment extended eastward. A mid-Mississippian regression then led to sandstone (Mattson Formation) as a westward-prograding delta.

Thin Permian and Triassic successions record marine deposition in a shallow water, shelf setting. These successions are separated from other units by hiatuses.

Jurassic and Early Cretaceous strata are absent from the Coal River map area. This time interval coincides with the Cordilleran orogeny (Nelson *et al.*, 2013), manifested by deformation and thickening of the sedimentary succession through folding and thrust faulting. Cretaceous silt and sand depositional basins located immediately east of the map area record development of foreland basins associated with deformation and uplift in the hinterland (including Coal River map area). Deformation was accompanied by low-grade to medium-grade regional metamorphism, as well as exhumation and erosion of earlier sedimentary formations. At the presently exposed structural level, deformation had essentially ceased before the intrusion of only slightly deformed mid-Cretaceous granitic stocks.

Farther east in Northwest Territories and Alberta, thrust faulting continued into the Paleocene. The entire exposed Coal River stratigraphy is presumed to have passively moved eastward along a basal detachment located at an unknown deeper structural level. Consequently the exposed early Paleozoic alkali basalt and the Cretaceous intrusions are structurally separated from their deep sources of partial melting.

Extension along south-trending, post-orogenic, normal faults locally preserved Eocene fluvial sediment with coal horizons (Rock River basin sediment). Intermontane basins in the Cordillera formed between major thrust sheets and along dextral strike-slip faults. These latter may be a response to re-orientation of relative movement between the Pacific and North American tectonic plates.

Mineral occurrences include Irish-type or MVT Zn-Pb replacements in carbonate rocks, massive sulphide mantos, tungsten and base metal skarns, and precious metal, intrusion-related veins and replacement deposits. Potential exists for sedimentary exhalative Zn-Pb ± Ba deposits, although none have been noted to date.

Carbonaceous sedimentary successions are overmature for source hydrocarbon potential. Conventional oil or gas reservoirs are probably not present. Potential does exist for unconventional tight shale gas resource. Coal resources have been identified in the late Eocene Rock River basin sediments.

## **ACKNOWLEDGEMENTS**

Fieldwork was a jointly funded collaboration between the Yukon Geological Survey (YGS) and the Geological Survey of Canada (GSC) through the federal Geomapping for Energy and Minerals (GEM) Program. Isotopic dating and paleontologic analyses were arranged by the GSC. Yukon Geological Survey funded Abbott's follow-up fieldwork in 2010, subsequent fossil identifications and geochemical analyses.

We thank Victoria Gold Corp for use of their exploration camp at Quartz Lake, and Reggie, David and James O'Farrell for use of Grizzly Creek Lodge on Upper Toobally Lake. Martina Bezzola, Casey Cardinal, Gavin Clarkson, Kristy Long, and Sarah Shoniker provided excellent field assistance. Aurora Geosciences, Helidynamics, Trans North, Black Sheep Aviation, Northern Rockies Air Charter and Beth Hunt worked to smooth logistical operations. Office-related challenges were solved by Janice Moor and Laurie Fahr. Monica Nordling helped geo-reference data for the geology map (Plate 1).

We acknowledge the Liard First Nation for their interest in this project which occurs in their traditional territory; in particular Alex Macmillan shared his knowledge of the early exploration history of the area.

Sandy McCracken and Godfrey Nowlan (both GSC) undertook the conodont fossil identification. Jim Crowley (Boise State University) completed the isotopic geochronology of the intrusions and tuff in the area. The manuscript was reviewed by David Moynihan, Yukon Geological Survey, and Karen Fallas, Geological Survey of Canada.

## REFERENCES

- Abbott, G., 1981. A new geological map of the upper Coal River area. *In: Yukon Geology and Exploration 1979-80*, Exploration and Geological Services Division, Yukon Region, Indian and Northern Affairs Canada, p. 51-54.
- Abbott, G., 1997. Geology of the upper Hart River area, eastern Ogilvie Mountains, Yukon Territory (116A/10, 116A/11). Exploration and Geological Services Division, Yukon, Indian and Northern Affairs Canada, Bulletin 9, 92 p.
- Abbott, J.G., Gordey, S.P. and Tempelman-Kluit, D.J., 1986. Setting of stratiform, sediment-hosted lead-zinc deposits in Yukon and northeastern British Columbia. *In: Mineral Deposits of Northern Cordillera*, J.A. Morin (ed.), Canadian Institute of Mining and Metallurgy, Special Volume 37, p. 1-18; *reprinted in Field trip Guidebook*, 8<sup>th</sup> IAGOD symposium, 1990, Geological Survey of Canada, Open File 2169, p. 69-98.
- Aitken, J.D., 1991. The Ice Brook Formation and post-Rapitan, Late Proterozoic glaciation, Mackenzie Mountains, Northwest Territories. Geological Survey of Canada, Bulletin 404, 43 p.
- Armitage, A. and Gray, P.D., 2012. Technical report on the Hyland gold property in the Yukon Territory, Canada. Technical report filed with SEDAR on November 15, 2012, 66 p.
- Bailey, D.K., 1985. Fluids, melts, flowage and styles of eruption in an alkaline ultramafic magmatism. *Transactions of the Geological Society of South Africa*, vol. 88, p. 449-457.
- Bamber, E.W. and Mamet, B.L., 1978. Carboniferous biostratigraphy and correlation, northeastern British Columbia and southwestern District of Mackenzie. Geological Survey of Canada, Bulletin 266, 65 p.
- Bamber, E.W., Taylor, G.C. and Proctor, R.M., 1968. Carboniferous and Permian stratigraphy of northeastern British Columbia. Geological Survey of Canada, Paper 68-15, 25 p.
- Barberi, F., Santacroe, R. and Varet, J., 1982. Chemical aspects of rift magmatism. *In: Continental and oceanic rifts*, G. Pálmason (ed.), American Geophysical Union, Washington, DC, p. 223-258.
- Bassett, H.C. and Stout, J.G., 1966. Devonian of western Canada. *In: International Symposium on the Devonian System*, vol. 1, D.H. Oswald (ed.), Alberta Society of Petroleum Geologists, p. 717-752.
- Beranek, L.P., Mortensen, J.K., Lane, L.S., Allen, T.L., Fraser, T.A., Hadlari, T. and Zantvoort, W.G., 2010. Detrital zircon geochronology of the western Ellesmerian clastic wedge, northwestern Canada: Insights on Arctic tectonics and the evolution of the northern Cordillera miogeocline. *Geological Society of America Bulletin*, vol. 122, no. 11/12, p. 1899-1911.
- Bostock, H.S., 1966. Notes on glaciation in central Yukon Territory. Geological Survey of Canada, Paper 68-15, 25 p.
- Cabanis, B. and Lecolle, M., 1989. The La/10-Y/15-Nb/8 diagram; a tool for distinguishing volcanic series and discovering crustal mixing and/or contamination. *Comptes Rendus de l'Académie des Sciences*, vol. 309, p. 2023-2029 (in French with an English abstract).
- Carne, R.C., 1996. Report on 1995 test pitting program on the Cuz property southeast Yukon Territory. Unpublished Yukon mineral assessment report #093537, 24 p.

- Cecile, M.P., 1982. The Lower Paleozoic Misty Creek embayment, Selwyn Basin, Yukon and Northwest Territories. Geological Survey of Canada, Bulletin 335, 78 p.
- Cecile, M.P., 2000. Geology of the northeastern Nidderly Lake map area, east-central Yukon and adjacent Northwest Territories. Geological Survey of Canada, Bulletin 553, 120 p.
- Cecile, M.P., Morrow, D.W. and Williams, G.K., 1997. Early Paleozoic (Cambrian to Early Devonian) tectonic framework, Canadian Cordillera. *Bulletin of Canadian Petroleum Geology*, vol. 45, no. 1, p. 54-74.
- Cecile, M.P. and Norford, B.S., 1979. Basin to platform transition, Lower Paleozoic Strata of Ware and Trutch map areas, northeastern British Columbia. *In: Current Research, Part A, Geological Survey of Canada, Paper 79-1A*, p. 219-226.
- Cecile, M.P. and Norford, B.S., 1991. Ordovician and Silurian assemblages. *In: Chapter 7, Cambrian to Middle Devonian Assemblages, Geology of the Cordilleran Orogen in Canada*, H. Gabrielse and C.J. Yorath (eds.), Geological Survey of Canada, Geology of Canada, no. 4, p. 184-196 (also Geological Society of America, *The Geology of North America*, vol. G-2).
- Cecile, M.P. and Norford, B.S., 1993. Ordovician and Silurian; Subchapter 4c. *In: Sedimentary Cover of the Craton in Canada*, D.F. Stott and J.D. Aitkin (eds.), Geological Survey of Canada, Geology of Canada, no. 5, p. 125-149 (also Geological Society of America, *The Geology of North America*, vol. D-1).
- Colpron, M., Logan, J.M. and Mortensen, J.K., 2002. U-Pb zircon age constraint for late Neoproterozoic rifting and initiation of the lower Paleozoic passive margin of western Laurentia. *Canadian Journal of Earth Sciences*, vol. 39, p. 133-143.
- Dawson, K.M. and Orchard, M.J., 1982. Regional metallogeny of the northern Cordillera: Biostratigraphy, correlation and metallogenic significance of bedded barite occurrences in eastern Yukon and western District of Mackenzie. *In: Current Research, Part C, Geological Survey of Canada, Paper 82-1C*, p. 31-38.
- Dixon, J., 2009. The Lower Triassic Shale member of the Montney Formation in the subsurface of northeast British Columbia. Geological Survey of Canada, Open File 6274, 9 p.
- Douglas, R.J.W. and Norris, D.K., 1960. Virginia Falls and Sibbeston Lake map – areas, Northwest Territories, 95F and G. Geological Survey of Canada, Paper 60-19, 26 p.
- Douglas, R.J.W., Gabrielse, H., Wheeler, J.O., Stott, D.F. and Belyea, H.R., 1970. Geology of western Canada. *In: Geology and Economic Minerals of Canada*, R.J.W. Douglas (ed.), Geological Survey of Canada, Economic Geology Report No. 1, p. 365-448.
- Duk-Rodkin, A., Barendregt, R.W., Froese, D.G., Weber, F., Enkin, R., Smith, I.R., Zazula, G.D., Waters, P. and Klassen, R., 2004. Timing and extent of Plio-Pleistocene glaciations in north-western Canada and east-central Alaska. *In: Quaternary Glaciations – Extent and Chronology, Part II*, J. Ehlers and P.L. Gibbard (eds.), Elsevier, p. 313-345.
- Duk-Rodkin, A., Barendregt, R.W., Tarnocai, C. and Phillips, F.M., 1996. Late Tertiary to late Quaternary record in the Mackenzie Mountains, Northwest Territories, Canada: stratigraphy, paleosols, paleomagnetism and chlorine-36. *Canadian Journal of Earth Sciences*, vol. 33, p. 875-895.

- Eisbacher, G.H., 1978. Re-definition and subdivision of the Rapitan Group, Mackenzie Mountains. Geological Survey of Canada, Paper 77-35, 21 p.
- Eisbacher, G.H., 1981. Sedimentary tectonics and glacial record in the Windermere Supergroup, Mackenzie Mountains, northwestern Canada. Geological Survey of Canada, Paper 80-27, 40 p.
- Espitalié, J., Laporte, J.L., Madec, M., Marquis, F., Leplat, P., Paulet, J. and Boutefeu, A., 1977. Méthode rapide de caractérisation des roches mères de leur potentiel pétrolier et de leur degré d'évolution. *Revue de l'Institut Français du Pétrole*, vol. 32, p. 23-42.
- Eyles, N., 1990. Marine debris flows: Late Precambrian 'tillites' of the Avalonian-Cadomian orogenic belt. *Palaeogeography, palaeoclimatology, Palaeoecology*, vol. 79, p. 73-98.
- Fallas, K.M. and Lane, L.S., 2001. Geology of the Mount Martin, Fisherman Mount Flett map areas, Yukon Territory and Northwest Territories. Geological Survey of Canada, Current Research 2001-A5, 11 p.
- Fallas, K.M., Lane, L.S. and Pigage, L.C., 2014. Geology, La Biche River, Yukon Territory-Northwest Territories. Geological Survey of Canada, Canadian Geoscience Map 144, scale 1:250 000. doi: 10.4095/000000.
- Fallas, K.M., Richards, B.C. and Khudoley, A., 2002. Regional paleocurrent patterns of the Mississippian Mattson Formation from the La Biche, Kotaneelee, and Liard Ranges, Yukon and Northwest Territories. Canadian Society of Petroleum Geologists Annual Meeting abstract volume, Calgary, Alberta.
- Ferri, F., Hickin, A.S. and Huntley, D.H., 2011. Besa River Formation, western Liard Basin, British Columbia (NTS 094N): geochemistry and regional correlations. *In: Geoscience Reports 2011*, British Columbia Ministry of Energy and Mines, p. 1-18.
- Ferri, F., Rees, C., Nelson, J. and Legun, A., 1999. Geology and Mineral Deposits of the northern Kechika Trough between Gataga River and the 60<sup>th</sup> Parallel. British Columbia Ministry of Energy, Mines and Petroleum Resources, Bulletin 107, 122 p.
- Fischer, B.J. and Pope, M.C., 2012. Lower Cambrian carbonate succession-Sekwi Formation. *In: Geology of the central Mackenzie Mountains of the northern Canadian Cordillera, Sekwi Mountain (105P), Mount Eduni (106A), and northwestern Wrigley Lake (95M) map areas, Northwest Territories.* E. Martel, E.C. Turner and B.J. Fisher (eds.), NWT Special Volume 1, NWT Geoscience Office, p. 142-149.
- Fritz, W.H., 1972. Lower Cambrian trilobites from the Sekwi Formation type section, Mackenzie Mountains, northwestern Canada. Geological Survey of Canada, Bulletin 212, 90 p.
- Fritz, W.H., 1982. Vampire Formation, a new Upper Precambrian (?)/Lower Cambrian formation, Mackenzie Mountains, Yukon and Northwest Territories. *In: Current Research, Part B, Geological Survey of Canada, Paper 82-1B*, p. 83-92.
- Fritz, W.H., 1985. The basal contact of the Road River Group—a proposal for its location in the type area and in other selected areas of Northern Canadian Cordillera. *In: Current Research, Part B, Geological Survey of Canada, Paper 85-1B*, p. 205-215.

- Fritz, W.H., Narbonne, G. and Gordey, S.P., 1983. Strata and trace fossils near the Precambrian-Cambrian boundary, Mackenzie, Selwyn, and Wernecke mountains, Yukon and Northwest Territories. *In: Current Research, Part B, Geological Survey of Canada, Paper 83-1B*, p. 365-375.
- Gabrielse, H., 1963. Geology, Rabbit River, British Columbia. Geological Survey of Canada, Map 46-1962. Scale: 1:253,440.
- Gabrielse, H., 1967a. Geology, Watson Lake, Yukon Territory. Geological Survey of Canada, Preliminary Map 19-1966, 1 sheet, doi:10.4095/107732.
- Gabrielse, H., 1967b. Tectonic evolution of the northern Canadian Cordillera; Canadian Journal of Earth Sciences, vol. 4, p. 271-298.
- Gabrielse, H. and Blusson, S.L., 1968. Geology, Coal River, Yukon Territory-District of Mackenzie. Geological Survey of Canada, Map 11-1968, scale: 1:253,440.
- Gabrielse, H. and Blusson, S.L., 1969. Geology of Coal River map-area, Yukon Territory and District of Mackenzie (95D). Geological Survey of Canada, Paper 68-38, 22 p.
- Gabrielse, H., Blusson, S.L. and Roddick, J.A., 1973. Geology of Flat River, Glacier Lake, and Wrigley Lake map-areas, District of Mackenzie and Yukon Territory. Geological Survey of Canada, Memoir 366 (Parts I and II), 421 p.
- Gabrielse, H., Monger, J.W.H., Wheeler, J.O. and Yorath, C.J., 1991. Part A. Morphogeological belts, tectonic assemblages and terranes; Chapter 2. *In: Geology of the Cordilleran Orogen in Canada*, H. Gabrielse and C.J. Yorath (eds.), Geological Survey of Canada, Geology of Canada, no. 4, p. 15-28 (also Geological Society of America, The Geology of North America, vol. G-2).
- Gabrielse, H. and Price, L.L., 1963. Geology, McDame, Cassiar District, British Columbia. Geological Survey of Canada, "A" Series Map 1110A, 1 sheet, doi: 10.4095/107061.
- Gibson, D.W., 1993. Triassic; Subchapter 4G. *In: Sedimentary cover of the craton in Canada*, D.F. Stott and J.D. Aitken (eds.), Geological Survey of Canada, no. 5, p. 294-320 (also Geological Society of America, The Geology of North America, vol. D-1).
- Godwin, C.I., Gabites, J.E. and Andrew, A., 1988. Leadtable: a galena lead isotope data base for the Canadian Cordillera, with a guide to its use by explorationists. British Columbia Ministry of Energy, Mines and Petroleum Resources, Paper 1988-4, 188 p.
- Godwin, C.I. and Sinclair, A.J., 1982. Average lead isotope growth curves for shale-hosted zinc-lead deposits, Canadian Cordillera. *Economic Geology*, vol. 77, p. 675-689.
- Goodfellow, W.D., Cecile, M.P. and Leybourne, M.I., 1995. Geochemistry, petrogenesis and tectonic setting of lower Paleozoic alkalic and potassic volcanic rocks, Northern Canadian Cordilleran miogeocline. *Canadian Journal of Earth Sciences*, vol. 32, p. 1236-1254.
- Gordey, S.P., Abbott, J.G. and Orchard, M.J., 1982. Devono-Mississippian (Earn Group) and younger strata in east-central Yukon. *In: Current Research, Part B, Geological Survey of Canada, Paper 82-1B*, p. 93-100.
- Gordey, S.P. and Anderson, R.G., 1993. Evolution of the northern Cordilleran miogeocline, Nahanni map area (105I), Yukon and Northwest Territories. Geological Survey of Canada, Memoir 428, 214 p.

- Gordey, S.P., 1991. Devonian-Mississippian clastics of the Foreland and Omineca Belts. *In: Geology of the Cordilleran Orogen in Canada*, H. Gabrielse and C.J. Yorath (eds.), Geological Survey of Canada, Geology of Canada, no. 4, p. 230-242 (also Geological Society of North America, vol. G-2).
- Gordey, S.P., 2013. Evolution of the Selwyn Basin region, Sheldon Lake and Tay River map areas, central Yukon. Geological Survey of Canada, Bulletin 599, 176 p.
- Gordey, S.P. and Makepeace, A.J. (comps.), 2003. Yukon digital geology, version 2.0. Geological Survey of Canada, Open File 1749, also known as Yukon Geological Survey, Open File 2003-9(D), 2 CD-ROMS, 1:1 000 000 scale.
- Green, L.H., 1972. Geology of Nash Creek, Larsen Creek, and Dawson map areas, Yukon Territory. Geological Survey of Canada, Memoir 364, 157 p.
- Hadlari, T., Davis, W.J., Dewing, K., Heaman, L.M., Lemieux, Y., Ootes, L., Pratt, B.R. and Pyle, L.J., 2012. Two detrital zircon signatures for the Cambrian passive margin of northern Laurentia highlighted by new U-Pb results from Northern Canada. *Geological Society of America Bulletin*, vol. 124, no. 7-8, p. 1155-1168.
- Handfield, R.C., 1968. Sekwi Formation, a new lower Cambrian formation in the southern Mackenzie Mountains, District of Mackenzie (95L, 105I, 105P). Geological Survey of Canada, Paper 68-47, 23 p.
- Handfield, R.C., 1971. Archaeocyatha from the Mackenzie and Cassiar Mountains, Northwest Territories, Yukon Territory and British Columbia. Geological Survey of Canada, Bulletin 201, 119 p.
- Harker, R., 1961. Summary account of Carboniferous and Permian formations, southwestern District of Mackenzie. Geological Survey of Canada, Paper 61-1, 9 p.
- Harrison, J.C., 1982. Petrology of the 'Ting Creek' alkalic intrusion southeast Yukon. Unpublished MSc Thesis, University of Toronto, Toronto, Ontario, 301 p.
- Hart, C.J.R., Goldfarb, R.J., Lewis, L.L. and Mair, J.L., 2004. The northern cordilleran mid-Cretaceous plutonic province: Ilmentite/magnetite-series granitoids and intrusion-related mineralization. *Resource Geology*, vol. 54, p. 253-280.
- Hart, C.J.R. and Lewis, L.L., 2006. Gold mineralization in the upper Hyland River area: A non-magmatic origin. *In: Yukon Exploration and Geology 2005*, D.S. Emond, G.D. Bradshaw, L.L. Lewis and L.H. Weston (eds.), Yukon Geological Survey, p. 109-125.
- Heffernan, R.S., 2004. Temporal, geochemical, isotopic and metallogenic studies of Mid-Cretaceous magmatism in the Tintina Gold Province, southeastern Yukon and southwestern Northwest Territories, Canada. Unpublished MSc thesis, University of British Columbia, Vancouver, British Columbia, 83 p.
- Henderson, C.M., Bamber, E.W., Richards, B.C., Higgins, A.C. and McGugan, A., 1993. Permian. *In: Sedimentary cover of the North American Craton: Canada*, D.E. Stott and J.D. Aitken (eds.), Geological Survey of Canada, Geology of Canada, no. 6 (also Geological Society of America, The geology of North America, DNAG vol. D-1).
- Herbosch, A. and Verniers, J., 2011. What is the biostratigraphic value of the ichnofossil *Oldhamia* for the Cambrian: a review. *Geologica Belgica*, vol. 14, no. 3-4, p. 229-248.

- Hofmann, H.J. and Cecile, M.P., 1981. Occurrence of Oldhamia and other trace fossils in Lower Cambrian(?) argillites, Selwyn Mountains, Yukon. Geological Survey of Canada, Paper 81-1A, p. 281-289.
- Jackson, D.E. and Lenz, A.C., 1962. Zonation of Ordovician and Silurian graptolites in northern Yukon, Canada. American Association of Petroleum Geologists Bulletin, vol. 46, p. 30-45.
- Jackson, L.E., Jr., Ward, B., Duk-Rodkin, A. and Hughes, O.L., 1991. The last Cordilleran ice sheet in southern Yukon Territory. Géographie physique et Quaternaire, vol. 45, no. 3, p. 341-354.
- Jenner, G.A., 1996. Trace element geochemistry of igneous rocks: geochemical nomenclature and analytical geochemistry. *In*: Trace Element Geochemistry of Volcanic Rocks: Applications for massive sulphide exploration, D.A. Wyman (ed.), Geological Association of Canada, Short Course Notes, vol. 12, p. 51-77.
- Jennings, D.S. and Jilson, G.A., 1986. Geology and Sulphide Deposits of Anvil Range, Yukon. *In*: Mineral Deposits of the Northern Cordillera: Proceedings of the Mineral Deposits of Northern Cordillera Symposium, December 1983, J.A. Morin (ed.), Special Volume 37, Canadian Institute of Mining and Metallurgy, p. 319-361.
- Kennedy, K., 2010. Preliminary Quaternary geology of Coal River area (NTS 95D), Yukon. *In*: Yukon Exploration and Geology 2009, K.E. MacFarlane, L.H. Weston and L.R. Blackburn (eds.), Yukon Geological Survey, p. 197-212.
- Kidd, F.A., 1963. The Besa River Formation. Bulletin of Canadian Petroleum Geology, vol. 11, p. 369-372.
- Kindle, E.D., 1944. Geological reconnaissance along the Fort Nelson, Liard and Beaver rivers, northeastern British Columbia and southeastern Yukon. Geological Survey of Canada, Paper 44-16, 19 p.
- King, H.L., 1995. Report on diamond drilling Mel property, Yukon. Unpublished Yukon mineral assessment report #093353, 64 p.
- Kingston, D.R., 1951. Stratigraphic reconnaissance along the upper South Nahanni River, NWT. American Association of Petroleum Geologists Bulletin, vol. 35, no. 11, p. 2409-2426.
- Kiss, F., 2010a. Total magnetic field, Flat River Aeromagnetic Survey, NTS 95E (south half), Yukon. Yukon Geological Survey, Open File 2010-15.
- Kiss, F., 2010b. First vertical derivative of the magnetic field, Flat River Aeromagnetic Survey, NTS 95E (south half), Yukon. Yukon Geological Survey, Open File 2010-16.
- Kiss, F., 2010c. Total magnetic field, Aeromagnetic Survey, NTS 95E (north half), Yukon. Yukon Geological Survey, Open File 2010-17.
- Kiss, F., 2010d. First vertical derivative of the magnetic field, Flat River Aeromagnetic Survey, NTS 95E (north half), Yukon. Yukon Geological Survey, Open File 2010-18.
- Klassen, R.W., 1983. Surficial Geology, Coal River, Yukon Territory (95D, west half), Geological Survey of Canada, Map 13-1982 (1:250 000 scale).

- Klassen, R.W., 1987. The Tertiary Pleistocene stratigraphy of the Liard Plain, southeastern Yukon Territory. Geological Survey of Canada, Paper 86-17, 16 p.
- Lemieux, Y., Hadlari, T. and Simonetti, A., 2011. Detrital zircon geochronology and provenance of Devonian-Mississippian strata in the northern Canadian Cordilleran miogeocline. *Canadian Journal of Earth Sciences*, vol. 48, p. 515-541.
- Lenz, A.C., 1972. Ordovician to Devonian history of northern Yukon and adjacent District of Mackenzie. *Bulletin of Canadian Petroleum Geology*, vol. 20, no. 2, p. 321-361.
- Leslie, C.D., 2009. Detrital zircon geochronology and rift-related magmatism: central Mackenzie Mountains, Northwest Territories. Unpublished MSc thesis, University of British Columbia, Vancouver, British Columbia, 236 p.
- Long, D.G.F. and Sweet, A.R., 1994. Age and depositional environment of the Rock River coal basin, Yukon Territory, Canada. *Canadian Journal of Earth Sciences*, vol. 31, p. 865-880.
- Ludvigsen, R., 1975. Ordovician formations and faunas, southern Mackenzie Mountains. *Canadian Journal of Earth Sciences*, vol. 12, no. 4, p. 663-697.
- MacIntyre, D.G., 1992. Geological setting and genesis of sedimentary exhalative barite and barite-sulfide deposits, Gataga district, northeastern British Columbia. *Exploration and Mining Geology*, vol. 1, p. 1-20.
- Macdonald, F.A., Schmitz, M.D., Crowley, J.L., Roots, C.F., Jones, D.S., Maloof, A.C., Strauss, J.V., Cohen, P.A., Johnston, D.T. and Schrag, D.P., 2010. Calibrating the Cryogenian. *Science*, vol. 327, no. 5970, p. 1241-1243.
- MacNaughton, R.B., 2002. Sedimentology of Triassic siliciclastic strata, Mount Martin and Mount Merrill map areas, Yukon Territory. Geological Survey of Canada, Current Research, 2002-A4, 10 p.
- MacNaughton, R.B. and Narbonne, G.M., 1999. Evolution and ecology of Neoproterozoic-Lower Cambrian trace fossils, NW Canada. *Palaios*, vol. 14, p. 97-115.
- MacNaughton, R.B., Roots, C.F. and Martel, E., 2008. Neoproterozoic(?)Cambrian lithostratigraphy, northeast Sekwi Mountain map area, Mackenzie Mountains, Northwest Territories: new data from measured sections. Geological Survey of Canada, Current Research (Online) no. 2008-16, 17 p.
- Macqueen, R.W. and Thompson, R.I., 1978. Carbonate-hosted lead-zinc occurrences in northeastern British Columbia with emphasis on the Robb Lake deposit. *Canadian Journal of Earth Sciences*, vol. 15, p. 1737-1762.
- Martel, E., Turner, E.C. and Fischer, B.J. (eds.), 2012. Geology of the central Mackenzie Mountains of the northern Canadian Cordillera, Sekwi Mountain (105P), Mount Eduni (106A), and northwestern Wrigley Lake (95M) map-areas, Northwest Territories. NWT Special Volume 1, NWT Geoscience Office, 423 p.
- Mathews, W.H. (compiler), 1986. Physiographic map of the Canadian Cordillera. Geological Survey of Canada, Map 1701A, 1 sheet, 1:5 000 000 scale.

- McCracken, A.D., 2010a. Report on 4 Ordovician-Devonian conodont samples (1 barren) from the Sekwi, Road River, Muncho-McConnell Formations of the Coal River Project area, southeastern Yukon submitted by Charlie Roots (Geological Survey of Canada) and processed in the GSC Vancouver Conodont Laboratory. NTS 095D-01, 095D-12, 095D-13. Geological Survey of Canada, Report 2-ADM-2010, 4 p.
- McCracken, A.D., 2010b. Report on 33 Ordovician-Permian conodont samples (25 barren) from the Fantasque, Muncho-McConnell, Narchilla, Narchilla-Vampire, Otter Creek, Sekwi equivalent, Sunblood, Rabbitkettle, Road River, Road River-Besa River, Vampire formations, unnamed Silurian-Devonian strata, and the Hyland Group of the Coal River Project area, southeastern Yukon and northern British Columbia, submitted by Charlie Roots (Geological Survey of Canada) and processed in the GSC Calgary Conodont Laboratory. NTS 094M/13, 095D-01, 095D-02, 095D-03, 095D-05, 095D-07, 095D-10, 095D-11, 095D-12, 095D-13, 095D-14, 095D-15. Geological Survey of Canada, Report 3-ADM-2010, 14 p.
- McDougall, G., 1976. Report on the Deb property. NWT mineral assessment report #080508, 20 p.
- McMechan, M., Ferri, F. and MacDonald, L., 2012. Geology of the Toad River area (NTS 094N), northeast British Columbia. *In: Geoscience Reports 2012, British Columbia Ministry of Energy and Mines*, p. 17-39.
- Meschede, M., 1986. A method of discriminating between different types of mid-ocean ridge basalts and continental tholeiites with the Nb-Zr-Y diagram. *Chemical Geology*, vol. 56, p. 207-218.
- Miller, D.C., 1977. Geological and geochemical report on the Mel, Jean and Wet claims, Yukon. Unpublished Yukon mineral assessment report #090234, 19 p.
- Miller, D.C. and Wright, J., 1986. Mel barite-zinc-lead deposit, Yukon – an exploration case history. *In: Mineral Deposits of Northern Cordillera: Proceedings of the Mineral Deposits of Northern Cordillera Symposium, December 1983, J.A. Morin (ed.), Special Volume 37, Canadian Institute of Mining and Metallurgy*, p. 129-141.
- Morrow, D.W., 1978. The Dunedin Formation: A transgressive shelf carbonate sequence. Geological Survey of Canada, Paper 76-12, 35 p.
- Morrow, D.W., Cumming, G.L. and Aulstead, K.L., 1990. The gas-bearing Devonian Manetoe facies, Yukon and Northwest Territories. Geological Survey of Canada, Bulletin 400, 54 p.
- Morrow, D.W., 1999. Lower Paleozoic stratigraphy of northern Yukon Territory and northwestern District of Mackenzie. Geological Survey of Canada, Bulletin 538, 201 p.
- Morrow, D.W. and Geldsetzer, H.H.J., 1991. Lower and Middle Devonian assemblages. *In: Chapter 7, Cambrian to Middle Devonian Assemblages, Geology of the Cordilleran Orogen in Canada*, H. Gabrielse and C.J. Yorath (eds.), Geological Survey of Canada, Geology of Canada, no. 4, p. 196-217 (also Geological Society of America, *The Geology of North America*, vol. G-2).
- Mortensen, J.K., Hart, C.J.R., Murphy, D.C. and Heffernan, R.S., 2000. Temporal evolution of Early and mid-Cretaceous magmatism of the Tintina gold belt. *In: Tintina gold belt: Concepts, Exploration and discovery*, J. Jambour (ed.), British Columbia and Yukon Chamber of Mines, Special Volume 2, p. 49-57.

- Moynihan, D., 2014. Bedrock Geology of NTS 106B/04, Eastern Rackla Belt. *In: Yukon Exploration and Geology 2013*, K.E. MacFarlane, M.G. Nordling and P.J. Sack (eds.), Yukon Geological Survey, p. 147-167.
- Murphy, D.C., 1997. Geology of the McQuesten River Region, Northern McQuesten and Mayo Map Areas, Yukon Territory (115P/14, 15, 16; 105M/13, 14). Exploration and Geological Services Division, Yukon, Indian and Northern Affairs Canada, Bulletin 6, 122 p.
- Natural Resources Canada, 2009. Canadian Aeromagnetic data base, Geoscience Data Repository; Geological Survey of Canada, <http://gdrdap.agg.nrcan.gc.ca/geodap/home/Default.aspx?lang=e>, [accessed March 01, 2009].
- Nelson, J. and Colpron, M., 2007. Tectonics and metallogeny of the British Columbia, Yukon and Alaskan Cordillera, 1.8 Ga to the present. *In: Mineral Deposits of Canada: A synthesis of major deposit-types, district metallogeny, the evolution of geological provinces, and exploration methods*, W.D. Goodfellow (ed.), Geological Association of Canada, Mineral Deposits Division, Special Publication No. 5, p. 755-791.
- Nelson, J.L., Colpron, M. and Israel, S., 2013. The Cordillera of British Columbia, Yukon, and Alaska: Tectonics and Metallogeny. *In: Tectonics, Metallogeny, and Discovery: the North American Cordillera and similar accretionary settings*, M. Colpron, T. Bissig, B.G. Rusk and J.F.H. Thompson (eds.), Society of Economic Geologists, Special Publication Number 17, p. 53-109.
- Norford, B.S., 1967. Report on ten lots of fossils from the Coal River Map-area, District of Mackenzie and Yukon Territory (NTS 95D); collected by Drs. S.L. Blusson and H. Gabrielse, 1967. Geological Survey of Canada, Report No. S-D 8 BSN 1967, 2 p.
- Norford, B.S., 1968a. Report on forty lots of fossils collected from the Sekwi Mountains, Nahanni, Glacier Lake, Coal River, and Rabbit River Map-areas, Yukon Territory, District of Mackenzie, and British Columbia (NTS 94M; 95D&L; 105I&P); collected by Drs. S.L. Blusson and H. Gabrielse, 1967. Geological Survey of Canada, Report No. O-D 8 BSN 1968, 6 p.
- Norford, B.S., 1968b. Report on ten lots of fossils from the Coal River and Cry Lake Map-areas, Yukon and British Columbia (NTS 95D, 104I); collected by Drs. S.L. Blusson and H. Gabrielse, 1967. Geological Survey of Canada, Report No. O-S 4 BSN 1968, 2 p.
- Norford, B.S., 1984. Report on two lots of fossils from the Coal River Map-area, Yukon Territory (NTS 95D); submitted by D.C. Miller, Sulpetro Minerals Ltd. Geological Survey of Canada, Report No. C-01-BSN-1984, 1 p.
- NORMIN, The Northern Minerals Database, 2010. Northwest Territories Geoscience Office, Yellowknife, NT: [www.nwtgeoscience.ca](http://www.nwtgeoscience.ca), [accessed February 24, 2010].
- Norris, A.W., 1985. Stratigraphy of Devonian outcrop belts in northern Yukon Territory and northwestern District of Mackenzie (Operation Porcupine Area). Geological Survey of Canada, Memoir 410, 81 p.
- Nowlan, G., 2008. Report on six samples from Ordovician strata in the northern Toobally Lake and Coal River map areas, southeastern Yukon submitted for conodont analysis by Lee Pigage (Yukon Geological Survey); NTS 095D/06; 095D/08. Geological Survey of Canada, Report No. 003-GSN-2008, 5 p.

- Nowlan, G.S., 2010a. Report on ten samples from Ordovician strata in the Coal River Project area, southeastern Yukon that were submitted for conodont analysis by Charlie Roots (Geological Survey of Canada) and Grant Abbott and Lee Pigage (Yukon Geological Survey) and processed in the GSC Vancouver Conodont Laboratory; NTS 095D/01, 095D/02, 095D/03, 095D/10, 095D/11, 095D/12. Geological Survey of Canada, Report No. 003-GSN-2010, 8 p.
- Nowlan, G.S., 2010b. Report on two samples from Ordovician strata in the Coal River Project area, southeastern Yukon that were submitted for conodont analysis by Lee Pigage (Yukon Geological Survey) and processed in the GSC Vancouver Conodont Laboratory; NTS 95D/06. Geological Survey of Canada, Report 004-GSN-2010, 2 p.
- Nowlan, G.S., 2010c. Report on twenty-eight samples from Ordovician strata in the Coal River area of Yukon Territory submitted for conodont analysis by Charlie Roots (Geological Survey of Canada) and Grant Abbott (Yukon Geological Survey); NTS 095D/01; 095D/02; 095D/03; 095D/09; 095D/10; 095D/11; 095D/14; 095D/15; CON #1746. Geological Survey of Canada, Report 005-GSN-2010, 23 p.
- Orchard, M.J., 2009a. Report on 6 (3 productive) microfossil samples submitted for analysis by L. Pigage, Yukon Geological Survey (2007). Geological Survey of Canada, Report No. 003-MJO-2009, 4 p.
- Orchard, M.J., 2009b. Report on 3 (2 productive) microfossil samples submitted for analysis by C.F. Roots, Geological Survey of Canada (2008). Coal River map area (95 D/03, /07), Yukon Territory. Geological Survey of Canada, Report No. 19-MJO-2009, 2 p.
- Orchard, M.J., 2010. Report on 25 (14 productive) microfossil samples submitted for analysis by C.F. Roots, Geological Survey of Canada (2009). Coal River map area (95 D/01, /02, /03, /05, /11, /12, /13, 14), Yukon Territory. Geological Survey of Canada, Report No. 4-MJO-2010, 9 p.
- Paradis, S., Nelson, J.L. and Zantvoort, W., 1999. A new look at the Robb Lake carbonate-hosted lead-zinc deposit, northeastern British Columbia. *In: Cordillera and Pacific margin/Interior Plains and Arctic Canada/Cordillère et marge du Pacifique/Plaines intérieures et régions arctique du Canada.* Geological Survey of Canada, Current Research no. 1999-A/B, p. 61-70.
- Patton, W.J.H., 1958. Mississippian succession in the South Nahanni River area, Northwest Territories. *In: Jurassic and Carboniferous in Western Canada*, Goodman, A.J. (ed.), American Association of Petroleum Geologists, J.A. Allan Memorial Volume, p. 302-326.
- Pearce, J.A., 1996. A user's guide to basalt discrimination diagrams. *In: Trace Element Geochemistry of Volcanic Rocks: Applications for Massive Sulphide Exploration*, D.A. Wyman (ed.), Geological Association of Canada, Short Course Notes, vol. 12, p. 79-113.
- Pearce, J.A., 2008. Geochemical fingerprinting of oceanic basalts with applications to ophiolite classification and the search for Archean oceanic crust. *Lithos*, vol. 100, p. 14-48, doi: 10.1016/j.lithos.2007.06.016.
- Pearce, J.A. and Cann, J.R., 1973. Tectonic setting of basic volcanic rocks determined using trace element analyses. *Earth and Planetary Science Letters*, vol. 19, p. 290-300.
- Peng, S., Babcock, L.E. and Cooper, R.A., 2012. The Cambrian Period. *In: The Geologic Time Scale 2012*, F. Gradstein, J. Ogg, M. Schmitz and G. Ogg (eds), Elsevier, vol. 2, p. 437-488.

- Peters, K.E., 1986. Guidelines for evaluating petroleum source rock using programmed pyrolysis. *American Association of Petroleum Geologists Bulletin*, vol. 70, p. 318-329.
- Pigage, L.C., 2004a. Preliminary geology of NTS 95D/8 (north Toobally Lakes area), southeast Yukon. Yukon Geological Survey, Open File 2004-19, scale 1:50 000.
- Pigage, L.C., 2004b. Bedrock geology compilation of the Anvil District (parts of NTS 105K/2, 3, 5, 6, 7 and 11), central Yukon. Yukon Geological Survey, Bulletin 15, 103 p.
- Pigage, L.C., 2006. Stratigraphy summary for southeast Yukon (95D/8 and 95C/5). *In: Yukon Exploration and Geology 2005*, D.S. Emond, G.D. Bradshaw, L.L. Lewis and L.H. Weston (eds.), Yukon Geological Survey, p. 267-285.
- Pigage, L.C., 2007. Preliminary geology map of NTS 95D/6. Yukon Geological Survey, Open File 2007-4, scale 1:50 000.
- Pigage, L.C., 2008. Preliminary bedrock geology for NTS 95D/6 (Otter Creek area), southeast Yukon. *In: Yukon Exploration and Geology 2007*, D.S. Emond, L.R. Blackburn, R.P. Hill and L.H. Weston (eds.), Yukon Geological Survey, p. 237-255.
- Pigage, L.C., 2009. Bedrock geology of NTS 95C/5 (Pool Creek) and NTS 95D/8 map sheets, southeast Yukon. Yukon Geological Survey, Bulletin 16, 150 p.
- Pigage, L.C. and MacNaughton, R.B., 2004. Reconnaissance geology of northern Toobally Lake (95D/8), southeast Yukon. *In: Yukon Exploration and Geology 2003*, D.S. Emond and L.L. Lewis (eds.), Yukon Geological Survey, p. 199-219.
- Pigage, L.C., Abbott, J.G. and Roots, C.F., 2011. Bedrock geology of Coal River map area (NTS 95D), Yukon. Yukon Geological Survey, Open File 2011-1, scale 1:250 000.
- Pigage, L.C., Crowley, J.L., Pyle, L.J., Abbott, J.G., Roots, C.F. and Schmitz, M.D., 2012. U-Pb zircon age of an Ordovician tuff in southeast Yukon: implications for the age of the Cambrian-Ordovician boundary. *Canadian Journal of Earth Sciences*, vol. 49, p. 732-741.
- Pigage, L.C., Crowley, J.L., Roots, C.F. and Abbott, J.G., 2014. Geochemistry and U-Pb zircon geochronology of mid-Cretaceous Tay River suite intrusions in southeast Yukon. *In: Yukon Exploration and Geology 2013*, K.E. MacFarlane, M.G. Nordling and P.J. Sack (eds.), Yukon Geological Survey, p. 169-174.
- Pohler, S.M.L. and Orchard, M.J., 1990. Ordovician conodont biostratigraphy, western Canadian Cordillera. Geological Survey of Canada, Paper 90-15, 37 p.
- Pugh, D.C., 1983. Pre-Mesozoic geology in the subsurface of Peel River map area, Yukon Territory and District of Mackenzie. Geological Survey of Canada, Memoir 401, 61 p.
- Pyle, L.J., 2004. Biostratigraphy Report. Seventeen samples submitted for conodont microfossil analysis, collected by Lee Pigage (Yukon Geological Survey), map sheet NTS 95D/8. Report No. LJP04-02, 12 p.
- Pyle, L.J. and Barnes, C.R., 2000. Upper Cambrian to Lower Silurian stratigraphic framework of platform-to-basin facies, northeastern British Columbia. *Bulletin of Canadian Petroleum Geology*, vol. 48, no. 2, p. 123-149.

- Rainbird R.H., Heaman, L.M. and Young G., 1992. Sampling Laurentia: Detrital zircon geochronology offers evidence for an extensive Neoproterozoic river system originating from the Grenville orogen. *Geology*, vol. 20, p. 351-354, doi:10.1130/0091-7613.
- Rainbird, R.H., McNicoll, V.J., Thériault, J., Heaman, L.M., Abbott, J.G., Long, D.G.F. and Thorkelson, D.J., 1997. Pan-continental river system draining Grenville Orogen recorded by U-Pb and Sm-Nd geochronology of Neoproterozoic quartzarenites and mudrocks, northwestern Canada. *Journal of Geology*, vol. 105, p. 1-17.
- Rasmussen, K.L., 2013. The timing, composition, and petrogenesis of syn- to post-accretionary magmatism in the northern Cordilleran miogeocline, eastern Yukon and southwestern Northwestern Territories. Unpublished PhD thesis, University of British Columbia, Vancouver, Canada.
- Rasmussen, K.L., Mortensen, J.K., Falck, H. and Ullrich, T.D., 2007. The potential for intrusion-related mineralization within the South Nahanni MERA area, Selwyn and Mackenzie Mountains, Northwest Territories. *In: Mineral and Energy Resource Assessment of the greater Nahanni ecosystem under consideration for the expansion of the Nahanni National Park Reserve, Northwest Territories.* Geological Survey of Canada, Open File 5344, p. 203-278.
- Richards, B.C., 1989. Uppermost Devonian and lower Carboniferous stratigraphy, sedimentation and diagenesis, southwestern District of Mackenzie and southeastern Yukon Territory (NTS 95B, C, F and G). Geological Survey of Canada, Bulletin 390, 135 p.
- Richards, B.C., Bamber, E.W., Higgins, A.C. and Utting, J., 1993. Carboniferous; sub-chapter 4E. *In: Sedimentary Cover of the Craton in Canada.* D.F. Stott and J.D. Aitken (eds.), Geological Survey of Canada, Geology of Canada, no. 5, p. 202-271 (also Geological Society of America, The Geology of North America, vol. D-1).
- Rollinson, H., 1993. Using geochemical data: evaluation, presentation, interpretation. Longman Scientific & Technical, Harlow, 352 p.
- Rooney, A.D., Macdonald, F.A., Strauss, J.V., Dudas, F.O., Hallmann, C. and Selby, D., 2014. Re-Os geochronology and coupled Os-Sr isotope constraints on the Sturtian snowball Earth. *Proceedings of the National Academy of Sciences*, vol. 111 (1), p. 51-56.
- Roots, C.F., 1997. Geology of the Mayo Map Area, Yukon Territory (105M). Exploration and Geological Services Division, Yukon, Indian and Northern Affairs Canada, Bulletin 7, 82 p.
- Roots, C.F., 1988. Cambro-Ordovician volcanic rocks in eastern Dawson map-area, Ogilvie Mountains, Yukon. *In: Yukon Geology, Vol. 2, Yukon Geological Survey*, p. 81-87.
- Roots, E.F., Green, L.H., Roddick, J.A. and Blusson, S.L., 1966. Geology, Frances Lake, Yukon Territory and District of Mackenzie. Geological Survey of Canada, Preliminary Map 6-1966, 1 sheet, doi:10.4095/107736.
- Rutgers, A.T.C., 1958. Stoddart Formation of northeastern British Columbia. *In: Jurassic and Carboniferous of western Canada.* A.J. Goodman (ed.), American Association of Petroleum Geologists, John Andrew Allen Memorial Volume, p. 327-330.
- Shervais, J., 1982. Ti-V plots and the petrogenesis of modern and ophiolitic lavas. *Earth and Planetary Science Letters*, vol. 59, p. 101-118.

- Smith, I.R., 2000. Preliminary report on surficial geology investigations of La Biche River map area, southeast Yukon Territory. Geological Survey of Canada, Current Research 2000-B3, 9 p.
- Stammers, M.A., 1983. Geological and Geochemical report on the Chuck 1 and 2 mineral claims. NWT mineral assessment report #081665, 18 p.
- Stockwell, J.E., 1975. Project 914, Geological/geochemical reconnaissance. Unpublished Yukon mineral assessment report #092014, 171 p.
- Sun, S.S. and McDonough, W.F., 1989. Chemical and isotopic systematics of oceanic basalts; implications for mantle composition and processes. *In: Magmatism in the ocean basins*, A.D. Saunders and M.J. Norry (eds.), Geological Society of London, London, vol. 42, p. 313-345.
- Sweet, A.R., 1983. Applied Research Report on 16 samples from the Rock River coal field, Yukon Territories (NTS 95D/11) as requested by D. Long. Geological Survey of Canada, Paleontology Report No. 11-ARS-1983, 7 p.
- Taylor, G.C. and MacKenzie, W.S., 1970. Devonian stratigraphy of northeastern British Columbia. Geological Survey of Canada, Bulletin 186, 62 p.
- Taylor, G.C. and Stott, D.F., 1999. Geology, Toad River, British Columbia. Geological Survey of Canada, Map 1955A, 1 sheet, 1:250 000 scale, doi:10.4095/210819.
- Tempelman-Kluit, D.J., 1970. Stratigraphy and structure of the "Keno Hill Quartzite" in Tombstone River-Upper Klondike River map-areas, Yukon Territory. Geological Survey of Canada, Bulletin 180, 102 p.
- Thompson, R.I., 1989. Stratigraphy, tectonic evolution and structural analysis of the Halfway River map area (94B), northern Rocky Mountains, British Columbia. Geological Survey of Canada, Memoir 425, 119 p., 10 maps.
- Thompson, R.I. and Roots, C.F., 1982. Ogilvie Mountains Project, Yukon: Part A: a new regional mapping program. Geological Survey of Canada, Current Research, Part A, Paper 82-1A, p. 411-414.
- Tipnis, R.S., Chatterton, B.D.E. and Ludvigsen, R., 1978. Ordovician conodont biostratigraphy of the southern District of Mackenzie, Canada. *In: Western and Arctic Canadian Biostratigraphy*, C.R. Stelck and B.D.E. Chatterton (eds.), Geological Association of Canada, Special Paper 18, p. 39-91.
- Utting, J., 2006. Palynological investigation of 2 outcrop samples of unknown age from Yukon, submitted by R.B. MacNaughton, Geological Survey of Canada (Calgary) and L. Pigage, Yukon Geological Survey, mapsheet 095D/08. Geological Survey of Canada, Report No. 04-JU-2006, 3 p.
- Vaillancourt, P., 1983. Geology of pyrite-sphalerite-galena concentrations in Proterozoic quartzite at Quartz Lake, southeastern Yukon. *In: Yukon Exploration and Geology 1982*, Yukon Geological Survey, Indian & Northern Affairs Canada/Department of Indian & Northern Development: Exploration & Geological Services Division, p. 73-77.
- Vulimiri, M., 1986. Geological report on the Chuck 1 mineral claim Caribou River area. Unpublished NWT mineral assessment report #082082, 19 p.
- Wheeler, J.O. and McFeely, P. (comps.), 1991. Tectonic Assemblage Map of the Canadian Cordillera and adjacent parts of the United States of America. Geological Survey of Canada, Map 1712A, scale 1:2 000 000.

- Wheeler, K.L., Forbes, R.B., Weber, F.R. and Reinhardt, C.D., 1986. The lithostratigraphy, petrology and geochemistry of the Ordovician Fossil Creek volcanics, White Mountains, east-central Alaska. United States Geological Survey, Alaska accomplishments, p. 70-73.
- Winchester, J.A. and Floyd, P.A., 1977. Geochemical discrimination of different magma series and their differentiation products using immobile elements. *Chemical Geology*, vol. 20, p. 325-343.
- Wood, D.A., 1980. The application of a Th-Hf-Ta diagram to problems of tectonomagmatic classification and to establishing the nature of crustal contamination of basaltic lavas of the British Tertiary Volcanic Province. *Earth and Planetary Science Letters*, vol. 45, p. 326-336.
- Wright, J. and Miller, D.C., 1986. Rock River coal basin: geology, gravity survey and interpretation. *In: Mineral Deposits of Northern Cordillera: Proceedings of the Mineral Deposits of Northern Cordillera Symposium, December 1983, J.A. Morin (ed.), Special Volume 37, Canadian Institute of Mining and Metallurgy*, p. 362-371.
- Yukon MINFILE - A database of mineral occurrences. Yukon Geological Survey, <[www.geology.gov.yk.ca/databases\\_gis.html](http://www.geology.gov.yk.ca/databases_gis.html)>.

## APPENDIX A - PALEONTOLOGY

**Table A1.** Fossil collections, arranged by formation.

Paleontology - NTS 95D				
Map ID	GSC ID	Fossil Type	Age Range	Reference
<b>Unit Es</b>				
1	73840, 68958, 68957, 68956, 68955	trilobite; archeocyathid	Early Cambrian (Series 2; Stage 3)	Handfield (1971)
2		trilobite	Early Cambrian (Series 2; Stage 4)	Bohach, L. (2009 pers comm)
<b>Unit COOC</b>				
3	C-092627	trilobite; brachiopod	Cambrian (Furongian) - Early Ordovician (Tremadocian)	Miller and Wright (1986); Norford (1984)
4	C-061554	trilobite; brachiopod	Cambrian (Furongian) - Early Ordovician (Tremadocian)	Miller and Wright (1986); Norford (1984)
5	C-535898	conodont	late Early Ordovician (Floian) - Late Ordovician (Sandbian)	Nowlan (2010c)
<b>Unit COC</b>				
6	C-417157	conodont	Early Ordovician (Tremadocian)	Pigage (2009); Pyle (2004)
7	C-535867	conodont	Middle Ordovician (Dapingian)	Orchard (2010); Nowlan (2010a)
<b>Unit COR</b>				
8	O-081023	brachiopod; trilobite	Early Ordovician (Tremadocian - Floian)	Norford (1968a)
9	O-081025	brachiopod; trilobite	Early Ordovician (late Tremadocian - early Floian)	Gabrielse and Blusson (1969)
10	O-081026	trilobite	Early Ordovician (late Tremadocian - early Floian)	Norford (1968a)
11	V-000005	conodont	Early Ordovician (early Tremadocian)	Nowlan (2010b)
12	C-535864	conodont	Early Ordovician (late Floian)	Nowlan (2010a)
13	V-000386	conodont	Early Ordovician	Orchard (2009b)
14	C-535939	conodont	Early Ordovician (early Tremadocian)	Nowlan (2010c)
15	C-535940	conodont	Early Ordovician (early to middle Floian)	Nowlan (2010c)
16	C-535951	conodont	Early Ordovician (Tremadocian)	Nowlan (2010c)
17	C-535953	conodont	Early Ordovician (late Tremadocian - Floian)	Nowlan (2010c)
18	C-535881	conodont	Early Ordovician (late Tremadocian - Floian)	Orchard (2010); Nowlan (2010a)
19	C-535963	conodont	Early Ordovician (late Tremadocian - early Floian)	Nowlan (2010c)
20	C-535964	conodont	Early Ordovician (late Floian)	Orchard (2010); Nowlan (2010c)
21	C-535966	conodont	Early Ordovician (late Tremadocian - early Floian)	Nowlan (2010c)

**APPENDIX A - PALEONTOLOGY**, continued

**Table A1, continued.** Fossil collections, arranged by formation.

<b>Paleontology - NTS 95D</b>				
<b>Map ID</b>	<b>GSC ID</b>	<b>Fossil Type</b>	<b>Age Range</b>	<b>Reference</b>
<b>Unit OSu</b>				
22	O-079251	gastropod	Late Ordovician (late Sandbian - late Katian)	Gabrielse and Blusson (1969)
23	O-079252	gastropod	Middle Ordovician (Dapingian) - Late Ordovician (Sandbian)	Gabrielse and Blusson (1969)
24	O-079253	brachiopod; gastropod	Early Ordovician (Floian) - Late Ordovician (early Katian)	Gabrielse and Blusson (1969)
25	O-079254	gastropod; brachiopod	Late Ordovician (late Sandbian - early Katian)	Gabrielse and Blusson (1969)
26	O-079153	trilobite; brachiopod	Middle Ordovician (Dapingian) - Late Ordovician (Sandbian)	Gabrielse and Blusson (1969)
27	O-079246	brachiopod	Cambrian (Furongian) - Devonian	Norford (1968b)
28	O-079247	brachiopod	Ordovician - Present	Norford (1968b)
29	C-417165	conodont	Early Ordovician (middle Tremadocian)	Pigage (2009); Pyle (2004)
30	C-417159	conodont	Middle Ordovician (Darrivillian)	Pigage (2009); Pyle (2004)
31	C-417166	conodont	Early Ordovician (Floian) - Middle Ordovician (Darrivillian)	Pigage (2009); Pyle (2004)
32	C-417167	conodont	Early Ordovician (Floian) - Middle Ordovician (Dapingian)	Pigage (2009); Pyle (2004)
33	C-417163	conodont	Late Ordovician (Sandbian)	Pigage (2009); Pyle (2004)
34	C-307428	conodont	Middle Ordovician (Dapingian)	Nowlan (2008)
35	C-307626	conodont	Ordovician	Nowlan (2008)
36	C-307629	conodont	Middle Ordovician (Dapingian)	Nowlan (2008)
37	C-307630	conodont	Early Ordovician - Middle Ordovician (Dapingian)	Nowlan (2008)
38	C-307631	conodont	Middle Ordovician (Darrivillian)	Nowlan (2008)
39	C-307632	conodont	Middle Ordovician (Dapingian)	Nowlan (2008)
40	V-000007	conodont	Middle Ordovician - Middle Devonian	Nowlan (2010b)
41	V-000387	conodont	Early Ordovician	Orchard (2009b)
42	C-535932	conodont	earliest Middle Ordovician (early Dapingian)	Nowlan (2010c)
43	C-535866	conodont	Middle Ordovician (Dapingian)	Orchard (2010); Nowlan (2010a)
44	C-535934	conodont	late Early Ordovician (Floian)	Nowlan (2010c)
45	C-535869	conodont	Middle Ordovician (Dapingian)	Orchard (2010); Nowlan (2010a)
46	C-535870	conodont	Middle Ordovician (Dapingian - Darrivillian)	Orchard (2010); Nowlan (2010a)

**APPENDIX A - PALEONTOLOGY**, continued

**Table A1, continued.** Fossil collections, arranged by formation.

<b>Paleontology - NTS 95D</b>				
<b>Map ID</b>	<b>GSC ID</b>	<b>Fossil Type</b>	<b>Age Range</b>	<b>Reference</b>
<b>Unit OSu (continued)</b>				
47	C-535878	conodont	Early Ordovician (Tremadocian - Floian)	Orchard (2010); Nowlan (2010a)
48	C-535942	conodont	Early Ordovician (Tremadocian - Floian)	Nowlan (2010c)
49	C-535943	conodont	Early Ordovician (late Tremadocian - Floian)	Nowlan (2010c)
50	C-535945	conodont	Early Ordovician (late Tremadocian - early Floian)	Nowlan (2010c)
51	C-535949	conodont	late Early Ordovician (Floian)	Nowlan (2010c)
52	C-535872	conodont	Early Ordovician - Middle Ordovician	Orchard (2010); Nowlan (2010a)
53	C-535874	conodont	Middle Ordovician (Dapingian)	Orchard (2010); Nowlan (2010a)
54	C-535959	conodont	late Early Ordovician (late Floian)	Nowlan (2010c)
55	C-535883	conodont	Early Ordovician - early Middle Ordovician	Orchard (2010); Nowlan (2010a)
56	C-535888	conodont	latest Early Ordovician (latest Floian)	Nowlan (2010c)
57	C-535960	conodont	Early Ordovician (late Tremadocian - early Floian)	Nowlan (2010c)
58	C-535890	conodont	latest Early Ordovician (latest Floian)	Nowlan (2010c)
59	C-535961	conodont	earliest Early Ordovician (Tremadocian)	Nowlan (2010c)
60	C-535892	conodont	latest Early Ordovician (late Floian)	Nowlan (2010c)
61	C-535893	conodont	late Early Ordovician (middle - latest Floian)	Nowlan (2010c)
62	C-535894	conodont	Early Ordovician (Floian)	Nowlan (2010c)
63	C-535901	conodont	late Middle Ordovician (middle Darrivilian) - early Late Ordovician (early Sandbian)	Nowlan (2010c)
64	C-535904	conodont	earliest Middle Ordovician (early Dapingian)	Nowlan (2010c)
65	C-535908	conodont	Early Ordovician (Tremadocian)	Nowlan (2010c)
66	C-535909	conodont	Early Ordovician (middle to late Floian)	Nowlan (2010c)
67	C-535910	conodont	Early Ordovician (Floian) - Late Ordovician (Sandbian)	Nowlan (2010c)
<b>Unit SDc</b>				
68	O-079240	coral	Silurian	Gabrielse and Blusson (1969)
69	O-079241	coral	Middle Ordovician - Permian	Norford (1968b)
70	V-000008	conodont	Early Devonian?	Orchard (2009a)

**APPENDIX A - PALEONTOLOGY**, continued

**Table A1, continued.** Fossil collections, arranged by formation.

<b>Paleontology - NTS 95D</b>				
<b>Map ID</b>	<b>GSC ID</b>	<b>Fossil Type</b>	<b>Age Range</b>	<b>Reference</b>
<b>Unit SDc (continued)</b>				
71	C-537288	conodont	Middle Ordovician - Middle Devonian	Orchard (2010); McCracken (2010a)
72	C-535948	conodont	Middle Ordovician - Middle Devonian	McCracken (2010b)
73	C-535891	conodont	Early Devonian (Lochkovian - Emsian)	McCracken (2010b)
74	C-535906	conodont	Early Devonian (early to late Emsian)	McCracken (2010b)
75	C-535907	conodont	Silurian	Nowlan (2010c)
76		2-hole crinoid	Early Devonian (Emsian) - Middle Devonian (Eifelian)	visual identification
77		2-hole crinoid	Early Devonian (Emsian) - Middle Devonian (Eifelian)	visual identification
<b>Unit SDRR</b>				
78	O-079161	graptolite	Silurian (late Llandovery - Telychian)	Gabrielse and Blusson (1969); Norford (1967)
79	O-081024	tentaculitid; graptolite	Early Devonian	Gabrielse and Blusson (1969)
80	O-081032	coral	Late Ordovician - Silurian (Pridoli)	Gabrielse and Blusson (1969)
81	O-079154	graptolite	Silurian (late Llandovery - Telychian)	Gabrielse and Blusson (1969); Norford (1967)
82	O-081028	graptolite; tentaculitid	Early Devonian	Gabrielse and Blusson (1969)
83	O-081027	graptolite; tentaculitid	Early Devonian (early Emsian)	Gabrielse and Blusson (1969)
84	O-079155	graptolite	Early Devonian (Emsian)	Gabrielse and Blusson (1969); Norford (1967)
85	O-079243	graptolite	Silurian (late Llandovery - Telychian)	Gabrielse and Blusson (1969); Norford (1967)
86	O-079244	graptolite; brachiopod	Silurian (late Llandovery - Telychian)	Gabrielse and Blusson (1969); Norford (1967)
87	O-079245	graptolite; brachiopod	Silurian	Gabrielse and Blusson (1969); Norford (1967)
88	O-079242	graptolite	Early Devonian	Gabrielse and Blusson (1969); Norford (1967)
89	O-079249	graptolite	Early Devonian	Gabrielse and Blusson (1969); Norford (1967)
90	C-535933	conodont	Early Devonian (late Emsian) - latest Middle Devonian	McCracken (2010b)
91	C-535861	conodont	Silurian (late Pridoli) - Early Devonian (early Lockhovian)	Orchard (2010); McCracken (2010a)
92		graptolite		visual identification
93		graptolite		visual identification

## APPENDIX A - PALEONTOLOGY, continued

**Table A1, continued.** Fossil collections, arranged by formation.

Paleontology - NTS 95D				
Map ID	GSC ID	Fossil Type	Age Range	Reference
94		graptolite		visual identification
<b>Unit SMRB</b>				
95	O-079151	graptolite	Silurian (late Llandovery - Telychian)	Gabrielse and Blusson (1969); Norford (1967)
96	O-079152	graptolite	Silurian (late Llandovery - Telychian)	Gabrielse and Blusson (1969); Norford (1967)
97	C-535902	conodont	Middle Devonian	McCracken (2010b)
98	C-535903	conodont	Middle Devonian	McCracken (2010b)
99	C-535876	conodont	Middle Devonian (Eifelian - Givetian)	McCracken (2010a)
100	C-535956	conodont	Middle Devonian (latest Eifelian - Givetian)	McCracken (2010b)
101		2-hole crinoid	Early Devonian (Emsian) - Middle Devonian (Eifelian)	visual identification
<b>Unit PF</b>				
102	C-417156	conodont	Permian	Pigage (2009); Pyle (2004)
103	C-535965	conodont	Pennsylvanian - Early Permian, possibly Late Permian	McCracken (2010b)
<b>Unit TRGT</b>				
104	C-404735	palynology	Early Triassic	Pigage (2009); Utting (2006)
<b>Unit ERRS</b> (all samples taken from diamond drill holes)				
105	C-082595	palynology	Late Eocene (Priabonian)	Long and Sweet (1994)
106	C-082596	palynology	Late Eocene (Priabonian)	Long and Sweet (1994)
107	C-082597	palynology	Late Eocene (Priabonian)	Long and Sweet (1994); Sweet, 1983

## References

Gabrielse, H. and Blusson, S.L., 1969. Geology of Coal River map-area, Yukon Territory and District of Mackenzie (95D). Geological Survey of Canada, Paper 68-38, 22 p.

Handfield, R.S., 1971. Archaeocyatha from the Mackenzie and Cassiar Mountains, Northwest Territories, Yukon Territory and British Columbia, Geological Survey of Canada, Bulletin 201, 119 p.

Long, D.F. and Sweet, A.R., 1994. Age and depositional environment of the Rock River coal basin, Yukon Territory, Canada. Canadian Journal of Earth Sciences, vol. 31, p. 865-880.

McCracken, A.D., 2010a. Geological Survey of Canada, Paleontology Report No. 2-ADM-2010, 4 p.

McCracken, A.D., 2010b. Geological Survey of Canada, Paleontology Report No. 3-ADM-2010, 14 p.

- Miller, D.C. and Wright, J., 1986. Mel barite-zinc-lead deposit, Yukon - an exploration case history. *In: Mineral Deposits of Northern Cordillera*, J.A. Morin (ed.), Canadian Institute of Mining and Metallurgy, Special Volume 37, p. 129-141.
- Orchard, M.J., 2009a. Geological Survey of Canada, Paleontology Report No. 003-MJO-2009, 4 p.
- Orchard, M.J., 2009b. Geological Survey of Canada, Paleontology Report No. 19-MJO-2009, 2 p.
- Orchard, M.J., 2010. Geological Survey of Canada, Paleontology Report No. 4-MJO-2010, 11 p.
- Pigage, L.C., 2009. Bedrock geology of NTS 95C/5 (Pool Creek) and NTS 95D/8 map sheets, southeast Yukon. Yukon Geological Survey, Bulletin 16, 150 p.
- Pyle, L.J., 2004. Biostratigraphy Report No. LJP04-02, 12 p.
- Norford, B.S., 1967. Geological Survey of Canada, Paleontology Report No. S-D 8 BSN 1967, 2 p.
- Norford, B.S., 1968a. Geological Survey of Canada, Paleontology Report No. O-D 8 BSN 1968, 6 p.
- Norford, B.S., 1968b. Geological Survey of Canada, Paleontology Report No. O-S 4 BSN 1968, 2 p.
- Norford, B.S., 1984. Geological Survey of Canada, Paleontology Report No. C-01-BSN-1984, 1 p.
- Nowlan, G.S., 2008. Geological Survey of Canada, Paleontology Report No. 003-GSN-2008, 5 p.
- Nowlan, G.S., 2010a. Geological Survey of Canada, Paleontology Report No. 003-GSN-2010, 8 p.
- Nowlan, G.S., 2010b. Geological Survey of Canada, Paleontology Report No. 004-GSN-2010, 2 p.
- Nowlan, G.S., 2010c. Geological Survey of Canada, Paleontology Report No. 005-GSN-2010, 23 p.
- Sweet, A.R., 1983. Geological survey of Canada, Paleontology Report No. 11-ARS-1983, 7 p.
- Utting, J., 2006. Geological Survey of Canada, Paleontology Report no. 04-JU-2006, 3 p.

## APPENDIX B - DETRITAL ZIRCON ANALYSES

**Table B1.** Detrital zircon sample locations.

Sample ID	Field Station	Unit	UTM East	UTM North	Longitude	Latitude	Analytical Laboratory
09LP014-1	09LP014	PY	569 497	6 695 908	-127.7390	60.3936	Isotope Geology Laboratory, Boise State University
09TOA098	09TOA098	PEVN	582 139	6 742 420	-127.4903	60.8087	Isotope Geology Laboratory, Boise State University
09TOA094	09TOA094	PEVN	593 057	6 724 637	-127.2982	60.6467	TERRA, Memorial University
09TOA095	09TOA095	Cs	590 771	6 723 883	-127.3403	60.6404	Isotope Geology Laboratory, Boise State University
09TOA096	09TOA096	Cs	590 449	6 724 166	-127.3461	60.6430	TERRA, Memorial University
09LP093-1	09LP093	OSs	658 912	6 734 865	-126.0870	60.7114	Isotope Geology Laboratory, Boise State University
09LP090-2	09LP090	MM	634 909	6 692 950	-126.5550	60.3505	Isotope Geology Laboratory, Boise State University

All coordinates are NAD83 datum, zone 9.

### LA-ICPMS Methods, Isotope Geology Laboratory, Boise State University

Zircon grains were separated from rocks using standard techniques and mounted in epoxy and polished until the centres of the grains were exposed. Cathodoluminescence (CL) images were obtained with a JEOL JSM-1300 scanning electron microscope and Gatan MiniCL. Zircon was analysed by laser ablation inductively coupled plasma mass spectrometry (LA-ICPMS) using a ThermoElectron X-Series II quadrupole ICPMS and New Wave Research UP-213 Nd:YAG UV (213 nm) laser ablation system. In-house analytical protocols, standard materials, and data reduction software were used for acquisition and calibration of U-Pb dates and a suite of high field strength elements (HFSE) and rare earth elements (REE). Zircon was ablated with a laser spot width of 25  $\mu\text{m}$  using fluence and pulse rates of 5  $\text{J}/\text{cm}^2$  and 10 Hz, respectively, during a 45 second analysis (15 sec gas blank, 30 sec ablation) that excavated a pit  $\sim 25 \mu\text{m}$  deep. Ablated material was carried by a 1.2 L/min He gas stream to the nebulizer flow of the plasma. Dwell times were 5 ms for Si and Zr; 100 ms for  $^{49}\text{Ti}$  and  $^{207}\text{Pb}$ , 40 ms for  $^{238}\text{U}$ ,  $^{232}\text{Th}$ ,  $^{202}\text{Hg}$ ,  $^{204}\text{Pb}$ ,  $^{206}\text{Pb}$  and  $^{208}\text{Pb}$  isotopes; and 10 ms for all other HFSE and REE. Background count rates for each analyte were obtained prior to each spot analysis and subtracted from the raw count rate for each analyte. Ablation pits that appear to have intersected glass or mineral inclusions were identified by time-resolved data that show large fluctuations in Ti or P, and were rejected. Similarly, pits that appear contaminated by common Pb were rejected based on an intensity of mass 204 above baseline. For concentration calculations, background-subtracted count rates for each analyte were internally normalized to  $^{29}\text{Si}$  and calibrated with respect to NIST SRM-610 and -612 glasses as the primary standards. Temperature was calculated from the Ti-in-zircon thermometer (Watson et al., 2006). Because there are no constraints on the activity of  $\text{TiO}_2$  in the source rocks, an average value in crustal rocks of 0.6 was used.

For U-Pb and  $^{207}\text{Pb}/^{206}\text{Pb}$  dates, instrumental fractionation of the background-subtracted ratios was corrected and dates were calibrated with respect to interspersed measurements of the Plesovice zircon

standard (Sláma et al., 2008). Two analyses of Plesovice were done for every 10 analyses of unknown zircon; a polynomial fit to the standard analyses yields each sample-specific fractionation factor. Signals at mass 204 were indistinguishable from zero following subtraction of mercury backgrounds measured during the gas blank (<1000 cps  $^{202}\text{Hg}$ ), and thus dates are reported without common Pb correction. Radiogenic isotope ratio and age error propagation for all analyses includes uncertainty contributions from counting statistics and background subtraction. For spot analyses that are individually interpreted (e.g., detrital zircon analyses), the uncertainty from the standard calibration is propagated into the error on each date. This uncertainty is the standard deviation of the time-varying U/Pb fractionation factor and the standard error of the mean of the time-invariant, smaller  $^{207}\text{Pb}/^{206}\text{Pb}$  fractionation factor. For groups of analyses that are collectively interpreted from a weighted mean date, a weighted mean date is first calculated using Isoplot 3.0 (Ludwig, 2003) using errors on individual dates that do not include the standard calibration uncertainties, and then the standard calibration uncertainty is propagated into the error on the weighted mean date. Data were collected from samples 09LP014 and 09TOA098 in one experiment in May 2011 (experiment 1), and from samples 09LP090, 09LP093, and 09TOA095 in three experiments (experiments 2-4) in one session in July 2012. Standard calibration uncertainties for  $^{207}\text{Pb}/^{206}\text{Pb}$  dates are 0.9, 0.9, 0.7, and 0.8% ( $2\sigma$ ) for experiments 1-4, respectively. Standard calibration uncertainty for  $^{206}\text{Pb}/^{238}\text{U}$  dates are 3.3, 3.3, 4.8, and 1.8% ( $2\sigma$ ) for experiments 1-4, respectively. Age interpretations are based on  $^{207}\text{Pb}/^{206}\text{Pb}$  dates for >1000 Ma zircon. These analyses are <17% discordant. The  $^{206}\text{Pb}/^{238}\text{U}$  dates are used for <1000 Ma zircon. Errors on the  $^{207}\text{Pb}/^{206}\text{Pb}$  and  $^{206}\text{Pb}/^{238}\text{U}$  dates from individual LA-ICPMS analyses are given at  $2\sigma$ , as are the errors on the weighted mean dates.

Two zircon secondary reference materials were treated as unknowns to assess accuracy, interspersed as groups of two analyses for every 20 unknown analyses. Weighted mean dates are calculated using Isoplot 3.0 (Ludwig, 2003) from errors on individual dates that do not include the standard calibration uncertainties. However, errors on weighted mean dates include the standard calibration uncertainties within each experiment (propagated in quadrature) and are given at  $2\sigma$ . FC1 zircon (1098 Ma from unpublished chemical abrasion thermal ionization mass spectrometry (CA-TIMS) data, Boise State University) yielded weighted mean  $^{207}\text{Pb}/^{206}\text{Pb}$  dates of  $1105 \pm 15$  (MSWD=1.5, n=24),  $1098 \pm 20$  (MSWD=0.4, n=4),  $1117 \pm 38$  (MSWD=1.2, n=4), and  $1087 \pm 21$  (MSWD=1.0, n=4) from experiments 1-4, respectively. Weighted mean  $^{206}\text{Pb}/^{238}\text{U}$  dates are  $1131 \pm 34$  (MSWD=1.0, n=24),  $1121 \pm 37$  (MSWD=0.9, n=4),  $1124 \pm 52$  (MSWD=0.3, n=4) and  $1122 \pm 24$  (MSWD=0.3, n=4) from experiments 1-4, respectively. Seiland zircon (530 Ma from unpublished CA-TIMS data, Boise State University) yielded weighted mean  $^{206}\text{Pb}/^{238}\text{U}$  dates of  $540 \pm 19$  (MSWD=1.4, n=10),  $537 \pm 25$  (MSWD=1.2, n=10), and  $534 \pm 10$  (MSWD=0.5, n=10) from experiments 2-4, respectively. These results show that accurate  $^{207}\text{Pb}/^{206}\text{Pb}$  and  $^{206}\text{Pb}/^{238}\text{U}$  dates were obtained.

## References

- Ludwig, K.R., 2003. User's Manual for Isoplot 3.00. Berkeley Geochronology Center: Berkeley, CA, 70 p.
- Sláma, J., Košler, J., Condon, D.J., Crowley, J.L., Gerdes, A., Hanchar, J.M., Horstwood, M.S.A., Morris, G.A., Nasdala, L., Norberg, N., Schaltegger, U., Schoene, B., Tubrett, M.N., Whitehouse, M.J., 2008. Plesovice zircon - A new natural reference material for U-Pb and Hf isotopic microanalysis. *Chemical Geology*, vol. 249, p. 1-35.
- Sun, S.S. and McDonough, W.F., 1989. Chemical and isotopic systematics of oceanic basalts; implications for mantle composition and processes. *In: Magmatism in the ocean basins*. A.D. Saunders and M.J. Norry (eds.), Geological Society of London, London, vol. 42, p. 313-345.
- Watson, E.B., Wark, D.A. and Thomas, J.B., 2006. Crystallization thermometers for zircon and rutile. *Contributions to Mineralogy and Petrology*, vol. 151, p. 413-433.

## LAM-ICP-MS Methods, INCO Innovation Centre, Memorial University

Analyses were completed at the INCO Innovation Centre at Memorial University, St. John's, Newfoundland. The data set was acquired through Laser Ablation Microprobe Inductively Coupled Plasma Mass Spectrometry (LAM ICP-MS). Bennett and Tubrett (2010) present a detailed description of the methodology; this section summarizes from that more complete description.

Zircon grains were extracted using standard crushing techniques, a Wilfley™ table, heavy liquids, a Frantz™ isodynamic separator, and hand-picking in ethanol under a binocular microscope. The grains were mounted in epoxy with standard reference materials and polished to expose grain cores to a 0.25 µm finish using an automated Struers Tegrasytem™ polisher.

U/Pb and Pb/Pb isotopic ratios were measured using a Finnigan ELEMENT XR double focusing magnetic sector field ICP-MS coupled to a Geolas 193 nm excimer laser. A 10 µm laser beam was rastered over the sample surface at a velocity of 10 µm/second to create a 20 µm x 20 µm to 40 µm x 40 µm square. Laser energy was set at 5J/cm<sup>2</sup> with a laser repetition rate of 10 Hz.

An internal standard tracer solution introduced during laser ablation of the solid sample was used to correct for instrumental mass bias. Data were collected on the unknown zircon grains and several reference standards. Typically 10 unknown grains were measured for every 6-8 analyses of the reference materials. During ablation U and Pb isotopes and tracer solution signals were acquired in time-resolved, peak-jumping, pulse-counting mode with one point measured per peak. Raw data were corrected for dead time of the electron multiplier and processed off line in the Excel spreadsheet program LAMdate (Košler et al., 2002). No common Pb correction was applied to the data.

### References

- Bennett, V. and Tubrett, M., 2010. U-Pb isotopic age dating by LAM ICP-MS, INCO Innovation Centre, Memorial University: Sample preparation methodology and analytical techniques. *In*: Yukon Exploration and Geology 2009, K.E. MacFarlane, L.H. Weston and L.R. Blackburn (eds.), Yukon Geological Survey, p. 47-55.
- Košler, J., Foneland, H., Sylvester, P.J., Tubrett, M. and Pedersen, R., 2002. U-Pb dating of detrital zircons for sediment provenance studies – a comparison of laser ablation ICP-MS and SIMS technique. *Chemical Geology*, vol. 182, p. 605-618.

**APPENDIX B - DETRITAL ZIRCON ANALYSES**, continued

**Table B2a.** Detrital zircon U-Pb geochronologic analyses from sample **09LP014** in the Yusezyu Formation (PY) - Isotope Geology Laboratory, Boise State University

Analysis	U (ppm)	Th (ppm)	Pb* (ppm)	Th/U	Corrected isotope ratios												Apparent ages (Ma)						% disc.
					$\frac{^{206}\text{Pb}^*}{^{207}\text{Pb}^*}$	$\pm 2\sigma$ (%)	$\frac{^{207}\text{Pb}^*}{^{235}\text{U}^*}$	$\pm 2\sigma$ (%)	$\frac{^{206}\text{Pb}^*}{^{238}\text{U}}$	$\pm 2\sigma$ (%)	error corr.	$\frac{^{238}\text{U}}{^{206}\text{Pb}^*}$	$\pm 2\sigma$ (%)	$\frac{^{207}\text{Pb}^*}{^{206}\text{Pb}^*}$	$\pm 2\sigma$ (%)	error corr.	$\frac{^{207}\text{Pb}^*}{^{206}\text{Pb}^*}$	$\pm 2\sigma$ (Ma)	$\frac{^{207}\text{Pb}^*}{^{235}\text{U}}$	$\pm 2\sigma$ (Ma)	$\frac{^{206}\text{Pb}^*}{^{238}\text{U}^*}$	$\pm 2\sigma$ (Ma)	
09LP014-1 L 50	46.47	26.63	29.97	0.57	5.255	3.095	12.598	6.174	0.480	5.342	0.87	2.083	5.342	0.190	3.095	0	2745	51	2650	58	2528	112	8
09LP014-1 L 79	80.84	56.61	56.18	0.70	5.275	2.211	13.080	5.090	0.500	4.584	0.90	1.998	4.584	0.190	2.211	0	2739	36	2685	48	2616	99	4
09LP014-1 L 85	29.30	46.86	22.76	1.60	5.290	2.796	12.721	5.580	0.488	4.828	0.87	2.049	4.828	0.189	2.796	-0.0	2734	46	2659	53	2562	102	6
09LP014-1 L 90	39.15	14.31	25.99	0.37	5.299	2.513	13.297	5.129	0.511	4.472	0.87	1.957	4.472	0.189	2.513	-0.0	2731	41	2701	48	2661	97	3
09LP014-1 L 39	100.14	70.61	71.36	0.71	5.309	2.126	13.180	4.749	0.507	4.246	0.89	1.971	4.246	0.188	2.126	0	2728	35	2693	45	2646	92	3
09LP014-1 XL 2	132.46	183.71	107.62	1.39	5.314	1.906	13.191	4.873	0.508	4.485	0.92	1.967	4.485	0.188	1.906	0.0	2726	31	2693	46	2650	97	3
09LP014-1 L 43	118.28	105.94	84.08	0.90	5.322	1.512	12.619	4.581	0.487	4.324	0.94	2.053	4.324	0.188	1.512	0	2724	25	2652	43	2558	91	6
09LP014-1 XL 17	21.44	16.39	15.45	0.76	5.383	3.252	12.831	5.077	0.501	3.899	0.77	1.996	3.899	0.186	3.252	0.0	2705	54	2667	48	2618	84	3
09LP014-1 L 92	76.51	42.54	51.17	0.56	5.391	2.070	12.716	4.831	0.497	4.365	0.90	2.011	4.365	0.186	2.070	-0.0	2703	34	2659	45	2602	93	4
09LP014-1 L 13	122.91	78.65	84.67	0.64	5.396	1.696	12.854	4.602	0.503	4.278	0.93	1.988	4.278	0.185	1.696	0.0	2701	28	2669	43	2627	92	3
09LP014-1 L 95	121.61	172.06	97.45	1.41	5.402	1.719	12.646	5.148	0.495	4.853	0.94	2.019	4.853	0.185	1.719	0	2699	28	2654	48	2594	104	4
09LP014-1 L 63	41.94	59.03	33.23	1.41	5.430	2.335	12.450	5.100	0.490	4.534	0.89	2.039	4.534	0.184	2.335	0	2691	39	2639	48	2572	96	4
09LP014-1 L 16	130.57	130.21	94.41	1.00	5.490	1.771	12.469	4.578	0.496	4.222	0.92	2.014	4.222	0.182	1.771	0	2673	29	2640	43	2598	90	3
09LP014-1 L 33	118.09	37.81	77.09	0.32	5.490	1.866	12.823	4.423	0.511	4.010	0.91	1.958	4.010	0.182	1.866	0	2672	31	2667	42	2659	87	0
09LP014-1 L 8	60.17	42.95	42.59	0.71	5.492	2.563	12.629	4.993	0.503	4.284	0.86	1.988	4.284	0.182	2.563	-0.0	2672	42	2652	47	2627	92	2
09LP014-1 XL 7	155.31	133.71	115.94	0.86	5.507	1.467	12.807	3.518	0.512	3.198	0.91	1.955	3.198	0.182	1.467	-0.0	2667	24	2666	33	2663	70	0
09LP014-1 L 84	145.95	85.27	89.98	0.58	5.601	2.616	11.300	5.021	0.459	4.285	0.85	2.179	4.285	0.179	2.616	-0.0	2639	43	2548	47	2435	87	8
09LP014-1 XL 12	32.21	23.63	22.01	0.73	5.688	2.979	11.776	4.371	0.486	3.198	0.73	2.058	3.198	0.176	2.979	0	2614	50	2587	41	2553	67	2
09LP014-1 XL 1	174.32	53.14	98.31	0.30	5.738	1.914	10.737	4.284	0.447	3.833	0.89	2.238	3.833	0.174	1.914	-0.0	2599	32	2501	40	2381	76	8
09LP014-1 L 76	184.73	91.67	111.34	0.50	6.064	1.585	10.386	4.570	0.457	4.286	0.94	2.189	4.286	0.165	1.585	-0.0	2507	27	2470	42	2425	87	3
09LP014-1 XL 18	93.40	68.31	62.90	0.73	6.096	1.740	10.914	3.826	0.482	3.408	0.89	2.073	3.408	0.164	1.740	0	2498	29	2516	36	2538	72	-2
09LP014-1 L 71	139.25	164.85	91.07	1.18	6.208	1.610	9.508	4.357	0.428	4.048	0.93	2.336	4.048	0.161	1.610	0.0	2467	27	2388	40	2297	78	7
09LP014-1 XL 15	104.11	67.10	64.45	0.64	6.312	1.735	9.900	4.121	0.453	3.737	0.91	2.206	3.737	0.158	1.735	0	2439	29	2425	38	2410	75	1
09LP014-1 XL 4	32.88	45.54	23.07	1.39	6.329	3.043	9.573	4.972	0.439	3.932	0.79	2.276	3.932	0.158	3.043	0	2434	52	2395	46	2348	77	4
09LP014-1 XL 6	74.61	43.70	46.16	0.59	6.343	1.958	10.055	4.604	0.463	4.167	0.91	2.162	4.167	0.158	1.958	-0.0	2431	33	2440	43	2451	85	-1
09LP014-1 L 26	108.74	57.82	59.21	0.53	6.454	1.922	8.857	4.928	0.415	4.538	0.92	2.412	4.538	0.155	1.922	-0.0	2401	33	2323	45	2236	86	7
09LP014-1 XL 10	56.51	65.20	36.92	1.15	6.534	2.223	9.078	3.995	0.430	3.319	0.83	2.324	3.319	0.153	2.223	0.0	2380	38	2346	37	2307	64	3
09LP014-1 L 38	45.16	34.45	26.25	0.76	6.631	3.090	8.733	5.579	0.420	4.645	0.83	2.381	4.645	0.151	3.090	0.0	2355	53	2311	51	2260	89	4
09LP014-1 L 44	124.76	85.25	62.82	0.68	6.768	2.236	7.723	4.572	0.379	3.988	0.87	2.638	3.988	0.148	2.236	0	2320	38	2199	41	2072	71	11
09LP014-1 XL 11	88.57	47.16	49.97	0.53	6.929	1.747	8.674	4.249	0.436	3.873	0.91	2.294	3.873	0.144	1.747	0.0	2280	30	2304	39	2332	76	-2
09LP014-1 L 31	44.72	52.07	26.67	1.16	6.979	3.387	7.758	5.205	0.393	3.952	0.76	2.547	3.952	0.143	3.387	-0.0	2267	58	2203	47	2135	72	6
09LP014-1 L 62	77.38	63.59	38.04	0.82	7.217	2.353	6.714	6.274	0.351	5.817	0.93	2.846	5.817	0.139	2.353	0	2209	41	2074	55	1941	98	12
09LP014-1 XL 9	22.95	24.38	12.52	1.06	7.510	3.484	6.861	5.630	0.374	4.423	0.79	2.676	4.423	0.133	3.484	0	2140	61	2094	50	2047	78	4
09LP014-1 L 82	102.94	165.79	57.78	1.61	7.740	3.150	6.213	5.327	0.349	4.295	0.81	2.867	4.295	0.129	3.150	0	2087	55	2006	47	1929	72	8
09LP014-1 L 81	55.30	50.14	25.04	0.91	7.944	3.096	5.643	5.294	0.325	4.294	0.81	3.076	4.294	0.126	3.096	0	2041	55	1923	46	1815	68	11
09LP014-1 L 89	239.58	308.64	125.20	1.29	7.973	1.802	5.972	4.674	0.345	4.313	0.92	2.896	4.313	0.125	1.802	-0.0	2035	32	1972	41	1912	71	6
09LP014-1 L 101	141.47	84.30	64.98	0.60	7.987	2.048	6.058	4.720	0.351	4.252	0.90	2.850	4.252	0.125	2.048	0.0	2032	36	1984	41	1939	71	5
09LP014-1 L 75	122.59	84.79	57.17	0.69	8.007	2.571	5.995	5.506	0.348	4.869	0.88	2.872	4.869	0.125	2.571	-0.0	2027	46	1975	48	1926	81	5
09LP014-1 L 70	97.53	35.96	41.49	0.37	8.023	2.726	5.880	5.018	0.342	4.213	0.84	2.923	4.213	0.125	2.726	0.0	2024	48	1958	44	1897	69	6
<b>09LP014-1 L 61</b>	<b>37.40</b>	<b>32.22</b>	<b>17.52</b>	<b>0.86</b>	<b>8.030</b>	<b>4.957</b>	<b>5.621</b>	<b>7.025</b>	<b>0.327</b>	<b>4.977</b>	<b>0.71</b>	<b>3.055</b>	<b>4.977</b>	<b>0.125</b>	<b>4.957</b>	<b>-0.0</b>	<b>2022</b>	<b>88</b>	<b>1919</b>	<b>61</b>	<b>1826</b>	<b>79</b>	<b>10</b>
09LP014-1 L 25	97.48	63.61	44.11	0.65	8.052	2.143	5.909	4.801	0.345	4.296	0.89	2.898	4.296	0.124	2.143	0.0	2017	38	1963	42	1911	71	5
09LP014-1 L 96	49.47	38.41	22.39	0.78	8.080	3.654	5.697	5.861	0.334	4.582	0.78	2.995	4.582	0.124	3.654	0	2011	65	1931	51	1857	74	8



APPENDIX B - DETRITAL ZIRCON ANALYSES, continued

Table B2a, *continued*. Detrital zircon U-Pb geochronologic analyses from sample **09LP014** in the Yusezyu Formation (PY) - Isotope Geology Laboratory, Boise State University

Analysis	U (ppm)	Th (ppm)	Pb* (ppm)	Th/U	Corrected isotope ratios											Apparent ages (Ma)						% disc.	
					$\frac{^{206}\text{Pb}^*}{^{207}\text{Pb}^*}$	$\pm 2\sigma$ (%)	$\frac{^{207}\text{Pb}^*}{^{235}\text{U}^*}$	$\pm 2\sigma$ (%)	$\frac{^{206}\text{Pb}^*}{^{238}\text{U}^*}$	$\pm 2\sigma$ (%)	error corr.	$\frac{^{238}\text{U}}{^{206}\text{Pb}^*}$	$\pm 2\sigma$ (%)	$\frac{^{207}\text{Pb}^*}{^{206}\text{Pb}^*}$	$\pm 2\sigma$ (%)	error corr.	$\frac{^{207}\text{Pb}^*}{^{206}\text{Pb}^*}$	$\pm 2\sigma$ (Ma)	$\frac{^{207}\text{Pb}^*}{^{235}\text{U}^*}$	$\pm 2\sigma$ (Ma)	$\frac{^{206}\text{Pb}^*}{^{238}\text{U}^*}$		$\pm 2\sigma$ (Ma)
09LP014-1 L 98	106.59	83.25	43.98	0.78	8.859	2.341	4.694	5.103	0.302	4.534	0.89	3.315	4.534	0.113	2.341	0.0	1846	42	1766	43	1699	68	8
09LP014-1 L 80	293.97	128.77	114.58	0.44	8.864	1.818	4.879	4.616	0.314	4.243	0.92	3.188	4.243	0.113	1.818	-0.0	1845	33	1799	39	1759	65	5
09LP014-1 L 23	119.74	71.63	48.92	0.60	8.873	2.605	4.924	5.038	0.317	4.312	0.86	3.156	4.312	0.113	2.605	-0.0	1843	47	1806	43	1775	67	4
09LP014-1 L 66	150.56	79.04	63.85	0.52	8.895	1.947	5.097	5.438	0.329	5.077	0.93	3.041	5.077	0.112	1.947	0	1839	35	1836	46	1833	81	0
09LP014-1 L 64	169.97	187.89	77.30	1.11	8.970	1.990	4.745	4.573	0.309	4.117	0.90	3.239	4.117	0.111	1.990	0.0	1824	36	1775	38	1734	63	5
09LP014-1 L 6	89.30	26.87	35.20	0.30	8.972	2.337	4.992	4.565	0.325	3.922	0.86	3.079	3.922	0.111	2.337	0	1823	42	1818	39	1813	62	1
09LP014-1 L 1	100.78	72.74	44.41	0.72	8.979	2.468	5.063	4.792	0.330	4.107	0.86	3.033	4.107	0.111	2.468	0	1822	45	1830	41	1837	66	-1
09LP014-1 L 47	119.22	69.66	48.13	0.58	8.985	2.380	4.837	5.528	0.315	4.989	0.90	3.173	4.989	0.111	2.380	0.0	1821	43	1791	47	1766	77	3
09LP014-1 L 21	97.57	109.54	42.07	1.12	8.986	2.617	4.691	5.573	0.306	4.921	0.88	3.271	4.921	0.111	2.617	0.0	1820	47	1766	47	1720	74	6
09LP014-1 L 20	71.36	37.77	27.85	0.53	8.988	2.997	4.774	5.386	0.311	4.475	0.83	3.213	4.475	0.111	2.997	-0.0	1820	54	1780	45	1747	68	4
09LP014-1 L 65	87.09	77.80	37.72	0.89	8.997	2.597	4.719	4.866	0.308	4.116	0.85	3.248	4.116	0.111	2.597	-0.0	1818	47	1771	41	1730	62	5
09LP014-1 L 28	39.12	13.59	14.90	0.35	9.028	4.044	4.766	6.103	0.312	4.570	0.75	3.205	4.570	0.111	4.044	0.0	1812	73	1779	51	1751	70	3
09LP014-1 L 3	179.83	79.80	72.13	0.44	9.034	1.805	4.874	4.505	0.319	4.128	0.92	3.131	4.128	0.111	1.805	-0.0	1811	33	1798	38	1787	64	1
09LP014-1 L 73	32.14	15.30	13.06	0.48	9.043	4.005	4.923	6.269	0.323	4.823	0.77	3.097	4.823	0.111	4.005	0.0	1809	73	1806	53	1804	76	0
09LP014-1 L 12	148.32	66.37	60.08	0.45	9.053	1.859	4.955	4.582	0.325	4.188	0.91	3.074	4.188	0.110	1.859	0.0	1807	34	1812	39	1816	66	-0
09LP014-1 L 54	470.34	3.05	160.84	0.01	9.072	2.316	4.673	5.325	0.307	4.795	0.90	3.252	4.795	0.110	2.316	-0.0	1803	42	1762	45	1728	73	4
09LP014-1 L 53	112.40	32.51	41.06	0.29	9.072	3.316	4.672	6.024	0.307	5.029	0.83	3.253	5.029	0.110	3.316	-0.0	1803	60	1762	50	1728	76	4
09LP014-1 L 77	71.15	35.61	27.52	0.50	9.079	2.716	4.642	5.241	0.306	4.482	0.86	3.272	4.482	0.110	2.716	0	1802	49	1757	44	1719	68	5
09LP014-1 L 35	69.49	63.62	30.17	0.92	9.097	4.159	4.715	6.120	0.311	4.489	0.73	3.215	4.489	0.110	4.159	0	1798	76	1770	51	1746	69	3
09LP014-1 L 5	96.45	33.12	38.64	0.34	9.122	2.370	4.957	4.692	0.328	4.049	0.86	3.049	4.049	0.110	2.370	-0.0	1793	43	1812	40	1828	64	-2
09LP014-1 L 7	26.48	6.33	10.07	0.24	9.131	5.218	4.834	6.771	0.320	4.314	0.64	3.124	4.314	0.110	5.218	0	1791	95	1791	57	1790	67	0
09LP014-1 L 4	54.73	10.50	20.98	0.19	9.131	3.043	4.932	5.053	0.327	4.034	0.80	3.062	4.034	0.110	3.043	-0.0	1791	55	1808	43	1822	64	-2
09LP014-1 L 2	297.88	25.82	108.01	0.09	9.131	1.658	4.806	4.627	0.318	4.320	0.93	3.142	4.320	0.110	1.658	-0.0	1791	30	1786	39	1782	67	1
09LP014-1 L 48	105.00	60.54	43.35	0.58	9.135	2.316	4.869	5.352	0.323	4.825	0.90	3.100	4.825	0.109	2.316	0.0	1791	42	1797	45	1802	76	-1
09LP014-1 L 9	205.80	143.13	77.93	0.70	9.141	2.039	4.339	6.690	0.288	6.372	0.95	3.477	6.372	0.109	2.039	0.0	1789	37	1701	55	1630	92	9
09LP014-1 L 32	89.55	38.31	34.90	0.43	9.166	2.485	4.706	4.688	0.313	3.975	0.85	3.197	3.975	0.109	2.485	-0.0	1784	45	1768	39	1755	61	2
09LP014-1 L 67	200.19	150.19	80.76	0.75	9.237	2.017	4.485	4.386	0.300	3.895	0.89	3.328	3.895	0.108	2.017	-0.0	1770	37	1728	36	1694	58	4
09LP014-1 L 10	13.63	22.00	6.99	1.61	9.546	6.270	4.553	7.991	0.315	4.953	0.62	3.172	4.953	0.105	6.270	-0.0	1710	115	1741	67	1766	77	-3
09LP014-1 L 99	43.41	0.41	7.90	0.01	13.030	5.455	1.787	7.360	0.169	4.942	0.67	5.922	4.942	0.077	5.455	-0.0	1115	109	1041	48	1006	46	10
09LP014-1 L 83	245.61	107.09	30.17	0.44	15.783	4.858	0.898	6.843	0.103	4.820	0.70	9.724	4.820	0.063	4.858	0	720	103	651	33	631	29	12

Notes:

Yellow highlighted rows are samples that intersected inclusions.  
 Isotope ratios and ages are NOT corrected for initial common Pb.  
 Isotope ratio and apparent age errors include systematic calibration errors of 6.37100499011343% ( $^{208}\text{Pb}/^{232}\text{Th}$ ), 0.452188693209402% ( $^{207}\text{Pb}/^{206}\text{Pb}$ ), 1.63033394062177% ( $^{206}\text{Pb}/^{238}\text{U}$ ) (all 1-sigma).  
 Sweep-by-sweep downhole fractionation of U/Pb ratios NOT corrected via Si/Zr fractionation factor.  
 Backgrounds were monitored during sweeps 8 to 18. Sample counts were integrated from sweeps 35 to 80.  
 Ablation used a laser spot size of 25 microns, and a laser firing repetition rate of 10 Hz.





APPENDIX B - DETRITAL ZIRCON ANALYSES, continued

Table B2b, *continued*. Detrital zircon trace element analyses from sample **09LP014** in the Yusezyu Formation (PY) - Isotope Geology Laboratory, Boise State University

Analysis	Concentrations (ppm)																						
	P	Ti	Y	Zr	Nb	La	Ce	Pr	Nd	Sm	Eu	Gd	Tb	Dy	Ho	Er	Tm	Yb	Lu	Hf	Ta	Th	U
09LP014-1 L 23	360.504	11.113	802.946	526729.035	1.256	0.009	9.185	0.045	0.394	2.809	0.179	18.862	6.082	75.428	30.833	120.888	31.180	352.320	44.414	10359.339	0.668	71.630	119.737
09LP014-1 L 66	385.228	6.231	896.048	490560.697	0.751		6.703	0.043	1.250	4.104	0.444	20.615	7.607	91.725	33.142	138.324	34.106	367.890	42.700	8827.487	0.560	79.038	150.563
09LP014-1 L 64	128.610	8.633	276.598	476855.116	0.941		11.657	0.157	2.588	5.209	2.044	18.789	4.636	39.215	10.255	29.329	6.391	58.433	6.097	8284.555	0.870	187.891	169.972
09LP014-1 L 6	158.133	8.932	332.018	473572.021	0.372		9.010	0.044	0.726	1.804	0.678	8.465	2.729	30.281	11.516	48.608	12.848	162.170	20.122	7377.272	0.335	26.873	89.302
09LP014-1 L 1	193.872	17.521	459.480	473710.253	1.202		12.949	0.041	1.063	2.636	0.304	11.533	3.861	47.495	16.393	69.155	17.323	193.626	22.885	7897.739	0.709	72.743	100.784
09LP014-1 L 47	153.961	18.024	897.327	511842.431	1.057	0.011	22.090	0.409	7.503	13.840	2.240	42.176	10.761	105.552	32.202	125.524	30.247	311.434	37.675	8580.749	0.344	69.659	119.221
09LP014-1 L 21	279.729	11.822	1406.464	569602.219	1.881		12.640	0.324	5.687	11.426	1.999	52.778	14.386	156.505	52.494	202.035	46.272	452.410	54.235	9413.816	0.981	109.539	97.573
09LP014-1 L 20	90.675	17.800	312.654	572265.209	0.724	0.077	19.327	0.067	1.244	1.575	0.513	9.609	2.507	30.094	10.875	44.447	10.918	117.297	14.899	9996.496	0.573	37.766	71.359
09LP014-1 L 65	250.053	19.491	1137.454	485462.098	1.544		11.152	0.193	5.275	11.120	1.228	42.782	12.016	128.931	44.066	166.286	38.915	418.147	43.631	7551.138	0.394	77.799	87.087
09LP014-1 L 28	137.749	4.747	186.304	509805.329	0.554	0.051	5.970		0.239	0.568	0.341	3.713	1.315	15.327	5.952	24.852	6.986	86.659	10.401	8124.782	0.255	13.588	39.125
09LP014-1 L 3	259.627	4.092	433.463	460459.756	1.160	0.162	22.896	0.029	1.700	4.776	1.152	16.631	5.047	45.564	15.554	57.133	14.493	167.249	18.787	7814.864	0.650	79.798	179.834
09LP014-1 L 73	352.085	10.384	635.961	487324.048	0.414	0.110	11.971	0.121	2.932	4.197	0.237	21.326	5.911	68.449	23.164	92.098	25.023	281.104	33.457	6836.750	0.204	15.303	32.136
09LP014-1 L 12	625.644	11.137	1350.953	509957.450	0.938	0.038	6.236	0.006	1.502	3.985	0.434	30.164	9.800	127.390	49.229	212.563	54.212	605.082	70.767	10067.922	0.739	66.365	148.322
09LP014-1 L 54	402.615	2.226	451.084	543879.151	0.259		0.446		0.616	3.026	0.120	17.660	5.460	51.170	15.510	61.163	16.399	193.920	24.498	14487.594	0.475	3.055	470.343
09LP014-1 L 53	316.292	12.941	612.552	543501.077	0.841		1.771	0.080	1.136	2.870	0.073	18.216	6.106	65.274	22.146	88.475	20.366	214.441	27.244	9766.717	0.445	32.513	112.398
09LP014-1 L 77	184.350	13.855	270.902	504177.460	0.772	0.060	3.073		0.230	1.148	0.100	6.180	2.315	25.803	9.965	42.364	10.941	131.419	15.400	8965.993	0.503	35.606	71.146
09LP014-1 L 35	182.900	15.664	591.581	492231.268	3.391	0.037	51.994	0.052	0.911	2.195	0.678	14.445	4.478	58.727	22.744	91.218	23.573	286.016	32.612	8027.505	1.172	63.620	69.492
09LP014-1 L 5	303.642	16.905	841.498	458169.188	0.937	0.030	7.105	0.143	2.868	5.087	1.158	24.784	8.322	88.323	31.207	129.286	33.141	361.192	38.725	7899.913	0.516	33.120	96.446
09LP014-1 L 7	161.326	8.354	176.158	484364.378	0.699	0.030	3.881	0.023	0.527	0.840	0.536	5.095	1.486	15.533	5.924	25.110	7.076	93.497	11.974	5495.140	0.530	6.327	26.484
09LP014-1 L 4	117.788	6.233	283.471	463566.369	0.568		6.773		0.589	1.038	0.137	4.619	2.222	24.192	9.925	41.927	10.942	126.814	13.764	8049.774	0.303	10.502	54.727
09LP014-1 L 2	182.332	10.456	104.634	476072.879	0.221	0.016	2.355	0.015	2.256	4.331	0.458	15.848	2.945	19.244	4.444	10.731	1.666	14.554	1.442	8478.961	0.017	25.819	297.878
09LP014-1 L 48	152.500	12.707	699.467	513251.988	0.526	0.064	12.607	0.110	3.784	6.832	1.261	27.872	7.494	77.320	24.513	96.190	22.365	245.257	27.849	8278.832	0.247	60.536	104.997
09LP014-1 L 9	281.011	15.996	1198.869	480441.154	1.308		3.735	0.114	1.862	6.559	0.911	41.146	12.064	138.137	46.509	175.635	41.762	433.226	46.879	8721.082	0.912	143.129	205.801
09LP014-1 L 32	203.171	18.158	488.431	485757.056	0.974		17.031	0.191	1.884	5.051	1.772	21.400	4.977	56.123	17.878	69.080	16.973	192.838	21.924	7415.883	0.322	38.310	89.551
09LP014-1 L 67	163.871	15.312	1249.336	482964.924	0.864	0.002	10.296	0.503	8.579	12.821	1.627	44.826	13.503	147.691	47.584	187.385	41.676	439.935	47.714	8454.266	0.683	150.193	200.191
09LP014-1 L 10	279.218	49.660	566.752	497969.662	0.844		20.243	0.251	3.883	6.717	1.909	22.311	6.018	64.316	21.608	84.336	18.949	209.333	24.867	6687.570	0.356	21.996	13.634
09LP014-1 L 99	46.019	0.786	190.213	506345.039	0.359	0.022	0.020					0.714	0.426	7.930	5.580	39.094	16.567	274.230	44.064	12709.898	0.583	0.414	43.409
09LP014-1 L 83	106.596	6.062	893.510	528000.356	29.841	0.072	13.732	0.065	1.089	3.151		22.693	7.712	93.102	33.878	134.180	32.305	340.661	37.328	10501.252	12.705	107.090	245.608

Notes:

Yellow highlighted rows are samples that intersected inclusions.  
Trace element concentrations in ppm, calculated using mean count rate method.  
Sweep-by-sweep downhole fractionation of U/Pb ratios NOT corrected via Si/Zr fractionation factor.  
Backgrounds were monitored during sweeps 8 to 18. Sample counts were integrated from sweeps 35 to 80.  
Ablation used a laser spot size of 25 microns, and a laser firing repetition rate of 10 Hz.





APPENDIX B - DETRITAL ZIRCON ANALYSES, continued

Table B2c, continued. Detrital zircon calculated ratios and values from sample 09LP014 in the Yusezyu Formation (PY) - Isotope Geology Laboratory, Boise State University

Analysis	CI chondrite normalizing values from Sun and McDonough (1989)														Ti-in-zircon T (°C)	Ce/Ce*	Eu/Eu*	(Sm/Nd) cn	(Lu/Nd) cn	Lu/Hf	Nb/Ta	Nb/U	Th/U	Th/Y	Y/Hf
	0.237	0.612	0.095	0.467	0.153	0.058	0.206	0.037	0.254	0.057	0.166	0.026	0.17	0.025											
	La	Ce	Pr	Nd	Sm	Eu	Gd	Tb	Dy	Ho	Er	Tm	Yb	Lu											
09LP014-1 L 98	0.122	22.272	4.881	16.010	71.229	48.025	178.312	246.662	379.631	488.187	614.151	961.951	1536.67	1040.094	834	8.90	0.38	4.45	64.97	0.00	3.14	0.00	0.78	0.11	0.10
09LP014-1 L 80	0.487	8.695	0.641	2.763	30.538	8.077	141.992	280.810	501.126	827.699	1153.085	1850.646	3012.88	2415.641	770	15.42	0.09	11.05	874.43	0.01	1.51	0.00	0.44	0.10	0.13
09LP014-1 L 23	0.039	15.008	0.472	0.844	18.361	3.081	91.785	162.620	296.960	544.752	730.440	1222.727	2072.47	1748.577	807	58.73	0.06	21.76	2072.68	0.00	1.88	0.01	0.60	0.09	0.08
09LP014-1 L 66	0.011	10.953	0.455	2.678	26.826	7.663	100.319	203.398	361.123	585.549	835.794	1337.474	2164.06	1681.115	749	47.00	0.12	10.02	627.84	0.00	1.34	0.00	0.52	0.09	0.10
09LP014-1 L 64	0.042	19.048	1.657	5.543	34.044	35.237	91.432	123.960	154.392	181.180	177.214	250.645	343.72	240.040	781	22.43	0.56	6.14	43.31	0.00	1.08	0.01	1.11	0.68	0.03
09LP014-1 L 6	0.012	14.723	0.464	1.556	11.793	11.692	41.191	72.971	119.216	203.465	293.707	503.827	953.94	792.187	785	61.91	0.44	7.58	509.24	0.00	1.11	0.00	0.30	0.08	0.05
09LP014-1 L 1	0.011	21.158	0.435	2.276	17.229	5.245	56.121	103.234	186.987	289.634	417.853	679.347	1138.98	901.002	858	94.88	0.14	7.57	395.87	0.00	1.70	0.01	0.72	0.16	0.06
09LP014-1 L 47	0.045	36.096	4.301	16.067	90.460	38.619	205.238	287.722	415.559	568.945	758.454	1186.160	1831.96	1483.268	861	16.61	0.26	5.63	92.32	0.00	3.08	0.01	0.58	0.08	0.10
09LP014-1 L 21	0.085	20.654	3.408	12.178	74.682	34.458	256.828	384.658	616.163	927.454	1220.755	1814.607	2661.23	2135.250	814	11.83	0.21	6.13	175.33	0.01	1.92	0.02	1.12	0.08	0.15
09LP014-1 L 20	0.323	31.580	0.707	2.664	10.292	8.838	46.759	67.025	118.482	192.132	268.561	428.170	689.98	586.586	859	61.30	0.31	3.86	220.18	0.00	1.26	0.01	0.53	0.12	0.03
09LP014-1 L 65	0.051	18.223	2.034	11.296	72.679	21.178	208.186	321.292	507.603	778.544	1004.751	1526.090	2459.69	1717.758	870	17.48	0.15	6.43	152.07	0.01	3.92	0.02	0.89	0.07	0.15
09LP014-1 L 28	0.214	9.755	0.114	0.512	3.711	5.873	18.071	35.171	60.342	105.163	150.161	273.971	509.76	409.494	724	59.36	0.54	7.25	799.76	0.00	2.18	0.01	0.35	0.07	0.02
09LP014-1 L 3	0.685	37.412	0.305	3.640	31.219	19.864	80.931	134.957	179.385	274.807	345.214	568.342	983.82	739.649	711	75.53	0.35	8.58	203.18	0.00	1.79	0.01	0.44	0.18	0.06
09LP014-1 L 73	0.466	19.560	1.272	6.279	27.430	4.092	103.778	158.055	269.483	409.258	556.486	981.308	1653.55	1317.194	800	22.51	0.06	4.37	209.78	0.00	2.03	0.01	0.48	0.02	0.09
09LP014-1 L 12	0.160	10.190	0.066	3.216	26.046	7.476	146.782	262.025	501.535	869.775	1284.369	2125.958	3559.31	2786.113	808	90.21	0.09	8.10	866.25	0.01	1.27	0.01	0.45	0.05	0.13
09LP014-1 L 54		0.729	0.295	1.319	19.779	2.073	85.934	145.977	201.456	274.030	369.564	643.089	1140.71	964.478	661		0.04	14.99	730.96	0.00	0.55	0.00	0.01	0.01	0.03
09LP014-1 L 53	0.021	2.894	0.839	2.434	18.757	1.264	88.642	163.251	256.983	391.280	534.595	798.686	1261.42	1072.599	824	6.73	0.02	7.71	440.76	0.00	1.89	0.01	0.29	0.05	0.06
09LP014-1 L 77	0.254	5.021	0.110	0.492	7.501	1.732	30.072	61.907	101.588	176.054	255.975	429.040	773.05	606.301	831	27.58	0.09	15.25	1232.81	0.00	1.53	0.01	0.50	0.13	0.03
09LP014-1 L 35	0.156	84.957	0.542	1.951	14.345	11.696	70.294	119.740	231.209	401.830	551.166	924.451	1682.44	1283.923	845	243.32	0.28	7.35	658.03	0.00	2.89	0.05	0.92	0.11	0.07
09LP014-1 L 5	0.125	11.609	1.510	6.142	33.248	19.964	120.603	222.505	347.728	551.359	781.187	1299.631	2124.66	1524.591	853	14.20	0.26	5.41	248.23	0.00	1.82	0.01	0.34	0.04	0.11
09LP014-1 L 7	0.128	6.341	0.241	1.129	5.490	9.239	24.795	39.731	61.155	104.668	151.722	277.492	549.98	471.432	778	34.32	0.61	4.86	417.48	0.00	1.32	0.03	0.24	0.04	0.03
09LP014-1 L 4		11.068	0.282	1.262	6.786	2.367	22.479	59.407	95.242	175.360	253.337	429.102	745.97	541.895	749		0.16	5.38	429.52	0.00	1.87	0.01	0.19	0.04	0.04
09LP014-1 L 2	0.068	3.848	0.158	4.832	28.305	7.897	77.118	78.743	75.762	78.523	64.842	65.335	85.61	56.776	801	34.14	0.15	5.86	11.75	0.00	12.90	0.00	0.09	0.25	0.01
09LP014-1 L 48	0.271	20.599	1.158	8.103	44.652	21.744	135.629	200.372	304.411	433.086	581.206	877.052	1442.69	1096.415	822	28.83	0.24	5.51	135.30	0.00	2.13	0.01	0.58	0.09	0.08
09LP014-1 L 9	0.030	6.103	1.201	3.987	42.870	15.708	200.223	322.558	543.848	821.715	1061.239	1637.725	2548.39	1845.634	847	9.91	0.13	10.75	462.86	0.01	1.43	0.01	0.70	0.12	0.14
09LP014-1 L 32	0.050	27.828	2.005	4.034	33.013	30.558	104.135	133.068	220.956	315.870	417.399	665.615	1134.34	863.132	862	27.08	0.45	8.18	213.99	0.00	3.02	0.01	0.43	0.08	0.07
09LP014-1 L 67	0.010	16.824	5.295	18.370	83.794	28.054	218.133	361.049	581.462	840.703	1132.236	1634.359	2587.85	1878.488	842	6.34	0.19	4.56	102.26	0.01	1.27	0.00	0.75	0.12	0.15
09LP014-1 L 10	0.066	33.076	2.647	8.314	43.904	32.912	108.568	160.897	253.212	381.768	509.585	743.095	1231.37	979.033	992	24.38	0.43	5.28	117.76	0.00	2.37	0.06	1.61	0.04	0.08
09LP014-1 L 99	0.094	0.033					3.473	11.389	31.219	98.595	236.216	649.681	1613.12	1734.817	585					0.00	0.62	0.01	0.01	0.00	0.01
09LP014-1 L 83	0.304	22.439	0.679	2.333	20.595		110.426	206.209	366.544	598.545	810.758	1266.844	2003.89	1469.588	747	45.65		8.83	630.01	0.00	2.35	0.12	0.44	0.12	0.09

Notes:

Activity (SiO<sub>2</sub>) = 1; activity (TiO<sub>2</sub>) = 0.6.

Yellow highlighted rows are samples that intersected inclusions.

Trace element concentrations in ppm, calculated using mean count rate method.

Sweep-by-sweep downhole fractionation of U/Pb ratios NOT corrected via Si/Zr fractionation factor.

Backgrounds were monitored during sweeps 8 to 18. Sample counts were integrated from sweeps 35 to 80.

Ablation used a laser spot size of 25 microns, and a laser firing repetition rate of 10 Hz.

APPENDIX B - DETRITAL ZIRCON ANALYSES, continued

Table B3a. Detrital zircon U-Pb geochronologic analyses from sample 09TOA098 in the undivided Vampire-Narchilla unit (PЄVN) - Isotope Geology Laboratory, Boise State University

Analysis	U (ppm)	Th (ppm)	Pb* (ppm)	Th/U	Corrected isotope ratios											Apparent ages (Ma)						% disc.	
					$\frac{^{206}\text{Pb}^*}{^{207}\text{Pb}^*}$	$\pm 2\sigma$ (%)	$\frac{^{207}\text{Pb}^*}{^{235}\text{U}^*}$	$\pm 2\sigma$ (%)	$\frac{^{206}\text{Pb}^*}{^{238}\text{U}}$	$\pm 2\sigma$ (%)	error corr.	$\frac{^{238}\text{U}}{^{206}\text{Pb}^*}$	$\pm 2\sigma$ (%)	$\frac{^{207}\text{Pb}^*}{^{206}\text{Pb}^*}$	$\pm 2\sigma$ (%)	error corr.	$\frac{^{207}\text{Pb}^*}{^{206}\text{Pb}^*}$	$\pm 2\sigma$ (Ma)	$\frac{^{207}\text{Pb}^*}{^{235}\text{U}}$	$\pm 2\sigma$ (Ma)	$\frac{^{206}\text{Pb}^*}{^{238}\text{U}^*}$		$\pm 2\sigma$ (Ma)
09TOA098 M 158	127.28	73.88	119.47	0.58	3.724	1.956	24.593	4.086	0.664	3.587	0.878	1.505	3.587	0.269	1.956	-0.0	3297	31	3292	40	3284	92	0
09TOA098 L 138	24.50	14.01	17.89	0.57	5.010	3.275	14.734	5.180	0.535	4.014	0.775	1.868	4.014	0.200	3.275	0.0	2823	53	2798	49	2764	90	2
09TOA098 L 102	131.75	102.57	94.36	0.78	5.353	1.904	13.062	3.610	0.507	3.068	0.850	1.972	3.068	0.187	1.904	0	2714	31	2684	34	2644	67	3
09TOA098 L 110	118.15	104.23	86.84	0.88	5.436	1.759	13.006	3.636	0.513	3.183	0.875	1.950	3.183	0.184	1.759	0	2689	29	2680	34	2669	70	1
09TOA098 L 121	28.03	19.58	19.47	0.70	5.464	3.553	12.824	5.771	0.508	4.547	0.788	1.968	4.547	0.183	3.553	0.0	2680	59	2667	54	2649	99	1
09TOA098 L 109	22.54	20.71	16.86	0.92	5.546	2.846	12.855	4.939	0.517	4.036	0.817	1.934	4.036	0.180	2.846	-0.0	2656	47	2669	47	2687	89	-1
09TOA098 M 174	127.34	158.38	97.89	1.24	5.553	1.742	12.489	3.824	0.503	3.404	0.890	1.988	3.404	0.180	1.742	0.0	2654	29	2642	36	2627	73	1
09TOA098 M 203	127.34	158.38	97.89	1.24	5.553	1.742	12.489	3.824	0.503	3.404	0.890	1.988	3.404	0.180	1.742	0.0	2654	29	2642	36	2627	73	1
09TOA098 L 128	74.86	42.76	49.38	0.57	5.616	1.946	12.123	3.922	0.494	3.405	0.868	2.025	3.405	0.178	1.946	-0.0	2635	32	2614	37	2587	73	2
09TOA098 L 119	68.58	76.70	49.87	1.12	5.652	2.458	12.042	4.673	0.494	3.974	0.850	2.026	3.974	0.177	2.458	-0.0	2624	41	2608	44	2586	85	1
09TOA098 M 191	48.07	46.86	33.86	0.97	5.657	2.382	11.856	4.612	0.486	3.949	0.856	2.056	3.949	0.177	2.382	-0.00	2623	40	2593	43	2555	83	3
09TOA098 M 221	48.07	46.86	33.86	0.97	5.657	2.382	11.856	4.612	0.486	3.949	0.856	2.056	3.949	0.177	2.382	-0.0	2623	40	2593	43	2555	83	3
09TOA098 M 153	22.91	151.34	32.33	6.61	5.660	3.378	11.846	5.659	0.486	4.540	0.802	2.056	4.540	0.177	3.378	0	2622	56	2592	53	2555	96	3
09TOA098 L 139	21.19	6.68	13.29	0.32	5.668	4.034	12.037	5.529	0.495	3.781	0.684	2.021	3.781	0.176	4.034	0	2620	67	2607	52	2591	81	1
09TOA098 M 160	40.38	50.80	28.99	1.26	5.672	3.505	11.456	4.930	0.471	3.468	0.703	2.122	3.468	0.176	3.505	0.0	2618	58	2561	46	2489	72	5
09TOA098 M 155	45.97	96.35	39.64	2.10	5.685	2.596	12.183	4.638	0.502	3.843	0.829	1.991	3.843	0.176	2.596	0.0	2615	43	2619	44	2624	83	-0
09TOA098 M 163	189.83	88.02	114.20	0.46	5.975	1.954	10.716	3.703	0.464	3.146	0.850	2.153	3.146	0.167	1.954	0.0	2531	33	2499	34	2459	64	3
09TOA098 M 186	93.56	103.32	59.24	1.10	6.518	3.100	9.263	4.630	0.438	3.439	0.743	2.284	3.439	0.153	3.100	-0.0	2384	53	2364	42	2341	68	2
09TOA098 M 216	93.56	103.32	59.24	1.10	6.518	3.100	9.263	4.630	0.438	3.439	0.743	2.284	3.439	0.153	3.100	-0.0	2384	53	2364	42	2341	68	2
09TOA098 M 198	77.97	45.79	44.99	0.59	6.576	2.277	9.214	3.963	0.439	3.244	0.819	2.275	3.244	0.152	2.277	0	2369	39	2360	36	2348	64	1
09TOA098 M 227	77.97	45.79	44.99	0.59	6.576	2.277	9.214	3.963	0.439	3.244	0.819	2.275	3.244	0.152	2.277	0	2369	39	2360	36	2348	64	1
09TOA098 M 166	107.84	74.36	59.14	0.69	6.857	2.288	8.207	3.747	0.408	2.968	0.792	2.450	2.968	0.146	2.288	-0.0	2298	39	2254	34	2207	55	4
09TOA098 M 171	152.05	191.30	77.99	1.26	7.022	2.008	6.711	7.175	0.342	6.888	0.960	2.926	6.888	0.142	2.008	0.0	2257	35	2074	63	1895	113	16
09TOA098 L 126	62.08	78.57	34.78	1.27	7.216	5.125	6.815	6.816	0.357	4.494	0.659	2.804	4.494	0.139	5.125	-0.0	2210	89	2088	60	1966	76	11
09TOA098 M 180	165.72	111.85	85.70	0.67	7.528	2.119	7.122	3.978	0.389	3.367	0.846	2.572	3.367	0.133	2.119	0	2136	37	2127	35	2117	61	1
09TOA098 M 209	165.72	111.85	85.70	0.67	7.528	2.119	7.122	3.978	0.389	3.367	0.846	2.572	3.367	0.133	2.119	0	2136	37	2127	35	2117	61	1
09TOA098 L 111	57.58	82.59	34.38	1.43	7.578	3.209	6.942	4.361	0.382	2.952	0.677	2.621	2.952	0.132	3.209	0.0	2124	56	2104	39	2083	53	2
09TOA098 M 169	44.27	68.36	24.74	1.54	8.257	2.590	5.968	4.701	0.357	3.923	0.835	2.798	3.923	0.121	2.590	-0.0	1973	46	1971	41	1970	67	0
09TOA098 M 172	135.28	98.73	63.61	0.73	8.271	1.613	5.888	3.802	0.353	3.443	0.906	2.831	3.443	0.121	1.613	-0.0	1970	29	1959	33	1950	58	1
09TOA098 L 115	25.36	46.93	13.88	1.85	8.307	4.918	5.469	6.142	0.329	3.680	0.599	3.035	3.680	0.120	4.918	0.0	1962	88	1896	53	1836	59	6
09TOA098 M 165	72.66	80.80	37.26	1.11	8.312	2.830	5.882	5.186	0.355	4.346	0.838	2.820	4.346	0.120	2.830	0	1961	50	1959	45	1957	73	0
09TOA098 L 122	105.38	76.28	48.43	0.72	8.320	2.676	5.750	4.668	0.347	3.824	0.819	2.882	3.824	0.120	2.676	-0.0	1959	48	1939	40	1920	64	2
09TOA098 L 118	125.60	178.93	61.13	1.42	8.386	3.082	5.392	6.163	0.328	5.337	0.866	3.049	5.337	0.119	3.082	-0.0	1945	55	1884	53	1828	85	6
09TOA098 M 189	246.96	276.96	117.75	1.12	8.444	2.325	5.432	4.436	0.333	3.778	0.852	3.006	3.778	0.118	2.325	-0.0	1933	42	1890	38	1851	61	4
09TOA098 M 219	246.96	276.96	117.75	1.12	8.444	2.325	5.432	4.436	0.333	3.778	0.852	3.006	3.778	0.118	2.325	-0.0	1933	42	1890	38	1851	61	4
09TOA098 L 103	20.45	26.20	10.15	1.28	8.469	4.718	5.380	6.396	0.330	4.319	0.675	3.026	4.319	0.118	4.718	0.0	1927	85	1882	55	1841	69	4
09TOA098 M 177	117.12	69.90	49.47	0.60	8.518	2.580	5.295	4.313	0.327	3.456	0.801	3.057	3.456	0.117	2.580	0	1917	46	1868	37	1824	55	5
09TOA098 M 206	117.12	69.90	49.47	0.60	8.518	2.580	5.295	4.313	0.327	3.456	0.801	3.057	3.456	0.117	2.580	0	1917	46	1868	37	1824	55	5
09TOA098 L 145	55.38	24.90	23.61	0.45	8.529	3.815	5.498	5.091	0.340	3.370	0.662	2.940	3.370	0.117	3.815	-0.0	1915	68	1900	44	1887	55	1
09TOA098 L 106	232.07	282.27	103.01	1.22	8.532	2.003	4.896	3.818	0.303	3.251	0.851	3.301	3.251	0.117	2.003	0.0	1914	36	1801	32	1706	49	11
09TOA098 M 188	26.21	40.72	14.13	1.55	8.556	3.458	5.614	5.595	0.348	4.399	0.786	2.870	4.399	0.117	3.458	-0.0	1909	62	1918	48	1927	73	-1
09TOA098 M 218	26.21	40.72	14.13	1.55	8.556	3.458	5.614	5.595	0.348	4.399	0.786	2.870	4.399	0.117	3.458	-0.0	1909	62	1918	48	1927	73	-1

APPENDIX B - DETRITAL ZIRCON ANALYSES, continued

Table B3a, *continued*. Detrital zircon U-Pb geochronologic analyses from sample **09TOA098** in the undivided Vampire-Narchilla unit (**PCVN**) - Isotope Geology Laboratory, Boise State University

Analysis	U (ppm)	Th (ppm)	Pb* (ppm)	Th/U	Corrected isotope ratios											Apparent ages (Ma)						% disc.	
					$\frac{206Pb^*}{207Pb^*}$	$\pm 2\sigma$ (%)	$\frac{207Pb^*}{235U^*}$	$\pm 2\sigma$ (%)	$\frac{206Pb^*}{238U}$	$\pm 2\sigma$ (%)	error corr.	$\frac{238U}{206Pb^*}$	$\pm 2\sigma$ (%)	$\frac{207Pb^*}{206Pb^*}$	$\pm 2\sigma$ (%)	error corr.	$\frac{207Pb^*}{206Pb^*}$	$\pm 2\sigma$ (Ma)	$\frac{207Pb^*}{235U}$	$\pm 2\sigma$ (Ma)	$\frac{206Pb^*}{238U^*}$		$\pm 2\sigma$ (Ma)
09TOA098 L 105	50.65	14.56	19.86	0.29	8.576	2.637	5.217	4.300	0.324	3.397	0.790	3.082	3.397	0.117	2.637	0.0	1905	47	1855	37	1812	54	5
09TOA098 M 182	29.30	9.77	12.45	0.33	8.578	4.268	5.656	5.788	0.352	3.910	0.676	2.842	3.910	0.117	4.268	-0.0	1904	77	1925	50	1943	66	-2
09TOA098 M 212	29.30	9.77	12.45	0.33	8.578	4.268	5.656	5.788	0.352	3.910	0.676	2.842	3.910	0.117	4.268	-0.0	1904	77	1925	50	1943	66	-2
09TOA098 M 195	130.47	110.99	60.00	0.85	8.618	2.635	5.385	4.570	0.337	3.734	0.817	2.971	3.734	0.116	2.635	0.0	1896	47	1883	39	1870	61	1
09TOA098 M 225	130.47	110.99	60.00	0.85	8.618	2.635	5.385	4.570	0.337	3.734	0.817	2.971	3.734	0.116	2.635	0.0	1896	47	1883	39	1870	61	1
09TOA098 M 193	128.30	248.26	72.39	1.94	8.632	2.391	5.327	4.507	0.334	3.820	0.848	2.998	3.820	0.116	2.391	0.0	1893	43	1873	39	1855	62	2
09TOA098 M 223	128.30	248.26	72.39	1.94	8.632	2.391	5.327	4.507	0.334	3.820	0.848	2.998	3.820	0.116	2.391	0.0	1893	43	1873	39	1855	62	2
09TOA098 L 140	247.91	307.12	121.07	1.24	8.758	1.586	5.191	3.494	0.330	3.113	0.891	3.033	3.113	0.114	1.586	0.0	1867	29	1851	30	1837	50	2
09TOA098 M 181	199.47	233.90	90.93	1.17	8.769	2.194	4.912	3.887	0.312	3.209	0.826	3.201	3.209	0.114	2.194	-0.0	1865	40	1804	33	1752	49	6
09TOA098 M 210	199.47	233.90	90.93	1.17	8.769	2.194	4.912	3.887	0.312	3.209	0.826	3.201	3.209	0.114	2.194	-0.0	1865	40	1804	33	1752	49	6
09TOA098 L 130	80.54	37.79	31.75	0.47	8.807	2.757	4.926	4.258	0.315	3.245	0.762	3.178	3.245	0.114	2.757	0	1857	50	1807	36	1763	50	5
09TOA098 L 113	141.87	96.87	60.00	0.68	8.815	2.336	4.996	4.099	0.319	3.368	0.822	3.131	3.368	0.113	2.336	0	1855	42	1819	35	1787	53	4
09TOA098 M 178	53.88	16.89	20.47	0.31	8.816	2.789	4.939	4.695	0.316	3.777	0.804	3.167	3.777	0.113	2.789	0.0	1855	50	1809	40	1769	58	5
09TOA098 M 207	53.88	16.89	20.47	0.31	8.816	2.789	4.939	4.695	0.316	3.777	0.804	3.167	3.777	0.113	2.789	0.0	1855	50	1809	40	1769	58	5
09TOA098 M 192	125.00	28.88	48.58	0.23	8.820	2.078	5.140	4.513	0.329	4.006	0.888	3.042	4.006	0.113	2.078	-0.0	1854	38	1843	38	1832	64	1
09TOA098 M 222	125.00	28.88	48.58	0.23	8.820	2.078	5.140	4.513	0.329	4.006	0.888	3.042	4.006	0.113	2.078	-0.0	1854	38	1843	38	1832	64	1
09TOA098 L 120	162.28	91.93	69.83	0.57	8.841	2.154	5.305	4.170	0.340	3.570	0.856	2.940	3.570	0.113	2.154	0	1850	39	1870	36	1887	58	-2
09TOA098 M 168	56.58	18.11	22.62	0.32	8.853	3.023	5.139	4.591	0.330	3.456	0.753	3.030	3.456	0.113	3.023	-0.0	1847	55	1843	39	1838	55	0
09TOA098 M 161	162.40	48.23	62.27	0.30	8.865	2.665	4.982	4.680	0.320	3.847	0.822	3.122	3.847	0.113	2.665	-0.0	1845	48	1816	40	1791	60	3
09TOA098 L 144	39.16	8.93	14.37	0.23	8.883	3.447	4.870	5.054	0.314	3.697	0.731	3.188	3.697	0.113	3.447	0.0	1841	62	1797	43	1759	57	4
09TOA098 L 124	126.71	55.43	50.08	0.44	8.887	2.544	4.943	4.265	0.319	3.423	0.803	3.139	3.423	0.113	2.544	0.0	1840	46	1810	36	1783	53	3
09TOA098 M 154	56.44	17.80	21.96	0.32	8.895	3.795	5.033	5.659	0.325	4.197	0.742	3.080	4.197	0.112	3.795	0.0	1839	69	1825	48	1813	66	1
09TOA098 L 116	152.94	43.89	59.57	0.29	8.903	1.770	5.019	3.881	0.324	3.454	0.890	3.086	3.454	0.112	1.770	-0.0	1837	32	1822	33	1810	54	2
09TOA098 M 202	71.18	64.98	31.66	0.91	8.903	3.335	5.009	5.038	0.323	3.777	0.750	3.092	3.777	0.112	3.335	0	1837	60	1821	43	1807	60	2
09TOA098 M 230	71.18	64.98	31.66	0.91	8.903	3.335	5.009	5.038	0.323	3.777	0.750	3.092	3.777	0.112	3.335	0.00	1837	60	1821	43	1807	60	2
09TOA098 L 108	76.79	33.34	30.94	0.43	8.936	3.028	5.022	4.711	0.325	3.609	0.766	3.073	3.609	0.112	3.028	0	1831	55	1823	40	1816	57	1
09TOA098 M 162	110.17	52.72	42.82	0.48	8.946	2.141	4.784	4.304	0.310	3.733	0.867	3.222	3.733	0.112	2.141	0	1829	39	1782	36	1743	57	5
09TOA098 L 134	103.32	19.57	40.60	0.19	8.946	2.515	5.179	4.266	0.336	3.446	0.808	2.976	3.446	0.112	2.515	0	1829	46	1849	36	1868	56	-2
09TOA098 M 173	213.87	124.48	89.47	0.58	8.951	1.742	5.041	3.910	0.327	3.501	0.895	3.056	3.501	0.112	1.742	0.0	1828	32	1826	33	1825	56	0
09TOA098 L 107	195.87	108.82	80.64	0.56	8.952	1.586	4.958	3.711	0.322	3.355	0.904	3.106	3.355	0.112	1.586	-0.0	1827	29	1812	31	1799	53	2
09TOA098 M 190	139.25	121.77	59.64	0.87	8.968	2.472	4.827	4.790	0.314	4.103	0.857	3.185	4.103	0.112	2.472	-0.0	1824	45	1790	40	1760	63	4
09TOA098 M 220	139.25	121.77	59.64	0.87	8.968	2.472	4.827	4.790	0.314	4.103	0.857	3.185	4.103	0.112	2.472	-0.0	1824	45	1790	40	1760	63	4
09TOA098 L 114	162.57	107.10	69.86	0.66	8.979	2.340	5.025	3.990	0.327	3.233	0.810	3.056	3.233	0.111	2.340	0.0	1822	42	1824	34	1825	51	-0
09TOA098 L 136	159.28	30.32	62.05	0.19	8.983	2.282	5.112	4.415	0.333	3.780	0.856	3.002	3.780	0.111	2.282	0	1821	41	1838	37	1853	61	-2
09TOA098 M 156	90.82	82.67	41.38	0.91	9.018	2.313	5.137	4.707	0.336	4.099	0.871	2.976	4.099	0.111	2.313	0	1814	42	1842	40	1867	66	-3
09TOA098 L 133	343.32	176.01	138.17	0.51	9.028	1.846	4.873	4.080	0.319	3.638	0.892	3.134	3.638	0.111	1.846	-0.0	1812	34	1798	34	1785	57	1
09TOA098 M 167	202.30	101.22	81.33	0.50	9.034	1.812	4.895	3.888	0.321	3.440	0.885	3.118	3.440	0.111	1.812	0.0	1811	33	1801	33	1793	54	1
09TOA098 L 129	166.88	172.24	76.12	1.03	9.034	2.058	4.930	4.029	0.323	3.464	0.860	3.096	3.464	0.111	2.058	0.0	1811	37	1807	34	1804	55	0
09TOA098 L 142	203.05	107.07	79.76	0.53	9.078	2.219	4.714	4.384	0.310	3.781	0.862	3.222	3.781	0.110	2.219	-0.0	1802	40	1770	37	1743	58	3
09TOA098 M 184	318.74	38.93	114.03	0.12	9.089	1.901	4.742	4.148	0.313	3.687	0.889	3.199	3.687	0.110	1.901	0	1800	35	1775	35	1753	57	3
09TOA098 M 214	318.74	38.93	114.03	0.12	9.089	1.901	4.742	4.148	0.313	3.687	0.889	3.199	3.687	0.110	1.901	0	1800	35	1775	35	1753	57	3
09TOA098 L 137	102.46	45.70	41.01	0.45	9.102	2.510	4.877	4.346	0.322	3.548	0.816	3.106	3.548	0.110	2.510	0	1797	46	1798	37	1799	56	-0

APPENDIX B - DETRITAL ZIRCON ANALYSES, continued

Table B3a, continued. Detrital zircon U-Pb geochronologic analyses from sample **09TOA098** in the undivided Vampire-Narchilla unit (PCVN) - Isotope Geology Laboratory, Boise State University

Analysis	U (ppm)	Th (ppm)	Pb* (ppm)	Th/U	Corrected isotope ratios											Apparent ages (Ma)						% disc.	
					$\frac{^{206}\text{Pb}^*}{^{207}\text{Pb}^*}$	$\pm 2\sigma$ (%)	$\frac{^{207}\text{Pb}^*}{^{235}\text{U}^*}$	$\pm 2\sigma$ (%)	$\frac{^{206}\text{Pb}^*}{^{238}\text{U}^*}$	$\pm 2\sigma$ (%)	error corr.	$\frac{^{238}\text{U}}{^{206}\text{Pb}^*}$	$\pm 2\sigma$ (%)	$\frac{^{207}\text{Pb}^*}{^{206}\text{Pb}^*}$	$\pm 2\sigma$ (%)	error corr.	$\frac{^{207}\text{Pb}^*}{^{206}\text{Pb}^*}$	$\pm 2\sigma$ (Ma)	$\frac{^{207}\text{Pb}^*}{^{235}\text{U}^*}$	$\pm 2\sigma$ (Ma)	$\frac{^{206}\text{Pb}^*}{^{238}\text{U}^*}$		$\pm 2\sigma$ (Ma)
09TOA098 L 141	231.53	288.06	107.34	1.24	9.111	1.870	4.767	4.123	0.315	3.675	0.891	3.175	3.675	0.110	1.870	0	1795	34	1779	35	1765	57	2
09TOA098 L 131	29.58	48.54	14.43	1.64	9.149	4.514	4.696	6.332	0.312	4.441	0.701	3.209	4.441	0.109	4.514	0	1788	82	1767	53	1748	68	2
09TOA098 M 183	186.06	109.57	77.18	0.59	9.157	2.174	4.896	3.934	0.325	3.278	0.833	3.075	3.278	0.109	2.174	-0.0	1786	40	1802	33	1815	52	-2
09TOA098 M 213	186.06	109.57	77.18	0.59	9.157	2.174	4.896	3.934	0.325	3.278	0.833	3.075	3.278	0.109	2.174	-0.0	1786	40	1802	33	1815	52	-2
09TOA098 M 175	51.99	12.62	19.52	0.24	9.170	3.708	4.775	5.013	0.318	3.373	0.673	3.149	3.373	0.109	3.708	0	1784	68	1780	42	1778	52	0
09TOA098 M 204	51.99	12.62	19.52	0.24	9.170	3.708	4.775	5.013	0.318	3.373	0.673	3.149	3.373	0.109	3.708	0	1784	68	1780	42	1778	52	0
09TOA098 M 176	42.09	50.16	19.29	1.19	9.172	2.982	4.700	4.799	0.313	3.760	0.784	3.198	3.760	0.109	2.982	0.0	1783	54	1767	40	1754	58	2
09TOA098 M 205	42.09	50.16	19.29	1.19	9.172	2.982	4.700	4.799	0.313	3.760	0.784	3.198	3.760	0.109	2.982	0.0	1783	54	1767	40	1754	58	2
09TOA098 M 194	229.70	105.02	91.76	0.46	9.189	2.361	4.823	4.382	0.321	3.691	0.842	3.111	3.691	0.109	2.361	0	1780	43	1789	37	1797	58	-1
09TOA098 M 224	229.70	105.02	91.76	0.46	9.189	2.361	4.823	4.382	0.321	3.691	0.842	3.111	3.691	0.109	2.361	0	1780	43	1789	37	1797	58	-1
09TOA098 M 159	264.20	61.96	102.62	0.23	9.210	2.059	4.963	4.177	0.332	3.634	0.870	3.016	3.634	0.109	2.059	0.0	1776	38	1813	35	1846	58	-4
09TOA098 L 117	79.45	37.03	31.95	0.47	9.214	3.197	4.908	5.394	0.328	4.344	0.805	3.049	4.344	0.109	3.197	-0.0	1775	58	1804	46	1829	69	-3
09TOA098 M 185	42.20	14.35	16.83	0.34	9.219	3.885	4.930	5.210	0.330	3.471	0.666	3.033	3.471	0.108	3.885	-0.0	1774	71	1807	44	1837	55	-4
09TOA098 M 215	42.20	14.35	16.83	0.34	9.219	3.885	4.930	5.210	0.330	3.471	0.666	3.033	3.471	0.108	3.885	-0.0	1774	71	1807	44	1837	55	-4
09TOA098 M 197	216.11	96.82	81.94	0.45	9.235	1.924	4.564	3.866	0.306	3.353	0.867	3.271	3.353	0.108	1.924	0.0	1771	35	1743	32	1719	51	3
09TOA098 M 226	216.11	96.82	81.94	0.45	9.235	1.924	4.564	3.866	0.306	3.353	0.867	3.271	3.353	0.108	1.924	0.0	1771	35	1743	32	1719	51	3
09TOA098 L 132	52.28	17.14	20.69	0.33	9.254	3.499	4.875	5.128	0.327	3.748	0.731	3.056	3.748	0.108	3.499	0	1767	64	1798	43	1825	60	-3
09TOA098 L 143	60.00	16.19	22.53	0.27	9.270	3.645	4.711	4.813	0.317	3.143	0.653	3.157	3.143	0.108	3.645	-0.0	1764	67	1769	40	1774	49	-1
09TOA098 M 199	17.79	22.84	8.43	1.28	9.311	5.608	4.725	6.889	0.319	4.001	0.581	3.134	4.001	0.107	5.608	0.0	1756	103	1772	58	1785	62	-2
09TOA098 M 228	17.79	22.84	8.43	1.28	9.311	5.608	4.725	6.889	0.319	4.001	0.581	3.134	4.001	0.107	5.608	0.0	1756	103	1772	58	1785	62	-2
09TOA098 M 201	139.41	45.63	52.90	0.33	9.315	2.415	4.650	4.106	0.314	3.321	0.809	3.183	3.321	0.107	2.415	-0.0	1755	44	1758	34	1761	51	-0
09TOA098 M 229	139.41	45.63	52.90	0.33	9.315	2.415	4.650	4.106	0.314	3.321	0.809	3.183	3.321	0.107	2.415	-0.0	1755	44	1758	34	1761	51	-0
09TOA098 L 125	264.48	118.23	100.12	0.45	9.317	1.739	4.523	3.881	0.306	3.469	0.894	3.272	3.469	0.107	1.739	0	1754	32	1735	32	1719	52	2
09TOA098 L 112	188.64	19.25	67.04	0.10	9.337	2.201	4.600	3.906	0.311	3.227	0.826	3.210	3.227	0.107	2.201	-0.0	1751	40	1749	33	1748	49	0
09TOA098 M 157	116.53	66.00	46.52	0.57	9.411	2.754	4.654	4.700	0.318	3.809	0.810	3.148	3.809	0.106	2.754	0.0	1736	50	1759	39	1778	59	-2
09TOA098 M 187	149.23	74.07	58.71	0.50	9.583	2.990	4.574	4.572	0.318	3.460	0.757	3.146	3.460	0.104	2.990	0	1703	55	1744	38	1779	54	-4
09TOA098 M 217	149.23	74.07	58.71	0.50	9.583	2.990	4.574	4.572	0.318	3.460	0.757	3.146	3.460	0.104	2.990	0	1703	55	1744	38	1779	54	-4
09TOA098 L 127	86.56	87.74	35.30	1.01	9.916	2.689	4.081	4.390	0.294	3.471	0.790	3.407	3.471	0.101	2.689	-0.0	1640	50	1651	36	1659	51	-1
09TOA098 L 123	543.07	255.96	69.46	0.47	16.281	2.768	0.895	4.662	0.106	3.751	0.805	9.462	3.751	0.061	2.768	0	654	59	649	22	648	23	1
09TOA098 M 179	577.19	428.43	78.67	0.74	16.343	2.703	0.888	4.350	0.105	3.408	0.783	9.498	3.408	0.061	2.703	0.0	646	58	645	21	645	21	0
09TOA098 M 208	577.19	428.43	78.67	0.74	16.343	2.703	0.888	4.350	0.105	3.408	0.783	9.498	3.408	0.061	2.703	0.0	646	58	645	21	645	21	0
09TOA098 M 170	1309.28	768.36	166.89	0.59	16.378	1.536	0.860	3.698	0.102	3.364	0.910	9.785	3.364	0.061	1.536	0.0	641	33	630	17	627	20	2

Notes:

Yellow highlighted rows are samples that intersected inclusions.  
 Isotope ratios and ages are NOT corrected for initial common Pb.  
 Isotope ratio and apparent age errors include systematic calibration errors of 6.37100499011343% ( $^{208}\text{Pb}/^{232}\text{Th}$ ), 0.452188693209402% ( $^{207}\text{Pb}/^{206}\text{Pb}$ ), 1.63033394062177% ( $^{206}\text{Pb}/^{238}\text{U}$ ) (all 1-sigma).  
 Trace element concentrations in ppm, calculated using mean count rate method.  
 Sweep-by-sweep downhole fractionation of U/Pb ratios NOT corrected via Si/Zr fractionation factor.  
 Backgrounds were monitored during sweeps 8 to 18. Sample counts were integrated from sweeps 35 to 80.  
 Ablation used a laser spot size of 25 microns, and a laser firing repetition rate of 10 Hz.





APPENDIX B - DETRITAL ZIRCON ANALYSES, continued

Table B3b, *continued*. Detrital zircon trace element analyses from sample 09TOA098 in the undivided Vampire-Narchilla unit (PЄVN) - Isotope Geology Laboratory, Boise State University

Analysis	Concentrations (ppm)																						
	P	Ti	Y	Zr	Nb	La	Ce	Pr	Nd	Sm	Eu	Gd	Tb	Dy	Ho	Er	Tm	Yb	Lu	Hf	Ta	Th	U
09TOA098 M 183	177.820	13.957	548.063	525192.658	1.109	0.018	15.311	0.169	4.051	5.661	1.169	22.023	6.941	64.217	20.255	79.357	18.404	196.950	22.923	8387.932	0.597	109.571	186.055
09TOA098 M 213	177.820	13.957	548.063	525192.658	1.109	0.018	15.311	0.169	4.051	5.661	1.169	22.023	6.941	64.217	20.255	79.357	18.404	196.950	22.923	8387.932	0.597	109.571	186.055
09TOA098 M 175	219.544	7.925	611.794	511688.070	0.892		4.648		0.913	2.240	0.615	11.573	4.454	53.295	21.159	101.698	27.629	322.629	41.623	7650.709	0.282	12.618	51.993
09TOA098 M 204	219.544	7.925	611.794	511688.070	0.892		4.648		0.913	2.240	0.615	11.573	4.454	53.295	21.159	101.698	27.629	322.629	41.623	7650.709	0.282	12.618	51.993
09TOA098 M 176	252.354	28.668	650.781	503456.111	1.946		39.384	0.179	3.757	6.508	1.804	23.679	7.132	71.744	24.981	99.143	26.011	270.801	32.269	7040.600	0.715	50.156	42.091
09TOA098 M 205	252.354	28.668	650.781	503456.111	1.946		39.384	0.179	3.757	6.508	1.804	23.679	7.132	71.744	24.981	99.143	26.011	270.801	32.269	7040.600	0.715	50.156	42.091
09TOA098 M 194	226.440	8.541	559.430	492494.157	1.009	0.133	9.378	0.070	0.675	3.973	0.387	16.363	4.406	56.744	20.809	85.413	20.966	230.265	25.902	8429.749	0.896	105.020	229.702
09TOA098 M 224	226.440	8.541	559.430	492494.157	1.009	0.133	9.378	0.070	0.675	3.973	0.387	16.363	4.406	56.744	20.809	85.413	20.966	230.265	25.902	8429.749	0.896	105.020	229.702
09TOA098 M 159	584.052	8.344	1289.890	521762.710	1.486		3.509		0.770	2.040	0.077	18.587	8.459	111.671	45.017	219.813	59.395	652.755	82.635	11724.094	1.382	61.965	264.199
09TOA098 L 117	147.463	10.518	328.794	558144.768	0.347	0.027	14.365	0.087	1.207	3.205	0.650	12.770	3.203	35.398	10.881	46.239	11.708	122.775	16.957	8577.811	0.215	37.028	79.449
09TOA098 M 185	190.432	5.164	309.812	539852.330	0.328		3.313		0.473	0.497	0.144	6.020	1.999	28.021	10.624	49.646	14.458	174.806	25.361	7980.781	0.249	14.354	42.205
09TOA098 M 215	190.432	5.164	309.812	539852.330	0.328		3.313		0.473	0.497	0.144	6.020	1.999	28.021	10.624	49.646	14.458	174.806	25.361	7980.781	0.249	14.354	42.205
09TOA098 M 197	282.071	7.570	636.512	485994.791	1.796	0.687	9.682	0.287	1.913	2.432	0.220	16.950	5.219	66.386	23.107	97.605	23.399	249.286	26.984	9268.200	0.954	96.821	216.115
09TOA098 M 226	282.071	7.570	636.512	485994.791	1.796	0.687	9.682	0.287	1.913	2.432	0.220	16.950	5.219	66.386	23.107	97.605	23.399	249.286	26.984	9268.200	0.954	96.821	216.115
09TOA098 L 132	152.543	10.194	211.918	497284.232	0.617		13.213	0.020	0.247	0.902	0.211	6.276	1.788	21.150	7.193	30.456	7.895	90.222	10.690	8372.484	0.274	17.138	52.275
09TOA098 L 143	91.593	4.924	123.825	512452.002	0.143		5.356				0.134	2.962	0.674	10.317	4.117	19.372	5.857	75.236	11.278	9344.759	0.206	16.192	60.004
09TOA098 M 199	279.105	41.726	473.941	511407.729	1.129	0.000	21.848	0.176	2.656	5.101	1.212	16.716	4.758	56.133	17.999	72.590	17.614	188.932	22.147	7277.672	0.416	22.841	17.793
09TOA098 M 228	279.105	41.726	473.941	511407.729	1.129	0.000	21.848	0.176	2.656	5.101	1.212	16.716	4.758	56.133	17.999	72.590	17.614	188.932	22.147	7277.672	0.416	22.841	17.793
09TOA098 M 201	225.915	15.820	374.449	511547.292	0.996		4.475		0.787	0.407		8.194	3.016	38.643	12.720	58.887	14.549	153.445	17.615	9330.524	0.841	45.625	139.412
09TOA098 M 229	225.915	15.820	374.449	511547.292	0.996		4.475		0.787	0.407		8.194	3.016	38.643	12.720	58.887	14.549	153.445	17.615	9330.524	0.841	45.625	139.412
09TOA098 L 125	179.188	7.167	704.783	500187.619	1.967	0.094	9.123		1.172	2.599	0.144	16.972	5.836	71.736	26.321	107.400	26.149	262.220	30.371	9702.181	1.455	118.229	264.477
09TOA098 L 112	60.327	0.836	394.023	470230.445	1.028		3.910			0.658	0.466	5.779	2.219	32.732	12.937	61.447	17.105	229.598	28.136	8084.949	0.603	19.253	188.638
09TOA098 M 157	196.007	13.703	673.533	527939.117	1.887	0.123	5.263		1.166	2.653	0.307	16.711	5.926	69.701	24.578	105.547	24.544	243.483	30.862	9142.905	0.970	66.001	116.527
09TOA098 M 187	160.617	8.946	631.854	521943.590	1.698	0.190	5.861		0.291	2.614	0.096	13.379	4.930	60.001	22.031	93.748	22.853	232.266	28.048	9907.455	0.847	74.066	149.227
09TOA098 M 217	160.617	8.946	631.854	521943.590	1.698	0.190	5.861		0.291	2.614	0.096	13.379	4.930	60.001	22.031	93.748	22.853	232.266	28.048	9907.455	0.847	74.066	149.227
09TOA098 L 127	187.065	21.434	462.157	523259.966	2.271		13.969	0.078	1.900	2.527	0.534	13.868	4.014	48.359	16.999	69.000	17.441	176.391	21.836	8393.965	0.906	87.737	86.558
09TOA098 L 123	143.461	1.959	1809.624	509364.946	85.866	0.052	18.102	0.082	1.776	4.570	0.173	36.684	15.907	202.787	72.634	297.895	69.206	676.766	67.830	10646.782	30.419	255.963	543.072
09TOA098 M 179	196.929	6.197	2279.701	514056.505	74.320		17.305	0.237	5.280	12.175	0.204	58.303	22.070	267.884	91.028	353.510	78.820	754.991	76.443	9275.807	23.060	428.429	577.187
09TOA098 M 208	196.929	6.197	2279.701	514056.505	74.320		17.305	0.237	5.280	12.175	0.204	58.303	22.070	267.884	91.028	353.510	78.820	754.991	76.443	9275.807	23.060	428.429	577.187
09TOA098 M 170	147.354	4.180	3461.834	501751.271	133.058	0.212	25.903	0.290	3.685	10.044	0.123	61.965	25.302	332.612	127.244	561.256	133.334	1330.863	138.266	10952.087	42.358	768.358	1309.279

Notes:

Yellow highlighted rows are samples that intersected inclusions.

Trace element concentrations in ppm, calculated using mean count rate method.

Sweep-by-sweep downhole fractionation of U/Pb ratios NOT corrected via Si/Zr fractionation factor.

Backgrounds were monitored during sweeps 8 to 18. Sample counts were integrated from sweeps 35 to 80.

Ablation used a laser spot size of 25 microns, and a laser firing repetition rate of 10 Hz.





APPENDIX B - DETRITAL ZIRCON ANALYSES, continued

Table B3c, continued. Detrital zircon calculated ratios and values from sample 09TOA098 in the undivided Vampire-Narchilla unit (PCVN) - Isotope Geology Laboratory, Boise State University

Analysis	CI chondrite normalizing values from Sun and McDonough (1989)														Ti-in-zircon (T°C)	Ce/Ce*	Eu/Eu*	(Sm/Nd) <sub>cn</sub>	(Lu/Nd) <sub>cn</sub>	Lu/Hf	Nb/Ta	Nb/U	Th/U	Th/Y	Y/Hf
	0.237	0.612	0.095	0.467	0.153	0.058	0.206	0.037	0.254	0.057	0.166	0.026	0.17	0.025											
	La	Ce	Pr	Nd	Sm	Eu	Gd	Tb	Dy	Ho	Er	Tm	Yb	Lu											
09TOA098 L 141	0.076	116.712	4.700	12.429	60.764	21.155	168.674	311.895	604.971	1077.275	1808.356	3217.603	5580.520	4587.829	563	48.87	0.18	4.89	369.11	0.02	3.03	0.01	1.24	0.15	0.29
09TOA098 L 131	0.021	57.357	6.514	26.962	99.905	69.214	223.815	323.590	508.262	687.871	894.903	1328.354	2086.497	1498.802	888	17.55	0.43	3.71	55.59	0.01	2.93	0.04	1.64	0.05	0.14
09TOA098 M 183	0.077	25.019	1.781	8.675	37.001	20.164	107.168	185.589	252.824	357.865	479.497	721.737	1158.530	902.466	832	26.93	0.28	4.27	104.03	0.00	1.86	0.01	0.59	0.20	0.07
09TOA098 M 213	0.077	25.019	1.781	8.675	37.001	20.164	107.168	185.589	252.824	357.865	479.497	721.737	1158.530	902.466	832	26.93	0.28	4.27	104.03	0.00	1.86	0.01	0.59	0.20	0.07
09TOA098 M 175		7.594	0.437	1.956	14.642	10.609	56.318	119.083	209.824	373.838	614.487	1083.499	1897.819	1638.712	773		0.30	7.49	837.91	0.01	3.16	0.02	0.24	0.02	0.08
09TOA098 M 204		7.594	0.437	1.956	14.642	10.609	56.318	119.083	209.824	373.838	614.487	1083.499	1897.819	1638.712	773		0.30	7.49	837.91	0.01	3.16	0.02	0.24	0.02	0.08
09TOA098 M 176	0.047	64.353	1.883	8.045	42.538	31.107	115.228	190.688	282.458	441.366	599.054	1020.028	1592.948	1270.426	918	66.68	0.39	5.29	157.91	0.00	2.72	0.05	1.19	0.08	0.09
09TOA098 M 205	0.047	64.353	1.883	8.045	42.538	31.107	115.228	190.688	282.458	441.366	599.054	1020.028	1592.948	1270.426	918	66.68	0.39	5.29	157.91	0.00	2.72	0.05	1.19	0.08	0.09
09TOA098 M 194	0.559	15.324	0.734	1.446	25.968	6.666	79.627	117.803	223.401	367.654	516.089	822.180	1354.499	1019.775	780	23.71	0.13	17.96	705.21	0.00	1.13	0.00	0.46	0.19	0.07
09TOA098 M 224	0.559	15.324	0.734	1.446	25.968	6.666	79.627	117.803	223.401	367.654	516.089	822.180	1354.499	1019.775	780	23.71	0.13	17.96	705.21	0.00	1.13	0.00	0.46	0.19	0.07
09TOA098 M 159		5.733	0.368	1.649	13.334	1.326	90.450	226.177	439.651	795.355	1328.177	2329.223	3839.737	3253.346	778		0.03	8.09	1972.84	0.01	1.08	0.01	0.23	0.05	0.11
09TOA098 L 117	0.115	23.473	0.920	2.584	20.949	11.206	62.139	85.644	139.362	192.237	279.392	459.150	722.209	667.593	801	45.35	0.27	8.11	258.32	0.00	1.61	0.00	0.47	0.11	0.04
09TOA098 M 185		5.413	0.226	1.013	3.250	2.479	29.297	53.456	110.319	187.707	299.976	567.000	1028.272	998.484	732		0.15	3.21	985.76	0.00	1.32	0.01	0.34	0.05	0.04
09TOA098 M 215		5.413	0.226	1.013	3.250	2.479	29.297	53.456	110.319	187.707	299.976	567.000	1028.272	998.484	732		0.15	3.21	985.76	0.00	1.32	0.01	0.34	0.05	0.04
09TOA098 M 197	2.899	15.821	3.019	4.096	15.897	3.785	82.480	139.546	261.361	408.245	589.757	917.600	1466.390	1062.346	768	5.35	0.08	3.88	259.39	0.00	1.88	0.01	0.45	0.15	0.07
09TOA098 M 226	2.899	15.821	3.019	4.096	15.897	3.785	82.480	139.546	261.361	408.245	589.757	917.600	1466.390	1062.346	768	5.35	0.08	3.88	259.39	0.00	1.88	0.01	0.45	0.15	0.07
09TOA098 L 132	0.005	21.589	0.214	0.529	5.897	3.642	30.539	47.819	83.268	127.079	184.025	309.604	530.715	420.881	798	196.44	0.20	11.15	795.44	0.00	2.25	0.01	0.33	0.08	0.03
09TOA098 L 143		8.752				2.315	14.416	18.018	40.619	72.731	117.051	229.694	442.563	444.027	728					0.00	0.69	0.00	0.27	0.13	0.01
09TOA098 M 199	0.001	35.699	1.858	5.687	33.337	20.892	81.342	127.223	220.998	318.007	438.613	690.765	1111.362	871.918	968	38.41	0.36	5.86	153.31	0.00	2.71	0.06	1.28	0.05	0.07
09TOA098 M 228	0.001	35.699	1.858	5.687	33.337	20.892	81.342	127.223	220.998	318.007	438.613	690.765	1111.362	871.918	968	38.41	0.36	5.86	153.31	0.00	2.71	0.06	1.28	0.05	0.07
09TOA098 M 201		7.313	0.377	1.686	2.661		39.875	80.642	152.136	224.743	355.815	570.547	902.616	693.502	846			1.58	411.37	0.00	1.19	0.01	0.33	0.12	0.04
09TOA098 M 229		7.313	0.377	1.686	2.661		39.875	80.642	152.136	224.743	355.815	570.547	902.616	693.502	846			1.58	411.37	0.00	1.19	0.01	0.33	0.12	0.04
09TOA098 L 125	0.398	14.907	0.561	2.510	16.987	2.480	82.587	156.033	282.423	465.029	648.940	1025.437	1542.470	1195.706	763	31.09	0.05	6.77	476.39	0.00	1.35	0.01	0.45	0.17	0.07
09TOA098 L 112		<b>6.389</b>		<b>0.440</b>	<b>4.300</b>	<b>8.035</b>	<b>28.123</b>	<b>59.341</b>	<b>128.868</b>	<b>228.573</b>	<b>371.284</b>	<b>670.799</b>	<b>1350.575</b>	<b>1107.727</b>	<b>589</b>		<b>0.50</b>	<b>9.77</b>	<b>2515.96</b>	<b>0.00</b>	<b>1.71</b>	<b>0.01</b>	<b>0.10</b>	<b>0.05</b>	<b>0.05</b>
09TOA098 M 157	0.517	8.600	0.558	2.496	17.341	5.295	81.316	158.457	274.413	434.237	637.748	962.508	1432.255	1215.033	830	16.00	0.11	6.95	486.75	0.00	1.94	0.02	0.57	0.10	0.07
09TOA098 M 187	0.800	9.576	0.139	0.624	17.087	1.659	65.104	131.822	236.223	389.235	566.454	896.201	1366.270	1104.259	785	20.39	0.04	27.39	1770.34	0.00	2.00	0.01	0.50	0.12	0.06
09TOA098 M 217	0.800	9.576	0.139	0.624	17.087	1.659	65.104	131.822	236.223	389.235	566.454	896.201	1366.270	1104.259	785	20.39	0.04	27.39	1770.34	0.00	2.00	0.01	0.50	0.12	0.06
09TOA098 L 127	0.021	22.825	0.823	4.068	16.519	9.215	67.485	107.332	190.389	300.330	416.917	683.948	1037.592	859.676	881	54.12	0.22	4.06	211.31	0.00	2.51	0.03	1.01	0.19	0.06
09TOA098 L 123	0.221	29.579	0.860	3.803	29.869	2.989	178.510	425.330	798.373	1283.280	1799.968	2713.971	3980.977	2670.477	651	54.69	0.03	7.85	702.18	0.01	2.82	0.16	0.47	0.14	0.17
09TOA098 M 179	0.062	28.277	2.492	11.306	79.578	3.519	283.715	590.119	1054.660	1608.269	2136.015	3090.994	4441.126	3009.558	749	22.14	0.02	7.04	266.20	0.01	3.22	0.13	0.74	0.19	0.25
09TOA098 M 208	0.062	28.277	2.492	11.306	79.578	3.519	283.715	590.119	1054.660	1608.269	2136.015	3090.994	4441.126	3009.558	749	22.14	0.02	7.04	266.20	0.01	3.22	0.13	0.74	0.19	0.25
09TOA098 M 170	0.893	42.324	3.049	7.892	65.650	2.121	301.531	676.523	1309.495	2248.133	3391.275	5228.770	7828.604	5443.540	713	21.48	0.01	8.32	689.77	0.01	3.14	0.10	0.59	0.22	0.32

Notes:

Activity (SiO<sub>2</sub>) = 1; activity (TiO<sub>2</sub>) = 0.6.

Yellow highlighted rows are samples that intersected inclusions.

Trace element concentrations in ppm, calculated using mean count rate method.

Sweep-by-sweep downhole fractionation of U/Pb ratios NOT corrected via Si/Zr fractionation factor.

Backgrounds were monitored during sweeps 8 to 18. Sample counts were integrated from sweeps 35 to 80.

Ablation used a laser spot size of 25 microns, and a laser firing repetition rate of 10 Hz.

APPENDIX B - DETRITAL ZIRCON ANALYSES, continued

Table B4. Detrital zircon U-Pb geochronologic analyses from sample **09LP094** from the undivided Vampire-Narchilla unit (PCVN) - Memorial University

File Name	Measured Isotopic Ratios							Calculated Ages (Ma)							Concordia age (Ma)	2 $\sigma$ error (Ma)	MSWD (of concordance)	Probability	Th232 (ppm)	U238 (ppm)	Th/U (ratio)
	$\frac{^{207}\text{Pb}}{^{235}\text{U}}$	1 $\sigma$ error	$\frac{^{206}\text{Pb}}{^{238}\text{U}}$	1 $\sigma$ error	Rho	$\frac{^{207}\text{Pb}}{^{206}\text{Pb}}$	1 $\sigma$ error	$\frac{^{207}\text{Pb}}{^{235}\text{U}}$	1 $\sigma$ error (Ma)	$\frac{^{206}\text{Pb}}{^{238}\text{U}}$	1 $\sigma$ error (Ma)	$\frac{^{207}\text{Pb}}{^{206}\text{Pb}}$	1 $\sigma$ error (Ma)	U-Pb/Pb-Pb concordancy (%)							
ap16a31	2.063	0.224	0.145	0.012	0.388	0.116	0.001	1137	74	874	69	1892	14	46	956	125.66	10.01	0.002	1003	918	1.092
ap16a28	4.499	0.513	0.260	0.021	0.354	0.129	0.002	1731	95	1491	107	2085	30	72	1613	174.10	4.17	0.041	59	55	1.082
ap19a33	3.144	0.398	0.212	0.028	0.525	0.104	0.001	1444	98	1238	150	1698	15	73	1413	197.30	2.59	0.107	285	443	0.643
ap16a48	7.673	0.360	0.332	0.017	0.553	0.151	0.002	2193	42	1849	83	2358	18	78	2199	83.75	25.91	0.000	248	152	1.631
ap16a29	4.413	0.143	0.268	0.006	0.371	0.116	0.001	1715	27	1528	33	1899	14	80	1640	50.33	30.01	0.000	418	542	0.772
ap16a60	5.101	0.232	0.283	0.015	0.594	0.123	0.001	1836	39	1609	77	1997	15	81	1850	75.73	13.94	0.000	223	273	0.817
ap16a19	9.047	1.055	0.361	0.011	0.133	0.158	0.005	2343	107	1987	53	2433	58	82	2019	102.67	7.70	0.006	178	323	0.551
ap16a52	0.951	0.141	0.113	0.008	0.234	0.067	0.002	679	73	691	45	824	50	84	689	84.17	0.03	0.865	82	193	0.427
ap19a11	4.630	0.264	0.270	0.016	0.504	0.112	0.001	1755	48	1543	79	1827	13	84	1732	96.28	9.80	0.002	147	276	0.533
ap19a20	4.885	0.157	0.292	0.008	0.417	0.115	0.001	1800	27	1654	39	1887	15	88	1764	52.94	15.58	0.000	113	196	0.580
ap16a04	8.358	0.492	0.381	0.020	0.441	0.152	0.001	2271	53	2082	92	2365	14	88	2248	107.28	5.15	0.023	240	140	1.718
ap19a24	13.482	0.397	0.468	0.013	0.481	0.194	0.001	2714	28	2475	58	2780	9	89	2711	55.81	22.76	0.000	188	186	1.016
ap19a39	13.025	0.413	0.471	0.013	0.423	0.192	0.002	2681	30	2489	55	2759	19	90	2664	60.16	14.85	0.000	84	33	2.521
ap16a61	5.398	0.234	0.315	0.012	0.434	0.119	0.001	1885	37	1763	58	1947	14	91	1864	73.64	5.14	0.023	361	409	0.882
ap19a12	8.189	0.297	0.381	0.012	0.433	0.145	0.001	2252	33	2081	56	2288	11	91	2230	65.73	11.51	0.001	64	175	0.365
ap19a18	5.416	0.364	0.311	0.020	0.487	0.117	0.001	1887	58	1746	100	1918	18	91	1876	115.62	2.64	0.104	212	184	1.154
ap19a30	5.149	0.274	0.306	0.013	0.402	0.115	0.001	1844	45	1719	64	1880	18	91	1813	87.59	4.07	0.044	133	183	0.726
ap16a27	4.829	0.427	0.296	0.026	0.489	0.111	0.001	1790	74	1673	127	1815	16	92	1780	148.90	1.11	0.292	419	346	1.212
ap19a10	3.164	0.217	0.240	0.011	0.322	0.094	0.001	1448	53	1389	55	1501	23	93	1419	88.77	0.88	0.347	50	128	0.387
ap16a07	5.906	0.631	0.331	0.030	0.431	0.122	0.001	1962	93	1845	148	1981	17	93	1943	183.62	0.75	0.388	127	193	0.657
ap19a34	9.240	0.302	0.418	0.012	0.440	0.156	0.001	2362	30	2250	55	2408	10	93	2353	59.98	5.24	0.022	167	247	0.675
ap19a19	2.254	0.131	0.196	0.008	0.335	0.081	0.001	1198	41	1154	41	1218	30	95	1175	67.64	0.87	0.351	46	78	0.582
ap16a09	5.230	0.243	0.325	0.010	0.322	0.117	0.002	1857	40	1814	47	1914	28	95	1841	70.15	0.72	0.396	38	57	0.658
ap16a22	5.101	0.266	0.315	0.012	0.358	0.114	0.001	1836	44	1768	58	1862	19	95	1814	82.01	1.36	0.243	69	119	0.581
ap16a55	5.357	0.309	0.331	0.015	0.384	0.118	0.001	1878	49	1841	71	1931	13	95	1869	94.16	0.28	0.594	257	411	0.625
ap16a70	5.792	0.172	0.335	0.009	0.427	0.120	0.001	1945	26	1865	41	1952	12	96	1933	50.64	4.54	0.033	253	402	0.630
ap16a20	3.178	0.174	0.255	0.007	0.256	0.095	0.002	1452	42	1464	37	1528	30	96	1459	61.97	0.07	0.797	40	89	0.446
ap19a32	6.008	0.146	0.346	0.007	0.400	0.123	0.001	1977	21	1915	32	1997	13	96	1965	41.18	4.06	0.044	160	182	0.879
ap19a22	5.943	0.206	0.333	0.012	0.516	0.118	0.001	1968	30	1855	58	1929	14	96	1966	60.36	5.29	0.021	99	239	0.413
ap19a21	4.844	0.194	0.307	0.009	0.347	0.109	0.001	1793	34	1724	42	1790	22	96	1768	61.46	2.44	0.118	44	76	0.583
ap16a30	6.501	0.235	0.356	0.010	0.390	0.125	0.001	2046	32	1964	48	2032	20	97	2029	61.71	3.19	0.074	107	125	0.854
ap16a05	6.246	0.195	0.354	0.010	0.467	0.124	0.001	2011	27	1956	49	2014	20	97	2007	54.51	1.61	0.205	111	112	0.990
ap16a08	16.509	1.349	0.547	0.035	0.391	0.209	0.002	2907	78	2814	146	2895	17	97	2898	155.58	0.47	0.492	60	84	0.708
ap16a75	2.219	0.062	0.193	0.004	0.378	0.079	0.001	1187	19	1139	22	1169	18	97	1167	34.47	4.22	0.040	177	460	0.384
ap19a26	5.951	0.189	0.340	0.008	0.381	0.119	0.001	1969	28	1889	40	1934	17	98	1949	53.00	4.25	0.039	98	88	1.120
ap19a37	5.545	0.124	0.325	0.007	0.461	0.114	0.001	1908	19	1815	33	1857	16	98	1898	38.48	10.08	0.001	122	196	0.624
ap16a40	5.433	0.190	0.331	0.010	0.429	0.115	0.001	1890	30	1845	48	1886	15	98	1884	58.97	1.03	0.310	65	220	0.293
ap19a23	9.296	0.292	0.428	0.011	0.419	0.150	0.001	2368	29	2298	51	2348	12	98	2360	57.13	2.26	0.132	90	141	0.641
ap16a11	5.808	0.200	0.344	0.008	0.337	0.118	0.002	1948	30	1906	38	1928	26	99	1934	54.41	1.08	0.298	19	63	0.296
ap16a26	14.310	0.549	0.523	0.018	0.441	0.190	0.002	2770	36	2710	75	2739	16	99	2769	72.78	0.81	0.369	90	121	0.744
ap19a04	12.635	0.424	0.493	0.014	0.433	0.175	0.001	2653	32	2582	62	2608	9	99	2649	63.12	1.60	0.205	205	160	1.282

APPENDIX B - DETRITAL ZIRCON ANALYSES, continued

Table B4, continued. Detrital zircon U-Pb geochronologic analyses from sample 09LP094 from the undivided Vampire-Narchilla unit (PEVN) - Memorial University

File Name	Measured Isotopic Ratios							Calculated Ages (Ma)							Concordia age (Ma)	2σ error (Ma)	MSWD (of concordance)	Probability	Th232 (ppm)	U238 (ppm)	Th/U (ratio)
	$\frac{^{207}\text{Pb}}{^{235}\text{U}}$	1σ error	$\frac{^{206}\text{Pb}}{^{238}\text{U}}$	1σ error	Rho	$\frac{^{207}\text{Pb}}{^{206}\text{Pb}}$	1σ error	$\frac{^{207}\text{Pb}}{^{235}\text{U}}$	1σ error (Ma)	$\frac{^{206}\text{Pb}}{^{238}\text{U}}$	1σ error (Ma)	$\frac{^{207}\text{Pb}}{^{206}\text{Pb}}$	1σ error (Ma)	U-Pb/Pb-Pb concordancy (%)							
ap16a38	2.915	0.177	0.253	0.010	0.324	0.092	0.002	1386	46	1452	51	1463	44	99	1413	77.55	1.39	0.238	26	52	0.502
ap16a10	5.014	0.235	0.331	0.008	0.266	0.113	0.002	1822	40	1843	40	1854	34	99	1832	63.15	0.19	0.659	34	36	0.953
ap16a32	4.476	0.304	0.316	0.013	0.297	0.108	0.002	1726	56	1768	62	1774	30	100	1744	94.25	0.35	0.556	91	94	0.969
ap19a09	6.517	0.192	0.359	0.011	0.499	0.121	0.001	2048	26	1975	50	1977	17	100	2047	51.96	2.85	0.091	61	117	0.523
ap16a63	14.502	0.274	0.526	0.009	0.479	0.188	0.002	2783	18	2724	40	2725	14	100	2784	35.78	2.84	0.092	117	139	0.844
ap16a66	5.208	0.090	0.333	0.004	0.368	0.113	0.001	1854	15	1855	21	1850	11	100	1854	27.65	0.00	0.961	195	431	0.452
ap19a07	5.513	0.189	0.330	0.011	0.467	0.112	0.001	1903	29	1838	51	1833	11	100	1897	58.67	2.02	0.155	223	424	0.525
ap19a06	6.576	0.137	0.366	0.008	0.507	0.122	0.001	2056	18	2011	37	1993	13	101	2056	36.81	2.02	0.155	138	246	0.561
ap19a38	7.873	0.221	0.404	0.009	0.418	0.135	0.001	2217	25	2188	44	2165	15	101	2213	49.90	0.52	0.470	119	144	0.827
ap19a05	5.681	0.181	0.338	0.010	0.458	0.113	0.001	1929	28	1877	48	1851	14	101	1924	54.70	1.49	0.223	109	219	0.500
ap19a35	13.574	0.501	0.522	0.018	0.462	0.182	0.001	2720	35	2706	75	2668	12	101	2720	69.78	0.05	0.832	190	134	1.419
ap19a31	5.594	0.110	0.340	0.006	0.440	0.114	0.001	1915	17	1887	28	1858	10	102	1912	33.52	1.18	0.278	639	437	1.462
ap16a42	1.023	0.024	0.115	0.002	0.373	0.062	0.001	715	12	704	12	691	20	102	709	19.72	0.71	0.399	358	1085	0.330
ap19a13	5.629	0.226	0.342	0.008	0.302	0.114	0.002	1921	35	1897	40	1858	25	102	1911	59.80	0.28	0.594	14	42	0.345
ap16a44	5.329	0.126	0.339	0.006	0.374	0.112	0.001	1873	20	1882	29	1840	14	102	1875	38.18	0.09	0.760	161	353	0.454
ap16a15	5.734	0.244	0.344	0.011	0.372	0.114	0.002	1936	37	1907	52	1863	24	102	1929	69.58	0.32	0.573	8	77	0.106
ap19a17	6.723	0.231	0.368	0.011	0.429	0.121	0.002	2076	30	2020	51	1969	22	103	2069	60.17	1.43	0.232	43	44	0.968
ap16a39	5.520	0.159	0.344	0.009	0.479	0.114	0.001	1904	25	1905	45	1856	17	103	1904	49.30	0.00	0.968	74	196	0.376
ap16a37	5.595	0.192	0.351	0.010	0.426	0.114	0.001	1915	30	1937	49	1866	13	104	1918	57.83	0.24	0.627	182	414	0.439
ap16a33	6.171	0.237	0.376	0.009	0.322	0.121	0.001	2000	34	2057	43	1973	19	104	2018	59.98	1.55	0.213	84	120	0.704
ap19a25	5.798	0.127	0.346	0.007	0.439	0.112	0.001	1946	19	1915	32	1832	14	105	1942	37.34	1.16	0.282	67	151	0.445
ap16a72	14.481	0.302	0.541	0.011	0.486	0.181	0.001	2782	20	2788	46	2660	13	105	2782	39.60	0.02	0.882	87	102	0.856
ap16a41	4.698	0.116	0.320	0.007	0.419	0.105	0.001	1767	21	1792	32	1707	17	105	1771	40.16	0.66	0.417	96	195	0.490
ap16a65	5.402	0.237	0.347	0.010	0.333	0.111	0.001	1885	38	1921	49	1822	19	105	1896	67.66	0.51	0.476	29	136	0.215
ap16a53	6.462	0.254	0.374	0.014	0.470	0.119	0.002	2041	35	2049	65	1935	26	106	2041	68.87	0.02	0.891	147	106	1.393
ap16a17	7.093	0.164	0.404	0.008	0.429	0.128	0.005	2123	21	2187	37	2065	67	106	2128	40.47	3.66	0.056	44	113	0.390
ap16a43	11.533	0.304	0.518	0.011	0.405	0.168	0.002	2567	25	2689	47	2535	22	106	2575	48.60	7.81	0.005	203	52	3.899
ap16a50	5.774	0.299	0.367	0.013	0.348	0.116	0.001	1943	45	2017	62	1896	22	106	1961	82.33	1.42	0.234	103	114	0.902
ap16a73	5.208	0.130	0.340	0.007	0.433	0.108	0.001	1854	21	1886	35	1769	11	107	1858	41.61	0.99	0.319	132	506	0.261
ap16a76	6.320	0.165	0.374	0.010	0.522	0.117	0.001	2021	23	2047	48	1912	16	107	2020	45.74	0.39	0.530	255	364	0.700
ap16a62	5.434	0.159	0.354	0.007	0.357	0.112	0.001	1890	25	1956	35	1827	20	107	1906	46.39	3.44	0.064	31	95	0.325
ap16a77	5.905	0.172	0.363	0.008	0.375	0.113	0.001	1962	25	1998	37	1845	15	108	1969	47.90	0.98	0.322	139	308	0.453
ap16a51	7.005	0.224	0.411	0.009	0.330	0.126	0.001	2112	28	2218	40	2038	18	109	2138	51.77	6.84	0.009	93	147	0.634
ap16a54	5.566	0.181	0.363	0.009	0.402	0.112	0.001	1911	28	1996	45	1825	15	109	1923	53.88	4.03	0.045	225	396	0.567
ap16a71	3.071	0.199	0.260	0.010	0.294	0.087	0.002	1425	50	1490	51	1362	39	109	1455	79.77	1.18	0.276	21	63	0.336
ap16a59	5.343	0.172	0.351	0.009	0.408	0.108	0.001	1876	28	1941	44	1768	12	110	1885	53.32	2.47	0.116	144	525	0.273
ap16a16	6.618	0.194	0.395	0.008	0.341	0.119	0.001	2062	26	2144	36	1935	16	111	2082	47.56	5.01	0.025	115	196	0.587
ap16a64	7.137	0.157	0.414	0.007	0.365	0.121	0.001	2129	20	2231	30	1975	14	113	2147	37.06	12.01	0.001	151	249	0.606
ap16a74	2.681	0.196	0.240	0.011	0.313	0.081	0.001	1323	54	1387	57	1224	28	113	1351	89.05	0.96	0.328	55	133	0.409
ap16a49	6.585	0.205	0.402	0.010	0.419	0.118	0.001	2057	27	2177	48	1919	20	113	2068	53.68	7.13	0.008	180	145	1.243

APPENDIX B - DETRITAL ZIRCON ANALYSES, continued

Table B4, *continued*. Detrital zircon U-Pb geochronologic analyses from sample **09LP094** from the undivided Vampire-Narchilla unit (PЄVN) - Memorial University

File Name	Measured Isotopic Ratios							Calculated Ages (Ma)							Th232 (ppm)	U238 (ppm)	Th/U (ratio)				
	$\frac{^{207}\text{Pb}}{^{235}\text{U}}$	1 $\sigma$ error	$\frac{^{206}\text{Pb}}{^{238}\text{U}}$	1 $\sigma$ error	Rho	$\frac{^{207}\text{Pb}}{^{206}\text{Pb}}$	1 $\sigma$ error	$\frac{^{207}\text{Pb}}{^{235}\text{U}}$	1 $\sigma$ error (Ma)	$\frac{^{206}\text{Pb}}{^{238}\text{U}}$	1 $\sigma$ error (Ma)	$\frac{^{207}\text{Pb}}{^{206}\text{Pb}}$	1 $\sigma$ error (Ma)	U-Pb/Pb-Pb concordancy (%)				Concordia age (Ma)	2 $\sigma$ error (Ma)	MSWD (of concordance)	Probability
ap19a08	0.722	0.033	0.091	0.003	0.310	0.057	0.001	552	19	563	15	494	24	114	559	27.30	0.31	0.581	1098	489	2.245
ap16a06	12.459	0.483	0.543	0.020	0.471	0.155	0.002	2640	36	2797	83	2405	20	116	2636	73.09	4.49	0.034	30	80	0.371
ap16a18	6.811	0.493	0.405	0.025	0.423	0.112	0.002	2087	64	2193	114	1825	31	120	2096	125.90	1.01	0.314	20	67	0.291

APPENDIX B - DETRITAL ZIRCON ANALYSES, continued

Table B5a. Detrital zircon U-Pb geochronologic analyses from sample 09TOA095 from the Sekwi correlative unit (Cs) - Isotope Geology Laboratory, Boise State University

Analysis	U (ppm)	Th (ppm)	Pb* (ppm)	Th/U	Corrected isotope ratios								Apparent ages (ma)						% disc.				
					$\frac{206\text{Pb}^*}{207\text{Pb}^*}$	±2σ (%)	$\frac{207\text{Pb}^*}{235\text{U}^*}$	±2σ (%)	$\frac{206\text{Pb}^*}{238\text{U}}$	±2σ (%)	error corr.	$\frac{238\text{U}}{206\text{Pb}^*}$	±2σ (%)	$\frac{207\text{Pb}^*}{206\text{Pb}^*}$	±2σ (%)	error corr.	$\frac{207\text{Pb}^*}{206\text{Pb}^*}$	±2σ (Ma)		$\frac{207\text{Pb}^*}{235\text{U}}$	±2σ (Ma)	$\frac{206\text{Pb}^*}{238\text{U}^*}$	±2σ (Ma)
09TOA095 M 264	106.98	70.97	128.86	0.66	2.844	1.894	37.901	4.505	0.782	4.087	0.907	1.279	4.087	0.352	1.894	0.0	3714	29	3717	45	3724	116	-0
09TOA095 M 253	320.43	203.85	236.74	0.64	4.031	2.177	17.984	9.998	0.526	9.758	0.976	1.902	9.758	0.248	2.177	0.0	3172	35	2989	96	2724	217	14
09TOA095 M 299	203.40	255.43	148.86	1.26	4.954	1.534	13.550	5.850	0.487	5.646	0.965	2.054	5.646	0.202	1.534	0	2841	25	2719	55	2557	119	10
09TOA095 M 319	44.73	27.15	35.85	0.61	5.142	2.817	15.164	5.827	0.566	5.101	0.875	1.768	5.101	0.194	2.817	0.0	2780	46	2826	56	2889	119	-4
09TOA095 M 278	151.04	165.29	128.73	1.09	5.273	2.184	14.294	5.458	0.547	5.002	0.916	1.829	5.002	0.190	2.184	-0.0	2739	36	2769	52	2811	114	-3
09TOA095 M 306	114.19	28.11	74.38	0.25	5.382	2.803	13.128	7.717	0.512	7.190	0.932	1.951	7.190	0.186	2.803	-0.0	2705	46	2689	73	2667	157	1
09TOA095 M 303	60.88	66.16	51.45	1.09	5.383	3.936	14.200	8.849	0.554	7.925	0.896	1.804	7.925	0.186	3.936	0	2705	65	2763	84	2843	182	-5
09TOA095 M 251	132.27	74.99	98.19	0.57	5.429	2.287	13.799	5.516	0.543	5.020	0.910	1.840	5.020	0.184	2.287	-0.0	2691	38	2736	52	2798	114	-4
09TOA095 M 225	208.36	93.02	137.13	0.45	5.446	2.498	12.312	6.873	0.486	6.403	0.932	2.056	6.403	0.184	2.498	-0.0	2686	41	2629	65	2555	135	5
09TOA095 M 281	202.29	135.12	134.15	0.67	5.536	2.217	11.615	3.966	0.466	3.288	0.829	2.144	3.288	0.181	2.217	0	2659	37	2574	37	2467	67	7
09TOA095 M 231	22.50	23.71	16.45	1.05	5.618	4.168	11.946	8.586	0.487	7.506	0.874	2.054	7.506	0.178	4.168	0	2634	69	2600	80	2557	158	3
09TOA095 M 271	117.74	75.79	82.81	0.64	5.638	2.459	12.312	5.144	0.503	4.518	0.878	1.986	4.518	0.177	2.459	0.0	2628	41	2628	48	2628	98	-0
09TOA095 M 243	131.55	97.42	94.87	0.74	5.675	1.860	12.054	4.316	0.496	3.895	0.902	2.016	3.895	0.176	1.860	0	2617	31	2609	40	2597	83	1
09TOA095 M 267	70.10	72.77	58.77	1.04	5.693	1.935	13.248	5.155	0.547	4.778	0.927	1.828	4.778	0.176	1.935	0	2612	32	2697	49	2813	109	-8
09TOA095 M 247	151.22	82.61	101.02	0.55	5.711	1.758	11.781	4.594	0.488	4.245	0.924	2.049	4.245	0.175	1.758	0.0	2607	29	2587	43	2562	90	2
09TOA095 M 239	97.28	96.63	76.53	0.99	5.722	2.329	12.217	4.941	0.507	4.358	0.882	1.972	4.358	0.175	2.329	0	2604	39	2621	46	2644	95	-2
09TOA095 M 316	54.66	46.54	41.38	0.85	5.799	2.094	12.303	4.570	0.517	4.062	0.889	1.933	4.062	0.172	2.094	0	2581	35	2628	43	2688	89	-4
09TOA095 M 229	74.84	29.53	48.93	0.39	5.865	3.036	11.700	6.299	0.498	5.520	0.876	2.009	5.520	0.171	3.036	0	2563	51	2581	59	2604	118	-2
09TOA095 M 245	165.49	55.89	100.96	0.34	5.968	2.245	10.886	4.655	0.471	4.078	0.876	2.122	4.078	0.168	2.245	0	2533	38	2513	43	2489	84	2
09TOA095 M 259	145.37	38.57	78.96	0.27	6.100	2.220	9.902	4.710	0.438	4.154	0.882	2.283	4.154	0.164	2.220	0.0	2497	37	2426	43	2342	82	6
09TOA095 M 322	265.83	77.04	152.28	0.29	6.320	1.946	9.896	5.393	0.454	5.030	0.933	2.204	5.030	0.158	1.946	0	2437	33	2425	50	2411	101	1
09TOA095 M 270	225.34	52.57	125.00	0.23	6.547	1.892	9.463	4.356	0.449	3.924	0.901	2.225	3.924	0.153	1.892	0.0	2377	32	2384	40	2392	78	-1
09TOA095 M 230	125.25	118.55	81.01	0.95	6.687	2.788	8.954	6.587	0.434	5.968	0.906	2.303	5.968	0.150	2.788	-0.0	2341	48	2333	60	2325	116	1
09TOA095 M 246	41.46	20.80	21.47	0.50	7.582	2.926	7.134	6.252	0.392	5.525	0.884	2.549	5.525	0.132	2.926	-0.0	2123	51	2128	56	2133	100	-0
09TOA095 M 295	98.70	41.78	49.24	0.42	7.648	2.347	7.062	5.245	0.392	4.690	0.894	2.553	4.690	0.131	2.347	-0.0	2108	41	2119	47	2131	85	-1
09TOA095 M 226	197.81	151.95	105.49	0.77	7.714	3.066	6.721	6.561	0.376	5.800	0.884	2.659	5.800	0.130	3.066	-0.0	2093	54	2075	58	2058	102	2
09TOA095 M 304	188.21	112.91	74.70	0.60	7.854	2.697	5.381	6.249	0.307	5.637	0.902	3.262	5.637	0.127	2.697	-0.0	2061	48	1882	54	1724	85	16
09TOA095 M 327	201.77	113.61	104.01	0.56	7.867	2.373	6.839	4.086	0.390	3.326	0.814	2.563	3.326	0.127	2.373	0	2058	42	2091	36	2124	60	-3
09TOA095 M 282	155.99	37.64	72.53	0.24	7.994	2.470	6.419	4.849	0.372	4.173	0.861	2.687	4.173	0.125	2.470	0.0	2030	44	2035	43	2039	73	-0
09TOA095 M 261	217.50	326.17	94.58	1.50	8.107	2.097	4.805	9.594	0.283	9.362	0.976	3.539	9.362	0.123	2.097	-0.0	2005	37	1786	81	1604	133	20
09TOA095 M 274	240.15	210.46	103.06	0.88	8.213	2.105	5.463	7.520	0.325	7.220	0.960	3.073	7.220	0.122	2.105	0.0	1982	37	1895	65	1816	114	8
09TOA095 M 296	129.77	111.66	66.76	0.86	8.267	2.469	6.044	5.680	0.362	5.116	0.901	2.759	5.116	0.121	2.469	-0.0	1970	44	1982	49	1994	88	-1
09TOA095 M 309	136.49	42.25	58.51	0.31	8.282	2.397	5.838	7.471	0.351	7.076	0.947	2.852	7.076	0.121	2.397	0	1967	43	1952	65	1938	118	1
09TOA095 M 308	184.65	53.41	78.81	0.29	8.357	2.310	5.700	4.821	0.345	4.231	0.878	2.895	4.231	0.120	2.310	-0.0	1951	41	1931	42	1913	70	2
09TOA095 M 273	139.83	105.94	69.91	0.76	8.475	2.562	5.932	5.707	0.365	5.100	0.894	2.743	5.100	0.118	2.562	0.0	1926	46	1966	50	2004	88	-4
09TOA095 M 250	287.07	244.97	142.12	0.85	8.557	1.953	5.634	3.912	0.350	3.389	0.866	2.860	3.389	0.117	1.953	-0.0	1909	35	1921	34	1933	57	-1
09TOA095 M 265	131.77	179.83	68.05	1.36	8.588	2.065	5.410	5.469	0.337	5.064	0.926	2.968	5.064	0.116	2.065	-0.0	1902	37	1886	47	1872	82	2
09TOA095 M 293	171.95	63.87	71.52	0.37	8.596	2.497	5.358	6.056	0.334	5.517	0.911	2.994	5.517	0.116	2.497	0	1901	45	1878	52	1858	89	2
09TOA095 M 266	139.70	127.23	65.71	0.91	8.714	2.133	5.249	5.755	0.332	5.345	0.929	3.014	5.345	0.115	2.133	0.0	1876	38	1861	49	1847	86	2
09TOA095 M 321	74.90	43.84	36.39	0.59	8.731	2.928	5.779	5.250	0.366	4.357	0.830	2.733	4.357	0.115	2.928	0	1873	53	1943	45	2010	75	-7
09TOA095 M 238	215.79	76.40	91.22	0.35	8.752	2.330	5.284	5.234	0.335	4.686	0.895	2.982	4.686	0.114	2.330	0	1868	42	1866	45	1864	76	0
09TOA095 M 297	277.64	190.12	105.66	0.68	8.782	2.075	4.698	5.844	0.299	5.464	0.935	3.342	5.464	0.114	2.075	-0.0	1862	37	1767	49	1687	81	9

APPENDIX B - DETRITAL ZIRCON ANALYSES, continued

Table B5a, continued. Detrital zircon U-Pb geochronologic analyses from sample 09TOA095 from the Sekwi correlative unit (Єs) - Isotope Geology Laboratory, Boise State University

Analysis	U (ppm)	Th (ppm)	Pb* (ppm)	Th/U	Corrected isotope ratios							Apparent ages (ma)						% disc.					
					$\frac{206\text{Pb}^*}{207\text{Pb}^*}$	±2σ (%)	$\frac{207\text{Pb}^*}{235\text{U}^*}$	±2σ (%)	$\frac{206\text{Pb}^*}{238\text{U}}$	±2σ (%)	error corr.	$\frac{238\text{U}}{206\text{Pb}^*}$	±2σ (%)	$\frac{207\text{Pb}^*}{206\text{Pb}^*}$	±2σ (%)	error corr.	$\frac{207\text{Pb}^*}{206\text{Pb}^*}$		±2σ (Ma)	$\frac{207\text{Pb}^*}{235\text{U}^*}$	±2σ (Ma)	$\frac{206\text{Pb}^*}{238\text{U}^*}$	±2σ (Ma)
09TOA095 M 324	273.93	137.32	118.20	0.50	8.854	2.256	5.205	4.764	0.334	4.196	0.881	2.992	4.196	0.113	2.256	0	1847	41	1853	41	1859	68	-1
09TOA095 M 320	172.94	85.80	70.89	0.50	8.890	2.930	5.000	6.462	0.322	5.760	0.891	3.102	5.760	0.112	2.930	0.0	1840	53	1819	55	1801	91	2
09TOA095 M 254	116.38	83.96	51.87	0.72	8.908	2.443	5.113	4.546	0.330	3.833	0.843	3.027	3.833	0.112	2.443	0	1836	44	1838	39	1840	61	-0
09TOA095 M 317	33.03	61.42	20.68	1.86	8.916	3.362	5.542	5.803	0.358	4.729	0.815	2.790	4.729	0.112	3.362	-0.0	1835	61	1907	50	1975	80	-8
09TOA095 M 241	143.60	371.42	64.43	2.59	8.952	3.058	4.646	6.857	0.302	6.138	0.895	3.315	6.138	0.112	3.058	-0.0	1827	55	1757	57	1699	92	7
09TOA095 M 272	113.61	102.08	49.13	0.90	8.987	3.276	4.743	5.320	0.309	4.191	0.788	3.235	4.191	0.111	3.276	0.0	1820	59	1775	45	1737	64	5
09TOA095 M 236	174.57	62.50	70.04	0.36	9.139	2.622	4.877	6.030	0.323	5.430	0.900	3.093	5.430	0.109	2.622	0	1790	48	1798	51	1806	86	-1
09TOA095 M 288	14.28	25.93	8.09	1.82	9.162	6.630	4.914	10.097	0.327	7.615	0.754	3.062	7.615	0.109	6.630	0	1785	121	1805	85	1822	121	-2
09TOA095 M 269	62.52	45.77	28.68	0.73	9.272	3.544	4.946	5.543	0.333	4.261	0.769	3.006	4.261	0.108	3.544	-0.0	1763	65	1810	47	1851	69	-5
09TOA095 M 314	148.49	125.92	61.49	0.85	9.615	2.667	4.196	5.903	0.293	5.266	0.892	3.417	5.266	0.104	2.667	0	1697	49	1673	48	1655	77	2
09TOA095 M 328	112.50	106.16	47.98	0.94	9.827	2.572	4.151	6.609	0.296	6.088	0.921	3.380	6.088	0.102	2.572	-0.0	1656	48	1664	54	1671	90	-1
09TOA095 M 257	122.25	89.03	43.88	0.73	10.108	2.559	3.639	4.670	0.267	3.907	0.837	3.748	3.907	0.099	2.559	0.0	1604	48	1558	37	1525	53	5
09TOA095 M 235	22.96	21.64	9.25	0.94	10.353	7.090	3.641	8.930	0.273	5.430	0.608	3.658	5.430	0.097	7.090	0.0	1559	133	1559	71	1558	75	0
09TOA095 M 291	265.45	136.19	86.67	0.51	10.394	2.469	3.381	5.024	0.255	4.375	0.871	3.923	4.375	0.096	2.469	0	1552	46	1500	39	1464	57	6
09TOA095 M 313	74.56	101.97	34.08	1.37	10.406	3.067	3.875	5.627	0.292	4.717	0.838	3.419	4.717	0.096	3.067	-0.0	1550	58	1609	45	1654	69	-7
09TOA095 M 233	86.09	77.02	33.31	0.89	10.545	3.109	3.526	7.896	0.270	7.258	0.919	3.708	7.258	0.095	3.109	-0.0	1525	59	1533	62	1539	99	-1
09TOA095 M 222	195.19	73.50	62.33	0.38	10.695	2.457	3.313	5.517	0.257	4.940	0.895	3.891	4.940	0.094	2.457	0	1498	46	1484	43	1474	65	2
09TOA095 M 256	229.90	78.47	69.22	0.34	10.734	2.007	3.206	4.388	0.250	3.902	0.889	4.007	3.902	0.093	2.007	0.0	1491	38	1459	34	1436	50	4
09TOA095 M 326	54.55	22.45	17.13	0.41	10.889	4.403	3.178	6.437	0.251	4.696	0.730	3.984	4.696	0.092	4.403	0.0	1464	84	1452	50	1444	61	1
09TOA095 M 276	160.75	53.81	51.89	0.33	10.926	2.309	3.363	5.773	0.266	5.291	0.917	3.753	5.291	0.092	2.309	0	1458	44	1496	45	1523	72	-4
09TOA095 M 221	258.01	77.66	78.05	0.30	10.927	2.457	3.158	5.796	0.250	5.250	0.906	3.995	5.250	0.092	2.457	0	1457	47	1447	45	1440	68	1
09TOA095 M 223	89.18	51.73	28.01	0.58	10.976	2.626	3.012	6.604	0.240	6.059	0.918	4.171	6.059	0.091	2.626	0.0	1449	50	1411	50	1385	76	4
09TOA095 M 302	66.84	38.11	21.90	0.57	10.989	3.950	3.208	7.113	0.256	5.916	0.832	3.911	5.916	0.091	3.950	-0.0	1447	75	1459	55	1468	78	-1
09TOA095 M 307	276.78	88.10	85.45	0.32	11.007	2.549	3.211	5.790	0.256	5.199	0.898	3.901	5.199	0.091	2.549	-0.0	1443	49	1460	45	1471	68	-2
09TOA095 M 286	92.04	42.98	33.70	0.47	11.040	3.034	3.618	6.339	0.290	5.566	0.878	3.451	5.566	0.091	3.034	-0.0	1438	58	1554	50	1640	81	-14
09TOA095 M 310	123.25	71.05	40.53	0.58	11.100	2.129	3.176	5.848	0.256	5.447	0.931	3.911	5.447	0.090	2.129	-0.0	1427	41	1451	45	1468	72	-3
09TOA095 M 298	178.14	32.78	53.11	0.18	11.169	2.359	3.191	5.743	0.258	5.236	0.912	3.869	5.236	0.090	2.359	0.0	1416	45	1455	44	1482	69	-5
09TOA095 M 284	63.41	44.98	21.69	0.71	11.172	5.079	3.133	6.863	0.254	4.616	0.673	3.939	4.616	0.090	5.079	0.0	1415	97	1441	53	1458	60	-3
09TOA095 M 292	131.05	48.61	38.18	0.37	11.173	2.677	2.934	4.746	0.238	3.919	0.826	4.206	3.919	0.090	2.677	0.0	1415	51	1391	36	1375	49	3
09TOA095 M 277	165.79	54.90	50.72	0.33	11.234	2.389	3.100	4.579	0.253	3.906	0.853	3.960	3.906	0.089	2.389	0	1405	46	1433	35	1452	51	-3
09TOA095 M 287	121.52	60.91	37.38	0.50	11.291	3.649	2.957	6.759	0.242	5.690	0.842	4.130	5.690	0.089	3.649	-0.0	1395	70	1397	51	1398	72	-0
09TOA095 M 242	211.14	65.47	61.22	0.31	11.371	2.609	2.894	6.229	0.239	5.657	0.908	4.191	5.657	0.088	2.609	0	1381	50	1380	47	1380	70	0
09TOA095 M 258	156.45	63.52	45.22	0.41	11.595	2.563	2.833	5.458	0.238	4.818	0.883	4.197	4.818	0.086	2.563	-0.0	1344	50	1364	41	1378	60	-3
09TOA095 M 325	196.54	157.67	60.40	0.80	11.929	2.491	2.558	4.897	0.221	4.216	0.861	4.518	4.216	0.084	2.491	0	1289	48	1289	36	1289	49	-0
09TOA095 M 294	186.75	68.89	57.80	0.37	11.948	2.643	2.943	6.293	0.255	5.711	0.908	3.921	5.711	0.084	2.643	-0.0	1285	51	1393	48	1464	75	-14
09TOA095 M 285	124.13	49.80	36.10	0.40	11.999	3.588	2.710	6.719	0.236	5.680	0.845	4.240	5.680	0.083	3.588	-0.0	1277	70	1331	50	1365	70	-7
09TOA095 M 279	47.81	28.57	15.26	0.60	12.124	4.550	2.779	7.191	0.244	5.568	0.774	4.093	5.568	0.082	4.550	0	1257	89	1350	54	1409	70	-12
09TOA095 M 260	471.83	42.60	107.14	0.09	12.219	2.369	2.286	6.228	0.203	5.760	0.925	4.936	5.760	0.082	2.369	-0.0	1242	46	1208	44	1189	63	4
09TOA095 M 244	290.80	173.23	66.96	0.60	12.233	2.908	2.005	5.012	0.178	4.083	0.815	5.622	4.083	0.082	2.908	0.0	1239	57	1117	34	1055	40	15
09TOA095 M 290	65.88	20.21	17.99	0.31	12.265	4.079	2.592	7.623	0.231	6.440	0.845	4.337	6.440	0.082	4.079	-0.0	1234	80	1298	56	1337	78	-8
09TOA095 M 311	111.53	60.89	29.74	0.55	12.422	3.775	2.363	6.442	0.213	5.220	0.810	4.698	5.220	0.080	3.775	0.0	1209	74	1231	46	1244	59	-3
09TOA095 M 280	113.23	49.37	28.65	0.44	12.485	3.183	2.248	6.002	0.204	5.088	0.848	4.913	5.088	0.080	3.183	0.0	1199	63	1196	42	1194	55	0

APPENDIX B - DETRITAL ZIRCON ANALYSES, continued

Table B5a, *continued*. Detrital zircon U-Pb geochronologic analyses from sample **09TOA095** from the Sekwi correlative unit (Єs) - Isotope Geology Laboratory, Boise State University

Analysis	U (ppm)	Th (ppm)	Pb* (ppm)	Th/U	Corrected isotope ratios							Apparent ages (ma)						% disc.					
					$\frac{^{206}\text{Pb}^*}{^{207}\text{Pb}^*}$	$\pm 2\sigma$ (%)	$\frac{^{207}\text{Pb}^*}{^{235}\text{U}^*}$	$\pm 2\sigma$ (%)	$\frac{^{206}\text{Pb}^*}{^{238}\text{U}}$	$\pm 2\sigma$ (%)	error corr.	$\frac{^{238}\text{U}}{^{206}\text{Pb}^*}$	$\pm 2\sigma$ (%)	$\frac{^{207}\text{Pb}^*}{^{206}\text{Pb}^*}$	$\pm 2\sigma$ (%)	error corr.	$\frac{^{207}\text{Pb}^*}{^{206}\text{Pb}^*}$		$\pm 2\sigma$ (Ma)	$\frac{^{207}\text{Pb}^*}{^{235}\text{U}}$	$\pm 2\sigma$ (Ma)	$\frac{^{206}\text{Pb}^*}{^{238}\text{U}^*}$	$\pm 2\sigma$ (Ma)
09TOA095 M 224	98.85	173.17	33.70	1.75	12.510	2.836	2.124	7.273	0.193	6.698	0.921	5.190	6.698	0.080	2.836	0	1195	56	1156	50	1136	70	5
09TOA095 M 234	190.39	76.31	46.73	0.40	12.673	2.913	2.150	6.324	0.198	5.614	0.888	5.061	5.614	0.079	2.913	-0.0	1170	58	1165	44	1162	60	1
09TOA095 M 248	124.78	100.67	30.58	0.81	12.888	3.649	1.891	6.150	0.177	4.951	0.805	5.658	4.951	0.078	3.649	-0.0	1136	73	1078	41	1049	48	8
09TOA095 M 275	126.78	110.51	36.26	0.87	12.913	3.093	2.219	5.726	0.208	4.818	0.842	4.812	4.818	0.077	3.093	-0.0	1133	62	1187	40	1217	53	-7
09TOA095 M 237	154.58	43.22	36.67	0.28	13.033	2.662	2.114	4.527	0.200	3.662	0.809	5.005	3.662	0.077	2.662	-0.0	1114	53	1153	31	1174	39	-5
09TOA095 M 227	299.32	146.95	68.59	0.49	13.064	2.619	1.899	5.085	0.180	4.358	0.857	5.557	4.358	0.077	2.619	0	1109	52	1081	34	1067	43	4
09TOA095 M 312	194.61	104.02	45.13	0.53	13.093	2.613	1.921	5.838	0.182	5.221	0.894	5.482	5.221	0.076	2.613	-0.0	1105	52	1088	39	1080	52	2
09TOA095 M 300	179.73	107.26	42.18	0.60	13.152	4.049	1.897	7.888	0.181	6.769	0.858	5.526	6.769	0.076	4.049	0.0	1096	81	1080	52	1072	67	2
09TOA095 M 232	108.87	85.84	27.79	0.79	13.163	3.830	1.928	6.805	0.184	5.625	0.827	5.433	5.625	0.076	3.830	0	1094	77	1091	46	1089	56	0
09TOA095 M 255	153.49	159.52	35.91	1.04	13.176	4.053	1.781	7.706	0.170	6.554	0.851	5.877	6.554	0.076	4.053	0.0	1092	81	1038	50	1013	61	7
09TOA095 M 305	57.22	27.59	13.17	0.48	13.199	4.321	1.918	6.764	0.184	5.204	0.769	5.447	5.204	0.076	4.321	0.0	1089	87	1087	45	1087	52	0
09TOA095 M 323	177.66	23.94	39.11	0.13	13.209	2.530	2.036	4.928	0.195	4.229	0.858	5.127	4.229	0.076	2.530	-0.0	1087	51	1128	34	1149	45	-6
09TOA095 M 240	150.72	95.90	37.75	0.64	13.346	3.503	1.958	7.169	0.190	6.254	0.872	5.275	6.254	0.075	3.503	-0.0	1067	70	1101	48	1119	64	-5
09TOA095 M 283	228.98	65.58	53.64	0.29	13.518	3.275	2.023	7.123	0.198	6.325	0.888	5.043	6.325	0.074	3.275	-0.0	1041	66	1123	48	1166	67	-12
09TOA095 M 228	41.40	19.17	10.09	0.46	13.538	3.466	1.978	9.477	0.194	8.821	0.931	5.149	8.821	0.074	3.466	-0.0	1038	70	1108	64	1144	92	-10
09TOA095 M 262	89.69	46.04	18.70	0.51	13.747	4.356	1.682	6.745	0.168	5.150	0.763	5.962	5.150	0.073	4.356	0.0	1007	88	1002	43	1000	48	1
09TOA095 M 263	67.91	41.50	15.36	0.61	13.892	6.535	1.786	8.006	0.180	4.624	0.578	5.558	4.624	0.072	6.535	-0.0	985	133	1040	52	1067	45	-8

Notes:

Yellow highlighted rows are samples that intersected inclusions.  
 Isotope ratios and ages are NOT corrected for initial common Pb.  
 Isotope ratio and apparent age errors include systematic calibration errors of 5.88531041610563% ( $^{208}\text{Pb}/^{232}\text{Th}$ ), 0.384628088162782% ( $^{207}\text{Pb}/^{206}\text{Pb}$ ), 0.857953833283302% ( $^{206}\text{Pb}/^{238}\text{U}$ ) (all 1-sigma).  
 Trace element concentrations in ppm, calculated using mean count rate method.  
 Sweep-by-sweep downhole fractionation of U/Pb ratios NOT corrected via Si/Zr fractionation factor.  
 Backgrounds were monitored during sweeps 10 to 27. Sample counts were integrated from sweeps 36 to 69.  
 Ablation used a laser spot size of 25 microns, and a laser firing repetition rate of 10 Hz.





APPENDIX B - DETRITAL ZIRCON ANALYSES, continued

Table B5b, continued. Detrital zircon trace element analyses from sample 09TOA095 from the Sekwi correlative unit (Cs) - Isotope Geology Laboratory, Boise State University

Analysis	Concentrations (ppm)																						
	P	Ti	Y	Zr	Nb	La	Ce	Pr	Nd	Sm	Eu	Gd	Tb	Dy	Ho	Er	Tm	Yb	Lu	Hf	Ta	Th	U
09TOA095 M 248	410.647	21.741	1097.821	461554.927	3.147	3.491	33.043	0.841	6.998	7.569	1.372	27.743	9.624	107.772	40.906	169.328	47.025	544.078	59.101	6640.021	1.678	100.674	124.779
09TOA095 M 275	314.837	19.734	751.459	444615.299	3.472	0.040	34.213	0.007	1.267	3.687	0.888	17.752	6.133	74.724	28.895	126.328	33.684	401.639	42.005	7882.190	2.165	110.509	126.779
09TOA095 M 237	167.675	9.501	443.784	448561.080	3.652		6.425		0.837	1.581	0.090	7.969	3.484	45.362	16.390	71.446	21.216	241.439	23.681	7318.088	2.016	43.218	154.585
09TOA095 M 227	196.056	6.640	641.220	440453.022	8.530	0.023	10.979	0.184	3.159	6.453	0.572	23.671	7.469	83.642	25.881	90.063	21.422	230.441	22.213	7049.503	3.019	146.953	299.318
09TOA095 M 312	595.243	16.396	1155.422	449333.440	0.635	0.067	2.393	0.194	4.539	9.690	0.059	41.817	13.177	145.163	45.216	171.073	44.832	485.087	45.409	7667.136	0.359	104.016	194.612
09TOA095 M 300	220.003	13.697	583.967	474911.701	5.739	0.427	35.112	0.200	1.247	2.473	0.429	10.666	4.418	58.843	21.590	97.137	27.632	313.178	34.193	8328.287	3.321	107.258	179.733
09TOA095 M 232	197.082	25.551	609.886	480440.259	2.908	0.087	41.281	0.123	2.264	4.371	1.300	22.197	6.642	74.514	22.634	92.990	24.068	254.770	24.909	6771.026	1.637	85.841	108.866
09TOA095 M 255	646.082	38.988	1705.622	479373.024	6.874	15.535	45.575	5.665	31.648	14.794	1.638	54.000	18.066	200.984	67.530	278.508	68.153	688.050	74.284	6527.157	2.863	159.518	153.494
09TOA095 M 305	233.532	19.765	776.951	474346.196	1.699	0.035	2.648	0.064	1.435	4.544	0.223	23.731	7.767	92.790	30.894	120.090	27.758	293.389	28.411	7987.117	0.777	27.589	57.217
09TOA095 M 323	804.902	8.891	1578.501	446417.088	0.250		0.500	0.087	0.749	4.025	0.035	35.093	13.422	173.449	61.502	257.721	64.156	703.206	64.228	7994.335	0.259	23.942	177.663
09TOA095 M 240	222.733	9.226	650.382	425383.832	4.504		31.333	0.073	1.300	2.237	0.384	11.943	4.668	64.710	24.694	107.079	29.899	368.333	39.003	7404.489	2.083	95.895	150.716
09TOA095 M 283	145.727	5.249	586.486	473355.239	2.082		13.164	0.004	1.186	2.292	0.120	18.235	5.821	66.885	22.454	90.749	22.699	243.216	24.016	7895.578	1.195	65.580	228.984
09TOA095 M 228	177.241	20.748	331.119	455893.791	2.027		14.141	0.026	1.585	2.464	0.934	11.326	3.289	41.099	12.231	50.251	12.771	158.740	15.457	6626.069	0.665	19.169	41.400
09TOA095 M 262	191.258	11.144	619.683	508125.834	4.567	0.009	17.092	0.062	1.160	3.306	0.220	14.972	5.200	65.315	22.348	96.284	25.772	280.117	31.484	8278.753	2.039	46.039	89.686
09TOA095 M 263	328.200	31.226	865.774	524849.737	0.779		2.329	0.084	2.767	6.374	0.391	27.554	9.490	103.305	32.903	132.152	34.210	346.083	36.558	8677.677	0.420	41.498	67.911

Notes:

Yellow highlighted rows are samples that intersected inclusions.

Trace element concentrations in ppm, calculated using mean count rate method.

Sweep-by-sweep downhole fractionation of U/Pb ratios NOT corrected via Si/Zr fractionation factor.

Backgrounds were monitored between sweeps 10 to 27. Sample counts were integrated from sweeps 36 to 69.

Ablation used a laser spot size of 25 microns, and a laser firing repetition rate of 10 Hz.





APPENDIX B - DETRITAL ZIRCON ANALYSES, continued

Table B5c, *continued*. Detrital zircon calculated ratios and values from sample **09TOA095** from the Sekwi correlative unit (Єs) - Isotope Geology Laboratory, Boise State University

Analysis	CI chondrite normalizing values from Sun and McDonough (1989)														Ti-in-zircon T (°C)	Ce/Ce*	Eu/Eu*	(Sm/Nd) <sub>cn</sub>	(Lu/Nd) <sub>cn</sub>	Lu/Hf	Nb/Ta	Nb/U	Th/U	Th/Y	Y/Hf
	0.237	0.612	0.095	0.467	0.153	0.058	0.206	0.037	0.254	0.057	0.166	0.026	0.17	0.025											
	La	Ce	Pr	Nd	Sm	Eu	Gd	Tb	Dy	Ho	Er	Tm	Yb	Lu											
09TOA095 M 224	0.232	68.836	1.971	9.047	43.204	33.031	71.278	97.453	119.167	149.972	183.474	299.274	502.812	336.959	855	62.51	0.58	4.78	37.25	0.00	2.31	0.01	1.75	0.73	0.03
09TOA095 M 234	0.015	31.308	0.600	1.630	19.537	2.737	61.577	144.590	276.496	440.188	605.569	1077.929	1941.825	1270.692	806	101.85	0.07	11.99	779.72	0.00	2.18	0.02	0.40	0.12	0.08
09TOA095 M 248	14.731	53.991	8.853	14.985	49.468	23.661	135.004	257.314	424.298	722.715	1023.127	1844.117	3200.461	2326.821	883	4.58	0.26	3.30	155.27	0.01	1.88	0.03	0.81	0.09	0.17
09TOA095 M 275	0.169	55.904	0.073	2.712	24.100	15.314	86.383	163.977	294.190	510.507	763.314	1320.941	2362.581	1653.751	872	461.89	0.28	8.89	609.73	0.01	1.60	0.03	0.87	0.15	0.10
09TOA095 M 237		10.498	0.401	1.793	10.332	1.554	38.777	93.144	178.589	289.575	431.698	831.982	1420.231	932.331	791		0.06	5.76	520.11	0.00	1.81	0.02	0.28	0.10	0.06
09TOA095 M 227	0.098	17.940	1.937	6.765	42.180	9.864	115.188	199.695	329.300	457.270	544.188	840.063	1355.533	874.546	756	17.63	0.13	6.23	129.27	0.00	2.83	0.03	0.49	0.23	0.09
09TOA095 M 312	0.282	3.909	2.044	9.720	63.335	1.023	203.491	352.320	571.508	798.864	1033.676	1758.124	2853.451	1787.744	850	3.36	0.01	6.52	183.93	0.01	1.77	0.00	0.53	0.09	0.15
09TOA095 M 300	1.801	57.372	2.106	2.671	16.161	7.392	51.902	118.132	231.666	381.440	586.933	1083.622	1842.222	1346.187	830	29.37	0.22	6.05	504.02	0.00	1.73	0.03	0.60	0.18	0.07
09TOA095 M 232	0.367	67.453	1.299	4.849	28.567	22.408	108.015	177.598	293.364	399.886	561.874	943.853	1498.649	980.666	903	81.02	0.33	5.89	202.26	0.00	1.78	0.03	0.79	0.14	0.09
09TOA095 M 255	65.548	74.468	59.632	67.768	96.690	28.237	262.773	483.061	791.278	1193.116	1682.827	2672.672	4047.353	2924.443	958	1.19	0.16	1.43	43.15	0.01	2.40	0.04	1.04	0.09	0.26
09TOA095 M 305	0.148	4.326	0.672	3.073	29.702	3.850	115.480	207.670	365.316	545.836	725.618	1088.565	1725.816	1118.555	872	10.56	0.05	9.67	364.03	0.00	2.19	0.03	0.48	0.04	0.10
09TOA095 M 323	0.023	0.817	0.914	1.603	26.308	0.607	170.769	358.883	682.869	1086.615	1557.225	2515.915	4136.504	2528.648	784	1.74	0.01	16.41	1577.42	0.01	0.96	0.00	0.13	0.02	0.20
09TOA095 M 240	0.019	51.197	0.769	2.785	14.618	6.624	58.117	124.814	254.764	436.294	647.004	1172.494	2166.663	1535.546	788	129.86	0.18	5.25	551.44	0.01	2.16	0.03	0.64	0.15	0.09
09TOA095 M 283	0.001	21.510	0.038	2.540	14.979	2.069	88.733	155.635	263.326	396.708	548.335	890.160	1430.681	945.493	733	1091.05	0.04	5.90	372.24	0.00	1.74	0.01	0.29	0.11	0.07
09TOA095 M 228	0.007	23.107	0.269	3.395	16.104	16.100	55.115	87.947	161.806	216.091	303.630	500.843	933.763	608.526	877	167.56	0.45	4.74	179.24	0.00	3.05	0.05	0.46	0.06	0.05
09TOA095 M 262	0.038	27.928	0.653	2.483	21.605	3.800	72.859	139.031	257.145	394.832	581.776	1010.682	1647.748	1239.528	808	80.88	0.08	8.70	499.18	0.00	2.24	0.05	0.51	0.07	0.07
09TOA095 M 263	0.022	3.806	0.884	5.925	41.658	6.735	134.084	253.746	406.714	581.323	798.504	1341.583	2035.782	1439.286	929	8.40	0.08	7.03	242.91	0.00	1.86	0.01	0.61	0.05	0.10

Notes:

Activity (SiO<sub>2</sub>) = 1; activity (TiO<sub>2</sub>) = 0.6.  
 Yellow highlighted rows are samples that intersected inclusions.  
 Trace element concentrations in ppm, calculated using mean count rate method.  
 Sweep-by-sweep downhole fractionation of U/Pb ratios NOT corrected via Si/Zr fractionation factor.  
 Backgrounds were monitored between sweeps 10 to 27. Sample counts were integrated from sweeps 36 to 69.  
 Ablation used a laser spot size of 25 microns, and a laser firing repetition rate of 10 Hz.

APPENDIX B - DETRITAL ZIRCON ANALYSES, continued

Table B6. Detrital zircon U-Pb geochronologic analyses from sample 09TOA096 from the Sekwi correlative unit (Es) - Memorial University

File Name	Measured Isotopic Ratios							Calculated Ages (Ma)							Concordia age (Ma)	2σ error (Ma)	MSWD (of concordance)	Probability	Th232 (ppm)	U238 (ppm)	Th/U Ratio
	$\frac{^{207}\text{Pb}}{^{235}\text{U}}$	2σ error	$\frac{^{206}\text{Pb}}{^{238}\text{U}}$	2σ error	Rho	$\frac{^{207}\text{Pb}}{^{206}\text{Pb}}$	1σ error	$\frac{^{207}\text{Pb}}{^{235}\text{U}}$	1σ error (Ma)	$\frac{^{206}\text{Pb}}{^{238}\text{U}}$	1σ error (Ma)	$\frac{^{207}\text{Pb}}{^{206}\text{Pb}}$	1σ error (Ma)	U-Pb/Pb-Pb concordancy (%)							
ap29b04	5.106	0.294	0.334	0.016	0.429	0.110	0.001	1837	24	1856	40	1807	21	103	1840	47.81	0.26	0.613	87	109	0.794
ap29b05	13.116	0.648	0.524	0.024	0.455	0.189	0.004	2688	23	2718	50	2736	34	99	2688	46.63	0.46	0.498	126	101	1.251
ap29b06	2.762	0.211	0.232	0.014	0.405	0.083	0.001	1345	29	1344	38	1279	28	105	1345	53.20	0.00	0.971	127	145	0.875
ap29b07	9.720	0.807	0.465	0.040	0.516	0.143	0.002	2409	38	2462	88	2267	26	109	2406	76.25	0.50	0.479	37	55	0.676
ap29b08	5.997	0.215	0.361	0.012	0.451	0.117	0.001	1975	16	1987	28	1910	11	104	1976	30.99	0.21	0.647	172	324	0.529
ap29b09	4.704	0.500	0.386	0.024	0.292	0.090	0.002	1768	45	2103	56	1427	33	147	1861	74.73	31.00	0.000	69	60	1.146
ap29b10	5.567	0.280	0.354	0.012	0.347	0.115	0.001	1911	22	1954	29	1882	18	104	1922	39.73	2.03	0.154	33	127	0.259
ap29b11	5.964	0.308	0.350	0.015	0.412	0.120	0.001	1971	22	1936	36	1949	12	99	1965	43.80	1.07	0.302	166	288	0.578
ap29b12	2.945	0.288	0.247	0.018	0.364	0.088	0.001	1394	37	1424	45	1382	25	103	1404	66.36	0.42	0.515	246	157	1.566
ap29b13	5.870	0.464	0.374	0.024	0.410	0.113	0.001	1957	34	2047	57	1844	21	111	1968	66.61	2.86	0.091	31	134	0.230
ap29b17	6.244	0.455	0.363	0.019	0.361	0.147	0.022	2011	32	1995	45	2315	257	86	2007	59.99	0.12	0.730	73	79	0.923
ap29b18	0.994	0.059	0.114	0.004	0.328	0.062	0.001	701	15	693	13	678	22	102	696	22.32	0.21	0.646	457	589	0.776
ap29b19	5.332	0.451	0.318	0.026	0.475	0.114	0.001	1874	36	1779	62	1864	23	95	1866	72.22	2.99	0.084	68	106	0.641
ap29b20	6.151	0.282	0.374	0.015	0.448	0.129	0.012	1997	20	2047	36	2087	164	98	2001	39.63	2.33	0.127	53	162	0.329
ap29b21	33.866	1.546	0.746	0.035	0.511	0.320	0.002	3606	23	3593	64	3568	11	101	3607	44.20	0.06	0.810	104	217	0.480
ap29b22	5.886	0.361	0.350	0.017	0.389	0.114	0.002	1959	27	1933	40	1863	24	104	1954	51.10	0.46	0.496	71	76	0.931
ap29b23	3.702	0.224	0.254	0.013	0.429	0.102	0.001	1572	24	1461	34	1656	17	88	1544	46.97	11.94	0.001	230	239	0.965
ap29b24	4.990	0.378	0.325	0.020	0.397	0.111	0.001	1818	32	1815	48	1822	15	100	1817	61.35	0.00	0.953	86	242	0.356
ap29b25	5.495	0.346	0.344	0.013	0.312	0.113	0.001	1900	27	1904	32	1846	23	103	1901	47.27	0.01	0.908	113	118	0.959
ap29b26	2.628	0.450	0.222	0.030	0.390	0.088	0.001	1309	63	1290	78	1373	17	94	1302	115.07	0.06	0.814	278	504	0.551
ap29b27	10.319	0.460	0.471	0.021	0.488	0.155	0.002	2464	21	2489	45	2398	17	104	2463	41.27	0.41	0.521	116	95	1.222
ap29b28	4.901	0.330	0.326	0.016	0.367	0.114	0.001	1802	28	1818	39	1864	20	98	1806	52.84	0.16	0.689	119	142	0.841
ap29b29	5.499	0.283	0.337	0.013	0.371	0.118	0.001	1900	22	1871	31	1919	16	97	1893	41.76	0.94	0.331	80	213	0.377
ap29b30	12.022	0.374	0.496	0.016	0.517	0.173	0.003	2606	15	2598	34	2591	32	100	2607	29.02	0.07	0.790	744	434	1.715
ap29b31	5.512	0.441	0.344	0.022	0.392	0.119	0.002	1903	34	1908	52	1943	30	98	1903	65.92	0.01	0.919	61	102	0.605
ap29b34	5.794	0.435	0.337	0.019	0.380	0.123	0.001	1946	33	1872	46	2003	21	93	1927	62.16	2.66	0.103	159	139	1.144
ap29b35	14.045	0.998	0.547	0.033	0.428	0.183	0.002	2753	34	2815	69	2683	14	105	2755	67.08	0.97	0.326	155	112	1.384
ap29b36	4.877	0.368	0.319	0.021	0.436	0.109	0.001	1798	32	1785	51	1787	14	100	1797	62.41	0.08	0.783	153	289	0.530
ap29b38	13.782	0.848	0.537	0.029	0.439	0.181	0.002	2735	29	2769	61	2659	19	104	2736	58.17	0.40	0.528	101	74	1.358
ap29b39	13.456	0.830	0.521	0.033	0.508	0.183	0.001	2712	29	2701	69	2680	9	101	2713	58.00	0.03	0.857	227	327	0.694
ap29b40	1.948	0.333	0.185	0.020	0.316	0.080	0.001	1098	57	1093	54	1185	36	92	1095	90.45	0.00	0.947	140	136	1.030
ap29b41	2.047	0.247	0.189	0.019	0.417	0.078	0.001	1131	41	1118	52	1151	22	97	1127	76.29	0.07	0.796	84	306	0.275
ap29b42	5.197	0.260	0.329	0.014	0.416	0.112	0.001	1852	21	1835	33	1830	14	100	1849	41.50	0.29	0.589	116	278	0.418
ap29b43	5.330	0.382	0.337	0.019	0.384	0.116	0.001	1874	31	1871	45	1898	21	99	1873	58.23	0.00	0.955	32	121	0.266
ap29b46	5.953	0.334	0.359	0.018	0.454	0.116	0.001	1969	24	1975	43	1903	16	104	1970	48.32	0.03	0.872	245	206	1.192
ap29b47	1.985	0.151	0.182	0.013	0.468	0.076	0.001	1110	26	1080	35	1093	21	99	1103	49.45	0.86	0.353	213	403	0.529
ap29b48	5.815	0.213	0.351	0.010	0.397	0.117	0.001	1949	16	1941	24	1913	11	101	1947	30.57	0.11	0.741	384	374	1.027
ap29b49	15.097	0.820	0.538	0.028	0.486	0.195	0.002	2821	26	2776	60	2785	19	100	2823	51.56	0.77	0.381	25	58	0.434
ap29b50	5.827	0.299	0.363	0.014	0.366	0.115	0.001	1950	22	1999	32	1877	15	106	1961	41.70	2.30	0.129	86	241	0.358
ap29b51	6.645	0.424	0.379	0.017	0.357	0.123	0.002	2065	28	2070	40	2001	26	103	2066	52.88	0.01	0.905	55	62	0.885
ap29b52	6.182	0.385	0.394	0.017	0.347	0.115	0.002	2002	27	2142	39	1877	26	114	2032	50.17	12.56	0.000	81	77	1.057

APPENDIX B - DETRITAL ZIRCON ANALYSES, continued

Table B6, continued. Detrital zircon U-Pb geochronologic analyses from sample 09TOA096 from the Sekwi correlative unit (Cs) - Memorial University

File Name	Measured Isotopic Ratios							Calculated Ages (Ma)							Concordia age (Ma)	2σ error (Ma)	MSWD (of concordance)	Probability	Th232 (ppm)	U238 (ppm)	Th/U Ratio
	$\frac{^{207}\text{Pb}}{^{235}\text{U}}$	2σ error	$\frac{^{206}\text{Pb}}{^{238}\text{U}}$	2σ error	Rho	$\frac{^{207}\text{Pb}}{^{206}\text{Pb}}$	1σ error	$\frac{^{207}\text{Pb}}{^{235}\text{U}}$	1σ error (Ma)	$\frac{^{206}\text{Pb}}{^{238}\text{U}}$	1σ error (Ma)	$\frac{^{207}\text{Pb}}{^{206}\text{Pb}}$	1σ error (Ma)	U-Pb/Pb-Pb concordancy (%)							
ap29b53	6.030	0.291	0.357	0.017	0.505	0.118	0.001	1980	21	1970	41	1919	16	103	1980	42.07	0.08	0.781	118	218	0.539
ap29b54	5.795	0.585	0.358	0.033	0.452	0.115	0.001	1946	44	1974	78	1880	20	105	1948	86.63	0.16	0.687	220	128	1.717
ap30b03	8.347	0.471	0.401	0.020	0.441	0.152	0.001	2269	26	2172	46	2370	14	92	2261	51.11	5.62	0.018	189	155	1.223
ap30b04	5.168	0.384	0.338	0.018	0.356	0.115	0.002	1847	32	1875	43	1880	30	100	1855	58.36	0.42	0.517	45	47	0.956
ap30b06	5.622	0.289	0.341	0.015	0.436	0.117	0.001	1919	22	1890	37	1912	15	99	1916	43.65	0.79	0.374	148	202	0.731
ap30b07	2.030	0.379	0.224	0.029	0.348	0.070	0.002	1126	64	1302	77	942	72	138	1181	109.77	4.82	0.028	11	20	0.541
ap30b09	5.561	0.676	0.363	0.026	0.293	0.114	0.002	1910	52	1997	61	1866	33	107	1942	88.63	1.65	0.199	11	53	0.198
ap30b10	13.212	1.248	0.544	0.040	0.389	0.180	0.003	2695	45	2799	83	2655	28	105	2703	87.49	1.76	0.185	11	19	0.587
ap30b11	10.337	0.345	0.434	0.013	0.447	0.174	0.001	2465	15	2326	29	2593	10	90	2456	31.00	29.04	0.000	122	288	0.422
ap30b12	6.515	0.368	0.355	0.017	0.434	0.130	0.001	2048	25	1959	41	2098	18	93	2036	49.37	5.47	0.019	142	114	1.239
ap30b15	12.522	0.731	0.508	0.026	0.438	0.184	0.001	2644	27	2650	56	2688	13	99	2645	54.80	0.01	0.908	131	104	1.257
ap30b16	10.783	0.568	0.425	0.021	0.479	0.182	0.001	2505	24	2284	48	2674	11	85	2498	49.20	27.76	0.000	177	180	0.981
ap30b17	5.364	0.276	0.361	0.015	0.411	0.111	0.001	1879	22	1985	36	1822	22	109	1893	42.53	9.88	0.002	27	118	0.232
ap30b18	6.047	0.625	0.392	0.026	0.315	0.114	0.002	1983	45	2132	59	1865	29	114	2024	79.57	5.78	0.016	10	70	0.144
ap30b19	10.218	0.784	0.496	0.026	0.347	0.152	0.002	2455	35	2598	57	2372	20	110	2478	66.98	6.55	0.010	162	97	1.675
ap30b20	5.542	0.471	0.340	0.024	0.420	0.114	0.002	1907	37	1886	58	1858	25	102	1904	71.47	0.16	0.693	16	63	0.245
ap30b21	1.965	0.304	0.182	0.019	0.339	0.080	0.002	1103	52	1075	52	1207	51	89	1089	85.71	0.22	0.638	9	47	0.181
ap30b22	2.300	0.256	0.220	0.017	0.342	0.079	0.002	1212	39	1284	44	1164	44	110	1240	67.05	2.27	0.132	10	72	0.133
ap30b23	7.575	1.596	0.451	0.070	0.369	0.132	0.005	2182	94	2400	156	2121	60	113	2211	179.52	2.09	0.148	10	11	0.933
ap30b24	4.442	0.448	0.335	0.024	0.360	0.102	0.002	1720	42	1864	59	1661	39	112	1753	76.69	5.97	0.015	7	31	0.215
de22a07	10.182	0.595	0.421	0.024	0.493	0.151	0.001	2451	27	2266	55	2362	9	96	2450	54.09	15.34	0.000	81	267	0.305
de22a08	5.516	0.308	0.321	0.013	0.364	0.112	0.001	1903	24	1793	32	1826	11	98	1868	45.21	11.77	0.001	92	266	0.346
de22a09	6.085	0.369	0.334	0.018	0.440	0.116	0.001	1988	26	1857	43	1892	11	98	1969	52.59	11.33	0.001	127	301	0.423
de22a10	5.784	0.498	0.340	0.019	0.331	0.113	0.001	1944	37	1888	47	1847	19	102	1924	67.52	1.30	0.255	20	101	0.195
de22a11	5.464	0.609	0.335	0.022	0.294	0.114	0.002	1895	48	1862	53	1863	26	100	1881	81.14	0.29	0.589	31	45	0.696
de22a12	6.577	0.577	0.363	0.020	0.310	0.121	0.001	2056	39	1998	47	1976	19	101	2034	68.78	1.30	0.255	124	73	1.690
de22a13	5.775	0.296	0.333	0.012	0.351	0.112	0.001	1943	22	1855	29	1839	19	101	1914	41.29	8.74	0.003	99	89	1.114
de22a14	7.256	0.496	0.369	0.018	0.363	0.130	0.001	2143	30	2024	43	2097	15	96	2111	58.33	7.88	0.005	60	119	0.503
de22a15	1.753	0.195	0.171	0.009	0.244	0.075	0.001	1028	36	1018	26	1075	30	95	1021	46.15	0.07	0.791	61	78	0.781
de22a18	5.518	0.398	0.334	0.016	0.331	0.112	0.001	1903	31	1859	39	1828	13	102	1888	55.97	1.19	0.275	54	137	0.396
de22a19	12.360	0.812	0.443	0.023	0.396	0.184	0.001	2632	31	2366	51	2690	9	88	2585	62.32	30.94	0.000	156	237	0.657
de22a20	5.626	0.477	0.327	0.022	0.391	0.112	0.001	1920	37	1824	53	1834	16	99	1897	70.42	3.59	0.058	52	125	0.417
de22a21	12.073	0.951	0.464	0.031	0.423	0.166	0.001	2610	37	2458	68	2522	11	97	2596	74.05	6.09	0.014	187	115	1.630
de22a22	5.690	0.456	0.331	0.023	0.425	0.109	0.001	1930	35	1843	55	1790	17	103	1916	68.11	2.96	0.085	85	94	0.911
de22a23	5.844	0.514	0.335	0.020	0.338	0.114	0.001	1953	38	1863	48	1868	22	100	1921	69.85	3.20	0.074	45	90	0.497
de22a24	6.207	0.696	0.346	0.028	0.358	0.120	0.002	2005	49	1914	66	1952	23	98	1978	92.35	1.86	0.173	63	44	1.428
de22a25	6.657	0.631	0.383	0.018	0.242	0.130	0.002	2067	42	2089	41	2092	25	100	2078	64.91	0.18	0.670	27	41	0.666
de22a26	2.820	0.241	0.226	0.012	0.314	0.084	0.001	1361	32	1312	32	1281	22	102	1335	52.43	1.71	0.191	56	179	0.310
de22a29	6.031	0.316	0.346	0.014	0.386	0.113	0.001	1980	23	1915	34	1844	11	104	1966	43.94	4.11	0.043	100	335	0.300
de22a30	5.653	0.345	0.326	0.015	0.368	0.113	0.001	1924	26	1818	36	1841	11	99	1893	49.81	8.83	0.003	125	244	0.513
de22a31	11.877	0.627	0.463	0.019	0.398	0.166	0.001	2595	25	2452	43	2522	10	97	2576	49.22	12.84	0.000	90	171	0.524
de22a32	5.157	0.438	0.329	0.013	0.235	0.113	0.001	1846	36	1831	32	1848	20	99	1837	53.08	0.11	0.737	89	88	1.004

APPENDIX B - DETRITAL ZIRCON ANALYSES, continued

Table B6, *continued*. Detrital zircon U-Pb geochronologic analyses from sample **09TOA096** from the Sekwi correlative unit (Cs) - Memorial University

File Name	Measured Isotopic Ratios							Calculated Ages (Ma)							Th232 (ppm)	U238 (ppm)	Th/U Ratio				
	$\frac{^{207}\text{Pb}}{^{235}\text{U}}$	2 $\sigma$ error	$\frac{^{206}\text{Pb}}{^{238}\text{U}}$	2 $\sigma$ error	Rho	$\frac{^{207}\text{Pb}}{^{206}\text{Pb}}$	1 $\sigma$ error	$\frac{^{207}\text{Pb}}{^{235}\text{U}}$	1 $\sigma$ error (Ma)	$\frac{^{206}\text{Pb}}{^{238}\text{U}}$	1 $\sigma$ error (Ma)	$\frac{^{207}\text{Pb}}{^{206}\text{Pb}}$	1 $\sigma$ error (Ma)	U-Pb/Pb-Pb concordancy (%)				Concordia age (Ma)	2 $\sigma$ error (Ma)	MSWD	Probability
																				(of concordance)	
de22a33	1.873	0.119	0.169	0.006	0.263	0.075	0.001	1072	21	1005	16	1067	21	94	1023	28.27	8.48	0.004	80	228	0.352
de22a34	5.395	0.331	0.327	0.011	0.278	0.112	0.001	1884	26	1826	27	1825	18	100	1855	43.23	3.23	0.072	22	85	0.265
de22a35	7.196	0.683	0.394	0.019	0.252	0.135	0.002	2136	42	2139	44	2163	27	99	2138	67.92	0.00	0.951	16	31	0.500
de22a36	14.530	0.815	0.502	0.031	0.548	0.181	0.001	2785	27	2623	66	2660	9	99	2798	51.89	8.57	0.003	163	166	0.983
de22a37	3.119	0.402	0.237	0.020	0.327	0.088	0.001	1437	50	1373	52	1385	23	99	1406	83.87	1.19	0.275	57	114	0.502
de22a40	15.645	0.925	0.557	0.029	0.436	0.182	0.001	2855	28	2854	59	2674	14	107	2855	56.35	0.00	0.974	231	52	4.480
de22a41	15.183	0.747	0.526	0.022	0.420	0.185	0.001	2827	23	2726	46	2696	10	101	2820	46.90	5.89	0.015	85	125	0.684
de22a42	5.513	0.367	0.330	0.015	0.345	0.111	0.001	1903	29	1837	37	1813	19	101	1881	52.63	2.94	0.086	44	80	0.550
de22a43	2.594	0.120	0.211	0.006	0.308	0.079	0.001	1299	17	1233	16	1165	19	106	1261	27.02	11.45	0.001	116	275	0.423
de22a44	4.982	0.490	0.321	0.020	0.312	0.106	0.001	1816	42	1795	48	1728	19	104	1808	72.22	0.16	0.693	59	92	0.644
de22a45	2.542	0.309	0.211	0.015	0.298	0.082	0.001	1284	44	1232	41	1248	24	99	1254	68.94	1.04	0.307	56	118	0.472
de22a46	3.043	0.315	0.234	0.016	0.339	0.086	0.001	1418	40	1355	43	1348	22	100	1389	68.20	1.79	0.181	45	109	0.413
de22a47	5.287	0.419	0.320	0.015	0.298	0.113	0.001	1867	34	1790	37	1856	23	96	1831	57.76	3.29	0.070	28	51	0.552
de22a48	2.158	0.207	0.182	0.013	0.384	0.077	0.001	1168	33	1079	37	1126	17	96	1127	58.94	5.14	0.023	132	312	0.422
de22a51	14.600	0.623	0.512	0.019	0.429	0.186	0.001	2790	20	2665	40	2703	12	99	2782	40.62	11.98	0.001	32	69	0.459
de22a52	4.801	0.422	0.330	0.014	0.237	0.115	0.002	1785	37	1839	33	1872	33	98	1815	54.40	1.55	0.214	51	41	1.239
de22a53	5.189	0.556	0.322	0.018	0.258	0.112	0.001	1851	46	1800	43	1839	18	98	1823	71.31	0.85	0.357	86	111	0.773
de22a54	2.060	0.195	0.194	0.009	0.245	0.078	0.001	1135	32	1145	24	1145	33	100	1142	43.09	0.07	0.798	43	57	0.758

APPENDIX B - DETRITAL ZIRCON ANALYSES, continued

Table B7a. Detrital zircon U-Pb geochronologic analyses from sample **09LP093** in unit OSs - Isotope Geology Laboratory, Boise State University

Analysis	U (ppm)	Th (ppm)	Pb* (ppm)	Th/U	Corrected isotope ratios								Apparent ages (Ma)						% disc.				
					$\frac{206\text{Pb}^*}{207\text{Pb}^*}$	±2σ (%)	$\frac{207\text{Pb}^*}{235\text{U}^*}$	±2σ (%)	$\frac{206\text{Pb}^*}{238\text{U}}$	±2σ (%)	error corr.	$\frac{238\text{U}}{206\text{Pb}^*}$	±2σ (%)	$\frac{207\text{Pb}^*}{206\text{Pb}^*}$	±2σ (%)	error corr.	$\frac{207\text{Pb}^*}{206\text{Pb}^*}$	±2σ (Ma)		$\frac{207\text{Pb}^*}{235\text{U}}$	±2σ (Ma)	$\frac{206\text{Pb}^*}{238\text{U}^*}$	±2σ (Ma)
09LP093 L 29	165.71	154.42	143.65	0.93	4.441	1.668	17.366	6.981	0.559	6.779	0.971	1.788	6.779	0.225	1.668	-0.0	3018	27	2955	67	2864	157	5
09LP093 L 73	334.09	157.44	240.16	0.47	4.865	1.618	15.142	5.517	0.534	5.274	0.956	1.872	5.274	0.206	1.618	0	2871	26	2824	53	2759	118	4
09LP093 L 57	121.87	79.11	97.21	0.65	4.927	2.000	15.621	5.892	0.558	5.542	0.941	1.792	5.542	0.203	2.000	-0.0	2850	33	2854	56	2859	128	-0
09LP093 L 1	119.18	59.62	80.57	0.50	5.215	2.030	13.546	6.412	0.512	6.082	0.949	1.952	6.082	0.192	2.030	0.0	2757	33	2719	61	2666	133	3
09LP093 L 81	38.87	68.48	33.09	1.76	5.217	4.784	13.506	8.025	0.511	6.443	0.803	1.957	6.443	0.192	4.784	-0.0	2757	79	2716	76	2661	140	3
09LP093 L 28	190.73	75.47	127.49	0.40	5.255	2.322	13.175	7.685	0.502	7.325	0.953	1.991	7.325	0.190	2.322	0.0	2745	38	2692	73	2623	158	4
09LP093 L 2	169.58	272.87	138.75	1.61	5.256	1.851	13.289	6.314	0.507	6.037	0.956	1.974	6.037	0.190	1.851	0.0	2744	30	2700	60	2642	131	4
09LP093 L 97	224.54	141.91	156.94	0.63	5.303	1.711	13.212	6.071	0.508	5.825	0.959	1.968	5.825	0.189	1.711	-0.0	2730	28	2695	57	2649	127	3
09LP093 L 55	107.32	45.33	77.18	0.42	5.317	2.388	13.880	7.242	0.535	6.837	0.944	1.869	6.837	0.188	2.388	-0.0	2726	39	2742	69	2763	154	-1
09LP093 L 12	211.30	219.96	159.34	1.04	5.328	1.688	12.994	7.248	0.502	7.049	0.973	1.992	7.049	0.188	1.688	0.0	2722	28	2679	68	2623	152	4
09LP093 L 95	43.31	82.03	37.47	1.89	5.360	3.010	12.946	6.969	0.503	6.285	0.902	1.987	6.285	0.187	3.010	0.0	2712	50	2676	66	2628	136	3
09LP093 L 53	79.80	46.80	58.52	0.59	5.366	2.701	13.400	7.254	0.522	6.732	0.928	1.917	6.732	0.186	2.701	-0.0	2710	45	2708	69	2706	149	0
09LP093 L 17	136.81	142.68	106.61	1.04	5.389	1.612	13.160	6.035	0.514	5.815	0.964	1.944	5.815	0.186	1.612	0.0	2703	27	2691	57	2675	127	1
09LP093 L 90	79.86	72.03	57.92	0.90	5.400	1.981	13.060	6.816	0.512	6.522	0.957	1.955	6.522	0.185	1.981	0.0	2700	33	2684	64	2663	142	1
09LP093 L 72	141.35	288.59	130.94	2.04	5.419	2.054	13.006	6.932	0.511	6.621	0.955	1.956	6.621	0.185	2.054	0	2694	34	2680	65	2662	144	1
09LP093 L 46	220.92	193.48	164.07	0.88	5.422	2.283	12.313	6.902	0.484	6.514	0.944	2.065	6.514	0.184	2.283	0.0	2693	38	2629	65	2546	137	5
09LP093 L 104	69.38	38.42	49.11	0.55	5.464	2.262	13.266	6.715	0.526	6.323	0.942	1.902	6.323	0.183	2.262	0.0	2680	37	2699	63	2723	140	-2
09LP093 L 35	136.17	78.83	100.37	0.58	5.482	2.261	13.266	7.412	0.527	7.059	0.952	1.896	7.059	0.182	2.261	-0.0	2675	37	2699	70	2731	157	-2
09LP093 L 10	270.06	254.88	193.38	0.94	5.539	1.325	12.182	6.006	0.489	5.857	0.975	2.043	5.857	0.181	1.325	0	2658	22	2619	56	2568	124	3
09LP093 L 50	186.61	96.57	139.32	0.52	5.604	2.804	13.482	6.652	0.548	6.032	0.907	1.825	6.032	0.178	2.804	0	2638	47	2714	63	2817	138	-7
09LP093 L 85	209.47	106.32	137.74	0.51	5.662	1.525	12.302	5.941	0.505	5.742	0.966	1.980	5.742	0.177	1.525	-0.0	2621	25	2628	56	2636	124	-1
09LP093 L 30	65.28	44.56	45.21	0.68	5.670	2.316	11.913	7.378	0.490	7.006	0.949	2.041	7.006	0.176	2.316	-0.0	2619	39	2598	69	2570	148	2
09LP093 L 4	104.45	99.72	71.22	0.95	5.697	1.600	11.584	6.122	0.479	5.909	0.965	2.089	5.909	0.176	1.600	-0.0	2611	27	2571	57	2521	123	3
09LP093 L 71	343.05	175.83	223.13	0.51	5.797	1.717	11.654	6.048	0.490	5.799	0.959	2.041	5.799	0.173	1.717	0	2582	29	2577	57	2570	123	0
09LP093 L 43	124.70	74.54	91.03	0.60	5.838	2.315	12.314	7.168	0.521	6.784	0.946	1.918	6.784	0.171	2.315	-0.0	2570	39	2629	67	2705	150	-5
09LP093 L 8	201.17	237.14	138.22	1.18	5.965	1.587	10.682	6.215	0.462	6.009	0.967	2.164	6.009	0.168	1.587	0.0	2534	27	2496	58	2449	122	3
09LP093 L 27	53.69	31.03	34.63	0.58	5.980	2.823	10.889	6.579	0.472	5.942	0.903	2.118	5.942	0.167	2.823	-0.0	2530	47	2514	61	2493	123	1
09LP093 L 68	230.89	150.91	149.08	0.65	5.988	1.875	10.768	6.520	0.468	6.245	0.958	2.138	6.245	0.167	1.875	0	2528	31	2503	61	2473	128	2
09LP093 L 109	159.69	59.11	94.74	0.37	6.010	2.238	10.598	6.913	0.462	6.541	0.946	2.165	6.541	0.166	2.238	0	2522	38	2489	64	2448	133	3
09LP093 L 65	126.17	68.79	82.51	0.55	6.030	1.828	11.125	7.918	0.487	7.704	0.973	2.055	7.704	0.166	1.828	0.0	2516	31	2534	74	2556	163	-2
09LP093 L 74	111.35	41.65	65.69	0.37	6.150	1.942	10.408	6.891	0.464	6.612	0.959	2.154	6.612	0.163	1.942	0.0	2483	33	2472	64	2458	135	1
09LP093 L 33	127.01	52.97	78.69	0.42	6.180	2.378	10.556	7.805	0.473	7.434	0.952	2.114	7.434	0.162	2.378	-0.0	2475	40	2485	72	2497	154	-1
09LP093 L 5	154.00	120.73	95.09	0.78	6.192	1.413	10.003	6.171	0.449	6.007	0.973	2.226	6.007	0.161	1.413	0	2471	24	2435	57	2392	120	3
09LP093 L 79	214.03	133.03	127.46	0.62	6.233	1.534	9.990	8.286	0.452	8.142	0.983	2.214	8.142	0.160	1.534	-0.0	2460	26	2434	76	2402	163	2
09LP093 L 102	227.15	283.21	152.84	1.25	6.325	1.924	9.590	6.493	0.440	6.202	0.955	2.273	6.202	0.158	1.924	0	2436	33	2396	60	2350	122	4
09LP093 L 36	145.62	61.22	81.53	0.42	6.751	2.150	8.765	6.709	0.429	6.355	0.947	2.330	6.355	0.148	2.150	0	2324	37	2314	61	2302	123	1
09LP093 L 58	178.59	167.01	119.37	0.94	6.824	2.605	9.177	7.210	0.454	6.723	0.932	2.202	6.723	0.147	2.605	0	2306	45	2356	66	2414	135	-5
09LP093 L 86	278.65	155.81	132.98	0.56	7.592	2.481	6.790	6.711	0.374	6.235	0.929	2.675	6.235	0.132	2.481	-0.0	2121	43	2084	59	2048	109	3
09LP093 L 98	370.24	101.60	166.44	0.27	7.785	1.856	6.577	5.853	0.371	5.551	0.948	2.693	5.551	0.128	1.856	-0.0	2077	33	2056	52	2036	97	2
09LP093 L 7	107.89	103.44	52.35	0.96	8.078	2.345	5.928	6.887	0.347	6.475	0.940	2.879	6.475	0.124	2.345	0.0	2012	42	1965	60	1922	108	4
09LP093 L 84	89.09	90.56	41.73	1.02	8.315	2.582	5.616	6.798	0.339	6.288	0.925	2.953	6.288	0.120	2.582	0.0	1960	46	1919	59	1880	103	4
09LP093 L 64	355.01	21.03	143.60	0.06	8.349	2.599	5.861	7.820	0.355	7.376	0.943	2.818	7.376	0.120	2.599	0.0	1953	46	1955	68	1958	125	-0

APPENDIX B - DETRITAL ZIRCON ANALYSES, continued

Table B7a, continued. Detrital zircon U-Pb geochronologic analyses from sample 09LP093 in unit OSs - Isotope Geology Laboratory, Boise State University

Analysis	U (ppm)	Th (ppm)	Pb* (ppm)	Th/U	Corrected isotope ratios							Apparent ages (Ma)						% disc.					
					$\frac{^{206}\text{Pb}^*}{^{207}\text{Pb}^*}$	$\pm 2\sigma$ (%)	$\frac{^{207}\text{Pb}^*}{^{235}\text{U}^*}$	$\pm 2\sigma$ (%)	$\frac{^{206}\text{Pb}^*}{^{238}\text{U}}$	$\pm 2\sigma$ (%)	error corr.	$\frac{^{238}\text{U}}{^{206}\text{Pb}^*}$	$\pm 2\sigma$ (%)	$\frac{^{207}\text{Pb}^*}{^{206}\text{Pb}^*}$	$\pm 2\sigma$ (%)	error corr.	$\frac{^{207}\text{Pb}^*}{^{206}\text{Pb}^*}$		$\pm 2\sigma$ (Ma)	$\frac{^{207}\text{Pb}^*}{^{235}\text{U}}$	$\pm 2\sigma$ (Ma)	$\frac{^{206}\text{Pb}^*}{^{238}\text{U}^*}$	$\pm 2\sigma$ (Ma)
09LP093 L 93	324.97	200.70	142.90	0.62	8.358	1.542	5.584	6.447	0.338	6.260	0.971	2.954	6.260	0.120	1.542	0	1951	28	1914	56	1879	102	4
09LP093 L 103	92.31	76.88	41.82	0.83	8.418	2.330	5.335	6.192	0.326	5.737	0.927	3.070	5.737	0.119	2.330	-0.0	1938	42	1875	53	1818	91	6
09LP093 L 107	195.09	86.89	83.82	0.45	8.441	2.752	5.569	7.990	0.341	7.502	0.939	2.933	7.502	0.118	2.752	-0.0	1933	49	1911	69	1891	123	2
09LP093 L 48	177.61	71.33	78.97	0.40	8.450	2.758	5.684	7.072	0.348	6.512	0.921	2.871	6.512	0.118	2.758	0.0	1931	49	1929	61	1927	108	0
09LP093 L 100	156.46	60.96	63.00	0.39	8.455	2.016	5.302	6.779	0.325	6.472	0.955	3.076	6.472	0.118	2.016	-0.0	1930	36	1869	58	1815	102	6
<b>09LP093 L 18</b>	<b>90.68</b>	<b>162.76</b>	<b>50.53</b>	<b>1.79</b>	<b>8.474</b>	<b>2.670</b>	<b>5.300</b>	<b>6.464</b>	<b>0.326</b>	<b>5.887</b>	<b>0.911</b>	<b>3.070</b>	<b>5.887</b>	<b>0.118</b>	<b>2.670</b>	<b>-0.0</b>	<b>1926</b>	<b>48</b>	<b>1869</b>	<b>55</b>	<b>1818</b>	<b>93</b>	<b>6</b>
09LP093 L 106	131.21	40.92	53.54	0.31	8.488	2.850	5.453	7.457	0.336	6.891	0.924	2.979	6.891	0.118	2.850	0	1923	51	1893	64	1866	112	3
09LP093 L 88	93.56	101.30	44.08	1.08	8.491	2.075	5.464	6.184	0.336	5.825	0.942	2.972	5.825	0.118	2.075	0	1923	37	1895	53	1870	95	3
09LP093 L 20	210.71	137.88	91.41	0.65	8.529	1.658	5.223	6.134	0.323	5.905	0.963	3.095	5.905	0.117	1.658	0.0	1915	30	1856	52	1805	93	6
09LP093 L 15	241.00	198.91	109.00	0.83	8.598	2.099	5.188	6.161	0.324	5.793	0.940	3.091	5.793	0.116	2.099	0	1900	38	1851	52	1807	91	5
09LP093 L 62	46.91	46.72	23.56	1.00	8.605	4.239	5.476	7.999	0.342	6.784	0.848	2.926	6.784	0.116	4.239	0.0	1899	76	1897	69	1895	111	0
09LP093 L 40	169.99	54.23	70.53	0.32	8.607	2.357	5.329	6.487	0.333	6.044	0.932	3.006	6.044	0.116	2.357	-0.0	1898	42	1874	55	1851	97	2
09LP093 L 16	94.67	62.89	40.60	0.66	8.620	2.471	5.134	6.292	0.321	5.786	0.920	3.115	5.786	0.116	2.471	-0.0	1896	44	1842	53	1795	91	5
09LP093 L 75	370.84	132.04	155.06	0.36	8.621	1.826	5.480	6.210	0.343	5.936	0.956	2.918	5.936	0.116	1.826	-0.0	1895	33	1898	53	1899	98	-0
09LP093 L 21	72.37	30.15	30.24	0.42	8.677	2.915	5.266	7.250	0.331	6.638	0.916	3.018	6.638	0.115	2.915	0.0	1884	52	1863	62	1845	106	2
<b>09LP093 L 101</b>	<b>155.92</b>	<b>69.80</b>	<b>60.43</b>	<b>0.45</b>	<b>8.679</b>	<b>2.747</b>	<b>4.878</b>	<b>6.583</b>	<b>0.307</b>	<b>5.982</b>	<b>0.909</b>	<b>3.257</b>	<b>5.982</b>	<b>0.115</b>	<b>2.747</b>	<b>-0.0</b>	<b>1883</b>	<b>49</b>	<b>1799</b>	<b>55</b>	<b>1726</b>	<b>91</b>	<b>8</b>
09LP093 L 80	117.09	69.72	49.71	0.60	8.686	1.982	5.332	6.391	0.336	6.076	0.951	2.977	6.076	0.115	1.982	0	1882	36	1874	55	1867	98	1
09LP093 L 3	85.53	99.44	39.06	1.16	8.698	2.981	5.052	6.903	0.319	6.226	0.902	3.138	6.226	0.115	2.981	-0.0	1879	54	1828	59	1783	97	5
09LP093 L 87	239.43	107.80	97.45	0.45	8.699	1.646	5.236	5.965	0.330	5.733	0.961	3.027	5.733	0.115	1.646	0	1879	30	1858	51	1840	92	2
09LP093 L 26	145.98	42.90	57.76	0.29	8.707	2.780	5.139	7.457	0.325	6.920	0.928	3.082	6.920	0.115	2.780	0.0	1877	50	1843	63	1812	109	3
09LP093 L 38	96.02	56.36	40.47	0.59	8.708	2.837	4.994	8.057	0.315	7.541	0.936	3.171	7.541	0.115	2.837	0.0	1877	51	1818	68	1767	117	6
09LP093 L 83	166.17	78.84	69.43	0.47	8.724	2.140	5.351	6.927	0.339	6.588	0.951	2.953	6.588	0.115	2.140	0	1874	39	1877	59	1880	107	-0
09LP093 L 56	171.70	44.55	70.58	0.26	8.743	2.259	5.346	6.765	0.339	6.377	0.943	2.950	6.377	0.114	2.259	-0.0	1870	41	1876	58	1882	104	-1
09LP093 L 31	52.27	12.32	21.09	0.24	8.751	3.202	5.255	7.786	0.334	7.097	0.912	2.998	7.097	0.114	3.202	-0.0	1868	58	1862	66	1855	114	1
09LP093 L 59	101.65	78.32	49.88	0.77	8.765	2.743	5.533	7.414	0.352	6.888	0.929	2.843	6.888	0.114	2.743	-0.0	1866	50	1906	64	1943	116	-4
09LP093 L 60	70.18	75.76	37.79	1.08	8.774	3.168	5.634	7.418	0.359	6.707	0.904	2.789	6.707	0.114	3.168	-0.0	1864	57	1921	64	1975	114	-6
09LP093 L 94	44.62	24.81	17.72	0.56	8.776	3.429	4.886	6.837	0.311	5.915	0.865	3.216	5.915	0.114	3.429	0	1863	62	1800	58	1745	90	6
09LP093 L 61	456.72	414.37	217.89	0.91	8.780	2.521	5.201	7.162	0.331	6.703	0.936	3.019	6.703	0.114	2.521	0.0	1862	46	1853	61	1844	108	1
09LP093 L 63	64.73	31.81	29.02	0.49	8.781	3.849	5.462	8.924	0.348	8.051	0.902	2.875	8.051	0.114	3.849	-0.0	1862	69	1895	77	1924	134	-3
09LP093 L 76	205.60	169.68	89.59	0.83	8.796	1.545	5.071	6.150	0.324	5.953	0.968	3.091	5.953	0.114	1.545	0.0	1859	28	1831	52	1807	94	3
09LP093 L 54	230.61	70.66	93.57	0.31	8.816	2.011	5.159	7.476	0.330	7.201	0.963	3.031	7.201	0.113	2.011	0	1855	36	1846	64	1838	115	1
09LP093 L 42	127.15	22.93	51.45	0.18	8.817	2.541	5.344	6.984	0.342	6.506	0.931	2.926	6.506	0.113	2.541	0	1855	46	1876	60	1895	107	-2
09LP093 L 96	189.75	102.97	66.99	0.54	8.830	2.569	4.282	10.525	0.274	10.207	0.970	3.647	10.207	0.113	2.569	0.0	1852	46	1690	87	1562	142	16
09LP093 L 22	165.43	36.41	64.27	0.22	8.834	2.634	5.095	6.925	0.326	6.404	0.925	3.064	6.404	0.113	2.634	0.0	1851	48	1835	59	1821	102	2
<b>09LP093 L 52</b>	<b>365.79</b>	<b>121.20</b>	<b>132.41</b>	<b>0.33</b>	<b>8.839</b>	<b>2.425</b>	<b>4.552</b>	<b>7.282</b>	<b>0.292</b>	<b>6.867</b>	<b>0.943</b>	<b>3.427</b>	<b>6.867</b>	<b>0.113</b>	<b>2.425</b>	<b>-0.0</b>	<b>1850</b>	<b>44</b>	<b>1741</b>	<b>61</b>	<b>1651</b>	<b>100</b>	<b>11</b>
09LP093 L 13	300.13	211.20	128.28	0.70	8.858	1.795	4.950	6.992	0.318	6.758	0.966	3.145	6.758	0.113	1.795	-0.0	1846	32	1811	59	1780	105	4
09LP093 L 91	192.45	79.96	77.17	0.42	8.861	2.104	5.074	6.212	0.326	5.845	0.941	3.067	5.845	0.113	2.104	-0.0	1846	38	1832	53	1819	93	1
09LP093 L 51	70.12	12.85	28.38	0.18	8.861	2.573	5.328	7.066	0.342	6.581	0.931	2.921	6.581	0.113	2.573	-0.0	1846	47	1873	60	1898	108	-3
09LP093 L 47	43.74	18.94	18.28	0.43	8.865	3.568	5.040	7.063	0.324	6.095	0.863	3.086	6.095	0.113	3.568	0	1845	65	1826	60	1809	96	2
09LP093 L 24	146.29	76.52	60.22	0.52	8.877	2.090	4.917	6.581	0.317	6.240	0.948	3.159	6.240	0.113	2.090	-0.0	1843	38	1805	56	1773	97	4
09LP093 L 34	109.08	78.53	51.70	0.72	8.878	2.745	5.373	7.150	0.346	6.602	0.923	2.890	6.602	0.113	2.745	0	1842	50	1881	61	1915	109	-4
09LP093 L 78	157.25	15.81	60.25	0.10	8.883	2.008	5.231	7.037	0.337	6.745	0.958	2.967	6.745	0.113	2.008	0.0	1841	36	1858	60	1872	110	-2

APPENDIX B - DETRITAL ZIRCON ANALYSES, continued

Table B7a, *continued*. Detrital zircon U-Pb geochronologic analyses from sample **09LP093** in unit OSs - Isotope Geology Laboratory, Boise State University

Analysis	U (ppm)	Th (ppm)	Pb* (ppm)	Th/U	Corrected isotope ratios								Apparent ages (Ma)						% disc.				
					$\frac{^{206}\text{Pb}^*}{^{207}\text{Pb}^*}$	$\pm 2\sigma$ (%)	$\frac{^{207}\text{Pb}^*}{^{235}\text{U}^*}$	$\pm 2\sigma$ (%)	$\frac{^{206}\text{Pb}^*}{^{238}\text{U}}$	$\pm 2\sigma$ (%)	error corr.	$\frac{^{238}\text{U}}{^{206}\text{Pb}^*}$	$\pm 2\sigma$ (%)	$\frac{^{207}\text{Pb}^*}{^{206}\text{Pb}^*}$	$\pm 2\sigma$ (%)	error corr.	$\frac{^{207}\text{Pb}^*}{^{206}\text{Pb}^*}$	$\pm 2\sigma$ (Ma)		$\frac{^{207}\text{Pb}^*}{^{235}\text{U}}$	$\pm 2\sigma$ (Ma)	$\frac{^{206}\text{Pb}^*}{^{238}\text{U}^*}$	$\pm 2\sigma$ (Ma)
09LP093 L 67	101.70	59.77	41.75	0.59	8.892	2.733	4.861	6.965	0.313	6.406	0.920	3.190	6.406	0.112	2.733	0.0	1839	49	1795	59	1758	99	4
09LP093 L 110	199.56	116.50	88.10	0.58	8.928	2.968	5.184	7.016	0.336	6.357	0.906	2.979	6.357	0.112	2.968	0.0	1832	54	1850	60	1866	103	-2
09LP093 L 105	63.92	56.11	27.71	0.88	8.934	3.070	4.738	6.774	0.307	6.038	0.891	3.257	6.038	0.112	3.070	0.0	1831	56	1774	57	1726	91	6
09LP093 L 69	386.65	114.73	156.17	0.30	8.941	1.720	5.154	6.559	0.334	6.329	0.965	2.992	6.329	0.112	1.720	0.0	1830	31	1845	56	1859	102	-2
09LP093 L 66	66.95	26.67	27.38	0.40	8.945	2.638	5.054	7.937	0.328	7.486	0.943	3.050	7.486	0.112	2.638	0.0	1829	48	1828	67	1828	119	0
09LP093 L 70	134.48	47.98	52.99	0.36	8.968	2.525	4.941	6.702	0.321	6.208	0.926	3.112	6.208	0.112	2.525	0	1824	46	1809	57	1796	97	2
09LP093 L 25	185.16	93.02	77.21	0.50	8.975	2.205	4.975	6.982	0.324	6.625	0.949	3.088	6.625	0.111	2.205	0	1823	40	1815	59	1809	104	1
09LP093 L 99	98.35	122.08	46.72	1.24	9.001	3.450	4.847	7.020	0.316	6.113	0.871	3.160	6.113	0.111	3.450	-0.0	1817	63	1793	59	1772	95	2
09LP093 L 82	274.31	198.46	106.76	0.72	9.023	2.266	4.561	5.976	0.298	5.530	0.925	3.351	5.530	0.111	2.266	-0.0	1813	41	1742	50	1684	82	7
09LP093 L 45	97.88	69.12	46.96	0.71	9.030	3.687	5.271	8.244	0.345	7.374	0.894	2.897	7.374	0.111	3.687	-0.0	1812	67	1864	70	1912	122	-6
09LP093 L 49	128.54	42.95	53.23	0.33	9.042	3.013	5.100	6.611	0.334	5.884	0.890	2.990	5.884	0.111	3.013	0.0	1809	55	1836	56	1860	95	-3
09LP093 L 11	171.26	45.06	62.03	0.26	9.068	1.725	4.621	7.210	0.304	7.000	0.971	3.291	7.000	0.110	1.725	0.0	1804	31	1753	60	1711	105	5
09LP093 L 41	253.85	87.68	99.82	0.35	9.115	2.394	4.769	7.491	0.315	7.098	0.948	3.171	7.098	0.110	2.394	-0.0	1794	44	1780	63	1767	110	2
09LP093 L 108	173.80	80.55	70.20	0.46	9.188	2.845	4.826	7.792	0.322	7.254	0.931	3.110	7.254	0.109	2.845	-0.0	1780	52	1789	66	1797	114	-1
09LP093 L 44	124.74	72.57	53.19	0.58	9.240	2.920	4.741	7.402	0.318	6.802	0.919	3.148	6.802	0.108	2.920	0	1770	53	1774	62	1778	106	-0
09LP093 L 37	140.08	171.22	62.91	1.22	9.481	2.534	4.171	7.223	0.287	6.763	0.936	3.487	6.763	0.105	2.534	0	1722	47	1668	59	1626	97	6
09LP093 L 92	151.06	95.93	57.88	0.64	9.620	2.510	4.278	6.585	0.298	6.088	0.925	3.350	6.088	0.104	2.510	0.0	1696	46	1689	54	1684	90	1
09LP093 L 6	295.02	184.51	80.66	0.63	11.219	1.738	2.657	7.310	0.216	7.100	0.971	4.626	7.100	0.089	1.738	-0.0	1407	33	1316	54	1262	81	10

Notes:

Yellow highlighted rows are samples that intersected inclusions.

Isotope ratios and ages are NOT corrected for initial common Pb.

Isotope ratio and apparent age errors include systematic calibration errors of 3.69819596935203% ( $^{208}\text{Pb}/^{232}\text{Th}$ ), 0.334539294582954% ( $^{207}\text{Pb}/^{206}\text{Pb}$ ), 2.39239549711403% ( $^{206}\text{Pb}/^{238}\text{U}$ ) (all 1-sigma).

Sweep-by-sweep downhole fractionation of U/Pb ratios NOT corrected via Si/Zr fractionation factor.

Backgrounds were monitored during sweeps 10 to 27. Sample counts were integrated from sweeps 36 to 69.

Ablation used a laser spot size of 25 microns, and a laser firing repetition rate of 10 Hz.





APPENDIX B - DETRITAL ZIRCON ANALYSES, continued

Table B7b, continued. Detrital zircon trace element analyses from sample 09LP093 in unit OSs - Isotope Geology Laboratory, Boise State University

Analysis	Concentrations (ppm)																						
	P	Ti	Y	Zr	Nb	La	Ce	Pr	Nd	Sm	Eu	Gd	Tb	Dy	Ho	Er	Tm	Yb	Lu	Hf	Ta	Th	U
09LP093 L 105	189.401	229.132	461.608	438508.847	6.507	0.410	42.116	0.140	1.688	2.791	0.399	11.138	3.859	47.309	16.311	72.188	19.124	216.732	26.425	6386.267	1.157	56.112	63.923
09LP093 L 69	247.519	5.880	855.192	546804.619	4.950		27.210	0.037	1.069	2.543	0.153	13.069	6.177	78.792	31.622	144.100	41.924	480.260	57.565	9161.294	2.701	114.726	386.652
09LP093 L 66	161.925	12.730	416.942	518004.748	0.480	0.009	19.219	0.061	1.687	4.524	0.958	15.994	4.901	47.153	16.384	65.225	17.044	192.976	21.530	5642.358	0.342	26.675	66.954
09LP093 L 70	246.266	14.204	490.623	563364.176	1.129		12.738	0.044	0.847	3.450	0.548	11.570	4.271	47.964	17.471	74.450	20.258	231.108	27.629	10109.815	0.966	47.981	134.482
09LP093 L 25	157.480	16.399	429.121	524950.197	1.015	0.089	15.957	0.085	1.466	4.047	0.668	14.987	4.519	49.898	16.552	61.700	15.731	157.712	16.681	8223.625	0.411	93.022	185.157
09LP093 L 99	165.681	5.126	1100.424	559721.883	1.031		37.166	0.148	2.342	8.102	2.036	35.043	11.333	127.989	43.240	170.435	42.818	444.682	50.417	8219.180	0.451	122.080	98.350
09LP093 L 82	252.489	14.356	777.920	656903.875	1.468		13.703	0.197	2.466	4.564	0.789	23.054	7.758	80.573	27.219	114.151	27.164	260.974	37.603	11578.959	0.722	198.461	274.308
09LP093 L 45	138.918	12.583	306.281	474532.426	2.239		21.142	0.026	0.963	2.064	0.323	8.325	2.899	33.690	11.939	52.564	14.046	160.883	16.139	7878.596	1.402	69.118	97.884
09LP093 L 49	180.447	12.034	420.361	445406.997	1.011		3.931	0.029	0.590	1.521	0.253	10.993	3.745	45.951	16.726	65.138	17.641	201.061	21.545	7552.218	0.692	42.953	128.537
09LP093 L 11	127.491	6.681	514.930	590625.428	0.548		3.316	0.054	0.787	1.358	0.522	10.642	3.934	47.774	17.643	82.926	22.987	259.298	31.859	8519.860	0.396	45.058	171.263
09LP093 L 41	248.584	9.723	670.560	454503.176	4.108		6.126	0.053	1.407	2.530	0.253	15.978	5.969	75.264	25.915	106.658	27.933	312.534	31.949	7207.975	2.443	87.683	253.848
09LP093 L 108	204.475	15.388	917.782	514821.013	0.970	0.004	4.837	0.083	2.214	4.689	0.527	27.198	9.101	105.629	35.981	135.397	32.629	343.101	33.366	7561.764	0.437	80.550	173.802
09LP093 L 44	173.479	13.434	632.713	455776.061	1.017		17.743	0.035	1.242	4.593	1.060	20.444	6.221	70.706	23.254	87.700	22.273	248.863	25.110	6896.722	0.478	72.569	124.741
09LP093 L 37	458.133	2771.253	1003.505	428063.717	15.171	7.824	36.233	2.307	14.357	11.673	2.105	34.086	10.019	115.452	39.514	154.285	40.034	434.198	46.592	5413.354	1.355	171.220	140.078
09LP093 L 92	227.033	7.130	1320.545	610458.815	5.993	0.012	61.666	0.092	1.706	5.782	1.465	24.151	9.501	123.675	48.311	217.973	61.533	672.569	85.787	9219.842	1.836	95.927	151.058
09LP093 L 6	797.545	39.324	3320.349	652469.680	7.688	9.236	61.729	7.794	48.839	30.591	8.030	84.470	28.194	327.088	114.362	470.439	112.452	1098.148	140.195	13100.247	3.402	184.514	295.018

Notes:

Yellow highlighted rows are samples that intersected inclusions.

Trace element concentrations in ppm, calculated using mean count rate method.

Backgrounds were monitored during sweeps 10 to 27. Sample counts were integrated from sweeps 36 to 69.

Ablation used a laser spot size of 25 microns, and a laser firing repetition rate of 10 Hz.





APPENDIX B - DETRITAL ZIRCON ANALYSES, continued

Table B7c, *continued*. Detrital zircon calculated ratios and values from sample **09LP093** in unit OSs - Isotope Geology Laboratory, Boise State University

Analysis	CI chondrite normalizing values from Sun and McDonough (1989)														Ti-in-zircon T (°C)	Ce/Ce*	Eu/Eu*	(Sm/Nd) <sub>cn</sub>	(Lu/Nd) <sub>cn</sub>	Lu/Hf	Nb/Ta	Nb/U	Th/U	Th/Y	Y/Hf
	0.237	0.612	0.095	0.467	0.153	0.058	0.206	0.037	0.254	0.057	0.166	0.026	0.17	0.025											
	La	Ce	Pr	Nd	Sm	Eu	Gd	Tb	Dy	Ho	Er	Tm	Yb	Lu											
09LP093 L 67	0.059	54.651	2.086	9.085	39.211	35.934	111.343	174.303	236.316	336.890	439.585	714.371	1089.017	823.397	863	50.96	0.48	4.32	90.64	0.00	2.03	0.01	0.59	0.11	0.09
09LP093 L 110	0.005	47.278	0.209	3.284	19.977	13.454	50.345	79.255	133.983	182.052	256.262	477.745	790.607	547.870	805	442.28	0.38	6.08	166.82	0.00	2.61	0.01	0.58	0.39	0.05
09LP093 L 105	1.730	68.817	1.471	3.614	18.241	6.876	54.201	103.186	186.256	288.177	436.184	749.974	1274.895	1040.372	1261	43.00	0.19	5.05	287.84	0.00	5.63	0.10	0.88	0.12	0.07
09LP093 L 69	0.010	44.461	0.387	2.290	16.619	2.645	63.598	165.166	310.204	558.699	870.693	1644.074	2825.059	2266.355	744	224.04	0.07	7.26	989.71	0.01	1.83	0.01	0.30	0.13	0.09
09LP093 L 66	0.039	31.403	0.638	3.612	29.570	16.511	77.830	131.050	185.640	289.465	394.109	668.411	1135.151	847.641	822	92.74	0.31	8.19	234.68	0.00	1.41	0.01	0.40	0.06	0.07
09LP093 L 70	0.011	20.814	0.459	1.815	22.548	9.454	56.300	114.199	188.835	308.681	449.847	794.430	1359.461	1087.774	834	88.55	0.24	12.42	599.41	0.00	1.17	0.01	0.36	0.10	0.05
09LP093 L 25	0.374	26.073	0.892	3.139	26.449	11.517	72.928	120.825	196.447	292.446	372.807	616.884	927.720	656.735	850	41.18	0.23	8.43	209.23	0.00	2.47	0.01	0.50	0.22	0.05
09LP093 L 99	0.039	60.728	1.561	5.014	52.953	35.105	170.524	303.011	503.894	763.960	1029.817	1679.131	2615.776	1984.904	731	75.93	0.31	10.56	395.84	0.01	2.29	0.01	1.24	0.11	0.13
09LP093 L 82	0.052	22.390	2.073	5.279	29.827	13.599	112.185	207.432	317.217	480.898	689.736	1065.260	1535.140	1480.415	835	21.08	0.19	5.65	280.41	0.00	2.03	0.01	0.72	0.26	0.07
09LP093 L 45	0.007	34.546	0.269	2.063	13.489	5.571	40.509	77.522	132.639	210.930	317.610	550.833	946.372	635.390	821	250.97	0.21	6.54	308.02	0.00	1.60	0.02	0.71	0.23	0.04
09LP093 L 49	0.008	6.424	0.302	1.264	9.940	4.363	53.492	100.127	180.910	295.511	393.585	691.795	1182.709	848.218	816	41.48	0.14	7.86	670.83	0.00	1.46	0.01	0.33	0.10	0.06
09LP093 L 11	0.014	5.419	0.571	1.684	8.878	9.001	51.784	105.194	188.088	311.708	501.063	901.434	1525.282	1254.275	756	18.52	0.30	5.27	744.73	0.00	1.38	0.00	0.26	0.09	0.06
09LP093 L 41	0.014	10.010	0.562	3.012	16.533	4.355	77.752	159.610	296.315	457.869	644.462	1095.420	1838.438	1257.826	793	34.77	0.09	5.49	417.55	0.00	1.68	0.02	0.35	0.13	0.09
09LP093 L 108	0.017	7.904	0.875	4.742	30.644	9.091	132.352	243.335	415.861	635.701	818.111	1279.557	2018.243	1313.635	843	17.72	0.11	6.46	277.04	0.00	2.22	0.01	0.46	0.09	0.12
09LP093 L 44	0.009	28.992	0.368	2.660	30.021	18.277	99.486	166.339	278.372	410.849	529.907	873.452	1463.901	988.583	828	153.59	0.28	11.28	371.60	0.00	2.13	0.01	0.58	0.11	0.09
09LP093 L 37	33.013	59.204	24.280	30.742	76.291	36.297	165.867	267.885	454.537	698.119	932.234	1569.972	2554.108	1834.320	2072	2.07	0.30	2.48	59.67	0.01	11.20	0.11	1.22	0.17	0.19
09LP093 L 92	0.052	100.761	0.968	3.653	37.790	25.255	117.523	254.035	486.908	853.553	1317.059	2413.048	3956.286	3377.433	762	197.49	0.33	10.34	924.48	0.01	3.26	0.04	0.64	0.07	0.14
09LP093 L 6	38.970	100.865	82.038	104.581	199.938	138.455	411.047	753.843	1287.748	2020.529	2842.530	4409.888	6459.695	5519.507	960	1.67	0.45	1.91	52.78	0.01	2.26	0.03	0.63	0.06	0.25

Notes:

Activity (SiO<sub>2</sub>) = 1; activity (TiO<sub>2</sub>) = 0.6.

Yellow highlighted rows are samples that intersected inclusions.

Trace element concentrations in ppm, calculated using mean count rate method.

Backgrounds were monitored between sweeps 10 to 27. Sample counts were integrated from sweeps 36 to 69.

Ablation used a laser spot size of 25 microns, and a laser firing repetition rate of 10 Hz.

APPENDIX B - DETRITAL ZIRCON ANALYSES, continued

Table B8a. Detrital zircon U-Pb geochronologic analyses from sample **09LP090** in Mattson Formation (MM) - Isotope Geology Laboratory, Boise State University

Analysis	U (ppm)	Th (ppm)	Pb* (ppm)	Th/U	Corrected isotope ratios											Apparent ages (Ma)						% disc.	
					$\frac{^{206}\text{Pb}^*}{^{207}\text{Pb}^*}$	$\pm 2\sigma$ (%)	$\frac{^{207}\text{Pb}^*}{^{235}\text{U}^*}$	$\pm 2\sigma$ (%)	$\frac{^{206}\text{Pb}^*}{^{238}\text{U}^*}$	$\pm 2\sigma$ (%)	error corr.	$\frac{^{238}\text{U}}{^{206}\text{Pb}^*}$	$\pm 2\sigma$ (%)	$\frac{^{207}\text{Pb}^*}{^{206}\text{Pb}^*}$	$\pm 2\sigma$ (%)	error corr.	$\frac{^{207}\text{Pb}^*}{^{206}\text{Pb}^*}$	$\pm 2\sigma$ (Ma)	$\frac{^{207}\text{Pb}^*}{^{235}\text{U}^*}$	$\pm 2\sigma$ (Ma)	$\frac{^{206}\text{Pb}^*}{^{238}\text{U}^*}$		$\pm 2\sigma$ (Ma)
09LP090 L 115	112.93	226.81	125.43	2.01	3.731	1.749	22.485	5.469	0.608	5.182	0.947	1.644	5.182	0.268	1.749	-0.0	<b>3294</b>	<b>27</b>	3205	53	3064	126	7
09LP090 L 132	103.28	44.78	86.13	0.43	4.449	2.828	18.724	7.080	0.604	6.490	0.917	1.655	6.490	0.225	2.828	0	3015	45	3028	68	3047	158	-1
09LP090 L 129	681.46	23.10	502.83	0.03	4.465	1.801	18.447	5.552	0.597	5.252	0.946	1.674	5.252	0.224	1.801	0	3010	29	3013	53	3019	127	-0
09LP090 L 195	51.47	25.89	39.72	0.50	4.931	2.427	15.683	5.359	0.561	4.778	0.892	1.783	4.778	0.203	2.427	0.0	2849	40	2858	51	2870	111	-1
09LP090 L 216	779.52	16.87	506.70	0.02	5.133	2.401	14.527	5.166	0.541	4.573	0.885	1.849	4.573	0.195	2.401	-0.0	2783	39	2785	49	2787	103	-0
09LP090 L 156	32.34	35.27	27.83	1.09	5.159	4.253	14.696	8.518	0.550	7.380	0.866	1.818	7.380	0.194	4.253	-0.0	<b>2775</b>	<b>70</b>	2796	81	2825	169	-2
09LP090 L 184	50.42	52.36	39.93	1.04	5.249	2.758	13.709	6.491	0.522	5.876	0.905	1.916	5.876	0.190	2.758	0.0	2746	45	2730	61	2707	130	1
09LP090 L 176	296.08	156.71	198.42	0.53	5.258	1.383	13.250	5.448	0.505	5.270	0.967	1.979	5.270	0.190	1.383	-0.0	2744	23	2698	51	2636	114	4
09LP090 L 170	148.07	48.86	95.78	0.33	5.283	1.416	13.270	5.416	0.508	5.228	0.965	1.967	5.228	0.189	1.416	-0.0	2736	23	2699	51	2650	114	3
09LP090 L 153	187.22	109.67	123.33	0.59	5.287	2.410	12.277	8.265	0.471	7.906	0.957	2.124	7.906	0.189	2.410	0	2735	40	2626	78	2487	163	9
09LP090 L 148	552.44	162.90	372.42	0.29	5.355	2.063	13.437	5.565	0.522	5.168	0.929	1.916	5.168	0.187	2.063	-0.0	2714	34	2711	53	2707	114	0
09LP090 L 166	33.12	30.32	23.73	0.92	5.680	3.296	12.110	7.957	0.499	7.242	0.910	2.005	7.242	0.176	3.296	-0.0	2616	55	2613	75	2609	155	0
09LP090 L 133	30.68	20.93	22.49	0.68	5.872	4.128	12.133	7.356	0.517	6.088	0.828	1.935	6.088	0.170	4.128	0.0	<b>2561</b>	<b>69</b>	2615	69	2685	134	-5
09LP090 L 145	63.27	40.84	46.21	0.65	6.199	3.174	11.878	11.083	0.534	10.619	0.958	1.872	10.619	0.161	3.174	0	2469	54	2595	104	2758	238	-12
09LP090 L 147	599.85	241.98	231.00	0.40	8.186	2.585	5.129	5.969	0.305	5.380	0.901	3.284	5.380	0.122	2.585	0	1988	46	1841	51	1714	81	14
09LP090 L 130	287.37	106.59	126.32	0.37	8.209	2.861	5.886	6.323	0.350	5.639	0.892	2.854	5.639	0.122	2.861	0.0	1983	51	1959	55	1937	94	2
09LP090 L 178	811.27	206.71	331.79	0.25	8.401	1.919	5.610	5.473	0.342	5.125	0.937	2.926	5.125	0.119	1.919	0	<b>1942</b>	<b>34</b>	1918	47	1895	84	2
09LP090 L 192	227.42	26.83	90.34	0.12	8.423	2.546	5.608	6.004	0.343	5.437	0.906	2.919	5.437	0.119	2.546	0	1937	46	1917	52	1899	89	2
09LP090 L 131	423.40	145.42	168.29	0.34	8.522	2.036	5.181	5.797	0.320	5.428	0.936	3.123	5.428	0.117	2.036	-0.0	1916	37	1850	49	1791	85	7
09LP090 L 140	133.97	30.64	57.21	0.23	8.593	2.689	5.724	6.801	0.357	6.247	0.919	2.803	6.247	0.116	2.689	0	1901	48	1935	59	1967	106	-3
09LP090 L 146	124.43	74.54	57.52	0.60	8.634	3.260	5.559	7.603	0.348	6.869	0.903	2.873	6.869	0.116	3.260	-0.0	1893	59	1910	65	1926	114	-2
09LP090 L 155	47.46	90.96	28.10	1.92	8.939	4.284	5.037	7.175	0.327	5.755	0.802	3.062	5.755	0.112	4.284	0.0	1830	78	1826	61	1822	91	0
09LP090 L 188	165.33	40.77	67.92	0.25	9.093	3.329	5.220	6.134	0.344	5.152	0.840	2.905	5.152	0.110	3.329	0	1799	61	1856	52	1907	85	-6
09LP090 L 144	107.46	61.64	44.80	0.57	9.130	2.405	4.745	7.373	0.314	6.969	0.945	3.183	6.969	0.110	2.405	-0.0	1792	44	1775	62	1761	107	2
09LP090 L 201	410.63	137.54	159.31	0.33	9.143	1.779	4.746	4.891	0.315	4.557	0.932	3.177	4.557	0.109	1.779	0.0	1789	32	1775	41	1764	70	1
09LP090 L 111	113.75	64.21	45.97	0.56	9.144	2.695	4.804	5.563	0.319	4.867	0.875	3.139	4.867	0.109	2.695	-0.0	1789	49	1786	47	1783	76	0
09LP090 L 123	428.24	149.88	163.90	0.35	9.146	1.743	4.696	5.174	0.312	4.871	0.942	3.210	4.871	0.109	1.743	-0.0	1788	32	1767	43	1748	75	2
09LP090 L 185	241.74	82.37	99.33	0.34	9.151	2.383	5.090	5.643	0.338	5.115	0.906	2.960	5.115	0.109	2.383	0	1787	43	1834	48	1876	83	-5
09LP090 L 114	137.56	55.84	51.22	0.41	9.219	1.649	4.544	5.415	0.304	5.158	0.953	3.292	5.158	0.108	1.649	-0.0	1774	30	1739	45	1710	77	4
09LP090 L 165	250.67	114.65	99.35	0.46	9.225	2.084	4.755	5.395	0.318	4.976	0.922	3.144	4.976	0.108	2.084	-0.0	1773	38	1777	45	1780	77	-0
09LP090 L 211	416.97	92.00	155.75	0.22	9.231	1.826	4.696	4.986	0.314	4.639	0.931	3.181	4.639	0.108	1.826	-0.0	1772	33	1766	42	1762	72	1
09LP090 L 143	125.35	44.08	47.80	0.35	9.308	3.077	4.549	7.184	0.307	6.491	0.904	3.257	6.491	0.107	3.077	-0.0	1756	56	1740	60	1726	98	2
09LP090 L 181	36.35	23.66	14.67	0.65	9.315	5.311	4.506	7.885	0.304	5.828	0.739	3.285	5.828	0.107	5.311	0	1755	97	1732	66	1713	88	2
09LP090 L 137	465.77	135.37	183.54	0.29	9.340	2.337	4.779	6.415	0.324	5.974	0.931	3.089	5.974	0.107	2.337	-0.0	1750	43	1781	54	1808	94	-3
09LP090 L 212	34.32	5.78	12.92	0.17	9.358	4.453	4.748	7.031	0.322	5.441	0.774	3.103	5.441	0.107	4.453	-0.0	1747	82	1776	59	1801	85	-3
09LP090 L 202	39.63	14.98	15.08	0.38	9.361	3.157	4.488	6.102	0.305	5.222	0.856	3.282	5.222	0.107	3.157	0	1746	58	1729	51	1714	79	2
09LP090 L 112	161.32	43.93	60.32	0.27	9.424	2.150	4.621	4.779	0.316	4.268	0.893	3.166	4.268	0.106	2.150	0	1734	39	1753	40	1770	66	-2
09LP090 L 198	52.12	44.62	21.82	0.86	9.775	4.255	4.189	7.048	0.297	5.618	0.797	3.367	5.618	0.102	4.255	-0.0	1666	79	1672	58	1676	83	-1
09LP090 L 219	1106.44	124.74	377.18	0.11	9.781	2.661	4.217	6.704	0.299	6.153	0.918	3.343	6.153	0.102	2.661	0.0	1665	49	1677	55	1687	91	-1
09LP090 L 190	221.05	53.54	73.51	0.24	9.784	2.678	3.917	6.046	0.278	5.420	0.897	3.597	5.420	0.102	2.678	-0.0	1665	50	1617	49	1581	76	5
09LP090 L 116	68.45	78.43	28.83	1.15	9.808	3.249	4.018	6.767	0.286	5.936	0.877	3.499	5.936	0.102	3.249	0	1660	60	1638	55	1621	85	2

APPENDIX B - DETRITAL ZIRCON ANALYSES, continued

Table B8a, *continued*. Detrital zircon U-Pb geochronologic analyses from sample **09LP090** in Mattson Formation (MM) - Isotope Geology Laboratory, Boise State University

Analysis	U (ppm)	Th (ppm)	Pb* (ppm)	Th/U	Corrected isotope ratios											Apparent ages (Ma)						% disc.	
					$\frac{206\text{Pb}^*}{207\text{Pb}^*}$	$\pm 2\sigma$ (%)	$\frac{207\text{Pb}^*}{235\text{U}^*}$	$\pm 2\sigma$ (%)	$\frac{206\text{Pb}^*}{238\text{U}}$	$\pm 2\sigma$ (%)	error corr.	$\frac{238\text{U}}{206\text{Pb}^*}$	$\pm 2\sigma$ (%)	$\frac{207\text{Pb}^*}{206\text{Pb}^*}$	$\pm 2\sigma$ (%)	error corr.	$\frac{207\text{Pb}^*}{206\text{Pb}^*}$	$\pm 2\sigma$ (Ma)	$\frac{207\text{Pb}^*}{235\text{U}}$	$\pm 2\sigma$ (Ma)	$\frac{206\text{Pb}^*}{238\text{U}^*}$		$\pm 2\sigma$ (Ma)
09LP090 L 149	159.50	34.90	50.51	0.22	9.861	2.605	3.739	6.100	0.267	5.516	0.904	3.740	5.516	0.101	2.605	0	1650	48	1580	49	1527	75	7
09LP090 L 206	320.33	110.29	115.49	0.34	9.907	1.975	4.103	5.943	0.295	5.605	0.943	3.392	5.605	0.101	1.975	0	1641	37	1655	49	1665	82	-1
09LP090 L 204	172.13	59.44	63.79	0.35	9.997	2.555	4.165	5.375	0.302	4.728	0.880	3.312	4.728	0.100	2.555	-0.0	1625	48	1667	44	1701	71	-5
09LP090 L 168	68.05	27.14	22.56	0.40	10.086	3.117	3.734	6.339	0.273	5.520	0.871	3.661	5.520	0.099	3.117	0.0	1608	58	1579	51	1557	76	3
09LP090 L 180	122.64	85.26	46.05	0.70	10.106	2.512	3.905	6.476	0.286	5.968	0.922	3.494	5.968	0.099	2.512	-0.0	1604	47	1615	52	1623	86	-1
09LP090 L 154	20.80	11.90	8.02	0.57	10.141	5.854	4.017	8.862	0.295	6.654	0.751	3.385	6.654	0.099	5.854	-0.0	1598	109	1638	72	1669	98	-4
09LP090 L 113	199.11	19.09	49.60	0.10	10.281	2.252	2.957	5.112	0.221	4.590	0.898	4.535	4.590	0.097	2.252	0.0	1572	42	1397	39	1285	53	18
<b>09LP090 L 205</b>	<b>369.47</b>	<b>151.85</b>	<b>130.70</b>	<b>0.41</b>	<b>10.380</b>	<b>2.112</b>	<b>3.767</b>	<b>5.671</b>	<b>0.284</b>	<b>5.263</b>	<b>0.928</b>	<b>3.526</b>	<b>5.263</b>	<b>0.096</b>	<b>2.112</b>	<b>0</b>	<b>1554</b>	<b>40</b>	<b>1586</b>	<b>45</b>	<b>1609</b>	<b>75</b>	<b>-4</b>
09LP090 L 141	144.30	51.70	49.43	0.36	10.541	3.130	3.635	6.955	0.278	6.211	0.893	3.599	6.211	0.095	3.130	0.0	1525	59	1557	55	1581	87	-4
<b>09LP090 L 191</b>	<b>22.97</b>	<b>24.88</b>	<b>8.09</b>	<b>1.08</b>	<b>10.626</b>	<b>5.943</b>	<b>3.021</b>	<b>7.699</b>	<b>0.233</b>	<b>4.894</b>	<b>0.636</b>	<b>4.295</b>	<b>4.894</b>	<b>0.094</b>	<b>5.943</b>	<b>-0.0</b>	<b>1510</b>	<b>112</b>	<b>1413</b>	<b>59</b>	<b>1349</b>	<b>60</b>	<b>11</b>
09LP090 L 150	265.57	103.84	88.64	0.39	10.797	3.338	3.437	6.822	0.269	5.950	0.872	3.716	5.950	0.093	3.338	0	1480	63	1513	54	1536	81	-4
09LP090 L 135	187.08	46.72	57.38	0.25	10.886	2.914	3.257	6.046	0.257	5.298	0.876	3.889	5.298	0.092	2.914	0	1465	55	1471	47	1475	70	-1
09LP090 L 117	111.00	48.61	33.23	0.44	11.074	2.830	3.012	5.559	0.242	4.785	0.861	4.133	4.785	0.090	2.830	0.0	1432	54	1411	42	1397	60	2
09LP090 L 217	73.65	41.29	23.12	0.56	11.108	3.164	3.029	6.608	0.244	5.801	0.878	4.098	5.801	0.090	3.164	0	1426	60	1415	50	1407	73	1
<b>09LP090 L 164</b>	<b>147.16</b>	<b>158.84</b>	<b>42.25</b>	<b>1.08</b>	<b>11.174</b>	<b>4.520</b>	<b>2.430</b>	<b>6.632</b>	<b>0.197</b>	<b>4.853</b>	<b>0.732</b>	<b>5.078</b>	<b>4.853</b>	<b>0.089</b>	<b>4.520</b>	<b>-0.0</b>	<b>1415</b>	<b>86</b>	<b>1252</b>	<b>48</b>	<b>1159</b>	<b>51</b>	<b>18</b>
09LP090 L 187	216.03	85.01	65.05	0.39	11.394	2.262	2.978	6.458	0.246	6.049	0.937	4.064	6.049	0.088	2.262	0	1377	43	1402	49	1418	77	-3
09LP090 L 214	68.70	31.17	21.28	0.45	11.549	4.001	2.939	6.413	0.246	5.012	0.781	4.062	5.012	0.087	4.001	-0.0	1351	77	1392	49	1419	64	-5
09LP090 L 163	720.64	159.52	184.19	0.22	11.583	2.125	2.627	5.371	0.221	4.933	0.918	4.532	4.933	0.086	2.125	0.0	1346	41	1308	40	1285	57	4
09LP090 L 199	50.77	24.40	14.77	0.48	11.650	4.489	2.719	6.903	0.230	5.243	0.760	4.352	5.243	0.086	4.489	0	1334	87	1334	51	1333	63	0
09LP090 L 138	833.72	32.13	208.70	0.04	11.755	2.846	2.670	8.568	0.228	8.081	0.943	4.393	8.081	0.085	2.846	-0.0	1317	55	1320	63	1322	97	-0
09LP090 L 121	101.45	72.22	28.06	0.71	11.817	3.673	2.425	6.371	0.208	5.206	0.817	4.811	5.206	0.085	3.673	-0.0	1307	71	1250	46	1217	58	7
09LP090 L 197	17.45	13.30	4.90	0.76	11.871	5.200	2.378	8.843	0.205	7.153	0.809	4.884	7.153	0.084	5.200	0.0	1298	101	1236	63	1201	78	7
09LP090 L 157	38.62	13.69	9.23	0.35	12.198	4.763	2.217	7.591	0.196	5.912	0.779	5.098	5.912	0.082	4.763	0.0	1245	93	1186	53	1155	62	7
09LP090 L 142	224.10	79.66	59.11	0.36	12.238	2.463	2.439	6.483	0.216	5.997	0.925	4.619	5.997	0.082	2.463	0	1239	48	1254	47	1263	69	-2
09LP090 L 215	207.89	120.45	53.20	0.58	12.341	2.642	2.192	5.610	0.196	4.949	0.882	5.097	4.949	0.081	2.642	0.0	1222	52	1178	39	1155	52	6
09LP090 L 173	51.83	25.88	11.27	0.50	12.555	5.542	1.969	8.179	0.179	6.015	0.735	5.577	6.015	0.080	5.542	-0.0	1188	109	1105	55	1063	59	11
09LP090 L 208	221.67	105.72	51.63	0.48	12.591	2.453	2.026	5.968	0.185	5.441	0.912	5.406	5.441	0.079	2.453	-0.0	1183	48	1124	41	1094	55	7
09LP090 L 179	538.70	294.32	136.54	0.55	12.602	1.877	2.223	5.768	0.203	5.454	0.946	4.922	5.454	0.079	1.877	0	1181	37	1188	40	1192	59	-1
09LP090 L 159	655.68	92.75	144.30	0.14	12.638	2.031	2.118	5.491	0.194	5.101	0.929	5.151	5.101	0.079	2.031	-0.0	1175	40	1155	38	1144	53	3
09LP090 L 119	123.03	41.86	29.59	0.34	12.705	3.236	2.184	6.553	0.201	5.698	0.870	4.970	5.698	0.079	3.236	-0.0	1165	64	1176	46	1182	62	-1
09LP090 L 207	152.62	71.21	38.18	0.47	12.724	2.668	2.173	6.875	0.201	6.336	0.922	4.987	6.336	0.079	2.668	0.0	1162	53	1172	48	1178	68	-1
09LP090 L 200	85.43	29.50	20.53	0.35	12.734	4.039	2.151	6.388	0.199	4.949	0.775	5.034	4.949	0.079	4.039	-0.0	1160	80	1165	44	1168	53	-1
09LP090 L 193	186.81	47.46	44.94	0.25	12.774	3.104	2.207	6.225	0.205	5.396	0.867	4.890	5.396	0.078	3.104	-0.0	1154	62	1183	43	1199	59	-4
09LP090 L 126	120.17	59.04	29.49	0.49	12.837	2.726	2.102	6.552	0.196	5.958	0.909	5.110	5.958	0.078	2.726	-0.0	1144	54	1149	45	1152	63	-1
09LP090 L 162	45.14	29.92	9.61	0.66	13.064	6.698	1.740	8.948	0.165	5.933	0.663	6.066	5.933	0.077	6.698	0	1109	134	1023	58	984	54	11
09LP090 L 183	150.08	67.52	34.92	0.45	13.068	3.926	2.010	6.970	0.190	5.759	0.826	5.250	5.759	0.077	3.926	-0.0	1109	78	1119	47	1124	59	-1
09LP090 L 172	299.81	45.88	62.03	0.15	13.101	2.830	1.950	6.056	0.185	5.355	0.884	5.399	5.355	0.076	2.830	-0.0	1104	57	1098	41	1096	54	1
09LP090 L 189	67.84	40.70	18.14	0.60	13.113	4.236	2.158	8.273	0.205	7.106	0.859	4.873	7.106	0.076	4.236	0	1102	85	1168	57	1203	78	-9
09LP090 L 177	1138.64	437.49	234.55	0.38	13.198	1.768	1.811	5.136	0.173	4.822	0.939	5.769	4.822	0.076	1.768	0	1089	35	1049	34	1031	46	5
09LP090 L 125	156.41	55.70	34.19	0.36	13.226	3.309	1.893	6.386	0.182	5.462	0.855	5.506	5.462	0.076	3.309	0.0	1085	66	1079	42	1076	54	1
09LP090 L 220	438.14	211.60	98.85	0.48	13.238	2.925	1.888	6.809	0.181	6.149	0.903	5.517	6.149	0.076	2.925	0.0	1083	59	1077	45	1074	61	1
09LP090 L 209	35.69	18.40	8.58	0.52	13.307	6.622	1.951	8.688	0.188	5.625	0.647	5.311	5.625	0.075	6.622	0	1072	133	1099	58	1112	57	-4

APPENDIX B - DETRITAL ZIRCON ANALYSES, continued

Table B8a, *continued*. Detrital zircon U-Pb geochronologic analyses from sample **09LP090** in Mattson Formation (MM) - Isotope Geology Laboratory, Boise State University

Analysis	U (ppm)	Th (ppm)	Pb* (ppm)	Th/U	Corrected isotope ratios							Apparent ages (Ma)						% disc.					
					$\frac{^{206}\text{Pb}^*}{^{207}\text{Pb}^*}$	$\pm 2\sigma$ (%)	$\frac{^{207}\text{Pb}^*}{^{235}\text{U}^*}$	$\pm 2\sigma$ (%)	$\frac{^{206}\text{Pb}^*}{^{238}\text{U}}$	$\pm 2\sigma$ (%)	error corr.	$\frac{^{238}\text{U}}{^{206}\text{Pb}^*}$	$\pm 2\sigma$ (%)	$\frac{^{207}\text{Pb}^*}{^{206}\text{Pb}^*}$	$\pm 2\sigma$ (%)	error corr.	$\frac{^{207}\text{Pb}^*}{^{206}\text{Pb}^*}$		$\pm 2\sigma$ (Ma)	$\frac{^{207}\text{Pb}^*}{^{235}\text{U}}$	$\pm 2\sigma$ (Ma)	$\frac{^{206}\text{Pb}^*}{^{238}\text{U}^*}$	$\pm 2\sigma$ (Ma)
09LP090 L 120	73.81	135.55	20.62	1.84	13.309	4.622	1.689	7.628	0.163	6.069	0.796	6.135	6.069	0.075	4.622	0.0	<b>1072</b>	<b>93</b>	1004	49	973	55	9
09LP090 L 174	309.63	241.77	71.51	0.78	13.354	2.079	1.861	6.024	0.180	5.653	0.939	5.549	5.653	0.075	2.079	0.0	<b>1065</b>	<b>42</b>	1067	40	1068	56	-0
09LP090 L 213	170.25	110.88	44.06	0.65	13.359	2.902	2.033	5.926	0.197	5.166	0.872	5.076	5.166	0.075	2.902	0	<b>1065</b>	<b>58</b>	1127	40	1159	55	-9
09LP090 L 127	210.83	132.65	45.20	0.63	13.502	2.956	1.677	6.579	0.164	5.877	0.893	6.090	5.877	0.074	2.956	0.0	<b>1043</b>	<b>60</b>	1000	42	980	53	6
09LP090 L 151	42.55	40.92	9.52	0.96	13.530	5.020	1.553	8.072	0.152	6.322	0.783	6.561	6.322	0.074	5.020	-0.0	<b>1039</b>	<b>101</b>	952	50	915	54	12
09LP090 L 175	310.05	37.28	55.03	0.12	13.568	3.501	1.631	8.618	0.161	7.875	0.914	6.230	7.875	0.074	3.501	0	<b>1033</b>	<b>71</b>	982	54	960	70	7
09LP090 L 203	200.39	4.79	40.19	0.02	13.581	3.318	1.882	6.652	0.185	5.765	0.867	5.395	5.765	0.074	3.318	0.0	<b>1031</b>	<b>67</b>	1075	44	1096	58	-6
09LP090 L 218	103.67	37.66	23.26	0.36	13.636	4.297	1.877	6.501	0.186	4.878	0.750	5.388	4.878	0.073	4.297	0	<b>1023</b>	<b>87</b>	1073	43	1098	49	-7
09LP090 L 139	107.97	30.46	22.97	0.28	13.649	3.853	1.811	7.829	0.179	6.815	0.871	5.577	6.815	0.073	3.853	0	<b>1021</b>	<b>78</b>	1050	51	1063	67	-4
09LP090 L 210	202.32	119.72	46.56	0.59	13.724	2.813	1.781	5.730	0.177	4.992	0.871	5.643	4.992	0.073	2.813	0	<b>1010</b>	<b>57</b>	1038	37	1052	48	-4
09LP090 L 167	62.11	58.76	15.46	0.95	13.813	5.309	1.829	8.228	0.183	6.286	0.764	5.459	6.286	0.072	5.309	-0.0	<b>997</b>	<b>108</b>	1056	54	1084	63	-9
09LP090 L 118	364.57	140.84	73.09	0.39	13.882	1.834	1.646	5.332	0.166	5.006	0.939	6.035	5.006	0.072	1.834	0.0	<b>987</b>	<b>37</b>	988	34	988	46	-0
09LP090 L 194	284.30	165.19	59.29	0.58	13.920	2.765	1.600	5.668	0.162	4.948	0.873	6.191	4.948	0.072	2.765	0	<b>981</b>	<b>56</b>	970	35	965	44	2
09LP090 L 182	117.21	112.68	27.00	0.96	14.038	3.844	1.623	7.518	0.165	6.461	0.859	6.052	6.461	0.071	3.844	0	<b>964</b>	<b>78</b>	979	47	986	59	-2
09LP090 L 134	140.54	40.04	28.69	0.28	14.144	3.366	1.674	6.003	0.172	4.970	0.828	5.824	4.970	0.071	3.366	0	<b>949</b>	<b>69</b>	999	38	1021	47	-8
09LP090 L 171	290.88	151.95	51.23	0.52	14.207	2.611	1.419	6.946	0.146	6.437	0.927	6.841	6.437	0.070	2.611	0.0	<b>940</b>	<b>54</b>	897	41	879	53	6
09LP090 L 186	152.86	1.42	26.50	0.01	14.589	3.859	1.529	6.702	0.162	5.480	0.818	6.181	5.480	0.069	3.859	0	<b>885</b>	<b>80</b>	942	41	967	49	-9
09LP090 L 152	143.78	12.97	17.13	0.09	14.684	3.410	0.979	6.117	0.104	5.078	0.830	9.586	5.078	0.068	3.410	-0.0	872	71	693	31	<b>640</b>	<b>31</b>	27
09LP090 L 161	171.01	37.46	19.59	0.22	15.446	4.887	0.864	7.096	0.097	5.145	0.725	10.328	5.145	0.065	4.887	0	766	103	632	33	<b>596</b>	<b>29</b>	22
09LP090 L 158	32.45	12.49	2.82	0.38	19.417	11.970	0.515	14.434	0.073	8.067	0.559	13.783	8.067	0.052	11.970	-0.0	263	275	422	50	<b>452</b>	<b>35</b>	-71
09LP090 L 196	191.20	170.39	19.16	0.89	18.347	4.569	0.536	6.781	0.071	5.010	0.739	14.022	5.010	0.055	4.569	0	392	103	436	24	<b>444</b>	<b>22</b>	-13
09LP090 L 124	649.56	879.87	68.91	1.35	18.068	2.890	0.525	5.852	0.069	5.088	0.870	14.537	5.088	0.055	2.890	0	426	64	428	20	<b>429</b>	<b>21</b>	-1
09LP090 L 122	360.74	76.67	27.96	0.21	17.408	3.526	0.543	6.312	0.069	5.235	0.829	14.592	5.235	0.057	3.526	-0.0	509	78	440	23	<b>427</b>	<b>22</b>	16
09LP090 L 128	279.43	175.33	24.62	0.63	17.457	4.577	0.538	7.352	0.068	5.753	0.783	14.693	5.753	0.057	4.577	0	502	101	437	26	<b>424</b>	<b>24</b>	16

Notes:

Yellow highlighted rows are samples that intersected inclusions.  
 Isotope ratios and ages are NOT corrected for initial common Pb.  
 Isotope ratio and apparent age errors include systematic calibration errors of 4.82108305642064% ( $^{208}\text{Pb}/^{232}\text{Th}$ ), 0.431914068815385% ( $^{207}\text{Pb}/^{206}\text{Pb}$ ), 1.64420908282226% ( $^{206}\text{Pb}/^{238}\text{U}$ ) (all 1-sigma).  
 Sweep-by-sweep downhole fractionation of U/Pb ratios NOT corrected via Si/Zr fractionation factor.  
 Backgrounds were monitored during sweeps 10 to 27. Sample counts were integrated from sweeps 36 to 69.  
 Ablation used a laser spot size of 25 microns, and a laser firing repetition rate of 10 Hz.





APPENDIX B - DETRITAL ZIRCON ANALYSES, continued

Table B8b, continued. Detrital zircon trace element analyses from sample 09LP090 in Mattson Formation (MM) - Isotope Geology Laboratory, Boise State University

Analysis	Concentrations (ppm)																						
	P	Ti	Y	Zr	Nb	La	Ce	Pr	Nd	Sm	Eu	Gd	Tb	Dy	Ho	Er	Tm	Yb	Lu	Hf	Ta	Th	U
09LP090 L 127	195.639	20.152	610.418	499648.906	6.990		51.392	0.161	1.536	3.905	0.521	13.686	5.295	62.526	22.912	94.778	27.611	305.478	33.435	8349.793	3.758	132.652	210.829
09LP090 L 151	376.028	26.406	1275.043	486514.853	1.305		4.514	0.157	3.781	8.658	0.432	41.071	13.663	152.583	47.772	183.586	44.627	459.335	43.819	6995.448	0.625	40.921	42.551
09LP090 L 175	670.592	6.511	1841.566	637863.652	0.768		0.946	0.029	0.942	2.358	0.016	20.039	10.847	160.546	65.484	301.359	75.994	784.462	97.478	12095.783	0.654	37.281	310.052
09LP090 L 203	68.800	0.574	112.126	480282.265	4.880	0.232	3.141	0.045	0.169	0.398	0.003	1.987	0.901	16.808	7.161	33.578	9.656	132.204	13.298	9194.006	4.048	4.792	200.389
09LP090 L 218	198.493	9.409	384.145	484917.948	4.749	0.035	32.018	0.053	0.873	1.533	0.380	9.130	2.900	37.406	13.593	59.731	17.726	207.968	21.917	7806.998	3.010	37.664	103.670
09LP090 L 139	183.809	6.259	357.371	470577.236	3.351		9.986	0.053	0.478	1.339	0.055	7.017	2.234	31.767	13.143	57.959	17.056	211.717	21.675	6971.615	1.998	30.457	107.973
09LP090 L 210	205.938	15.390	426.221	476593.051	3.070		28.526	0.009	0.783	1.846	0.422	10.561	3.675	47.021	16.401	68.213	20.622	257.525	25.899	7275.279	1.888	119.724	202.322
09LP090 L 167	252.694	16.902	597.430	598693.499	3.281	0.039	14.011	0.049	1.380	2.890	0.271	15.636	5.481	67.293	23.190	95.281	24.381	238.790	27.882	10032.079	1.356	58.764	62.105
09LP090 L 118	208.804	5.707	1149.029	559561.551	17.419	0.127	14.963	0.056	1.836	5.467	0.318	30.182	10.789	125.318	45.480	182.578	44.961	452.096	48.159	10800.591	7.287	140.839	364.568
09LP090 L 194	428.684	8.674	1158.848	460746.093	2.878		9.407	0.095	1.871	4.335	0.100	28.597	10.473	129.163	46.019	179.303	45.571	486.059	42.924	8249.393	1.795	165.191	284.296
09LP090 L 182	77.964	4.426	408.894	533036.331	6.603	0.325	38.069	0.037	0.666	0.929	0.201	4.914	2.020	26.736	11.521	64.813	21.957	326.540	44.669	9865.051	2.063	112.678	117.205
09LP090 L 134	134.209	9.307	453.517	484405.114	1.749	0.008	7.880	0.000	0.496	1.556	0.116	9.397	3.457	46.012	16.567	69.307	20.266	220.395	22.805	7985.909	1.062	40.040	140.538
09LP090 L 171	277.664	4.751	1136.368	661337.071	4.315	0.014	10.820		0.858	2.604	0.048	20.751	8.660	106.772	41.223	177.675	42.382	405.755	54.497	13691.798	3.188	151.947	290.878
09LP090 L 186	54.039	2.178	174.211	507661.011	0.147		0.136				0.130	1.035	0.766	12.305	5.514	30.314	10.174	150.106	20.729	7167.442	0.009	1.420	152.858
09LP090 L 152	104.815	2.325	273.266	459278.457	1.292		0.769		0.133	0.958	0.109	4.672	1.717	26.592	9.817	42.372	11.731	134.863	12.764	8239.922	1.334	12.969	143.777
09LP090 L 161	339.770	7.421	555.248	532673.691	4.184	0.056	7.176	0.080	1.257	2.858	0.489	11.367	3.745	54.097	21.330	94.999	30.802	401.225	46.062	9180.418	2.178	37.457	171.006
09LP090 L 158	100.184	11.013	185.018	512747.242	0.150	0.046	4.638	0.040	0.270	0.672	0.239	3.422	1.527	19.440	6.745	28.959	8.104	98.131	10.782	6816.566	0.179	12.489	32.452
09LP090 L 196	206.258	16.796	892.552	458192.682	0.652	0.104	5.072	0.254	4.502	5.341	1.705	22.753	8.086	93.565	32.632	133.655	37.556	426.727	43.080	4987.787	0.731	170.391	191.196
09LP090 L 124	512.282	16.532	2760.061	539355.602	2.465	0.010	29.315	0.718	10.944	20.094	9.164	90.376	28.329	313.117	104.333	421.316	108.488	1172.904	131.061	6642.730	0.890	879.868	649.564
09LP090 L 122	792.533	5.157	1899.751	557197.217	2.318	0.026	2.661	0.097	2.067	6.226	0.189	37.881	15.448	196.062	70.984	299.376	75.314	803.514	84.556	10027.353	2.220	76.669	360.745
09LP090 L 128	160.839	17.804	1047.819	515442.476	0.611	0.014	8.873	0.410	6.348	9.705	0.947	36.731	10.858	115.815	39.422	161.935	42.382	423.473	43.250	7064.838	0.468	175.326	279.427

Notes:

Yellow highlighted rows are samples that intersected inclusions.

Trace element concentrations in ppm, calculated using mean count rate method.

Backgrounds were monitored during sweeps 10 to 27. Sample counts were integrated from sweeps 36 to 69.

Ablation used a laser spot size of 25 microns, and a laser firing repetition rate of 10 Hz.





APPENDIX B - DETRITAL ZIRCON ANALYSES, continued

Table B8c, *continued*. Detrital zircon calculated ratios and values from sample **09LP090** in Mattson Formation (MM) - Isotope Geology Laboratory, Boise State University

Analysis	CI chondrite normalizing values from Sun and McDonough (1989)														Ti-in-zircon T (°C)	Ce/Ce*	Eu/Eu*	(Sm/Nd) <sub>cn</sub>	(Lu/Nd) <sub>cn</sub>	Lu/Hf	Nb/Ta	Nb/U	Th/U	Th/Y	Y/Hf
	0.237	0.612	0.095	0.467	0.153	0.058	0.206	0.037	0.254	0.057	0.166	0.026	0.170	0.025											
	La	Ce	Pr	Nd	Sm	Eu	Gd	Tb	Dy	Ho	Er	Tm	Yb	Lu											
09LP090 L 174	0.137	31.795	5.465	19.388	79.133	48.774	260.586	495.024	876.848	1464.452	2109.270	3321.875	4813.367	4482.874	873	11.35	0.29	4.08	231.22	0.01	1.17	0.01	0.78	0.11	0.22
09LP090 L 213	0.022	26.821	0.877	2.317	21.735	1.710	84.591	183.331	345.130	580.938	830.122	1503.360	2489.536	1590.819	776	59.65	0.03	9.38	686.57	0.01	2.36	0.10	0.65	0.13	0.11
09LP090 L 127	0.043	83.974	1.697	3.289	25.525	8.986	66.598	141.571	246.165	404.803	572.677	1082.771	1796.930	1316.323	874	96.56	0.20	7.76	400.19	0.00	1.86	0.03	0.63	0.22	0.07
09LP090 L 151	0.041	7.376	1.648	8.097	56.586	7.443	199.857	365.313	600.720	844.022	1109.280	1750.060	2701.968	1725.157	907	8.73	0.06	6.99	213.06	0.01	2.09	0.03	0.96	0.03	0.18
09LP090 L 175	0.008	1.546	0.310	2.018	15.409	0.283	97.513	290.023	632.072	1156.960	1820.897	2980.157	4614.484	3837.726	754	9.74	0.01	7.64	1901.64	0.01	1.17	0.00	0.12	0.02	0.15
09LP090 L 203	0.981	5.133	0.474	0.363	2.599	0.046	9.671	24.086	66.173	126.512	202.890	378.683	777.669	523.533	565	7.05	0.01	7.17	1443.99	0.00	1.21	0.02	0.02	0.04	0.01
09LP090 L 218	0.147	52.317	0.558	1.870	10.019	6.551	44.429	77.552	147.266	240.157	360.911	695.137	1223.341	862.862	790	148.27	0.24	5.36	461.51	0.00	1.58	0.05	0.36	0.10	0.05
09LP090 L 139	0.014	16.316	0.562	1.024	8.754	0.941	34.144	59.743	125.067	232.203	350.203	668.853	1245.392	853.330	750	56.63	0.04	8.54	832.95	0.00	1.68	0.03	0.28	0.09	0.05
09LP090 L 210	0.002	46.612	0.090	1.677	12.067	7.278	51.392	98.270	185.123	289.772	412.164	808.689	1514.854	1019.630	843	1007.94	0.23	7.19	607.90	0.00	1.63	0.02	0.59	0.28	0.06
09LP090 L 167	0.165	22.894	0.520	2.955	18.887	4.678	76.089	146.550	264.932	409.721	575.714	956.134	1404.648	1097.709	853	66.84	0.10	6.39	371.50	0.00	2.42	0.05	0.95	0.10	0.06
09LP090 L 118	0.538	24.450	0.586	3.932	35.735	5.481	146.872	288.475	493.377	803.542	1103.190	1763.187	2659.390	1896.037	741	43.52	0.06	9.09	482.22	0.00	2.39	0.05	0.39	0.12	0.11
09LP090 L 194	0.025	15.371	1.005	4.006	28.335	1.725	139.158	280.024	508.518	813.048	1083.400	1787.083	2859.172	1689.910	782	29.85	0.02	7.07	421.87	0.01	1.60	0.01	0.58	0.14	0.14
09LP090 L 182	1.370	62.203	0.388	1.426	6.072	3.468	23.913	53.997	105.260	203.553	391.618	861.066	1920.824	1758.621	718	70.77	0.23	4.26	1233.64	0.00	3.20	0.06	0.96	0.28	0.04
09LP090 L 134	0.033	12.877	0.005	1.062	10.171	1.998	45.727	92.440	181.151	292.701	418.773	794.727	1296.444	897.820	789	676.02	0.07	9.58	845.65	0.00	1.65	0.01	0.28	0.09	0.06
09LP090 L 171	0.061	17.680	0.411	1.838	17.023	0.834	100.979	231.556	420.361	728.314	1073.562	1662.058	2386.794	2145.543	724	74.97	0.01	9.26	1167.32	0.00	1.35	0.01	0.52	0.13	0.08
09LP090 L 186		0.222				2.241	5.035	20.485	48.445	97.419	183.168	398.984	882.978	816.086	659					0.00	16.47	0.00	0.01	0.01	0.02
09LP090 L 152		1.257	0.064	0.285	6.262	1.885	22.736	45.898	104.691	173.439	256.025	460.028	793.309	502.537	664		0.13	22.00	1765.47	0.00	0.97	0.01	0.09	0.05	0.03
09LP090 L 161	0.236	11.726	0.844	2.692	18.680	8.438	55.315	100.133	212.979	376.852	574.012	1207.939	2360.149	1813.462	766	21.70	0.23	6.94	673.71	0.01	1.92	0.02	0.22	0.07	0.06
09LP090 L 158	0.192	7.579	0.416	0.578	4.394	4.117	16.650	40.825	76.534	119.164	174.976	317.796	577.241	424.491	806	24.90	0.39	7.60	733.94	0.00	0.84	0.00	0.38	0.07	0.03
09LP090 L 196	0.441	8.287	2.672	9.640	34.907	29.397	110.719	216.204	368.365	576.534	807.583	1472.769	2510.161	1696.073	853	5.33	0.40	3.62	175.95	0.01	0.89	0.00	0.89	0.19	0.18
09LP090 L 124	0.042	47.901	7.554	23.434	131.334	157.999	439.788	757.448	1232.743	1843.344	2545.713	4254.441	6899.436	5159.866	851	12.61	0.55	5.60	220.19	0.02	2.77	0.00	1.35	0.32	0.42
09LP090 L 122	0.110	4.349	1.024	4.426	40.693	3.254	184.336	413.035	771.899	1254.139	1808.916	2953.479	4726.552	3328.970	732	7.67	0.03	9.19	752.12	0.01	1.04	0.01	0.21	0.04	0.19
09LP090 L 128	0.057	14.499	4.316	13.593	63.430	16.334	178.739	290.327	455.965	696.499	978.457	1662.022	2491.017	1702.762	859	6.63	0.13	4.67	125.27	0.01	1.31	0.00	0.63	0.17	0.15

Notes:

Activity (SiO<sub>2</sub>) = 1; activity (TiO<sub>2</sub>) = 0.6.

Yellow highlighted rows are samples that intersected inclusions.

Trace element concentrations in ppm, calculated using mean count rate method.

Backgrounds were monitored between sweeps 10 to 27. Sample counts were integrated from sweeps 36 to 69.

Ablation used a laser spot size of 25 microns, and a laser firing repetition rate of 10 Hz.

## APPENDIX C - WHOLE ROCK GEOCHEMISTRY

**Table C1.** Analyses for volcanic rocks in the undivided Vampire-Narchilla unit. All coordinates are NAD83 datum, zone 9. (See analytical notes at the end of the table.)

Sample		07LP044A	07LP044B	07LP055	Sample		09TOA006
Station		07LP044	07LP044	07LP055	Station		09TOA006
Rock		flow	flow	diabase	Rock		diabase
Unit		PcVN-v	PcVN-v	PcVN-v	Unit		PcVN-v
UTM E		594608	594608	594412	UTM E		594385
UTM N		6706355	6706355	6714284	UTM N		6714232
SiO <sub>2</sub> (%)	FUS XRF	47.14	46.93	44.27	SiO <sub>2</sub> (%)	FUS ICP	45.61
Al <sub>2</sub> O <sub>3</sub> (%)	FUS XRF	16.90	16.62	16.79	Al <sub>2</sub> O <sub>3</sub> (%)	FUS ICP	16.25
FeO (%)	TITR	NA	NA	NA	FeO (%)	TITR	7.10
Fe <sub>2</sub> O <sub>3</sub> (%)	DIFF	NA	NA	NA	Fe <sub>2</sub> O <sub>3</sub> (%)	DIFF	4.06
Fe <sub>2</sub> O <sub>3</sub> * (%)	FUS XRF	10.61	10.50	12.50	Fe <sub>2</sub> O <sub>3</sub> * (%)	FUS ICP	11.95
MnO (%)	FUS XRF	0.204	0.213	0.253	MnO (%)	FUS ICP	0.222
MgO (%)	FUS XRF	2.63	2.61	3.71	MgO (%)	FUS ICP	3.53
CaO (%)	FUS XRF	5.93	6.36	8.57	CaO (%)	FUS ICP	7.43
Na <sub>2</sub> O (%)	FUS XRF	4.86	4.84	3.68	Na <sub>2</sub> O (%)	FUS ICP	3.5
K <sub>2</sub> O (%)	FUS XRF	2.18	2.18	2.20	K <sub>2</sub> O (%)	FUS ICP	2.71
TiO <sub>2</sub> (%)	FUS XRF	2.07	2.06	2.74	TiO <sub>2</sub> (%)	FUS ICP	2.816
P <sub>2</sub> O <sub>5</sub> (%)	FUS XRF	1.25	1.23	1.91	P <sub>2</sub> O <sub>5</sub> (%)	FUS ICP	1.94
L.O.I. (%)		5.81	6.11	3.00	L.O.I. (%)		2.31
<b>Total (%)</b>		<b>99.58</b>	<b>99.65</b>	<b>99.62</b>	<b>Total (%)</b>		<b>97.48</b>
Au (ppb)	INAA	NA	NA	NA	Au (ppb)	INAA	-2
As (ppm)	INAA	NA	NA	NA	As (ppm)	INAA	-0.5
Br (ppm)	INAA	NA	NA	NA	Br (ppm)	INAA	-0.5
Cr (ppm)	INAA	NA	NA	NA	Cr (ppm)	INAA	-5
Ir (ppm)	INAA	NA	NA	NA	Ir (ppm)	INAA	-5
Sc (ppm)	INAA	1.164	1.304	1.395	Sc (ppm)	INAA	7.0
Se (ppm)	INAA	NA	NA	NA	Se (ppm)	INAA	-3
Sb (ppm)	INAA	NA	NA	NA	Sb (ppm)	INAA	0.3
Sc (ppm)	FUS ICP	NA	NA	NA	Sc (ppm)	FUS ICP	8
Be (ppm)	FUS ICP	NA	NA	NA	Be (ppm)	FUS ICP	2
V (ppm)	FUS ICP-MS	56	97	56	V (ppm)	FUS ICP	115
Cr (ppm)	FUS ICP-MS	-20	-20	-20	Cr (ppm)	FUS ICP-MS	-20
Co (ppm)	FUS ICP-MS	13	12	18	Co (ppm)	FUS ICP-MS	17
Ni (ppm)	FUS ICP-MS	-20	-20	-20	Ni (ppm)	FUS ICP-MS	-20
Cu (ppm)	FUS ICP-MS	-10	-10	20	Cu (ppm)	FUS ICP-MS	-10
Zn (ppm)	FUS ICP-MS	90	80	170	Zn (ppm)	FUS ICP-MS	110
Ga (ppm)	FUS ICP-MS	21	20	19	Ga (ppm)	FUS ICP-MS	18
Ge (ppm)	FUS ICP-MS	1.6	1.4	1.5	Ge (ppm)	FUS ICP-MS	1.6
As (ppm)	FUS ICP-MS	-5	-5	11	As (ppm)	FUS ICP-MS	-5
Rb (ppm)	FUS ICP-MS	43	41	34	Rb (ppm)	FUS ICP-MS	41
Sr (ppm)	FUS ICP-MS	296	307	2320	Sr (ppm)	FUS ICP	2106
Y (ppm)	FUS ICP-MS	46.6	46.9	44.5	Y (ppm)	FUS ICP-MS	43.1
Zr (ppm)	FUS ICP-MS	103	73	24	Zr (ppm)	FUS ICP-MS	401

## APPENDIX C - WHOLE ROCK GEOCHEMISTRY, continued

**Table C1, continued.** Analyses for volcanic rocks in the undivided Vampire-Narchilla unit. All coordinates are NAD83 datum, zone 9. (See analytical notes at the end of the table.)

Sample		07LP044A	07LP044B	07LP055	Sample		09TOA006
Station		07LP044	07LP044	07LP055	Station		09TOA006
Nb (ppm)	FUS ICP-MS	113	111	80	Nb (ppm)	FUS ICP-MS	115
Mo (ppm)	FUS ICP-MS	-2	-2	3	Mo (ppm)	FUS ICP-MS	-2
Ag (ppm)	FUS ICP-MS	-0.5	-0.5	-0.5	Ag (ppm)	FUS ICP-MS	1.1
In (ppm)	FUS ICP-MS	-0.1	-0.1	-0.1	In (ppm)	FUS ICP-MS	-0.1
Sn (ppm)	FUS ICP-MS	7	2	2	Sn (ppm)	FUS ICP-MS	2
Sb (ppm)	FUS ICP-MS	3.1	1.2	-0.2	Sb (ppm)	FUS ICP-MS	0.5
Cs (ppm)	FUS ICP-MS	1.0	0.8	1.0	Cs (ppm)	FUS ICP-MS	1.0
Ba (ppm)	FUS ICP-MS	828	826	974	Ba (ppm)	FUS ICP	1095
La (ppm)	FUS ICP-MS	105	102	88.1	La (ppm)	FUS ICP-MS	94.7
Ce (ppm)	FUS ICP-MS	211	206	187	Ce (ppm)	FUS ICP-MS	209
Pr (ppm)	FUS ICP-MS	27.1	26.9	25.3	Pr (ppm)	FUS ICP-MS	25.0
Nd (ppm)	FUS ICP-MS	93.7	91.9	90.8	Nd (ppm)	FUS ICP-MS	101
Sm (ppm)	FUS ICP-MS	15.80	15.60	15.90	Sm (ppm)	FUS ICP-MS	17.8
Eu (ppm)	FUS ICP-MS	4.82	4.81	5.16	Eu (ppm)	FUS ICP-MS	4.98
Gd (ppm)	FUS ICP-MS	13.10	12.90	13.50	Gd (ppm)	FUS ICP-MS	13.8
Tb (ppm)	FUS ICP-MS	1.83	1.80	1.86	Tb (ppm)	FUS ICP-MS	1.56
Dy (ppm)	FUS ICP-MS	9.20	9.17	8.96	Dy (ppm)	FUS ICP-MS	9.22
Ho (ppm)	FUS ICP-MS	1.65	1.63	1.61	Ho (ppm)	FUS ICP-MS	1.64
Er (ppm)	FUS ICP-MS	4.51	4.48	4.25	Er (ppm)	FUS ICP-MS	4.31
Tm (ppm)	FUS ICP-MS	0.616	0.613	0.575	Tm (ppm)	FUS ICP-MS	0.557
Yb (ppm)	FUS ICP-MS	3.82	3.74	3.37	Yb (ppm)	FUS ICP-MS	3.39
Lu (ppm)	FUS ICP-MS	0.552	0.530	0.480	Lu (ppm)	FUS ICP-MS	0.514
Hf (ppm)	FUS ICP-MS	2.8	1.9	0.6	Hf (ppm)	FUS ICP-MS	7.8
Ta (ppm)	FUS ICP-MS	8.60	8.51	5.99	Ta (ppm)	FUS ICP-MS	7.93
W (ppm)	FUS ICP-MS	1.1	1.0	1.1	W (ppm)	FUS ICP-MS	0.7
Tl (ppm)	FUS ICP-MS	0.12	0.12	0.14	Tl (ppm)	FUS ICP-MS	0.06
Pb (ppm)	FUS ICP-MS	-5	-5	6	Pb (ppm)	FUS ICP-MS	5
Bi (ppm)	FUS ICP-MS	0.2	0.1	0.2	Bi (ppm)	FUS ICP-MS	-0.1
Th (ppm)	FUS ICP-MS	12.30	12.00	10.00	Th (ppm)	FUS ICP-MS	7.73
U (ppm)	FUS ICP-MS	2.76	2.73	4.10	U (ppm)	FUS ICP-MS	1.76

\* Total iron reported as Fe<sub>2</sub>O<sub>3</sub>.

### Notes:

Samples were analyzed at Activation Laboratories Ltd., Ancaster, Ontario, Canada.

Major oxides and most minor elements were determined by X-Ray Fluorescence (XRF) on a fusion sample containing a lithium metaborate/tetraborate flux, in 2007.

Those determined by Inductively Coupled Plasma (ICP) were performed in 2009, also on a fusion sample.

FeO was determined by titration.

Au, As, Br, Cr, Ir, Sc, Se, Sb were determined by Instrumental Neutron Activation Analysis (INAA).

Trace elements and REE were analyzed by ICP-Mass Spectrometry (MS) or ICP on a fusion sample.

An elemental abundance below the detection limit is shown as a negative value.

NA = not analyzed

## APPENDIX C - WHOLE ROCK GEOCHEMISTRY, continued

**Table C2a.** Analyses of dikes and volcanic rocks within the Toobally and Crow formations (2003). All coordinates are NAD83 datum, zone 9. (See analytical notes at the end of the table.)

Sample		03LP003	03LP004	03LP010	03LP017	03LP021	03LP023	03LP028	03LP028%	03LP029
Station		03LP003	03LP004	03LP010	03LP017	03LP021	03LP023	03LP028	03LP028	03LP029
Rock		altered dyke/ sill	dyke/sill	altered dyke/ sill	altered dyke/ sill	dyke/sill	altered breccia	lapilli tuff	lapilli tuff	lapilli tuff
Unit		PT	PT	PT	PT	PT	EOC-v	EOC-v	EOC-v	EOC-v
UTM E		649 516	649 441	649 320	650 123	647 628	647 538	647 053	647 053	646 909
UTM N		6 698 177	6 698 146	6 694 834	6 698 395	6 697 581	6 697 584	6 697 555	6 697 555	6 697 722
SiO <sub>2</sub> (%)	FUS ICP	31.79	45.35	34.74	52.62	42.08	36.67	47.45		51.12
Al <sub>2</sub> O <sub>3</sub> (%)	FUS ICP	13.45	15.26	14.98	14.85	14.68	10.18	14.62		12.90
Fe <sub>2</sub> O <sub>3</sub> * (%)	FUS ICP	11.55	11.24	10.61	10.59	15.01	15.90	11.39		10.11
MnO (%)	FUS ICP	0.183	0.184	0.125	0.045	0.176	0.230	0.162		0.209
MgO (%)	FUS ICP	8.04	7.57	3.72	2.26	4.65	4.66	8.55		8.55
CaO (%)	FUS ICP	8.57	8.72	12.15	1.95	8.23	7.99	6.21		6.54
Na <sub>2</sub> O (%)	FUS ICP	1.62	2.41	2.91	0.16	2.88	0.12	3.87		3.10
K <sub>2</sub> O (%)	FUS ICP	2.00	2.07	1.45	2.71	0.47	1.43	0.63		0.76
TiO <sub>2</sub> (%)	FUS ICP	1.438	1.672	2.067	2.753	3.369	2.461	1.596		1.824
P <sub>2</sub> O <sub>5</sub> (%)	FUS ICP	0.31	0.32	0.20	0.34	0.37	0.43	0.18		0.25
L.O.I. (%)		19.68	4.31	15.64	10.88	6.92	18.56	4.35		3.34
<b>Total (%)</b>		<b>98.63</b>	<b>99.11</b>	<b>98.59</b>	<b>99.16</b>	<b>98.84</b>	<b>98.63</b>	<b>99.01</b>		<b>98.70</b>
Ba (ppm)	FUS ICP	389	814	268	260	337	92	326		295
Sr (ppm)	FUS ICP	198	257	526	52	698	76	380		732
Y (ppm)	FUS ICP	21	27	21	22	24	27	16		18
Sc (ppm)	FUS ICP	31	34	30	32	20	16	31		29
Zr (ppm)	FUS ICP	83	95	97	201	177	159	105		122
Be (ppm)	FUS ICP	2	1	1	2	2	1	1		1
V (ppm)	FUS ICP	226	258	249	272	270	178	193		156
V (ppm)	FUS ICP-MS	211	247	237	249	257	162	178	181	143
Cr (ppm)	FUS ICP-MS	314	271	528	254	-20	-20	279	291	250
Co (ppm)	FUS ICP-MS	39	38	52	69	47	26	45	45	34
Ni (ppm)	FUS ICP-MS	100	80	198	103	52	25	130	136	69
Cu (ppm)	FUS ICP-MS	-10	51	317	635	28	13	60	69	-10
Zn (ppm)	FUS ICP-MS	62	91	80	67	125	42	83	112	122
Ga (ppm)	FUS ICP-MS	14	16	18	17	20	14	15	15	15
Ge (ppm)	FUS ICP-MS	2	2	2	3	2	2	1	2	2
As (ppm)	FUS ICP-MS	-5	12	115	60	-5	21	-5	-5	-5
Rb (ppm)	FUS ICP-MS	50	27	54	69	14	36	10	10	13
Sr (ppm)	FUS ICP-MS	196	249	503	51	735	75	378	387	746
Y (ppm)	FUS ICP-MS	20	23	18	23	26	24	17	17	20
Zr (ppm)	FUS ICP-MS	87	105	110	210	200	172	110	112	133
Nb (ppm)	FUS ICP-MS	35	38	23	48	38	29	27	27	28
Mo (ppm)	FUS ICP-MS	3	>100	>100	2	2	>100	-2	-2	-2
Ag (ppm)	FUS ICP-MS	-0.5	-0.5	-0.5	-0.5	-0.5	-0.5	-0.5	-0.5	-0.5
In (ppm)	FUS ICP-MS	-0.2	-0.2	-0.2	-0.2	-0.2	-0.2	-0.2	-0.2	-0.2
Sn (ppm)	FUS ICP-MS	-1	-1	1	2	2	1	1	2	1
Sb (ppm)	FUS ICP-MS	-0.5	-0.5	-0.5	1.5	0.7	1.9	-0.5	0.7	-0.5
Cs (ppm)	FUS ICP-MS	7.8	3.3	3.1	4.1	2.2	1.4	0.8	0.8	-0.5
Ba (ppm)	FUS ICP-MS	396	828	275	264	362	95	336	340	313

## APPENDIX C - WHOLE ROCK GEOCHEMISTRY, continued

**Table C2a, continued.** Analyses of dikes and volcanic rocks within the Toobally and Crow formations (2003). All coordinates are NAD83 datum, zone 9. (See analytical notes at the end of the table.)

Sample		03LP003	03LP004	03LP010	03LP017	03LP021	03LP023	03LP028	03LP028%	03LP029
Station		03LP003	03LP004	03LP010	03LP017	03LP021	03LP023	03LP028	03LP028	03LP029
La (ppm)	FUS ICP-MS	29.9	31.4	15.7	23.6	34.1	21.6	14.9	15.6	25.3
Ce (ppm)	FUS ICP-MS	59.9	62.5	33.8	49.8	73.2	46.3	32.8	34.3	50.4
Pr (ppm)	FUS ICP-MS	6.53	6.86	4.12	5.58	8.19	5.45	3.92	4.02	5.64
Nd (ppm)	FUS ICP-MS	27.9	28.8	19.5	24.5	35.6	24.6	18.0	18.1	25.3
Sm (ppm)	FUS ICP-MS	5	5.6	4.4	4.9	6.8	6.0	3.9	3.9	5.0
Eu (ppm)	FUS ICP-MS	1.88	2.10	1.29	1.53	2.83	2.15	1.73	1.71	2.17
Gd (ppm)	FUS ICP-MS	5	5.8	4.6	5.4	6.8	6.5	4.3	4.2	5.3
Tb (ppm)	FUS ICP-MS	0.8	0.9	0.7	0.9	1.1	1.0	0.7	0.7	0.8
Dy (ppm)	FUS ICP-MS	4.1	4.7	3.8	5.0	5.5	5.0	3.6	3.6	4.3
Ho (ppm)	FUS ICP-MS	0.8	0.9	0.7	0.9	1.0	0.9	0.7	0.7	0.8
Er (ppm)	FUS ICP-MS	2.3	2.7	2.0	2.7	2.9	2.7	1.9	1.9	2.1
Tm (ppm)	FUS ICP-MS	0.32	0.36	0.27	0.39	0.38	0.36	0.26	0.26	0.28
Yb (ppm)	FUS ICP-MS	1.8	2.1	1.5	2.2	2.3	2.2	1.5	1.5	1.7
Lu (ppm)	FUS ICP-MS	0.3	0.32	0.23	0.33	0.34	0.33	0.23	0.23	0.25
Hf (ppm)	FUS ICP-MS	2.3	2.7	3.2	5.5	5.1	4.4	2.9	2.9	3.5
Ta (ppm)	FUS ICP-MS	1.9	2.2	1.3	3.2	2.3	1.8	1.7	1.5	1.6
W (ppm)	FUS ICP-MS	1	-1	-1	2	-1	-1	-1	-1	-1
Tl (ppm)	FUS ICP-MS	0.2	0.2	0.2	0.3	-0.1	0.3	-0.1	-0.1	-0.1
Pb (ppm)	FUS ICP-MS	-5	10	18	-5	7	14	-5	10	9
Bi (ppm)	FUS ICP-MS	-0.4	-0.4	-0.4	-0.4	-0.4	-0.4	-0.4	-0.4	-0.4
Th (ppm)	FUS ICP-MS	2.6	3.1	1.6	5.2	4.0	3.6	1.6	1.6	2.4
U (ppm)	FUS ICP-MS	0.7	0.8	0.4	1.4	0.9	0.8	0.4	0.4	0.6

\* Total iron reported as Fe<sub>2</sub>O<sub>3</sub>.  
% Replicate analysis.

### Notes:

Samples were analyzed at Activation Laboratories Ltd., Ancaster, Ontario, Canada.

Samples were crushed and then pulverized in a ceramic mill.

Major and minor elements were determined by Inductively Coupled Plasma (ICP) on a fusion sample.

Trace elements and REE were analyzed by ICP-Mass Spectrometry (MS) on a fusion sample.

An elemental abundance below the detection limit is shown as a negative value.

Upper detection limits are indicated with > upper limit.

NA = not analyzed

## APPENDIX C - WHOLE ROCK GEOCHEMISTRY, continued

**Table C2b(i).** Analyses of dikes and volcanic rocks within the Crow Formation (2004-2005). All coordinates are NAD83 datum, zone 9. (See analytical notes at the end of the table.)

Sample		05LP005-1	05LP008	04LP017	04LP018-1	04LP018-2	04LP052-1	04LP052-2	04LP052-3	04LP067(1)
Station		05LP005	05LP008	04LP017	04LP018	04LP018	04LP052	04LP052	04LP052	04LP067
Rock		flow	flow	volcani-clastic	flow	flow	flow	flow	flow	flow
Unit		EOC-v	EOC-v	EOC-v	EOC-v	EOC-v	EOC-v	EOC-v	EOC-v	EOC-v
UTM E		653 170	650 376	647 676	647 392	647 392	648 485	648 485	648 485	647 299
UTM N		6702 526	6698 707	6689 077	6688 779	6688 779	6701 937	6701 937	6701 937	6688 532
SiO <sub>2</sub> (%)	FUS XRF	47.37	27.87	41.18	47.94	54.73	48.08	43.57	47.46	47.38
Al <sub>2</sub> O <sub>3</sub> (%)	FUS XRF	18.8	11.97	13.72	11.53	10.51	14.64	17.51	15.89	15.21
Cr <sub>2</sub> O <sub>3</sub> (%)	FUS XRF	0.03	0.06	-0.01	-0.01	0.18	0.05	0.06	0.10	-0.01
Fe <sub>2</sub> O <sub>3</sub> * (%)	FUS XRF	12.13	12.22	10.03	9.91	11.96	11.73	10.30	10.89	12.34
MnO (%)	FUS XRF	0.156	0.213	0.167	0.168	0.024	0.182	0.233	0.186	0.193
MgO (%)	FUS XRF	6.65	7.44	4.34	4.90	13.81	7.58	11.91	10.03	4.32
CaO (%)	FUS XRF	0.91	16.04	8.68	7.52	0.43	4.80	5.23	3.00	4.44
Na <sub>2</sub> O (%)	FUS XRF	4.96	1.91	0.10	2.55	0.03	4.26	2.76	3.45	4.63
K <sub>2</sub> O (%)	FUS XRF	0.34	0.08	3.67	0.91	0.02	1.62	1.39	2.86	0.57
TiO <sub>2</sub> (%)	FUS XRF	2.56	2.1	3.60	2.23	1.15	1.33	1.50	1.37	2.85
P <sub>2</sub> O <sub>5</sub> (%)	FUS XRF	0.28	0.27	1.12	0.50	0.11	0.44	0.48	0.44	0.62
LOI (%)		5.75	19.39	13.90	11.93	7.30	5.62	5.37	4.17	7.77
<b>Total (%)</b>		<b>99.94</b>	<b>99.56</b>	<b>100.50</b>	<b>100.08</b>	<b>100.25</b>	<b>100.33</b>	<b>100.32</b>	<b>99.85</b>	<b>100.31</b>
Sc (ppm)	INAA	33.4	34.8	10.9	12.8	18.0	16.7	20.2	17.6	15.4
V (ppm)	FUS ICP-MS	257	235	190	133	138	109	140	122	149
Cr (ppm)	FUS ICP-MS	180	310	29	-20	1,140	299	374	338	-20
Co (ppm)	FUS ICP-MS	14	33	23	46	73	33	42	41	41
Ni (ppm)	FUS ICP-MS	50	140	-20	113	449	162	199	188	-20
Cu (ppm)	FUS ICP-MS	50	60	12	33	-10	-10	-10	12	24
Zn (ppm)	FUS ICP-MS	90	150	42	-30	64	61	116	101	39
Ga (ppm)	FUS ICP-MS	21	15	21	14	12	16	22	19	16
Ge (ppm)	FUS ICP-MS	1.5	1.3	1.7	1.0	1.4	1.0	2.0	1.4	1.1
As (ppm)	FUS ICP-MS	-5	-5	-5	-5	-5	-5	-5	-5	-5
Rb (ppm)	FUS ICP-MS	8	2	116	19	-1	15	21	37	10
Sr (ppm)	FUS ICP-MS	254	180	422	73	25	175	647	259	52
Y (ppm)	FUS ICP-MS	21.3	19	38.4	20.4	10.0	23.6	30.1	27.1	21.9
Zr (ppm)	FUS ICP-MS	135	113	413	156	54	179	202	210	167
Nb (ppm)	FUS ICP-MS	22.5	17.7	137	32.4	11.9	86.7	99.1	106	34.1
Mo (ppm)	FUS ICP-MS	-2	-2	-2	-2	-2	-2	-2	-2	-2
Ag (ppm)	FUS ICP-MS	-0.5	-0.5	-0.5	-0.5	-0.5	-0.5	-0.5	-0.5	-0.5
In (ppm)	FUS ICP-MS	-0.1	-0.1	-0.1	-0.1	-0.1	-0.1	-0.1	-0.1	-0.1
Sn (ppm)	FUS ICP-MS	-1	-1	1	-1	-1	-1	-1	3	-1
Sb (ppm)	FUS ICP-MS	0.7	1	-0.2	-0.2	-0.2	-0.2	-0.2	0.2	-0.2
Cs (ppm)	FUS ICP-MS	1.4	0.1	3.2	1.5	0.1	0.2	0.5	0.5	0.7
Ba (ppm)	FUS ICP-MS	151	23	673	128	5	415	765	946	50
La (ppm)	FUS ICP-MS	20	6.28	159	12.3	5.66	49.8	64.4	66.2	23.4
Ce (ppm)	FUS ICP-MS	48.7	16.4	294	26.9	12.5	98.7	121	123	51.7
Pr (ppm)	FUS ICP-MS	6.21	2.35	32.0	3.31	1.46	9.97	12.4	12.3	6.23
Nd (ppm)	FUS ICP-MS	25.9	11.3	117	16.6	6.26	36.7	44.9	42.8	26.8
Sm (ppm)	FUS ICP-MS	5.62	3.31	18.8	5.46	1.46	6.55	8.02	7.34	7.29

**APPENDIX C - WHOLE ROCK GEOCHEMISTRY, continued**

**Table C2b(i), continued.** Analyses of dikes and volcanic rocks within the Crow Formation (2004-2005). All coordinates are NAD83 datum, zone 9. (See analytical notes at the end of the table.)

Sample		05LP005-1	05LP008	04LP017	04LP018-1	04LP018-2	04LP052-1	04LP052-2	04LP052-3	04LP067(1)
Station		05LP005	05LP008	04LP017	04LP018	04LP018	04LP052	04LP052	04LP052	04LP067
Eu (ppm)	FUS ICP-MS	2.44	1.46	5.61	2.10	0.484	2.24	3.24	2.61	2.83
Gd (ppm)	FUS ICP-MS	5.71	4	14.2	5.86	1.77	5.67	6.67	6.02	7.53
Tb (ppm)	FUS ICP-MS	0.88	0.69	1.91	0.88	0.34	0.91	1.05	0.98	1.12
Dy (ppm)	FUS ICP-MS	4.67	4.09	9.00	4.51	2.12	5.00	5.84	5.44	5.43
Ho (ppm)	FUS ICP-MS	0.86	0.72	1.45	0.77	0.41	0.94	1.09	0.99	0.89
Er (ppm)	FUS ICP-MS	2.32	1.83	3.73	2.07	1.08	2.73	3.04	2.79	2.30
Tm (ppm)	FUS ICP-MS	0.306	0.244	0.497	0.283	0.142	0.383	0.423	0.391	0.294
Yb (ppm)	FUS ICP-MS	1.77	1.37	2.92	1.67	0.81	2.27	2.62	2.48	1.72
Lu (ppm)	FUS ICP-MS	0.234	0.171	0.401	0.237	0.110	0.329	0.376	0.360	0.233
Hf (ppm)	FUS ICP-MS	3.5	2.9	9.5	3.8	1.5	4.1	4.3	4.4	4.4
Ta (ppm)	FUS ICP-MS	1.62	1.26	8.77	1.75	0.59	4.68	4.88	5.23	2.22
W (ppm)	FUS ICP-MS	-0.5	-0.5	1.7	0.9	-0.5	-0.5	-0.5	0.6	4.2
Tl (ppm)	FUS ICP-MS	0.1	0.05	0.82	0.17	-0.05	0.21	0.18	0.30	0.09
Pb (ppm)	FUS ICP-MS	-5	-5	10	-5	-5	6	9	9	-5
Bi (ppm)	FUS ICP-MS	-0.1	-0.1	2.7	1.4	0.9	1.5	2.1	1.5	0.6
Th (ppm)	FUS ICP-MS	1.96	1.68	14.8	2.04	0.88	6.89	7.32	7.67	2.56
U (ppm)	FUS ICP-MS	0.53	0.39	4.67	0.63	0.24	1.82	1.84	2.50	0.74

## APPENDIX C - WHOLE ROCK GEOCHEMISTRY, continued

**Table C2b(ii).** Analyses of dikes and volcanic rocks within the Crow Formation (2004-2005). All coordinates are NAD83 datum, zone 9. (See analytical notes at the end of the table.)

Sample		04LP067(2)	05LP037	05LP060	05LP064	05LP047	05LP047A	04LP030	04LP058	04LP062
Station		04LP067	05LP037	05LP060	05LP064	05LP047	05LP047	04LP030	04LP058	04LP062
Rock		flow	flow	flow?	flow	dyke/sill?	dyke/sill?	volcani-clastic	flow	flow
Unit		EOC-v	EOC-v	EOC-v	EOC-v	EOC-v	EOC-v	EOC-v	EOC-v	EOC-v
UTM E		647 299	646 474	648 589	648 671	643 488	643 488	640 489	638 839	639 536
UTM N		6688 532	6698 311	6701 885	6703 655	6698 498	6698 498	6698 856	6706 551	6708 455
SiO <sub>2</sub> (%)	FUS XRF	47.35	45.47	40.32	43.22	46.59	46.20	48.40	49.69	46.67
Al <sub>2</sub> O <sub>3</sub> (%)	FUS XRF	15.16	14.66	12.84	13.76	16.70	16.68	14.07	15.89	14.26
Cr <sub>2</sub> O <sub>3</sub> (%)	FUS XRF	-0.01	0.05	0.10	0.07	0.01	0.05	0.04	0.01	-0.01
Fe <sub>2</sub> O <sub>3</sub> * (%)	FUS XRF	12.38	11.29	13.63	14.21	11.33	11.40	11.54	10.83	14.61
MnO (%)	FUS XRF	0.193	0.118	0.132	0.216	0.158	0.163	0.166	0.138	0.136
MgO (%)	FUS XRF	4.28	9.38	8.85	11.59	5.15	5.18	7.64	6.14	5.02
CaO (%)	FUS XRF	4.43	5.04	8.34	5.74	10.67	10.66	8.78	4.41	6.28
Na <sub>2</sub> O (%)	FUS XRF	4.66	4.14	0.69	2.89	2.33	2.47	1.87	4.69	4.61
K <sub>2</sub> O (%)	FUS XRF	0.57	0.39	2.55	0.84	1.40	1.30	2.28	2.14	1.40
TiO <sub>2</sub> (%)	FUS XRF	2.84	1.75	1.73	1.78	2.26	2.22	2.42	2.86	3.91
P <sub>2</sub> O <sub>5</sub> (%)	FUS XRF	0.61	0.42	0.32	0.44	0.33	0.33	0.32	0.44	0.65
LOI (%)		7.77	7.21	10.03	4.53	2.14	2.52	2.83	3.15	2.19
<b>Total (%)</b>		<b>100.23</b>	<b>99.92</b>	<b>99.53</b>	<b>99.29</b>	<b>99.07</b>	<b>99.17</b>	<b>100.36</b>	<b>100.39</b>	<b>99.73</b>
Sc (ppm)	INAA		20.4	28.2	27.9	29.0	29.2	27.9	26.8	29.5
V (ppm)	FUS ICP-MS		116	164	163	209	222	255	247	314
Cr (ppm)	FUS ICP-MS		270	440	380	70	80	238	57	-20
Co (ppm)	FUS ICP-MS		33	37	47	31	31	42	40	34
Ni (ppm)	FUS ICP-MS		140	230	190	30	30	125	35	-20
Cu (ppm)	FUS ICP-MS		-10	-10	-10	50	50	74	68	13
Zn (ppm)	FUS ICP-MS		70	70	90	60	70	86	110	83
Ga (ppm)	FUS ICP-MS		16	15	14	18	18	19	20	20
Ge (ppm)	FUS ICP-MS		1.2	1.1	1.2	1.3	1.3	1.5	0.9	1.5
As (ppm)	FUS ICP-MS		-5	-5	-5	6	-5	-5	-5	-5
Rb (ppm)	FUS ICP-MS		8	64	12	27	25	35	23	15
Sr (ppm)	FUS ICP-MS		91	81	291	385	395	241	70	245
Y (ppm)	FUS ICP-MS		23.9	19.5	22.2	22.7	22.3	26.1	25.9	31.1
Zr (ppm)	FUS ICP-MS		145	101	120	180	177	176	245	186
Nb (ppm)	FUS ICP-MS		43.5	25.4	34.9	28.0	27.4	31.2	45.1	39.0
Mo (ppm)	FUS ICP-MS		-2	-2	-2	-2	-2	-2	2	-2
Ag (ppm)	FUS ICP-MS		-0.5	-0.5	-0.5	-0.5	-0.5	-0.5	-0.5	-0.5
In (ppm)	FUS ICP-MS		-0.1	-0.1	-0.1	-0.1	-0.1	-0.1	-0.1	-0.1
Sn (ppm)	FUS ICP-MS		-1	-1	-1	-1	-1	-1	-1	-1
Sb (ppm)	FUS ICP-MS		1.1	0.9	0.9	0.9	0.8	-0.2	-0.2	-0.2
Cs (ppm)	FUS ICP-MS		0.2	2.1	0.7	0.3	0.2	0.4	0.3	0.4
Ba (ppm)	FUS ICP-MS		40	168	371	249	227	288	147	193
La (ppm)	FUS ICP-MS		29.7	19.5	28.8	24.4	23.7	25.9	24.1	33.0
Ce (ppm)	FUS ICP-MS		60.4	42.8	60.6	56.7	52.9	56.7	57.4	75.7
Pr (ppm)	FUS ICP-MS		7.11	5.50	7.26	7.13	6.63	6.72	7.01	9.09
Nd (ppm)	FUS ICP-MS		28.0	22.4	28.7	28.3	26.7	28.0	28.0	38.6
Sm (ppm)	FUS ICP-MS		5.74	4.79	5.71	6.05	5.74	6.38	5.88	8.36

**APPENDIX C - WHOLE ROCK GEOCHEMISTRY, continued**

**Table C2b(ii), continued.** Analyses of dikes and volcanic rocks within the Crow Formation (2004-2005). All coordinates are NAD83 datum, zone 9. (See analytical notes at the end of the table.)

Sample		04LP067(2)	05LP037	05LP060	05LP064	05LP047	05LP047A	04LP030	04LP058	04LP062
Station		04LP067	05LP037	05LP060	05LP064	05LP047	05LP047	04LP030	04LP058	04LP062
Eu (ppm)	FUS ICP-MS		2.04	1.69	1.90	2.08	2.01	2.10	1.53	3.00
Gd (ppm)	FUS ICP-MS		5.61	4.72	5.50	5.56	5.39	6.15	5.54	8.44
Tb (ppm)	FUS ICP-MS		0.85	0.71	0.78	0.86	0.82	1.00	0.92	1.32
Dy (ppm)	FUS ICP-MS		4.73	3.91	4.37	4.71	4.68	5.51	5.19	6.88
Ho (ppm)	FUS ICP-MS		0.90	0.72	0.84	0.89	0.89	1.02	1.02	1.25
Er (ppm)	FUS ICP-MS		2.50	2.07	2.42	2.33	2.45	2.84	2.94	3.34
Tm (ppm)	FUS ICP-MS		0.349	0.280	0.333	0.328	0.336	0.383	0.418	0.453
Yb (ppm)	FUS ICP-MS		2.11	1.59	1.96	2.00	1.97	2.23	2.56	2.69
Lu (ppm)	FUS ICP-MS		0.299	0.223	0.287	0.294	0.270	0.314	0.367	0.358
Hf (ppm)	FUS ICP-MS		3.3	2.6	2.8	4.5	4.3	4.7	6.2	5.2
Ta (ppm)	FUS ICP-MS		2.47	1.51	2.18	1.96	1.91	1.87	2.57	2.46
W (ppm)	FUS ICP-MS		-0.5	-0.5	-0.5	-0.5	1.2	-0.5	1.1	1.1
Ti (ppm)	FUS ICP-MS		-0.05	0.20	0.06	0.09	0.09	0.18	0.10	0.10
Pb (ppm)	FUS ICP-MS		6	7	-5	-5	-5	-5	-5	6
Bi (ppm)	FUS ICP-MS		-0.1	-0.1	-0.1	-0.1	-0.1	0.6	0.5	1.0
Th (ppm)	FUS ICP-MS		4.79	2.52	3.47	3.36	2.95	2.52	4.44	2.89
U (ppm)	FUS ICP-MS		1.14	0.48	0.67	0.80	0.72	0.62	0.80	0.72

\* Total iron reported as Fe<sub>2</sub>O<sub>3</sub>.

**Notes:**

Samples were analyzed at Activation Laboratories Ltd., Ancaster, Ontario, Canada. Samples were crushed and then pulverized in a ceramic mill. Major oxides and most minor elements were determined by X-Ray Fluorescence (XRF) on a fusion sample. Sc was analyzed using Instrumental Neutron Activation Analysis (INAA). Trace elements and REE were analyzed by ICP-Mass Spectrometry (MS) at research detection limits on a fusion sample containing a lithium metaborate/tetraborate flux. An elemental abundance below the detection limit is shown as a negative value. NA = not analyzed

**APPENDIX C - WHOLE ROCK GEOCHEMISTRY**, continued

**Table C2c.** Analyses of volcanic rocks within the Crow Formation (2009-2010). All coordinates are NAD83 datum, zone 9. (See analytical notes at the end of the table.)

Sample		09TOA141E	09TOA149	09LP082-1	09LP083-2	10TOA024
Station		09TOA141	09TOA149	09LP082	09LP083	10TOA024
Rock		flow	flow	flow	tuff	flow
Unit		EOC-v	EOC-v	EOC-v	EOC-v	EOC-v
UTM E		633 677	640 254	632 218	633 122	637 550
UTM N		6715 218	6718 980	6762 262	6761 980	6718 719
SiO <sub>2</sub> (%)	FUS ICP	60.26	45.03	42.37	46.04	69.39
Al <sub>2</sub> O <sub>3</sub> (%)	FUS ICP	16.06	13.38	17.08	20.31	12.85
FeO (%)	TITR	1.31	5.43	6.35	3.90	1.11
Fe <sub>2</sub> O <sub>3</sub> (%)	DIFF	6.79	5.34	3.20	3.25	2.72
Fe <sub>2</sub> O <sub>3</sub> * (%)	FUS ICP	8.25	11.37	10.26	7.58	3.95
MnO (%)	FUS ICP	0.015	0.164	0.084	0.139	0.050
MgO (%)	FUS ICP	1.81	5.33	6.84	6.06	3.16
CaO (%)	FUS ICP	0.13	8.49	6.58	4.16	0.50
Na <sub>2</sub> O (%)	FUS ICP	0.58	4.29	3.09	3.19	0.65
K <sub>2</sub> O (%)	FUS ICP	7.68	0.19	2.43	3.79	4.48
TiO <sub>2</sub> (%)	FUS ICP	0.589	2.609	2.03	1.56	0.44
P <sub>2</sub> O <sub>5</sub> (%)	FUS ICP	0.08	0.33	0.30	0.21	0.34
L.O.I. (%)		2.99	8.26	8.60	6.41	2.75
<b>Total (%)</b>		<b>98.43</b>	<b>99.45</b>	<b>99.69</b>	<b>99.45</b>	<b>98.54</b>
Au (ppb)	INAA	-2	-2	-2	-2	NA
As (ppm)	INAA	-0.5	-0.5	-0.5	4.1	NA
Br (ppm)	INAA	-0.5	-0.5	-0.5	-0.5	NA
Cr (ppm)	INAA	-5	43	221	56	NA
Ir (ppm)	INAA	-5	-5	-5	-5	NA
Sc (ppm)	INAA	22.6	29.0	28.9	20.4	NA
Se (ppm)	INAA	-3	-3	-3	-3	NA
Sb (ppm)	INAA	0.3	-0.2	0.2	0.5	NA
Sc (ppm)	FUS ICP	24	33	32	22	9
Be (ppm)	FUS ICP	4	1	1	1.0	3
V (ppm)	FUS ICP	84	338	285	208	44
Cr (ppm)	FUS ICP-MS	-20	50	210	50	-20
Co (ppm)	FUS ICP-MS	4	34	37	28	15
Ni (ppm)	FUS ICP-MS	-20	40	70	30	-20
Cu (ppm)	FUS ICP-MS	-10	110	-10	30	-10
Zn (ppm)	FUS ICP-MS	40	150	100	120	50
Ga (ppm)	FUS ICP-MS	27	17	18	18	24
Ge (ppm)	FUS ICP-MS	1.9	2.0	1.1	0.9	2.0
As (ppm)	FUS ICP-MS	-5	-5	-5	5	-5
Rb (ppm)	FUS ICP-MS	143	3	37	67	126
Sr (ppm)	FUS ICP	21	133	108	102	15
Y (ppm)	FUS ICP-MS	51.7	26.2	20.8	14.9	51.4
Zr (ppm)	FUS ICP-MS	817	190	144	111	143

## APPENDIX C - WHOLE ROCK GEOCHEMISTRY, continued

**Table C2c, continued.** Analyses of volcanic rocks within the Crow Formation (2009-2010). All coordinates are NAD83 datum, zone 9. (See analytical notes at the end of the table.)

Sample		09TOA141E	09TOA149	09LP082-1	09LP083-2	10TOA024
Station		09TOA141	09TOA149	09LP082	09LP083	10TOA024
Nb (ppm)	FUS ICP-MS	108	36.2	26	23.4	51.9
Mo (ppm)	FUS ICP-MS	-2	-2	-2	-2	-2
Ag (ppm)	FUS ICP-MS	2.4	0.5	-0.5	-0.5	-0.5
In (ppm)	FUS ICP-MS	-0.1	-0.1	-0.1	-0.1	-0.1
Sn (ppm)	FUS ICP-MS	6	2	1	-1	9
Sb (ppm)	FUS ICP-MS	-0.2	-0.2	-0.2	0.3	-0.2
Cs (ppm)	FUS ICP-MS	3.6	0.3	5.0	2.1	2.5
Ba (ppm)	FUS ICP	628	43	204	288	289
La (ppm)	FUS ICP-MS	91.5	23.3	19.0	15.7	41.0
Ce (ppm)	FUS ICP-MS	195	53.1	42	34.5	88.1
Pr (ppm)	FUS ICP-MS	21.10	6.57	5.14	4.16	10.1
Nd (ppm)	FUS ICP-MS	77.9	28.0	22	17.1	38.4
Sm (ppm)	FUS ICP-MS	13.6	6.53	5.0	3.76	9.40
Eu (ppm)	FUS ICP-MS	3.26	2.08	1.44	1.33	1.140
Gd (ppm)	FUS ICP-MS	10.5	6.19	4.88	3.53	9.79
Tb (ppm)	FUS ICP-MS	1.70	0.96	0.78	0.56	1.68
Dy (ppm)	FUS ICP-MS	9.81	5.32	4.32	3.06	9.93
Ho (ppm)	FUS ICP-MS	1.98	0.96	0.77	0.58	1.91
Er (ppm)	FUS ICP-MS	5.74	2.57	2.11	1.56	5.43
Tm (ppm)	FUS ICP-MS	0.877	0.352	0.302	0.226	0.813
Yb (ppm)	FUS ICP-MS	6.07	2.19	1.85	1.39	5.25
Lu (ppm)	FUS ICP-MS	1.02	0.331	0.275	0.200	0.820
Hf (ppm)	FUS ICP-MS	17.0	4.2	3.2	2.5	4.3
Ta (ppm)	FUS ICP-MS	7.47	2.72	1.91	1.69	4.49
W (ppm)	FUS ICP-MS	-0.5	-0.5	-0.5	-0.5	-0.5
Tl (ppm)	FUS ICP-MS	0.18	-0.05	-0.05	0.09	0.32
Pb (ppm)	FUS ICP-MS	6	20	-5	7	-5
Bi (ppm)	FUS ICP-MS	-0.1	-0.1	-0.1	-0.1	-0.1
Th (ppm)	FUS ICP-MS	21.0	2.89	2.6	2.28	20.40
U (ppm)	FUS ICP-MS	2.75	0.74	0.66	0.48	4.57

\* Total iron reported as Fe<sub>2</sub>O<sub>3</sub>.

### Notes:

Samples were analyzed at Activation Laboratories Ltd., Ancaster, Ontario, Canada.

Samples were crushed and then pulverized in a mild steel mill.

Major elemental oxides and most minor elements were determined by Inductively Coupled Plasma (ICP) on a fusion sample.

FeO was determined by titration.

Au, As, Br, Cr, Ir, Sc, Se and Sb were determined by Instrumental Neutron Activation Analysis (INAA).

Trace elements and REE were analyzed by ICP-Mass Spectrometry (MS) at research detection limits on a fusion sample containing a lithium metaborate/tetraborate flux.

An elemental abundance below the detection limit is shown as a negative value.

NA = not analyzed

## APPENDIX C - WHOLE ROCK GEOCHEMISTRY, continued

**Table C3.** Analyses for volcanic rocks of the Rabbitkettle Formation. All coordinates are NAD83 datum, zone 9. (See analytical notes at the end of the table.)

Sample		J96-10 155.7m	J96-11 36.8m	07LP032	Sample		09LP003-3	09LP049-2	09RAS050D	09TOA161	09TOA165	09RAS168B extra
Station		drill hole	drill hole	07LP032	Station		09LP003-3	09LP049	09RAS050	09TOA161	09TOA165	09RAS168
Rock		flow/sill?	flow/sill?	flow	Rock		altered flow	flow	sill	flow	flow	flow
Unit		ЄOR-v	ЄOR-v	ЄOR-v	Unit		ЄOR-v	ЄOR-v	ЄOR-v	ЄOR-v	ЄOR-v	ЄOR-v
Easting		590 910	590 870	591 303	Easting		582 955	569 574	572 762	613 430	612 912	609 000
Northing		6 698 779	6 699 220	6 698 365	Northing		6 709 689	6 722 949	6 749 796	6 753 492	6 739 782	6 727 200
SiO <sub>2</sub> (%)	FUS XRF	44.31	43.44	43.97	SiO <sub>2</sub> (%)	FUS ICP	55.99	48.36	48.34	49.10	45.84	43.62
Al <sub>2</sub> O <sub>3</sub> (%)	FUS XRF	14.43	14.58	14.49	Al <sub>2</sub> O <sub>3</sub> (%)	FUS ICP	16.82	16.04	12.67	12.58	15.26	14.39
FeO (%)	TITR	NA	NA	NA	FeO (%)	TITR	4.51	6.19	6.59	8.10	6.41	9.40
Fe <sub>2</sub> O <sub>3</sub> (%)	DIFF	NA	NA	NA	Fe <sub>2</sub> O <sub>3</sub> (%)	DIFF	0.81	4.25	5.70	0.76	3.61	2.10
Fe <sub>2</sub> O <sub>3</sub> * (%)	FUS XRF	13.26	13.15	12.92	Fe <sub>2</sub> O <sub>3</sub> * (%)	FUS ICP	5.82	11.13	13.02	9.76	10.73	12.55
MnO (%)	FUS XRF	0.193	0.199	0.185	MnO (%)	FUS ICP	0.098	0.156	0.176	0.154	0.133	0.158
MgO (%)	FUS XRF	8.80	8.18	8.30	MgO (%)	FUS ICP	6.29	5.75	5.56	8.91	6.76	9.50
CaO (%)	FUS XRF	8.07	8.84	8.85	CaO (%)	FUS ICP	2.47	8.49	5.07	7.24	9.40	8.94
Na <sub>2</sub> O (%)	FUS XRF	2.54	2.35	2.68	Na <sub>2</sub> O (%)	FUS ICP	4.92	2.93	3.53	3.93	2.00	1.96
K <sub>2</sub> O (%)	FUS XRF	0.92	1.83	0.64	K <sub>2</sub> O (%)	FUS ICP	1.19	0.87	0.11	1.04	3.16	1.62
TiO <sub>2</sub> (%)	FUS XRF	2.88	2.90	2.92	TiO <sub>2</sub> (%)	FUS ICP	0.669	2.326	3.254	1.129	3.076	2.292
P <sub>2</sub> O <sub>5</sub> (%)	FUS XRF	0.53	0.52	0.52	P <sub>2</sub> O <sub>5</sub> (%)	FUS ICP	0.15	0.66	0.41	0.17	0.58	0.34
Cr <sub>2</sub> O <sub>3</sub> (%)	FUS XRF	0.02	0.02	0.02	Cr <sub>2</sub> O <sub>3</sub> (%)	FUS ICP	NA	NA	NA	NA	NA	NA
L.O.I. (%)		4.46	3.31	4.25	L.O.I. (%)		5.08	2.79	7.90	4.45	3.12	4.17
<b>Total (%)</b>		<b>100.41</b>	<b>99.32</b>	<b>99.75</b>	<b>Total (%)</b>		<b>99.49</b>	<b>99.51</b>	<b>100.10</b>	<b>98.47</b>	<b>100.10</b>	<b>99.55</b>
Au (ppb)	INAA	NA	NA	NA	Au (ppb)	INAA	-2	-2	-2	-2	-2	-2
As (ppm)	INAA	NA	NA	NA	As (ppm)	INAA	4.2	-0.5	11.8	-0.5	-0.5	2.2
Br (ppm)	INAA	NA	NA	NA	Br (ppm)	INAA	-0.5	-0.5	-0.5	-0.5	-0.5	-0.5
Cr (ppm)	INAA	NA	NA	NA	Cr (ppm)	INAA	107	107	42	337	346	491
Ir (ppm)	INAA	NA	NA	NA	Ir (ppm)	INAA	-5	-5	-5	-5	-5	-5
Sc (ppm)	INAA	26.5	26.7	26.8	Sc (ppm)	INAA	16.1	24.6	28.2	20.1	27.4	31.6
Se (ppm)	INAA	NA	NA	NA	Se (ppm)	INAA	-3	-3	-3	-3	-3	-3
Sb (ppm)	INAA	NA	NA	NA	Sb (ppm)	INAA	-0.2	-0.2	0.8	0.5	0.2	0.5
Sc (ppm)	FUS ICP	NA	NA	NA	Sc (ppm)	FUS ICP	19	28	31	22	31	36
Be (ppm)	FUS ICP	NA	NA	NA	Be (ppm)	FUS ICP	2	2	1	-1	-1	-1
V (ppm)	FUS ICP-MS	254	261	264	V (ppm)	FUS ICP	148	247	426	179	312	305
Cr (ppm)	FUS ICP-MS	280	280	270	Cr (ppm)	FUS ICP-MS	120	110	40	350	320	470
Co (ppm)	FUS ICP-MS	48	48	47	Co (ppm)	FUS ICP-MS	17	32	46	45	41	54
Ni (ppm)	FUS ICP-MS	140	140	140	Ni (ppm)	FUS ICP-MS	50	-20	-20	240	130	240
Cu (ppm)	FUS ICP-MS	70	70	50	Cu (ppm)	FUS ICP-MS	30	10	60	50	30	70
Zn (ppm)	FUS ICP-MS	140	110	140	Zn (ppm)	FUS ICP-MS	50	110	130	90	60	90
Ga (ppm)	FUS ICP-MS	20	19	20	Ga (ppm)	FUS ICP-MS	16	18	19	15	16	21
Ge (ppm)	FUS ICP-MS	1.6	1.4	1.4	Ge (ppm)	FUS ICP-MS	1.8	1.6	2.1	1.4	1.5	1.5
As (ppm)	FUS ICP-MS	-5	-5	-5	As (ppm)	FUS ICP-MS	8	-5	13	-5	-5	-5

**APPENDIX C - WHOLE ROCK GEOCHEMISTRY, continued**

**Table C3, continued.** Analyses for volcanic rocks of the Rabbitkettle Formation. All coordinates are NAD83 datum, zone 9. (See analytical notes at the end of the table.)

Sample		J96-10 155.7m	J96-11 36.8m	07LP032	Sample		09LP003-3	09LP049-2	09RAS050D	09TOA161	09TOA165	09RAS168B extra
Station		drill hole	drill hole	07LP032	Station		09LP003-3	09LP049	09RAS050	09TOA161	09TOA165	09RAS168
Rb (ppm)	FUS ICP-MS	20	32	9	Rb (ppm)	FUS ICP-MS	30	15	<1	13	47	17
Sr (ppm)	FUS ICP-MS	615	827	855	Sr (ppm)	FUS ICP	177	531	436	267	772	367
Y (ppm)	FUS ICP-MS	30.6	30.7	30.6	Y (ppm)	FUS ICP-MS	18.0	38.8	32.1	16.3	21.3	23.5
Zr (ppm)	FUS ICP-MS	272	271	271	Zr (ppm)	FUS ICP-MS	131	252	222	101	147	192
Nb (ppm)	FUS ICP-MS	55.9	56.2	56.9	Nb (ppm)	FUS ICP-MS	9.9	21.1	43.6	14.3	37.0	44.8
Mo (ppm)	FUS ICP-MS	2	-2	-2	Mo (ppm)	FUS ICP-MS	-2	-2	-2	-2	-2	-2
Ag (ppm)	FUS ICP-MS	0.9	0.6	< 0.5	Ag (ppm)	FUS ICP-MS	-0.5	0.7	0.6	-0.5	-0.5	0.6
In (ppm)	FUS ICP-MS	-0.1	-0.1	-0.1	In (ppm)	FUS ICP-MS	-0.1	-0.1	-0.1	-0.1	-0.1	-0.1
Sn (ppm)	FUS ICP-MS	2	2	3	Sn (ppm)	FUS ICP-MS	1	2	2	-1	1	1
Sb (ppm)	FUS ICP-MS	3.9	-0.2	-0.2	Sb (ppm)	FUS ICP-MS	-0.2	-0.2	0.9	-0.2	-0.2	0.4
Cs (ppm)	FUS ICP-MS	2.3	1.7	1.0	Cs (ppm)	FUS ICP-MS	1.7	1.8	1.7	2.9	2.9	1.7
Ba (ppm)	FUS ICP-MS	982	1080	1130	Ba (ppm)	FUS ICP	650	551	435	601	2951	1597
La (ppm)	FUS ICP-MS	47.8	46.6	45.3	La (ppm)	FUS ICP-MS	27.7	32.0	28.1	52.6	32.2	30.7
Ce (ppm)	FUS ICP-MS	95.5	93.6	92.4	Ce (ppm)	FUS ICP-MS	54.7	74.5	62.9	90.0	74.9	64.6
Pr (ppm)	FUS ICP-MS	11.9	11.8	12.1	Pr (ppm)	FUS ICP-MS	5.92	9.36	7.77	9.05	9.17	7.55
Nd (ppm)	FUS ICP-MS	43.7	42.4	42.6	Nd (ppm)	FUS ICP-MS	22.4	39.2	33.2	31.3	38.0	31.0
Sm (ppm)	FUS ICP-MS	8.65	8.26	8.39	Sm (ppm)	FUS ICP-MS	4.23	8.65	7.61	4.48	7.76	6.53
Eu (ppm)	FUS ICP-MS	2.66	2.68	2.52	Eu (ppm)	FUS ICP-MS	0.810	2.30	2.27	1.41	2.21	1.82
Gd (ppm)	FUS ICP-MS	7.64	7.65	7.68	Gd (ppm)	FUS ICP-MS	3.49	7.97	7.23	4.04	6.69	6.12
Tb (ppm)	FUS ICP-MS	1.19	1.16	1.17	Tb (ppm)	FUS ICP-MS	0.55	1.29	1.11	0.60	0.91	0.91
Dy (ppm)	FUS ICP-MS	6.09	5.93	6.01	Dy (ppm)	FUS ICP-MS	3.22	7.40	6.21	3.26	4.68	4.91
Ho (ppm)	FUS ICP-MS	1.10	1.09	1.06	Ho (ppm)	FUS ICP-MS	0.65	1.41	1.14	0.62	0.84	0.90
Er (ppm)	FUS ICP-MS	3.05	2.96	2.93	Er (ppm)	FUS ICP-MS	1.93	4.00	3.26	1.70	2.14	2.40
Tm (ppm)	FUS ICP-MS	0.413	0.400	0.399	Tm (ppm)	FUS ICP-MS	0.289	0.596	0.460	0.246	0.278	0.333
Yb (ppm)	FUS ICP-MS	2.46	2.46	2.46	Yb (ppm)	FUS ICP-MS	1.95	3.85	2.87	1.50	1.63	2.02
Lu (ppm)	FUS ICP-MS	0.381	0.365	0.362	Lu (ppm)	FUS ICP-MS	0.319	0.613	0.422	0.231	0.238	0.296
Hf (ppm)	FUS ICP-MS	6.3	6.3	6.3	Hf (ppm)	FUS ICP-MS	3.0	4.9	4.9	2.1	3.3	4.3
Ta (ppm)	FUS ICP-MS	4.35	4.27	4.29	Ta (ppm)	FUS ICP-MS	0.82	1.35	3.18	0.63	2.79	3.18
W (ppm)	FUS ICP-MS	0.8	0.7	0.8	W (ppm)	FUS ICP-MS	-0.5	-0.5	-0.5	-0.5	-0.5	-0.5
Tl (ppm)	FUS ICP-MS	0.12	0.08	0.06	Tl (ppm)	FUS ICP-MS	0.09	-0.05	-0.05	-0.05	0.10	-0.05
Pb (ppm)	FUS ICP-MS	5	-5	7	Pb (ppm)	FUS ICP-MS	28	6	-5	6	-5	-5

## APPENDIX C - WHOLE ROCK GEOCHEMISTRY, continued

**Table C3, continued.** Analyses for volcanic rocks of the Rabbitkettle Formation. All coordinates are NAD83 datum, zone 9. (See analytical notes at the end of the table.)

Sample		J96-10 155.7m	J96-11 36.8m	07LP032	Sample		09LP003-3	09LP049-2	09RAS050D	09TOA161	09TOA165	09RAS168B extra
Station		drill hole	drill hole	07LP032	Station		09LP003-3	09LP049	09RAS050	09TOA161	09TOA165	09RAS168
Bi (ppm)	FUS ICP-MS	0.1	-0.1	0.2	Bi (ppm)	FUS ICP-MS	-0.1	-0.1	-0.1	-0.1	-0.1	-0.1
Th (ppm)	FUS ICP-MS	7.29	6.83	6.99	Th (ppm)	FUS ICP-MS	8.15	3.36	4.30	2.82	6.81	4.08
U (ppm)	FUS ICP-MS	1.87	1.67	1.68	U (ppm)	FUS ICP-MS	1.98	0.7	1.04	0.85	0.66	1.04

\* Total iron reported as Fe<sub>2</sub>O<sub>3</sub>.

### Notes:

Samples were analyzed at Activation Laboratories Ltd., Ancaster, Ontario, Canada.

Samples were crushed and then pulverized in a mild steel mill.

Major oxides and most minor elements were determined by X-Ray Fluorescence (XRF) on a fusion sample containing a lithium metaborate/tetraborate flux, in 2007.

Those determined by Inductively Coupled Plasma (ICP) were performed in 2009, also on a fusion sample.

FeO was determined by titration.

Au, As, Br, Cr, Ir, Sc, Se, Sb were determined by Instrumental Neutron Activation Analysis (INAA).

Trace elements and REE were analyzed by ICP-Mass Spectrometry (MS) or ICP on a fusion sample.

An elemental abundance below the detection limit is shown as a negative value.

NA = not analyzed

## APPENDIX C - WHOLE ROCK GEOCHEMISTRY, continued

**Table C4.** Analyses of volcanic rocks within the Sunblood Formation. All coordinates are NAD83 datum, zone 9.

Sample		09LP072	09MBKL01
Station		09LP072	09MBKL001
Rock		flow	flow
Unit		OSu-v	OSu-v
UTM E		621 003	626 074
UTM N		6 684 592	6 705 020
SiO <sub>2</sub> (%)	FUS ICP	48.73	48.28
Al <sub>2</sub> O <sub>3</sub> (%)	FUS ICP	14.98	15.07
FeO (%)	TITR	5.80	10.20
Fe <sub>2</sub> O <sub>3</sub> (%)	DIFF	2.11	0.73
Fe <sub>2</sub> O <sub>3</sub> * (%)	FUS ICP	8.56	12.07
MnO (%)	FUS ICP	0.066	0.097
MgO (%)	FUS ICP	8.15	8.94
CaO (%)	FUS ICP	4.73	4.29
Na <sub>2</sub> O (%)	FUS ICP	0.71	2.44
K <sub>2</sub> O (%)	FUS ICP	5.2	2.1
TiO <sub>2</sub> (%)	FUS ICP	1.608	2.407
P <sub>2</sub> O <sub>5</sub> (%)	FUS ICP	0.27	0.28
L.O.I. (%)		7.20	2.09
<b>Total (%)</b>		<b>100.20</b>	<b>98.05</b>
Au (ppb)	INAA	-2	-2
As (ppm)	INAA	1.6	-0.5
Br (ppm)	INAA	-0.5	-0.5
Cr (ppm)	INAA	348	69
Ir (ppm)	INAA	-5	-5
Sc (ppm)	INAA	23.6	32.5
Se (ppm)	INAA	-3	-3
Sb (ppm)	INAA	-0.2	-0.2
Sc (ppm)	FUS ICP	25	35
Be (ppm)	FUS ICP	-1	1
V (ppm)	FUS ICP	226	307
Cr (ppm)	FUS ICP-MS	310	70
Co (ppm)	FUS ICP-MS	55	42
Ni (ppm)	FUS ICP-MS	160	40
Cu (ppm)	FUS ICP-MS	100	70
Zn (ppm)	FUS ICP-MS	60	90
Ga (ppm)	FUS ICP-MS	17	19
Ge (ppm)	FUS ICP-MS	0.8	1.2
As (ppm)	FUS ICP-MS	-5	-5
Rb (ppm)	FUS ICP-MS	40	32
Sr (ppm)	FUS ICP	123	197

continued...

Sample (cont.)		09LP072	09MBKL01
Station (cont.)		09LP072	09MBKL001
Y (ppm)	FUS ICP-MS	20.2	23.6
Zr (ppm)	FUS ICP-MS	130	190
Nb (ppm)	FUS ICP-MS	29.9	34.6
Mo (ppm)	FUS ICP-MS	-2	-2
Ag (ppm)	FUS ICP-MS	-0.5	0.6
In (ppm)	FUS ICP-MS	-0.1	-0.1
Sn (ppm)	FUS ICP-MS	1	2
Sb (ppm)	FUS ICP-MS	-0.2	-0.2
Cs (ppm)	FUS ICP-MS	3.2	4.2
Ba (ppm)	FUS ICP	517	875
La (ppm)	FUS ICP-MS	18.0	18.6
Ce (ppm)	FUS ICP-MS	38.9	46.2
Pr (ppm)	FUS ICP-MS	4.68	5.98
Nd (ppm)	FUS ICP-MS	19.4	26.5
Sm (ppm)	FUS ICP-MS	4.68	6.26
Eu (ppm)	FUS ICP-MS	0.996	1.74
Gd (ppm)	FUS ICP-MS	4.55	5.75
Tb (ppm)	FUS ICP-MS	0.74	0.88
Dy (ppm)	FUS ICP-MS	4.26	4.92
Ho (ppm)	FUS ICP-MS	0.81	0.90
Er (ppm)	FUS ICP-MS	2.20	2.41
Tm (ppm)	FUS ICP-MS	0.318	0.317
Yb (ppm)	FUS ICP-MS	1.96	2.01
Lu (ppm)	FUS ICP-MS	0.304	0.298
Hf (ppm)	FUS ICP-MS	3.1	4.2
Ta (ppm)	FUS ICP-MS	2.06	2.60
W (ppm)	FUS ICP-MS	0.9	-0.5
Tl (ppm)	FUS ICP-MS	0.49	0.21
Pb (ppm)	FUS ICP-MS	-5	-5
Bi (ppm)	FUS ICP-MS	-0.1	-0.1
Th (ppm)	FUS ICP-MS	5.0	3.55
U (ppm)	FUS ICP-MS	0.95	0.90

\* Total iron reported as Fe<sub>2</sub>O<sub>3</sub>.

### Notes:

Samples were analyzed at Activation Laboratories Ltd., Ancaster, Ontario, Canada.

Samples were crushed and then pulverized in a mild steel mill.

Major oxides and most minor elements were determined by X-Ray Fluorescence (XRF) on a fusion sample containing a lithium metaborate/tetraborate flux, in 2007.

Those determined by Inductively Coupled Plasma (ICP) were performed in 2009, also on a fusion sample.

FeO was determined by titration.

Au, As, Br, Cr, Ir, Sc, Se, Sb were determined by Instrumental Neutron Activation Analysis (INAA).

Trace elements and REE were analyzed by ICP-Mass Spectrometry (MS) or ICP on a fusion sample.

An elemental abundance below the detection limit is shown as a negative value.

NA = not analyzed

## APPENDIX D - ROCK-EVAL ANALYSES

Measured parameters for Rock-Eval-6

Parameter	Units	Mode	Description
S1	Mg HC/g rock	Pyrolysis	Free hydrocarbons
S2	Mg HC/g rock	Pyrolysis	Oil generation potential
Tpeak	°C	Pyrolysis	Temperature for S2 maximum release
S3	mgCO <sub>2</sub> /g rock	Pyrolysis	CO <sub>2</sub> from organic source
S3CO	mgCO/g rock	Pyrolysis	CO from organic source
S4CO <sub>2</sub>	mgCO <sub>2</sub> /g rock	Oxidation	CO <sub>2</sub> from organic source
S4CO	mgCO/g rock	Oxidation	CO from organic source
S5	mgCO <sub>2</sub> /g rock	Oxidation	CO <sub>2</sub> from mineral source
S5CO	mgCO/g rock	Oxidation	CO from mineral source

Calculated parameters from Rock-Eval-6

Parameter	Unit	Formula	Name
Tmax	°C	Calculated from Tps2-	Tmax
PI		S1/(S1+S2)	Production Index
PC	Wt %	Calculated from S1, S2, S3, S3CO, S3'CO	Pyrolysable organic carbon
RC CO	Wt %	Calculated from S4CO	Residual organic carbon (CO)
RC CO <sub>2</sub>	Wt %	Calculated from S4CO <sub>2</sub>	Residual organic carbon (CO <sub>2</sub> )
RC	Wt %	RC CO + RC CO <sub>2</sub>	Residual organic carbon
TOC	Wt %	PC + RC	Total organic carbon
HI	Mg HC/g TOC	S2*100/TOC	Hydrogen Index
OI	Mg CO <sub>2</sub> /g TOC	S3*100/TOC	Oxygen Index
OI CO	Mg CO/g TOC	S3CO*100/TOC	Oxygen Index CO
MinC	Wt %	pyroMinC + oximinC	Mineral Carbon

**Table D1.** Rock-Eval-6 analyses for samples collected from Coal River area (NTS 95D).

Sample	UTM E (m)	UTM N (m)	UTM Zone	Rock Type	Unit	Qty (mg)	S1 (mg HC/g rock)	S2 (mg HC/g rock)	PI	S3	Tmax (°C)	Tpeak (°C)	S3CO (mg CO/g rock)	PC (wt %)	TOC (wt %)	RC (wt %)	HI (mg HC/g TOC)	OICO (mg CO/g TOC)	OI	MinC (wt %)	S4CO	S4CO <sub>2</sub>	RCCO (wt %)	RCCO <sub>2</sub> (wt %)
<b>9107</b>					<b>standard</b>	70.7	0.73	12.13	0.06	0.51	441	478	0.21	1.10	5.10	4.00	238	4	10	4.3	18.6	117.3	0.800	3.20
09CYA010-1	579525	6708840	9N	black silty shale	SDRR	70.3	0.02	0.06	0.22	1.04	610	647	0.05	0.04	1.77	1.73	3	3	59	6.0	7.9	51.0	0.340	1.39
09LP039-2	579916	6716388	9N	black silty shale	SDRR	70.4	0.00	0.00	0.70	0.18	296	333	0.00	0.00	0.18	0.18	0	0	100	0.0	0.9	5.3	0.040	0.14
09LP074-1	623195	6684500	9N	black silty shale	SDRR	70.0	0.00	0.00	0.18	0.42	480	517	0.02	0.01	0.28	0.27	0	7	150	11.9	0.6	9.2	0.020	0.25
09LP058-1	559154	6658253	9N	limestone	SDRR contaminated	70.5	0.01	0.10	0.08	0.52	389	426	0.13	0.03	1.08	1.05	9	12	48	0.1	4.0	32.1	0.170	0.88
<b>9107</b>					<b>standard</b>	70.9	0.67	11.78	0.05	0.49	441	478	0.24	1.07	5.07	4.00	232	5	10	4.3	18.3	117.9	0.780	3.22
09LP062-1	617826	6683313	9N	silty shale	SDRR	70.5	0.01	0.01	0.32	0.32	485	522	0.02	0.01	0.27	0.26	4	7	119	13.0	0.8	8.4	0.030	0.23
09RAS106-1	647762	6668800	9N	black silty shale	DMBR	70.8	0.01	0.06	0.13	1.64	516	553	0.26	0.07	3.69	3.62	2	7	44	0.2	12.7	112.5	0.550	3.07
09LP093-2	658912	6734865	9N	black silty shale	SMRB	70.7	0.01	0.01	0.34	1.22	503	540	0.19	0.05	2.27	2.22	0	8	54	0.1	6.3	71.6	0.270	1.95
09LP077-1	657060	6712865	9N	mudstone	SMRB	50.2	0.01	0.02	0.20	1.99	500	537	0.31	0.08	7.36	7.28	0	4	27	0.2	31.3	217.8	1.340	5.94
<b>9107</b>					<b>standard</b>	70.6	0.72	12.11	0.06	0.50	442	479	0.19	1.10	5.02	3.92	241	4	10	4.4	18.3	115.0	0.780	3.14
10TOA035	559765	6660180	9N	black silty shale	SDRR	70.0	0.01	0.02	0.44	2.48	412	451	0.67	0.12	3.49	3.37	1	19	71	0.4	12.3	104.1	0.530	2.84
<b>9107</b>					<b>standard</b>	70.7	0.63	11.89	0.05	0.47	441	480	0.16	1.07	5.04	3.97	236	3	9	4.4	18.4	116.6	0.790	3.18